UNIVERSITY OF SOUTHAMPTON

Singular Partial Integro-Differential Equations Arising in Thin Aerofoil Theory

Timothy Richard Bislig Lattimer

Submitted for Ph.D. degree

Faculty of Mathematical Studies

October, 1996

UNIVERSITY OF SOUTHAMPTON

ABSTRACT

FACULTY OF MATHEMATICAL STUDIES

MATHEMATICS

Doctor of Philosophy

SINGULAR PARTIAL INTEGRO-DIFFERENTIAL EQUATIONS ARISING IN THIN AEROFOIL THEORY

by Timothy Richard Bislig Lattimer

A study is undertaken of three physical problems in which singular partial integro-differential equations arise. The equations result from applying thin aerofoil theory to two-dimensional potential flow over a free boundary. In all cases the work builds on existing steady models, for which ordinary singular integro-differential equations have been derived, to obtain time-dependent equations. The first of the physical problems examined is the sail equation, which describes the behaviour of a thin, flexible, inextensible sail in a high-Reynolds-number cross-flow at a small, but time-dependent, angle of incidence to the sail. A review of literature on the sail problem is presented. The unsteady equation is then solved numerically for various angles of incidence and sail masses. Variations of the unsteady sail equation are also derived to describe the sail as the sail mass becomes very small or very large, and to describe the flapping of a flag. An analytic expression is found for the low-mass sail given a particular set of functions for the angle of attack, for which the tension in the sail, and hence the lift, are zero.

The second problem examined is that of slot injection into a high-Reynolds-number cross-flow driven by an excess pressure in the slot. A literature review of slot injection to, and suction from, a free stream is presented, and then the unsteady injection problem is considered. Three different regimes are found for slot injection, according to the time scale of the pressure variations. Of these, the most important is the 'interactive' time scale, for which a third order singular partial integro-differential equation is obtained for the height of the shear layer separating the injected fluid from the free stream. For the other two cases, analytic solutions are found in terms of the known steady solutions. Discussion of the behaviour over more than one time scale is also presented. The numerical solution of the interactive equations, and singular partial integro-differential equations in general, is discussed, and it is concluded that in general integral transforms need not prevent stable numerical schemes from being found, and a condition for the numerical stability of finite difference schemes for singular partial integro-differential equations is obtained.

The third physical system discussed is suction from a high-Reynolds-number cross-flow. For this system a singular partial integro-differential equation is derived and solved, and closed form expressions for the mass transfer into the slot and the height of the shear layer are found. It is found that for a sudden change in the suction slot pressure, the mass transfer exhibits oscillatory decay to the steady solutions. The suction problem is related to the slot injection problem, and the transition between the two problems, when the slot pressure takes values both above and below the free stream pressure, is considered for various time scales, with equations unifying injection and suction presented for two different time scales. For changes over the shorter time scale it is shown how closed form solutions for the mass transfer may be found directly from the unsteady suction equations.

Contents

List of Figures

ACKNOWLEDGEMENTS

I would like to thank my supervisor, Alistair Fitt, for his time, help, and advice over the last three years. Thanks also to other members of the applied maths group for their help, in particular to Jeff Dewynne, for various ideas and practical help, and to Bob Craine.

I also acknowledge the Engineering and Physical Sciences Research Council, for their financial support.

Most of all I would like to thank my wife, Maxine, for her love, support, and strength, over the last three years, and particularly during the last few weeks of writing up.

PRINCIPAL NOTATION

Throughout, asterisks are used to denote non-dimensionalised variables, for example x^* denotes x divided by the characteristic length scale.

$b(x)$	$2\arcsin x^{\frac{1}{2}} - 2\log 2\, x^{\frac{1}{2}}(1-x)^{-\frac{1}{2}}$, i.e. the inverse finite-range Hilbert transform of $\log 1 - x$
c	$\begin{cases} \text{Courant number} \\ \text{Distance between masts of sail} \end{cases}$
$f(t)$	Slot pressure function
I_ν	Modified Bessel functions
J_ν	Bessel functions
k	Wave-number of instabilities
ℓ	Length of the sail
L	Width of the slot
n	Number of mesh points
p	Pressure
p_b	Pressure at the boundary, $y = S(x)$
p_∞	Pressure at infinity
Re	Reynolds number
$S(x)$	$\begin{cases} \text{Displacement of sail from the } x-\text{axis} \\ \text{Height of blown region} \end{cases}$
t	Time
T	Tension in the sail
u, v	Velocity components in the x and y directions
U_∞, U	Velocity of the cross-flow
v_w	Injection velocity
x, y	Cartesian co-ordinates
α	Angle of incidence of cross-flow to the sail
β	Tension parameter, given by $\beta^2 = T/(\rho' U^2)$
$\gamma(x)$	Source/sink/vortex strength at $(x, 0)$
δ	Small parameter in the sail problem, a measure of the displacement of the sail
ϵ	$\begin{cases} \text{Non-dimensional measure of the pressure difference between the slot and the free stream} \\ \text{Measure of the excess length of the sail, } \epsilon = (\ell - c)/c \end{cases}$
κ	Strength of singularity at leading edge of the sail
λ	Tension parameter for steady sail, $\lambda = 2\rho U^2 c/T = \mu/\beta^2$
μ	For unsteady sail, $\mu = 2\rho c/\rho'$
ξ	Variable of integration in $x-$direction
ρ	Density of fluid
ρ'	Mass per unit length of the sail
σ	Defined by $\sigma = \int_0^x S(\xi)d\xi$
ϕ	Velocity potential in blown region
Φ_O	Velocity potential in outer region
ψ	In sail problem, $\psi = S_x$
Ψ	Two-dimensional streamfunction : $(u, v) = (\Psi_y, -\Psi_x)$
ω	Frequency of instabilities
$\fint$	Cauchy Principal Value integral

Note that the term *Hilbert transform* is here used to denote the integral transform with Cauchy kernel, $(\xi - x)^{-1}$, over any region of integration.

Chapter 1

Introduction

A study is undertaken of singular partial integro-differential equations arising in unsteady two-dimensional fluid dynamics problems involving thin aerofoil theory. All the equations contain Hilbert transforms, for which some useful results are detailed in appendix A. This study is motivated in part by the study of the cooling of turbine blades, where cool gas passes through slots or holes onto the blade surface. The cooling gas is sucked from a channel inside the blade, and expelled into the free stream, see figure 1.1. The slot cooling system cools the blade down in two different ways : the cool

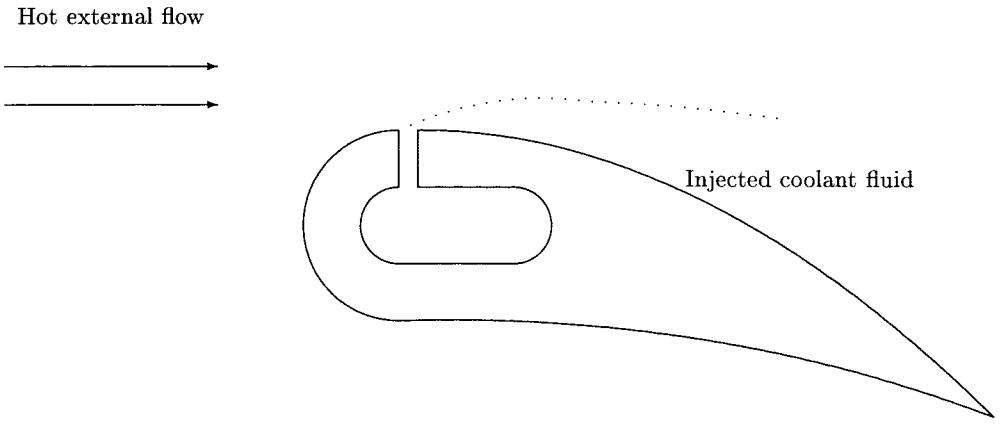

Figure 1.1: A schematic diagram of the film cooling system

air in the internal passages of the blade removes heat from the body of the blade, and the cooling air which is expelled into the free stream insulates the surface of the blade from the hot gases flowing past. A single blade may have many slots all over the surface of the blade, but they are usually concentrated at the leading edge of the blade, since it is this part which is usually subject to the most extreme heat. This cooling may have significant effects on the lifetime of the blade : Barry (1976) [5] showed that a variation of 20°C around a mean blade temperature of 900°C can halve or double the life of a blade. Unfortunately turbulent mixing downstream of the point at which the cooling gas is injected means that the heat from the external flow will penetrate the cooling layer downstream of the slot. Improved cooling of the blade will allow higher temperatures of the gas that enters the

turbine to be used. This in turn improves fuel efficiency, and it is the cooling mechanism which allows temperatures of approximately 1400°C (from Morland (1988) [60]) to be used in a modern commercial jet engine. Similar considerations apply to the related subject of slot injection from the leading edge of a Joukowski aerofoil. Hubbard & Riley (1995) [46] showed that slot injection may delay separation, and hence increase the lift of the aerofoil, as well as cool the surface downstream of separation. The flow will here be modelled by slot injection into a free stream.

The problem of suction into a slot from a free stream is also relevant to film cooling, as before the cooling air is emitted from the surface of the blade, it must be sucked from a channel inside the blade. It is also relevant to 'rim sealing', which again is related to modern gas turbines : between the rotating turbine disc and a stator hot mainstream gas may be ingested, which can severely affect disc temperatures. Again, air may be injected into the external flow in order to prevent this ingestion, see figure 1.2.

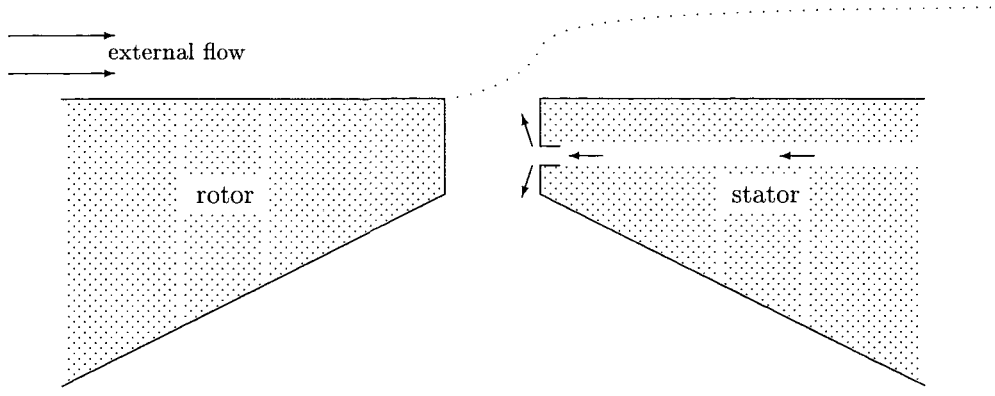

Figure 1.2: A schematic diagram of the rim seal. This an axisymmetric problem, with the rotor rotating out of the page.

This is essentially a three-dimensional problem and so will require further study, though it is hoped that examination of the two-dimensional system will provide at least a qualitative guide to the axisymmetric and fully three-dimensional problems. The relevance of slot suction to the rim seal problem is in the behaviour when the difference between the slot pressure and the external pressure can change sign so that slot injection can become slot suction, or vice versa. This is also relevant to a range of problems including the fluid flow produced by wind blowing past a nuclear reactor containment dome, discussed by Kapila and Drew (1987) [49]. In this problem the interior of the dome is maintained at a pressure less than that of the outside atmosphere so that contaminated air is prevented from seeping out of the dome through small gaps which lie between the segments from which the dome is constructed. However should atmospheric pressure drop below that in the dome then the problem will become an unsteady problem in which both blowing and sucking occur, so the 'blowing and sucking' problem will be of particular relevance.

Other related problems in which flows similar to those obtained for slot injection may occur include

convector heating from a flat plate, as studied by, for example, Smith & Riley (1979) [77], and flow of blood in branching arteries and veins. Moreover, analysis of the film cooling problem will provide some insight into other problems with 'blown-off' boundary layers, for example, flow down a step or past a blunt body, as studied by O'Malley et al (1991) [65]. The analysis of the equations derived will also be applicable to other physical problems in which similar integro-differential equations with Cauchy kernels, $(\xi - x)^{-1}$, arise, such as crack formation (e.g. Fitt et al (1995) [32]).

Three problems in particular are focussed upon. In all three cases the work is based on an existing steady model, but unsteady models have not previously been considered. The first problem considered is two-dimensional uniform irrotational flow of an inviscid fluid at a small angle of incidence to a thin, flexible, inextensible membrane. This problem is discussed in chapter 2. For a steady flow the shape of the membrane may be described by a linear integro-differential equation, usually referred to as the sail equation (the equation is usually attributed to Thwaites (1961) [91], but was originally derived by Voelz (1950) [107]), whose validity is dependent on the facts that the excess length of the sail, in other words the distance by which the length of the sail exceeds the distance between the masts, is small relative to the distance between the masts, and that the angle of inclination of the flow to the sail is small. All small variables in the problem, in particular the angle of incidence of the sail to the crossflow, and the deviation of the sail from a straight line between the masts, are scaled relative to the square-root of this excess length. Part of the motivation of the study of this equation is in order to provide further insight into the mathematics arising from the slot cooling problem, in that a similar type of equation is derived, although the sail equation, unlike the equation derived from slot injection, is linear. It is however an interesting and relevant problem in its own right, and is also relevant to the study of flexible-sail type wind-turbines, see for example Fleming & Probert (1984) [36]. By allowing the angle of inclination to depend on time, a more complicated, but still linear, time-dependent singular partial integro-differential equation has been derived. It is this time-dependent equation that is of particular interest, and which constitutes the new research of this chapter. The numerical solution of this equation is discussed, and results are presented, in chapter 3. Previously little work has been found on the study of singular partial integro-differential equations, in this or any other context, so the work on the unsteady sail equation is particularly important, not only in its own right, but also in relation to other problems, and in particular the unsteady slot injection and suction problems of chapters 5 and 6. Chapter 2 ends with a discussion of the limiting behaviour of the unsteady sail in the cases where the relative mass of the sail becomes large or small, and the case where the scaled angle of incidence of the crossflow to the sail becomes large. The consequences of this analysis for a flapping flag are also discussed, and another singular partial integro-differential equation is derived to describe the shape of the flag. This equation may be reduced to an ordinary integro-differential equation describing sinusoidal flapping of a flag in a steady cross-flow.

The second problem considered is that of injection from a slot into a uniform flow of a high-Reynolds-

number fluid, the 'blowing' problem, in two dimensions. The injection is driven by a small pressure difference between the slot and the external flow, and again linearised thin aerofoil theory applies. A small parameter is defined by the relative difference between the pressure at the bottom of the slot and the external pressure at infinity, with the other variables in the problem being dependent upon this small parameter. Chapter 4 contains a review of previous literature on the subject, which almost exclusively is concerned with the steady problem. Chapter 5 then examines the unsteady problem, in which the slot pressure is allowed to vary with time. Three different systems of equations are then derived according to the time scale of the change in the slot pressure, each system containing at least one singular partial integro-differential equation. The 'suction problem', again in two dimensions with the suction of a high Reynolds number fluid being driven by a pressure difference between the slot and the external flow, is discussed in chapter 6. Again, previous time-independent studies are discussed and then the relevant singular partial integro-differential equations are derived by allowing the slot pressure to vary with time. Unlike in the blowing problem, the equations derived are linear, and may be solved by analytic methods in some cases. The solutions are then given for some possible choices of slot pressure profiles (e.g. sinusoidal, linear, step function). The case where injection and suction both take place over a period of time is discussed in chapter 7, where equations unifying the two cases are presented for changes over two of the time scales defined. For the shorter of these time scales, the equations are similar to those of slot suction, and are solved by the same methods.

Chapters 8 and 9 then discuss attempts to solve the time-dependent blowing (i.e. injection) equations derived in chapter 5 numerically, and analyse the solution of singular partial integro-differential equations in general. It is found that if, as was the case with the unsteady sail equation, the highest derivatives in the equation are not contained in the transform, the integral transform does not affect numerical stability. If the transform does contain at least one of the highest derivatives, then although the presence of a singular integral will affect numerical stability, it is sometimes possible to find stable finite difference schemes to solve these equations numerically, and further that the behaviour of singular partial integro-differential equations is closely linked to those of the partial differential equations obtained by replacing the integral transform operator with the identity operator. A numerical solution is found for a particular singular partial integro-differential equation of this kind, and this is found to converge to the known solution. In the case of the time dependent slot injection equations, the associated partial differential equation is third order, which leads to formidable problems in finding a stable numerical scheme for the associated partial differential equation, and thus for the full system containing the singular integral. Chapter 10 gives a summary of the results obtained, and proposes some areas in which the analysis could be extended.

All the computations described here were done using a silicon graphics Indigo 2XL workstation, and FORTRAN coding. Where required, linear matrix equations were solved using NAG routine F04ATF, and Bessel functions were evaluated using NAG routine S18DEF.

Chapter 2

The Sail Equation

The sail equation of Voelz (1950) [107] and Thwaites (1961) [91] is similar to the steady slot injection equation of Fitt et al (1985) [34] in that it is a singular integro-differential equation containing a Cauchy kernel, for which no analytic solution has been found. Furthermore although in both cases there is a significant amount of literature on the physical problem which the equation addresses, there is very little literature on the unsteady problem. In both cases analysis of the unsteady problem leads to an equation with a singular partial integro-differential equation, and again this class of equation is not one that has previously been examined. The techniques in the derivation and the analysis of the sail equation, which is linear, will therefore be of use in the more complicated unsteady slot injection and suction equations. Furthermore the numerical problems posed by the sail equation will be similar to those of the slot injection equation.

2.1 The Aerodynamic Theory of Flexible Surfaces

Most studies of flow past a sail to date have been two-dimensional, one of the first mathematical models being completed by Cisotti (1932) [19]. In this study the sail was assumed to be non-porous, with the flow separating at the trailing edge of the sail (the "leach"), to form a quiescent wake. This differed from the work of Voelz (1950) [107], in whose model the sail was considered as a linear distribution of vortices, with the flow considered to be incompressible and irrotational, and the sail assumed to be non-porous and inextensible. It is this model upon which the analysis of the problem in this chapter will largely be based. This model applied thin aerofoil theory (see, for example, Van Dyke (1964) [99]), assuming that the sail deviates from a straight line connecting the masts by only a small amount, thus permitting linear asymptotics to be used, with the angle of attack of the cross-flow remaining small. From this a linear integro-differential equation for the shape of the sail depending on the ratio of the angle of attack to the excess length of the sail was derived. This equation was then numerically solved for a variety of sail lengths, and the lift, moment, and pressure distribution on the sail were also calculated. Bugler (1957) [11] undertook a more thorough analysis based on a similar model. However it is the work of Thwaites (1961) [91] which is most usually associated with

this problem. Thwaites's work was similar to that of Voelz, deriving the same equation, apparently independently, although Thwaites's equation extends the theory to apply to a porous sail where the flow through the sail is proportional to the pressure difference across it. Moreover Thwaites found solutions beyond the range examined by Voelz, in particular finding a range of solutions with zero lift for a non-zero angle of attack. (These are the even eigenvalues of section 2.2.3). Nielsen (1963) [63] independently completed a study similar to that of Thwaites based on Fourier series and numerical matrix techniques rather than integral equations, and found that numerically his results were in good agreement with those of Thwaites and Voelz. Nielsen also examined the three-dimensional problem, and performed some experiments. The experiments largely agreed with the numerical calculations, with errors being thought to be caused in part by porosity of the sail and boundary layer effects, although Chapleo (1968) [16] argued that errors may have been caused by overestimation of the lift due to camber. Barakat (1968) [4] studied the influence of the porosity of the sail and extended the theory to a two-lobed sail, and Tuck & Haselgrove (1972) [97] considered the problem in which the sail is not rigidly attached to the trailing edge but instead attached to a rope, or sheet, which is inflexible and fixed at one end. They found that as the length of the sheet increases the lift decreases but the stability of the sail increases. A three-dimensional linear analysis was completed by Nickel (1987) [62], using the 'lifting line theory' of Prandtl (1918) [70].

A more general study, valid for greater angles of incidence than those of Voelz or Thwaites was completed by Dugan (1970) [27] who used the behavioural model developed by Cisotti. This was a non-linear free-streamline model, allowing separation of the flow at the trailing edge, assuming constant tension in the sail. A non-linear singular integral equation was found and solved numerically, obtaining the sail profile and the drag, lift and moment experienced by the sail, although the model breaks down for small angles of attack. Vanden-Broeck (1982) [101] used a similar model to derive and numerically solve an integro-differential equation for arbitrary angles of incidence. Jackson (1983) [48] considered an extensible sail, and derived a non-linear equation for arbitrary angles of attack. Computational procedures were also applied for a viscous flow with a Reynolds number of between 2×10^3 and 10^4 for elastic, inextensible, and constant tension sails, by Smith & Shyy (1995b) [82] for steady flow, and Smith & Shyy (1995a) [81] for unsteady flow. Other unsteady analyses include that of Bäcker et al (1991) [2], for the related non-linear problem of fibres fluttering in an airspinning process, and that of Haselgrove & Tuck (1976) [45], who found that for a low-mass sail of infinite length there is a critical value of the sail tension, with the sail being stable or unstable to small disturbances according to whether the tension is less than or greater than the critical value. This work is the most similar to that of this chapter, in that it is applied to a linear inextensible sail, and thus is an extension of the equation derived by Voelz. However their work considered only a sail of zero mass, whereas the work of this chapter will consider sails of finite length and finite mass, as well as considering the asymptotic analysis as the sail length and sail mass tend towards zero or infinity. Their work also allowed vortices

to be shed from the sail, with a line vortex appearing downstream of the sail along the axis of the sail.

Although the models of Voelz, Thwaites, and Nielsen, and the equations derived, are essentially the same, comparisons to the steady results will be made using the work of Thwaites (1961) [91] (henceforth referred to as 'Thwaites'), as this is the most complete and detailed analysis of the theoretical steady problem.

2.2 The Sail Equation

The sail equation, as presented by Thwaites, concerns the uniform two-dimensional flow of an inviscid, incompressible fluid at low angle of incidence, α, past a porous, flexible, inextensible, thin sail of finite length. It gives a singular integro-differential equation for the shape of the sail. Figure 2.1 gives a schematic representation of the sail. Since the sail is taken to be of zero thickness, the flow just above

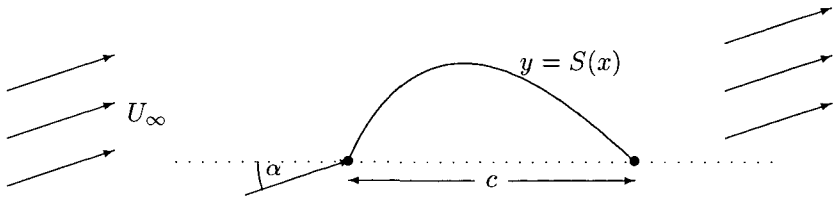

Figure 2.1: A Schematic Diagram of the Sail

the sail and the flow just below the sail will be parallel to the sail, so the sail contains no sources. There will however be a net lift on the sail, so the sail may be modelled as a distribution of vortices of strength $\gamma(x)$, lying on the line

$$y = S(x), \qquad 0 \leq x \leq c,$$

where $S(x)$ is small compared to c, so to lowest order the vortices lie on the x-axis between $x = 0$ and $x = c$. Let $c\delta$ be a measure of the size of $S(x)$, leaving the question of how δ relates to other variables in the problem open for now. Then using the fact that the potential corresponding to a vortex of strength γ at the point (x', y') in thin aerofoil theory is $\gamma \arctan\left(\frac{y-y'}{x-x'}\right)$, where γ is small (of order δ), the velocity potential, Φ, may be written as an order δ perturbation to the velocity potential of a uniform flow Ux, in the form

$$\Phi = U(x\cos\alpha + y\sin\alpha) + \frac{1}{2\pi}\int_0^c \gamma(\xi)\arctan\left(\frac{y}{\xi - x}\right)d\xi. \tag{2.1}$$

In order to relate $\gamma(x)$ to the shape of the sail $S(x)$ it is necessary to compare the direction of the flow just above the sail to that predicted by the potential. In order for this to be possible it is necessary to define the *porosity* of the sail, $\sigma(x)$. Thwaites defined the porosity $\sigma(x)$ of the sail for the purposes of

this problem by assuming that the velocity of the fluid through the sail in the y-direction is $\sigma(x)\gamma(x)$ (the velocity in the x-direction through the sail may be ignored as it will be of the order of $\delta\gamma(x)$). The flow just above the sail will therefore be the sum of two components : the tangential term from the fluid flowing over the sail, and the normal term from the fluid flowing through the sail. The second of these terms is $\sigma\gamma$ in the vertical direction and the first of these will be of magnitude $U(1+O(\delta))$ with a slope of $S'(x)$. Thus the slope of the total flow just above the sail will be

$$\lim_{y\to 0} v/u = S'(x) + \frac{\sigma\gamma}{U}, \tag{2.2}$$

where u and v denote the velocities in the x and y directions. Since $u = \Phi_x$, $v = \Phi_y$, the left-hand side of equation 2.2 may be written as

$$\lim_{y\to 0} v/u = \lim_{y\to 0} \frac{U\alpha + (2\pi)^{-1}\int_0^c \frac{\gamma(\xi)(\xi-x)}{(\xi-x)^2+y^2}d\xi + O(\alpha^3)}{U + (2\pi)^{-1}\int_0^c \frac{\gamma(\xi)y}{(\xi-x)^2+y^2}d\xi + O(\alpha^2)}.$$

The integral term in the denominator of this equation may be ignored, as it is of order δ and thus negligible compared to U. Thus after substitution from equation 2.2 the equation reduces to

$$\alpha + \frac{1}{2\pi U}\int_0^c \frac{\gamma(\xi)}{\xi - x}d\xi = S'(x) + \frac{\sigma\gamma}{U},$$

and hence

$$\frac{1}{\pi}\int_0^c \frac{\gamma(\xi)}{\xi - x}d\xi = 2U(S'(x) - \alpha) + 2\sigma(x)\gamma(x). \tag{2.3}$$

This equation relates $S'(x)$ to $\gamma(x)$. In order to relate $\gamma(x)$ to $S''(x)$ and thus obtain an integral equation for $S'(x)$ it is necessary to balance the lift on an element of the sail against the tension. Consider an element of the sail with length δs whose end-points are at $(x, S(x))$ and $(x+\delta x, S(x+\delta x))$ respectively. Comparison of forces in the x-direction shows that $\delta T = 0$ to lowest order. The y-component of the tension force, F_T, is given by

$$F_T = (T + \delta T)\sin(\psi + d\psi) - T\sin\psi, \tag{2.4}$$

where ψ is the angle that the sail makes with the horizontal, i.e. $\tan\psi = S_x$. This force F_T must be equal and opposite to the lift. The y-component of the aerodynamic force on the sail element, F_A, is

$$F_A = p_-\delta s\cos\psi - p_+\delta s\cos\psi, \tag{2.5}$$

where p_- and p_+ represent the values of the pressure just below and just above the sail respectively. Hence $p_- - p_+$, which will henceforth be denoted as Δp, is the lift at a given value of x.

This lift may be determined by Bernoulli's equation. The flow is irrotational and steady, so $p + \frac{1}{2}\rho(u^2+v^2)$ will be constant throughout the flow, where p represents the pressure, and ρ the fluid density. In particular

$$\lim_{y\to 0^-}(p + \frac{1}{2}\rho q^2) = \lim_{y\to 0^+}(p + \frac{1}{2}\rho q^2), \qquad 0 \le x \le c,$$

where $q^2 = u^2 + v^2 = u^2(1 + O(\delta^2))$ from equation 2.2. From equation 2.1 the right-hand side of the above equation is

$$\lim_{y\to 0^+} p + \frac{1}{2}\rho\left(U + \frac{1}{2\pi}\int_0^c \frac{\gamma(\xi)y}{(x-\xi)^2+y^2}d\xi\right)^2.$$

Using the fact that $\pm\frac{1}{\pi}\lim_{y\to 0\pm}\frac{y}{x^2+y^2}$ is the Dirac delta function, $\delta(x)$, the following result is obtained :

$$\lim_{y\to 0\pm} u^2 = U^2 + 2U\frac{1}{2\pi}\int_0^c \pm\gamma(\xi)\pi\delta(x-\xi)d\xi + o(\gamma^2).$$

It then follows that

$$\Delta p = \rho U\gamma(x).. \tag{2.6}$$

This may be substituted into the expressions for the tension and lift forces, equations 2.4 and 2.5. As the perturbation is small, $\tan\psi$ is equal to ψ to within order ψ^3, and in the limit as δs tends to zero, $\delta s/\delta x = 1 + O(\psi^2)$. Hence the relationship between γ and the aerodynamic force is

$$TS''(x) + \rho U\gamma(x) = 0. \tag{2.7}$$

This confirms that $\gamma(x)$ is of order δ as $S'(x) = O(\delta)$. We can now write the 'Sail Equation' in terms of $S(x)$:

$$\frac{-T}{\pi\rho U}\int_0^c \frac{S''(\xi)}{\xi - x}d\xi = 2U(S'(x) - \alpha) - \frac{2T}{\rho U}\sigma(x)S''(x). \tag{2.8}$$

The boundary conditions are $S(x) = 0$ at $x = 0$ and $x = c$ since the ends of the sail are fixed, and the requirement that the Kutta condition is satisfied at the trailing edge, $S''(x) = 0$ at $x = c$. This extra requirement is necessary due to the presence of the integral transform, whose inverse is non-unique (see section A.2.1). The physical interpretation given by the Kutta condition is that there is no separation at the trailing edge, so the flow re-attaches smoothly.

Henceforth it is convenient to work in terms of non-dimensional variables. In his original derivation of the equations Thwaites scaled $S(x)$ with $c\alpha$, with the assumption that α is small. In other words, the small parameter δ was taken to be α. This implies that the length of the sail must only exceed c, the distance between the ends of the sail, by an amount of order $c\alpha^2$, since the length of the sail is given by the integral of the square-root of $(1 + S'^2)$. Thus Thwaites defined the excess length of the sail, ϵ, by denoting the length of the sail as $c(1 + \epsilon)$, i.e.

$$c(1+\epsilon) = \int_0^c (1 + S'^2(x))^{\frac{1}{2}}dx. \tag{2.9}$$

With this definition, and Thwaites's scaling of S with α, ϵ is of order (α^2). Thwaites's variable ℓ/c is equivalent to ϵ^2 defined here.

The non-dimensionalisation used in this analysis, therefore, will scale $S(x)$ with $c\epsilon^{\frac{1}{2}}$, so the small parameter δ, will be $\epsilon^{\frac{1}{2}}$. (Note that since this analysis is only to first order in $\epsilon^{\frac{1}{2}}$, all terms of order ϵ will be negligible). There are several advantages to this scaling. The first of these is that since it is desired to progress from Thwaites's steady equation to a new, unsteady, equation, it makes sense to

re-scale with a parameter that will not be dependent on time. Although an unsteady system could be considered with a sail of varying length, but a fixed angle of attack, this is considered unrealistic and a sail with a fixed length and a variable angle of attack will be considered in the sections on the unsteady sail equation, from section 2.3 onwards. Furthermore even in the steady case it is preferable to scale with $\epsilon^{\frac{1}{2}}$ rather than α, as it allows α to be zero, or, equivalently, much less than $\epsilon^{\frac{1}{2}}$. Thwaites found the sail shapes corresponding to $\alpha = 0$, but considered them to be "meaningless" as a result of his choice of scaling. Using the same scaling, Chambers (1966) [15] interpreted the same solutions as being the free modes of a flag (for a discussion of how the sail equation relates to a flag, see section 2.9). In addition it is shown in section 2.7 that for both the steady and unsteady equation, with this choice of scaling there is no requirement for α to be of order $\epsilon^{\frac{1}{2}}$, although α must be small for the sail to represent a small perturbation to the free stream. The non-dimensionalisation used henceforth is therefore given by :-

$$\begin{aligned} x &= cx^*, \\ y &= c\epsilon^{\frac{1}{2}}y^*, \\ S(x) &= c\epsilon^{\frac{1}{2}}S^*(x^*), \\ \gamma(x) &= \frac{T\epsilon^{\frac{1}{2}}}{\rho U c}\gamma^*(x^*), \\ \lambda &= \frac{2\rho U^2 c}{T}, \\ \sigma(x) &= \sigma^*(x^*), \\ \alpha &= \epsilon^{\frac{1}{2}}\alpha^*, \\ \psi &= \epsilon^{\frac{1}{2}}S^{*\prime}(x^*). \end{aligned}$$

In terms of these variables equation 2.8 becomes

$$-\frac{1}{\pi}\int_0^1 \frac{S^{*\prime\prime}(\xi)}{(\xi - x^*)}d\xi = \lambda(S^{*\prime}(x^*) - \alpha^*) - 2\sigma^*(x^*)S^{*\prime\prime}(x^*), \tag{2.10}$$

with boundary conditions, as before, $S^*(0) = S^*(1) = 0$ and $S^{*\prime\prime}(1) = 0$. There is now a further condition, which enables λ to be determined, namely that the scaled excess length is unity. From equation 2.9 in non-dimensionalised co-ordinates this may be written as

$$1 = \frac{1}{2}\int_0^1 S^{*\prime 2}(x^*)dx^* + o(\epsilon). \tag{2.11}$$

This condition will be referred to as 'the length condition' and is important to both the steady and unsteady cases.

Henceforth the sail will be taken to be non-porous ($\sigma = 0$), for simplicity. Equation 2.10 may also be inverted by the methods discussed in section A.2.2 to give

$$S^{*\prime\prime}(x^*) = \frac{\lambda}{\pi}\frac{(1-x^*)^{\frac{1}{2}}}{x^{*\frac{1}{2}}}\int_0^1 \frac{\xi^{\frac{1}{2}}(S^{*\prime}(\xi) - \alpha^*)}{(1-\xi)^{\frac{1}{2}}(\xi - x^*)}d\xi. \tag{2.12}$$

Here the inversion has been chosen in order to give $S^{*\prime\prime}(1) = 0$.

2.2.1 Lift

Solution of the above equations give the sail shape, $S^*(x^*)$, and the tension parameter, λ, for a given ratio of angle of attack to excess sail length, α^*. From this other features of the flow may be deduced, for example the velocity just above and below the sail, the pressure coefficient at each point, the total lift on the sail, and the load on each mast. Of these, the total lift is the statistic of most interest in both the steady and the unsteady problem. It may easily be calculated in terms of S, by observing that the pressure difference across the sail at a given value of x^* is given by equation 2.6, and that the total lift is just the integral of the lift at each point over the sail. Hence, combining equations 2.6 and 2.7,

$$\begin{aligned}
\text{Total lift} &= \int_0^c \Delta p dx \\
&= \int_0^c \rho U \gamma(x) dx \\
&= -T \int_0^c \psi' dx \\
&= T(\psi(0) - \psi(1)) \\
&= T\epsilon^{\frac{1}{2}}(S^{*\prime}(0) - S^{*\prime}(1)) \\
&= \frac{2\rho U^2 c}{\lambda}\epsilon^{\frac{1}{2}}(S^{*\prime}(0) - S^{*\prime}(1)). \qquad (2.13)
\end{aligned}$$

The force on each mast may also be calculated, by considering an element of length dx at the end of the sail. Since, in this linear model, to lowest order all forces are horizontal, with the tension, T, being constant, the horizontal force on each mast will be a force of magnitude T (i.e. $2\rho U^2 c\lambda^{-1}$) inwards. In the vertical direction the force on the mast will be the same as the vertical component of the tension, which is $T\psi$, and so, in non-dimensionalised co-ordinates, the force on the leading mast will be $2\rho U^2 c\lambda^{-1}\epsilon^{\frac{1}{2}}S^{*\prime}(0)$, and the force on the trailing mast will be $-2\rho U^2 c\lambda^{-1}\epsilon^{\frac{1}{2}}S^{*\prime}(1)$. This confirms the expression for the lift given by equation 2.13, and moreover, since the expressions for the force on each mast will be the same for an unsteady sail, this demonstrates that equation 2.13 will be valid for an unsteady sail.

2.2.2 Numerical Solution of the Steady Equation

Voelz, Thwaites and Nielsen solved the sail equation in the form given by equation 2.12, for a given λ, by similar methods. The transformation $2x = 1 - \cos\theta$ was used and the solution was assumed to be given by Fourier series. Here, however, a finite difference method will be used, as this will also be appropriate to the unsteady equation, and the slot equations which are derived in chapter 5. In the form given by equation 2.12 there are two singularities : the $(\xi - x)^{-1}$ singularity in the integrand at $\xi = x^*$, and the square-root singularity at $x^* = 0$. However integration with respect to x^* will remove the latter of these, and weaken the former to give a logarithmic singularity, which will pose

no problems numerically. Since equation 2.12 gives, using equation A.8,

$$S^{*\prime\prime}(x^*) = \frac{\lambda}{\pi}\frac{(1-x^*)^{\frac{1}{2}}}{x^{*\frac{1}{2}}}\int_0^1 \frac{\xi^{\frac{1}{2}}S^{*\prime}(\xi)}{(1-\xi)^{\frac{1}{2}}(\xi-x^*)}d\xi - \lambda\alpha^*\sqrt{\frac{1-x^*}{x^*}}, \tag{2.14}$$

it follows from integration with respect to x^* that

$$\begin{aligned} S^{*\prime}(x^*) &= \frac{\lambda}{\pi}\int_0^1 \left(2\sqrt{\frac{\xi}{1-\xi}}\arcsin\sqrt{x^*} - \log\left|\frac{\sqrt{\frac{x^*}{1-x^*}} - \sqrt{\frac{\xi}{1-\xi}}}{\sqrt{\frac{x^*}{1-x^*}} + \sqrt{\frac{\xi}{1-\xi}}}\right|\right) S^{*\prime}(\xi)d\xi \\ &- \lambda\alpha^*\left(\arcsin\sqrt{x^*} + \sqrt{x^*}\sqrt{1-x^*}\right) + \psi_0. \end{aligned}$$

Here, ψ_0 is a constant, which is determined from the condition that S^* is zero at $x^* = 0$ and $x^* = 1$. The values of $S^{*\prime}$ at ξ_i will therefore be denoted by ψ_i for $0 \le i \le n$, where the ξ_i are a mesh with $\xi_i = i/n$, and $n+1$ is the number of points. With this notation the above equation becomes

$$\psi_i - \psi_0 - \frac{\lambda}{\pi}\sum_{k=0}^{n-1}(I(\xi_{k+1},\xi_i) - I(\xi_k,\xi_i))\psi_k \approx -\lambda\alpha^*\left(\arcsin\sqrt{\xi_i} + \sqrt{\xi_i}\sqrt{1-\xi_i}\right),$$

for $1 \le i \le n-1$. Here, $I(\xi, x)$ is given by

$$\begin{aligned} I_\xi(\xi,x) &= 2\sqrt{\frac{\xi}{1-\xi}}\arcsin\sqrt{x} - \log\left|\frac{\sqrt{\frac{x}{1-x}} - \sqrt{\frac{\xi}{1-\xi}}}{\sqrt{\frac{x}{1-x}} + \sqrt{\frac{\xi}{1-\xi}}}\right| \\ \Rightarrow I(\xi,x) &= 2\arcsin\sqrt{x}\arcsin\sqrt{\xi} - 2\sqrt{\xi}\sqrt{1-\xi}\arcsin\sqrt{x} + 2\sqrt{x}\sqrt{1-x}\arcsin\sqrt{\xi} \\ &- (\xi - x)\log\left|\frac{\sqrt{\frac{x}{1-x}} - \sqrt{\frac{\xi}{1-\xi}}}{\sqrt{\frac{x}{1-x}} + \sqrt{\frac{\xi}{1-\xi}}}\right|, \end{aligned}$$

via some simple, although rather long-winded, algebra. Hence a matrix equation for the variables ψ_i is obtained, for $0 \le i \le n-1$. The system is closed with the equation

$$\sum_{k=0}^{n-1}\psi_k = 0,$$

corresponding to the fact that the sail is fixed at both ends. The matrix is singular only for values of λ corresponding to $\alpha^* = 0$. In this case an extra condition is required to solve the matrix equation. Although this condition is the length condition, it is not possible to explicitly enter this into the matrix equation, as it is non-linear, so the solution may be found by imposing, $S^{*\prime} = 1$ at $x^* = 0$, say, and then re-scaling.

The matrix equation is solved for a given λ. This gives a solution, $\psi = S^{*\prime}$. This may not satisfy the length condition, equation 2.11. However, since the equation to be solved, equation 2.14, is invariant under the transformation $(S^*, \lambda, \alpha^*) \to (kS^*, \lambda, k\alpha^*)$ it follows that a scaled solution which does satisfy the length condition will be a solution for some α^*. In fact if the above scheme is solved for a given λ, with α^* set to 1, for example, then the correct value of α^* corresponding to that λ is given by

$$\sqrt{\frac{1}{\frac{1}{2}\int_0^1 S^{*\prime 2}\,dx^*}}.$$

Thus a plot of λ against α^* may be drawn, and is shown in figure 2.2, with the broken line representing the asymptotic behaviour of λ for large values of α^* (see section 2.2.4).

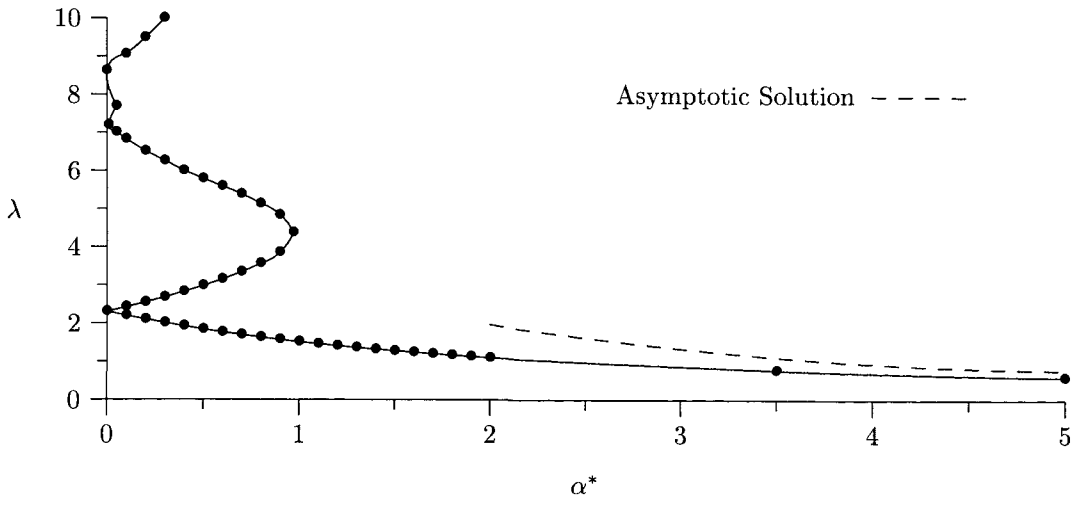

Figure 2.2: Calculated Values of λ Plotted Against α^*

The error in this scheme is the error in evaluating the integral of $I_\xi\psi$. Since the approximation made is that ψ is constant on the interval (ξ_k, ξ_{k+1}), the error will be of order $I_\xi\psi'\delta x$, where δx is the difference between mesh points. Since $I_\xi\psi'$ is order 1 everywhere, the error in this scheme is δx^{-1}, i.e. n^{-1}.

One interesting feature of the solutions is that for a given sail length and angle of attack, more than one solution is possible, each corresponding to a different value of λ. For example with $\alpha^* = 0.4$, λ may be 1.92866,2.82537, or 6.08502. (These values were obtained using the above numerical scheme with 200 mesh points). The corresponding sail shapes are illustrated in figure 2.3. The next section will go on to discuss this phenomenon, and how it relates to the eigenvalues of the problem.

2.2.3 Eigenvalues

A relationship between λ and α^* was determined from the numerical calculations described above and was expressed in figure 2.2. The obvious feature of this graph is that the relationship between λ and α^* is not one to one. To place this into context it is necessary to examine the existence of the eigenvalues of this problem, defined by the values of λ for which there is smooth separation at the leading edge, as well as the trailing edge.

Using the result given by equation A.8, equation 2.12 may be written

$$S^{*\prime\prime}(x^*) = \frac{\lambda}{\pi}\frac{(1-x^*)^{\frac{1}{2}}}{x^{*\frac{1}{2}}}\int_0^1 \frac{\xi^{\frac{1}{2}}S^{*\prime}(\xi)}{(1-\xi)^{\frac{1}{2}}(\xi - x^*)}d\xi - \lambda\alpha^*\sqrt{\frac{1-x^*}{x^*}}. \tag{2.15}$$

Consider the behaviour of S^* near $x^* = 1$. The α^* term suggests that $S^{*\prime\prime} \sim (1-x^*)^{\frac{1}{2}}$, which in turn suggests that $S^{*\prime}$ will analytically tend to a constant (which in general will be non-zero) so the coefficient of $(\xi - x^*)^{-1}$ will have a square-root singularity. Thus, according to equation A.12, the

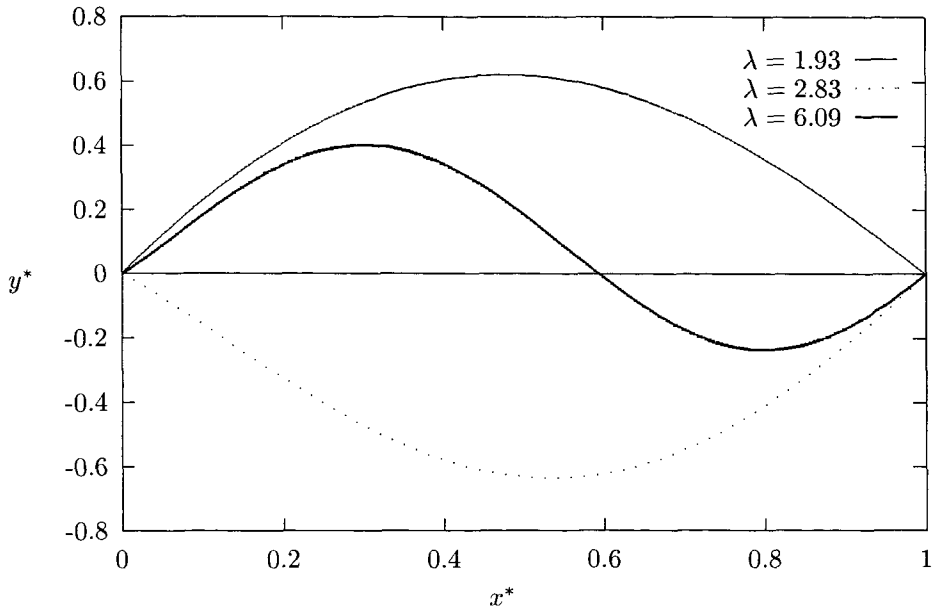

Figure 2.3: The Three Sail Shapes for $\alpha^* = 0.4$

integral transform will tend to a constant, and so both terms on the right-hand side will asymptotically tend towards a multiple of $(1-x^*)^{\frac{1}{2}}$. Since there is no reason for these terms to be equal the asymptotic behaviour of S^* near $x^* = 1$ will be given by $S^{*\prime\prime} \sim K(1-x^*)^{\frac{1}{2}}$, for some constant K.

Near $x^* = 0$, by similar reasoning, $S^{*\prime}$ will tend to a constant, so from equation A.12 the singular integral will tend to a constant. Thus both terms of equation 2.15 will exhibit square-root singularities at $x^* = 0$. Hence as x^* tends to zero,

$$S^{*\prime\prime} \sim \lambda \left(\frac{1}{\pi} \int_0^1 \frac{S^{*\prime}(\xi)}{\xi^{\frac{1}{2}}(1-\xi)^{\frac{1}{2}}} d\xi - \alpha^* \right) x^{*-\frac{1}{2}}. \tag{2.16}$$

Therefore there will almost always be a square-root singularity in the second derivative of S^* at $x^* = 0$, of which the strength is given by this equation. Note that the above equation does not imply that this singularity is proportional to λ as the sail shape $S^*(x^*)$ exhibits a non-linear dependency on λ. This singularity corresponds to non-smooth separation at the leading edge. However it is found that for certain discrete values of λ, i.e. certain values of α^*, the strength of the singularity given by the above equation will be zero, so there is smooth attachment at the leading edge. These values of λ are the eigenvalues of the problem, and for these values $S^{*\prime\prime}(0) = 0$.

These eigenvalues will be denoted by λ_i, with corresponding eigenfunctions $S_i^*(x^*)$, $i = 1, 2, \ldots$. The values of these eigenvalues may be found numerically. Equation 2.16 shows that any solution of the sail equation for which S^* is symmetric about $x = \frac{1}{2}$ will be an eigenfunction for the case when $\alpha^* = 0$. The eigenfunctions $S_i^*(x^*)$ corresponding to odd values of i turn out to be symmetric about $x = \frac{1}{2}$, whereas the eigenfunctions corresponding to even values of i are antisymmetric about $x = \frac{1}{2}$, i.e. $S_i^*(x^*) = (-1)^{i+1} S_i^*(1-x^*)$ for all eigenfunctions S_i^*. Thwaites obtained values for the first six eigenvalues, as shown in the table below, and these were confirmed by the numerical calculations

detailed in section 2.2.2.

	λ_1	λ_2	λ_3	λ_4	λ_5	λ_6
Eigenvalues	2.316	5.507	8.635	11.78	14.93	18.08

The solutions of the equations for other values of λ were also evaluated numerically, and another feature that becomes apparent is that the solutions are wholly concave only when $\lambda < \lambda_1$. In general for $\lambda_i < \lambda \leq \lambda_{i+1}$ the solution $y^* = S^*(x^*)$ will cross the x-axis i times between 0 and 1. Thus $S_1^*(x^*)$ is the only concave eigenfunction, and there are no concave eigenfunctions when $\alpha^* \neq 0$. Furthermore for any value of α^* there will be a solution with $\lambda \leq \lambda_1$. This puts the condition, observed by Thwaites and others, that a concave sail will only occur in the region $\lambda < \lambda_1$ into perspective, as a concave solution exists for all values of α^*. Furthermore this is the only solution for $\alpha^* > \alpha^*_{max}$, where α^*_{max} was found to be 0.971. This is consistent with the intuitive expectation that concave sails are those most commonly experienced in a steady flow.

The property of integral transforms given by section A.3 is also of relevance to this equation, although in order for it to be applied the singularity in u_{x^*} must be subtracted out. Hence it is best to consider a function u defined by

$$S^*_{x^*} = u(x^*) + 2\kappa\sqrt{\{x^*(1-x^*)\}},$$

where κ is the strength of the singularity given by equation 2.16. Note that the Hilbert transform of the derivative of $\sqrt{\{x^*(1-x^*)\}}$ may easily be evaluated by use of equation A.8. Substitution of the definition of u into equation 2.10 therefore gives

$$-\frac{1}{\pi}\fint_0^1 \frac{u_\xi}{\xi - x^*}d\xi + 2\kappa = \lambda\left(u + 2\kappa\sqrt{\{x^*(1-x^*)\}} - \alpha^*\right).$$

As u_x has no singularities, it will satisfy the requirements for equation A.10 to hold, so multiplication of both sides by u_{x^*} and integration from 0 to 1 yields

$$2\kappa(u(1)-u(0)) = \lambda\left(\frac{1}{2}u^2(1) - \frac{1}{2}u^2(0) + 2\kappa\int_0^1 u_{x^*}\sqrt{\{x^*(1-x^*)\}}\,dx^* - \alpha^*(u(1)-u(0))\right). \quad (2.17)$$

This provides a useful check on any numerical results obtained, and is particularly interesting when λ is an eigenvalue, for in this case κ is zero. From the above equation it follows that if κ is zero, either $u(0) = u(1)$ or $u(0) + u(1) = 2\alpha^*$. Recall that from the definition of u, if $\kappa = 0$ then $u = S^*_{x^*}$, and from equation 2.13 that the lift is proportional to $u(1) - u(0)$. The solutions for S^* corresponding to the odd eigenvalues are symmetric about $x^* = \frac{1}{2}$, so $u(0) = -u(1)$, so these will correspond to the case where $u(1) + u(0) = 2\alpha^* = 0$. The even eigenvalues give antisymmetric solutions so $u(1) = u(0)$ in this case. From equation 2.13 it follows that the lift is zero for any sails with non-zero angle of attack and smooth separation at the leading edge, but for sails with zero angle of attack there will be a non-zero lift.

2.2.4 The Sail Shape for Large Angles of Incidence

For small values of the tension parameter, λ, sometimes referred to as the *Weber number*, the function $S(x)$ will be of order λ and so equation 2.10 may be reduced to

$$\frac{1}{\pi}\int_0^1 \frac{S^{*\prime\prime}(\xi)}{\xi - x^*}d\xi = \lambda\alpha^* + o(\lambda^2). \tag{2.18}$$

This may be solved to give a solution for $S^{*\prime}(x)$ in the limit as $\lambda \to 0$, by the methods detailed in section A.2.3, bearing in mind that the solution must be chosen so that $S^{*\prime\prime} = 0$ at $x^* = 1$. Hence

$$S^{*\prime}(x^*) = \alpha^*\lambda\left(\frac{3\pi}{8} - \arcsin\sqrt{x^*} - \sqrt{x^*}\sqrt{1-x^*}\right), \tag{2.19}$$

and from this S^* may be found, see figure 2.4.

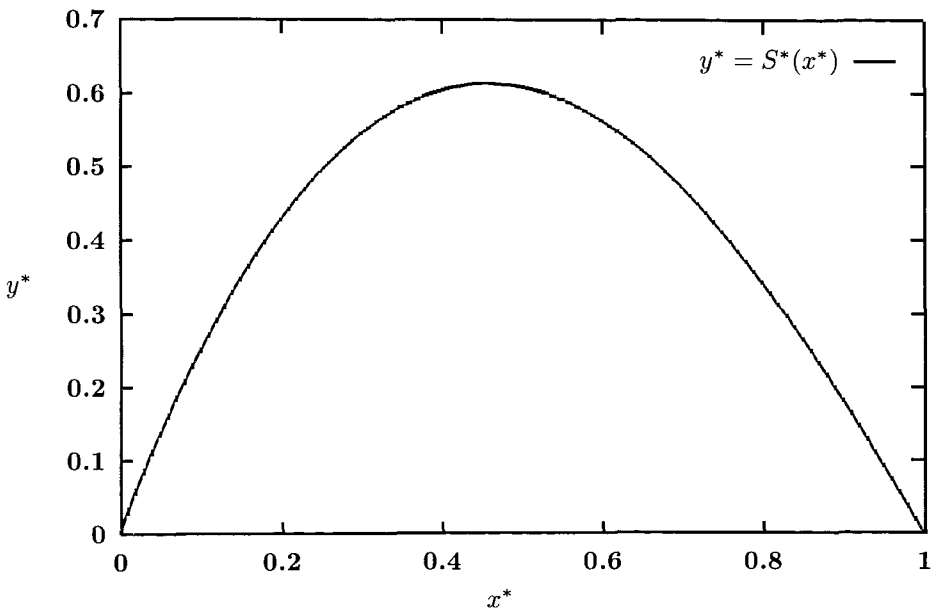

Figure 2.4: The Sail Shape Under Large Tension

Since, according to the length condition given by equation 2.11, $S^{*\prime}$ must be order 1, this gives that $\alpha^*\lambda$ must be order 1. Hence for a given sail length, this case, where the tension is high, corresponds to a high angle of incidence, or more precisely, to a high value of $\alpha\epsilon^{-\frac{1}{2}}$. The formula obtained by substituting the above expression for $S^{*\prime}$ into the length condition is

$$(\lambda\alpha^*)^2\left(\frac{3\pi^2}{64} - \frac{1}{3}\right) = 2 \tag{2.20}$$

for large values of α^*. The corresponding lift will follow from equation 2.13 to give

$$\frac{2\rho U^2 c}{\lambda}\epsilon^{\frac{1}{2}}(S^{*\prime}(0) - S^{*\prime}(1)) = \frac{\rho U^2 c}{\lambda}\pi\epsilon^{\frac{1}{2}}\sqrt{\frac{2}{\frac{3\pi^2}{64} - \frac{1}{3}}}. \tag{2.21}$$

2.3 An Unsteady Formulation of the Sail Equation

Thwaites's sail equation deals with a uniform flow at constant incidence α to a light, inextensible, porous sail. A more realistic case is when the angle, α, is a function of time. This will lead to a sail shape, $y = S(x,t)$ which will be dependent on time. This case has not previously been examined for a sail with non-zero mass. For simplicity the porosity of the sail will be taken to be zero, although it would not be particularly difficult to extend the analysis below to include the effects of porosity. The velocity potential for the flow, Φ, will be similar to that for the time independent case, i.e.

$$\Phi(x,y,t) = U(x\cos\alpha(t) + y\sin\alpha(t)) + \frac{1}{2\pi}\int_0^c \gamma(\xi,t)\arctan\left(\frac{y}{\xi - x}\right)d\xi, \tag{2.22}$$

where, as before, γ is the vortex strength at a given point on the sail, and c is the distance between the two fixed ends of the sail. As before the length of the sail is given as $c(1+\epsilon)$, thus defining the small parameter ϵ. The condition that the sail is a free boundary is

$$\frac{D}{Dt}(y - S(x,t)) = 0, \tag{2.23}$$

which reduces to

$$\frac{\Phi_y}{\Phi_x} = S_x + \frac{S_t}{\Phi_x}.$$

Substituting Φ from equation 2.22 gives

$$S_x + \frac{S_t}{U} = \alpha(t) + \frac{1}{2\pi U}\int_0^c \frac{\gamma(\xi,t)}{\xi - x}d\xi, \tag{2.24}$$

where, as in the steady case, α is assumed to be small, and terms of order α^2, i.e. ϵ, are ignored. All working is performed to order $\epsilon^{\frac{1}{2}}$, i.e. to order α.

In the steady case, γ was related to $S''(x)$ by the condition that the tension in the sail had to balance the lift given by the vortex γ, i.e. the pressure difference above and below the sail. In the unsteady case this is no longer the case since the sail is moving, so the equation becomes force = mass $\times$ acceleration. Using the notation of the steady sail, section 2.2, this equation applied to a finite element of the sail is

$$F_T + F_A = \rho'\delta s\frac{\partial^2 S}{\partial t^2}, \tag{2.25}$$

where ρ' is the mass per unit length of the sail. As before, the tension force, F_T, is given by equation 2.4. Bernoulli's equation will now include a time-dependent term, so it will be necessary to find Δp, and hence F_A, from the unsteady Bernoulli equation in the form

$$\lim_{y\to 0^+}(\Phi_t + p + \frac{1}{2}\rho q^2) = \lim_{y\to 0^-}(\Phi_t + p + \frac{1}{2}\rho q^2). \tag{2.26}$$

This may be written in the form

$$[\Phi_t]_{0^-}^{0^+} + [p]_{0^-}^{0^+} + \frac{1}{2}\rho\left[q^2\right]_{0^-}^{0^+} = 0. \tag{2.27}$$

It is easiest to consider the three terms separately. Equation 2.22 gives

$$\Phi_t = U\alpha'(t)(y\cos\alpha - x\sin\alpha) + \frac{1}{2\pi}\int_0^c \gamma_t(\xi,t)\arctan\left(\frac{y}{\xi - x}\right)d\xi. \tag{2.28}$$

The first term in this equation will be continuous over the boundary $y = 0$. The integrand in the second term will also be continuous except at $\xi = x$. However this part of the integral will not contribute to equation 2.27 since

$$\lim_{\epsilon\to 0}\int_{x-\epsilon}^{x+\epsilon} \arctan\left(\frac{y}{\xi - x}\right)d\xi = 0.$$

The pressure term in equation 2.26 will just be $[p]_{0-}^{0+}$ which is $-\Delta p$. The third term will be $\rho U\gamma(x,t)$ as evaluated in the steady case. Thus equation 2.26 becomes

$$\Delta p = \rho U\gamma(x,t).$$

This may be combined with equations 2.4, 2.5 and 2.25 to give

$$\rho' S_{tt}\delta s = T\cos\psi d\psi + \rho U\gamma\cos\psi\delta s,$$

and hence, in the limit as ψ tends to zero,

$$\rho U\gamma(x,t) + TS_{xx} = \rho' S_{tt}, \tag{2.29}$$

This gives us an expression for γ which may in turn be substituted into equation 2.24 to give the *time dependent sail equation*,

$$S_x + \frac{S_t}{U} = \alpha(t) + \frac{1}{2\pi\rho U^2}\int_0^c \frac{\rho' S_{tt}(\xi,t) - TS_{\xi\xi}(\xi,t)}{\xi - x}d\xi. \tag{2.30}$$

The boundary conditions will be the same as those of the steady case, namely $S(0,t) = S(1,t) = 0$, since the ends of the sails are fixed, and the Kutta condition $S''(1,t) = 0$. As expected, with all time derivatives set to zero, the steady sail equation, equation 2.8 is recovered.

This may also be expressed in non-dimensional co-ordinates defined similarly to those of the steady equation :

$$\begin{aligned}
x &= cx^*, \\
\xi &= c\xi^*, \\
t &= \frac{c}{U}t^*, \\
S(x,t) &= c\epsilon^{\frac{1}{2}}S^*(x^*,t^*), \\
\mu &= \frac{2\rho c}{\rho'}, \\
\beta &= \sqrt{\left(\frac{T}{\rho' U^2}\right)}, \\
\alpha(t) &= \epsilon^{\frac{1}{2}}\alpha^*(t^*).
\end{aligned}$$

In these co-ordinates equation 2.30 becomes

$$\frac{1}{\pi}\int_0^1 \frac{S^*_{t^*t^*} - \beta^2 S^*_{\xi^*\xi^*}}{\xi^* - x^*} d\xi^* = \mu(S^*_{x^*} + S^*_{t^*} - \alpha^*(t^*)), \tag{2.31}$$

with the boundary conditions $S^*(1,t^*) = S^*(0,t^*) = 0$ and $S^*_{x^*x^*}(1,t^*) = 0$. The initial conditions necessary are the values of S^* and $S^*_{t^*}$ at $t^* = 0$, say. The equation is dependent on two non-dimensional parameters, μ and β. (The parameter $\lambda = \frac{2\rho U^2 c}{T}$ in the steady sail equation is equal to $\mu\beta^{-2}$ in this notation). Of these, μ is dependent only on the initial conditions given and will clearly be constant in space and time in this model. However it is not immediately obvious that the tension, T, of the sail will be a constant over time, although it is a constant over x to first order, since shearing forces are neglected. The value of T, and hence β, must be chosen so that the solution of equation 2.31, $S(x,t)$, has constant length, as before, as given by the length condition, equation 2.11. Therefore a complete solution for $S^*(x^*,t^*)$ for a given β will not be a physical solution (i.e. a solution which conserves sail length) unless that solution satisfies equation 2.11 *for all values of* t^*. This may not be possible for constant values of β and so the tension, β, must be considered as a function of time.

The condition that the length be constant is not the only condition that could have been chosen. For an extensible sail, a linear relation between excess length and tension could have been used, for example

$$T = k\left(\frac{1}{2}\int_0^c S_x^2 dx - \ell_0\right),$$

where k is a constant, measuring the inextensibility of the sail, and ℓ_0 is the length of the sail under zero tension. In this case, the constant length condition is equivalent to having k infinitely large.

2.4 Similarity Solutions

If is often useful to find similarity solutions to partial differential equations. Power-law similarity solutions will exist for an equation in a function $S^*(x^*,t^*)$ if there exist γ and δ such that the equation is invariant under the transformation

$$(x^*, t^*, S^*) \longmapsto (kx^*, k^\gamma t^*, k^\delta S^*).$$

Consider the effect of such a transform upon the singular integral in the unsteady sail equation (equation 2.31), writing the integrand as $f(\xi,t^*)$, and denoting $(\overline{x},\overline{t},\overline{f})$ as $(kx^*,k^\gamma t^*,k^\delta f)$. The resulting expression will be

$$\int_0^1 \frac{f(\xi,t^*)}{\xi - x^*} d\xi = k^{-\delta}\int_0^{k^{-1}} \frac{\overline{f}(u,t^*)}{u - \overline{x}} du,$$

where the substitution $\xi = ku$ has been made. Immediately it may be seen that the resulting expression will not be of the same kind as the original expression as the upper limit of the range of integration has changed. Hence there can be no power-law similarity solutions to a partial integro-differential equation with a finite range of integration, although it will be seen in section 8.2 that such solutions

do exist in the slot injection problem, where the range of integration is semi-infinite. However for the unsteady sail equation it is possible that more complicated similarity solutions exist, although none have as yet been found.

2.5 An Unsteady Sail of Low Mass

The unsteady equation given above, equation 2.31, is dependent on three dimensionless parameters : α^*, the angle of incidence, β, the tension, and μ, an inverse measure of the mass of the sail. Of these the choice of β is governed by the length condition, so for a sail of a given length the shape will depend on only two parameters : α^* and μ. Consider the case where the mass of the sail is low, i.e. μ is large. Dividing the unsteady sail equation (equation 2.31) by μ gives

$$\frac{1}{\mu\pi}\int_0^1 \frac{S^*_{t^*t^*} - \beta^2 S^*_{\xi^*\xi^*}}{\xi^* - x^*} d\xi^* = S^*_{x^*} + S^*_{t^*} - \alpha^*(t^*), \tag{2.32}$$

which, assuming that β remains order 1, suggests that the right-hand side will tend to zero for large values of μ. However this is incorrect since the equation

$$S^*_{x^*} + S^*_{t^*} - \alpha^*(t^*) = 0$$

has the general solution

$$S^* = f(x^* - t^*) + \int_0^{t^*} \alpha^*(\tau) d\tau,$$

where f is an arbitrary function. Defining $A(t^*)$ such that $A_{t^*} = \alpha^*$, there will be a solution which satisfies the boundary conditions $S^*(0) = S^*(1) = 0$ if and only if

$$A(t-1) \equiv A(t),$$

which will not in general be the case. However for periodic functions A, i.e. periodic functions α^*, with period 1, it will be possible to obtain solutions which will have a finite tension. Note though that there is another condition on α^* created by the length condition, for this type of solution to exist, namely that

$$\frac{1}{2}\int_0^1 \alpha^2(t^*) dt^* = 1.$$

For example, if $\alpha^* = 2\cos 2n\pi t^*$, then the function

$$S(x^*, t^*) = \frac{1}{n\pi}\left(\sin 2n\pi(x^* - t^*) + \sin 2n\pi t^*\right) \tag{2.33}$$

will be a solution and will satisfy the length condition for all integer values of n. Functions α^* for which such solutions are possible may be thought of as eigenfunctions. Fig 2.5 shows a plot of this solution for $n = 1$, with t^* taking the values 0,0.2,0.4,0.6,0.8. The solution is periodic with period 1. Note that the attachment at the leading edge will be smooth for all t^*. Since equation 2.33 implies that $S^*_{x^*}$ will take the same value at $x^* = 0$ and $x^* = 1$ it follows that for these sail shapes the lift will be zero, from equation 2.13.

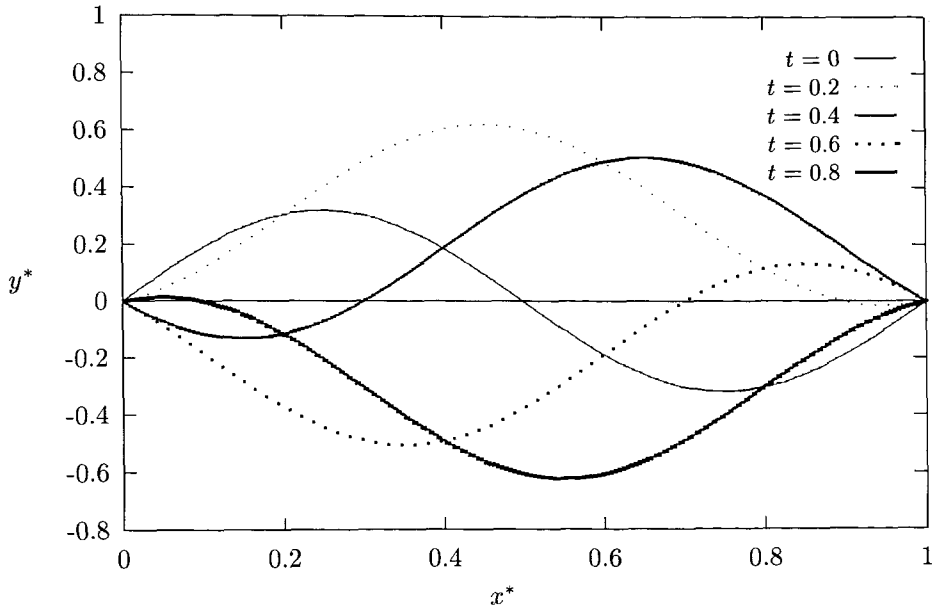

Figure 2.5: A Low Mass Sail Shape, With Order 1 Tension

For functions α^* that do not satisfy this condition, or are not periodic with period 1, a solution will not be possible with the above assumptions for large μ. This is because the assumption that β remains of order 1 is dangerously naive, particularly bearing in mind the dependence of the tension on the angle of incidence in the steady state problem (section 2.2.4). Hence in general for large values of μ it is reasonable to assume that β^2 will scale with μ so that only the $S^*_{t^*t^*}$ term will become negligible in equation 2.32 to give

$$-\frac{1}{\pi}\frac{\beta^2}{\mu}\int_0^1 \frac{S^*_{\xi^*\xi^*}}{\xi^* - x^*}d\xi^* = S^*_{x^*} + S^*_{t^*} - \alpha^*(t^*) + o(\mu^{-1}), \tag{2.34}$$

with the usual boundary conditions. Note that there is only one 'independent' non-dimensional parameter, as the parameter $\frac{\beta^2}{\mu}$ must be chosen such that the length condition is satisfied. The requirement that β^2 scales with μ is not a surprising one, since physically β^2 is a measure of the tension in the sail, and μ, being a measure of the relative densities of the sail and of air, is a measure of the relative importance of inertia to aerodynamical effects. For a sail with low mass inertia is relatively unimportant, and so only a high tension can act to balance the aerodynamical effects. Furthermore in the steady problem it is only the ratio of μ to β^2 which is important. The numerical solution of the above equation is considered in section 9.9.

The above analysis has assumed that α^* remains of order 1. For a sail of low mass with a high angle of incidence (i.e. high μ and high α^*) the α^* term dominates the right-hand side of equation 2.34, requiring that $\beta^2 = O(\mu\alpha^*)$ and giving essentially the same equation as that for the steady state solution for large α^*, namely

$$\frac{1}{\pi}\frac{\beta^2}{\mu}\int_0^1 \frac{S^*_{\xi^*\xi^*}}{\xi^* - x^*}d\xi^* = \alpha^*(t^*) + o(\mu^{-1}) + o(\alpha^{*-1}),$$

which will have the same solution as that for the steady state solution for large λ given by equation 2.19.

2.6 An Unsteady Sail of High Mass

For a sail of large mass per unit area, μ will be small. For order 1 values of α^* in the limit as $\mu \to 0$, the right-hand side of equation 2.31 will tend to zero and so the Hilbert transform of $S^*_{t^*t^*} - \beta^2 S^*_{x^*x^*}$ will be zero. This means that $S^*_{t^*t^*} - \beta^2 S^*_{x^*x^*}$ must be a constant multiple of $x^{*-\frac{1}{2}}(1-x^*)^{-\frac{1}{2}}$, and from the Kutta condition, $S_{x^*x^*} = 0$, it follows that

$$S^*_{t^*t^*} - \beta^2 S^*_{x^*x^*} = 0, \tag{2.35}$$

with the usual boundary conditions and the length condition. Note that in general it would appear that β will be order 1, since although the aerodynamic effects are now negligible, the inertia effects will be order 1, and thus the tension will be order 1 to balance this. In effect this is the wave equation with a non-constant velocity, caused by the requirement that the tension varies in such a way as to preserve length. In other words, the sail behaves like a string under non-constant tension, with the length being fixed not only on an order 1 level, but at the level defined by the perturbations of the string.

One immediate aspect of this equation is that unless β is zero there is no steady solution which satisfies both the boundary conditions and the length condition, so the sail will always be in motion for non-zero β.

To analyse this equation further, this equation may be posed in such a way as to make the coefficients of the highest derivatives constant by the introduction of a variable τ defined by $\frac{d\tau}{dt^*} = \beta$, recalling that β is a function of time. This reduces the equation to

$$S^*_{\tau\tau} + \gamma(\tau) S^*_{\tau} - S^*_{x^*x^*} = 0,$$

where $\gamma(\tau) = \frac{\beta'(t^*)}{\beta^2(t^*)}$. If $\Gamma(\tau)$ is defined by $\Gamma' = \gamma$, and $\overline{S}(x^*, \tau)$ by $\overline{S} = e^{\frac{1}{2}\Gamma} S$, then the first derivative in t^* may be eliminated to give

$$\overline{S}_{\tau\tau} - \overline{S}_{x^*x^*} + \overline{\gamma}(\tau)\overline{S} = 0,$$

where $\overline{\gamma}$ is defined by

$$\overline{\gamma} = -\frac{1}{4}\left(2\gamma'(\tau) + \gamma^2(\tau)\right).$$

Although a solution to this equation may be found for given functions $\overline{\gamma}$, using a Riemann function, for the purposes of this problem $\overline{\gamma}$ is unknown, and must be determined by the length condition. With this in mind, the fact that the boundary conditions are $S(0, t^*) = S(1, t^*) = 0$, suggests the use of separable solutions. Returning to the form suggested in equation 2.35, solutions of the form $X(x^*)T(t^*)$ must all satisfy

$$\frac{X''}{X} = \frac{1}{\beta^2}\frac{T''}{T} = \text{constant}.$$

From the boundary conditions it follows that $X(0) = X(1) = 0$ and so the constant in the above equation must be negative, giving solutions for X of the form $X_n = \sin n\pi x^*$ where n must be an integer. Since only linearly independent solutions need be considered, attention may be restricted to positive values of n. The corresponding T_n are the solutions of

$$T'' = -n^2\pi^2\beta^2 T, \tag{2.36}$$

which implies that $T_n(t^*) = T_1(nt^*)$. By multiplying both sides by $2T'$, this may be written

$$\frac{d}{dt^*}(T'^2) = -n^2\pi^2\beta^2\frac{d}{dt^*}T^2.$$

If β is now considered as a function of T, an implicit solution may be found,

$$t^* - t_0^* = \int_0^T \frac{dT_1}{\sqrt{A - 2n^2\pi^2\int_0^{T_1}\beta^2(T_2)T_2 dT_2}}, \tag{2.37}$$

where T_1 and T_2 are variables of integration and A and t_0^* are arbitrary constants. These constants may be determined by the initial values of T_n' and T_n. Without loss of generality $T_n(0)$ may be defined to be one. However since separable solutions cannot satisfy the length condition, it will be necessary to consider linear combinations of separable solutions to find an expression for the shape of the sail. For this reason the idea of considering β as a function of T is undesirable, since the above equation defines all the T_n, and β will have to take the same value for all T_n at any given time.

Any function of the form $\sum a_n X_n(x^*)T_n(t^*)$ will automatically satisfy equation 2.35 and the boundary conditions. The a_n may be determined by the initial conditions, bearing in mind that $T_n(0) = 1$, so the a_n will in fact be the coefficients of the Fourier sine series for $S(x,0)$. However to determine β the length condition must be applied, bearing in mind that the T_n depend on β according to equation 2.36. Applying the length condition, and recalling that $X_n = \sin n\pi x^*$, and that $T_n(t^*) = T_1(nt^*)$, gives

$$\begin{aligned}
\frac{1}{2}\int_0^1 S_{x^*}^2 dx^* &= 1, \\
\frac{1}{2}\int_0^1 \left(\sum_{n=1}^{\infty} a_n X_n'(x^*)T_n(t^*)\right)^2 dx^* &= 1, \\
\frac{1}{2}\int_0^1 \left(\sum_{n=1}^{\infty} n\pi a_n \cos n\pi x^* T_n(t^*)\right)^2 dx^* &= 1, \\
\frac{1}{2}\sum_{n=1}^{\infty} n^2\pi^2 a_n^2 T_1^2(nt^*) &= 1,
\end{aligned}$$

where use has been made of the usual orthogonality relations between the functions $\{\cos n\pi x^*\}$ when multiplying out the bracket to eliminate the cross-terms. This immediately shows that there will be no solution with constant β, since in this case $T_1(t^*) = \sin\beta\pi t^*$ and the series becomes a Fourier sine series, which cannot identically equal 1. (It also shows that, since X is a Fourier sine series, it must be odd). Furthermore it seems reasonable to expect that, for most choices of a_n (which depend

only on the initial conditions) there will be no possible β which will give T_1 so as to satisfy the above equation, and hence the length condition. Clearly something is wrong with the assumptions made, and again it must be that the assumption that β is order 1 that is flawed. Hence in the absence of aerodynamic forces there will not usually be a balance between the tension in the sail and inertia, and the sail will remain in steady state. This is clear for an initial value problem with zero initial time derivative, since as long as the initial value of S, $S^{(0)}(x^*)$ satisfies the length condition and the boundary conditions, it will give a solution for S for all values of t^* as long as $\beta = 0$. If the initial time derivative, $S^{(1)}(x^*)$ is non-zero, then the motion will remain linear, with $S = S^{(0)} + t^* S^{(1)}$, as long as the length condition is still satisfied, and then there will be an impulse in the tension parameter β which will either stop or reverse the motion. In section 2.8 it is shown by energy considerations that the motion will be reversed.

Naturally since the aerodynamic forces are negligible the size of α^* is no longer relevant, unless it is sufficiently large that $\alpha^*\mu$ is order 1. In this case, from equation 2.31, and using the result of equation A.8, the sail equation becomes

$$S^*_{t^*t^*} - \beta^2 S^*_{x^*x^*} = \alpha^* \mu \sqrt{\frac{1-x^*}{x^*}},$$

with the usual boundary conditions $S^* = 0$ at $x^* = 0$ and $x^* = 1$ and $S^*_{x^*x^*} = 0$ at $x^* = 1$. The tension therefore cannot be zero. This can be seen either by considering the length condition, or the behaviour near $x^* = 0$. In fact the solution will be the same as that for a large angle of incidence with an order 1 value of μ, as considered below, i.e. with the sail shape, S^*, being constant, and β^2 scaling with $\alpha^*\mu$. The reasons why this is so are discussed in the next section.

2.7 Large Angles of Incidence

Although α must be much less than one to satisfy some assumptions made in the derivation of the unsteady equations, there is no reason why α^* (defined by $\alpha\epsilon^{-\frac{1}{2}}$) should remain order 1. The behaviour for large α^* when μ is large or small has been discussed at the end of the two preceding sections. If μ is order 1 then in order for equation 2.31 to balance, β^2 must scale with α^*, and all other terms will become negligible leaving

$$\frac{1}{\pi} \int_0^1 \frac{S_{\xi^*\xi^*}}{\xi^* - x^*} d\xi^* = \mu \frac{\alpha^*}{\beta^2}. \tag{2.38}$$

Hence there will be a quasi-steady solution, which will be the same as the solution given by equation 2.19 for a high tension (or, equivalently, high angle of incidence) sail in the steady state case of section 2.2.4. Furthermore, since the solution of the above equation will scale with $\mu\alpha^*\beta^{-2}$, the length condition implies that this must be constant, and so β^2 will vary in proportion to α^*, and S^* will in fact be completely independent of time. By comparison with equation 2.20 it follows that

$$\beta^2(t^*) = \mu\alpha(t^*)\sqrt{\frac{3\pi^2}{128} - \frac{1}{6}}. \tag{2.39}$$

Physically this is because a high relative angle of incidence implies a high tension. (It also implies that the aerodynamic force on the sail is dominated by the uniform part of the flow, and not by the aerodynamic lift forces caused by the interaction of the sail with the flow). Hence the inertia of the sail becomes negligible relative to the forces on it and the equation of motion becomes a balance between the tension and the uniform part of the flow. Since there is only one sail shape which provides the right balance for this, this shape will remain constant as long as α^* is much greater than unity, even though α^* may vary with time.

2.8 The Energy Equation

In order to discuss the energy of this system it is convenient to re-write the unsteady sail equation of equation 2.31 in terms of two variables, which yields

$$S^*_{t^*t^*} - \beta^2 S^*_{x^*x^*} = \mu\gamma(x^*, t^*), \tag{2.40}$$

$$\frac{1}{\pi}\int_0^1 \frac{\gamma(\xi^*, t^*)}{\xi^* - x^*} d\xi^* = S^*_{x^*} + S^*_{t^*} - \alpha^*. \tag{2.41}$$

Since the first of these equations is essentially Newton's second law, with γ representing the aerodynamic force and the $S^*_{x^*x^*}$ term representing the force due to the tension, integration over the distance travelled in the direction of the force will give an expression for the energy of the system. Since the force is in the y direction the distance travelled against the force, for a given x^* is given by dS^* evaluated at fixed x^*, i.e. $S^*_{t^*}dt^*$. This suggests the idea of multiplying equation 2.40 by S_{t^*} and integrating over time, to give an expression for the energy at a given value of x^*. To obtain the total energy this must be integrated with respect to x^* between 0 and 1. On multiplying equation 2.40 by S_{t^*} and integrating over x^* the following result is obtained :

$$\frac{\partial}{\partial t^*}\left(\frac{1}{2}\int_0^1 {S^*_{t^*}}^2 dx^*\right) - \beta^2 \int_0^1 S^*_{t^*} S^*_{x^*x^*} dx^* = \mu \int_0^1 \gamma S^*_{t^*} dx^*.$$

Of these the first term clearly corresponds to the kinetic energy of the sail. The integral in the second term may be integrated by parts to give

$$[S_{t^*} S_{x^*}]_0^1 - \int_0^1 S^*_{x^*t^*} S_{x^*} dx^* = 0 - \frac{\partial}{\partial t^*}\left(\frac{1}{2}\int_0^1 {S^*_{x^*}}^2 dx^*\right) = 0,$$

observing that S_{t^*} is zero at both ends of the sail, and that the length condition means that the integral over $(0, 1)$ of $S^2_{x^*}$ is constant. Since this integral corresponds to the work done by the tension force on the sail is it not surprising that this will be zero if and only if the sail is inextensible, since an extensible sail could store energy. Thus the energy equation becomes a balance between the kinetic energy and the energy obtained from the aerodynamic lift. Therefore it remains to evaluate the contribution to the energy from the aerodynamic lift. It is possible to express this in terms of S^* only, but this does not provide any particular insight into the problem for order one values of μ, so for an

inextensible sail it is more convenient to write the energy equation as

$$\frac{\partial}{\partial t^*}\left(\frac{1}{2}\int_0^1 {S_{t^*}^*}^2 dx^*\right) = \mu\int_0^1 \gamma S_{t^*}^* dx^*. \tag{2.42}$$

However in the case where μ was taken to be small, in other words the high mass sail, the energy contribution from the aerodynamic force, which is proportional to μ, will also be small, and so only the kinetic energy term remains from equation 2.42, so it must be zero. Hence the kinetic energy of the sail is constant in the limit as μ tends to zero.

In the case where μ is small but $\alpha^*\mu$ is order 1, an expression for the energy may again be obtained, since in this case equation 2.41 becomes

$$\frac{1}{\pi}\int_0^1 \frac{\gamma(\xi^*, t^*)}{\xi^* - x^*} d\xi^* = -\alpha^*,$$

giving $\gamma = \alpha^*\sqrt{\frac{1-x^*}{x^*}}$ (see section A.2.3). Hence the energy equation, from equation 2.42 is

$$\frac{\partial}{\partial t^*}\left(\frac{1}{2}\int_0^1 {S_{t^*}^*}^2 dx^*\right) = \mu\alpha^*\int_0^1 S_{t^*}^*\sqrt{\frac{1-x^*}{x^*}} dx^*. \tag{2.43}$$

This shows that the sail may gain or lose kinetic energy in some cases, and in particular that if $S_{t^*}^*$ is of the same sign for all values of x^*, then the sail will gain kinetic energy if this sign is the same as that of α^*, and will lose kinetic energy if this is the opposite sign. This is the expected result, that a sail moving against the cross-flow will be doing work against the cross-flow and therefore will lose energy to it.

2.9 A Flag Flapping

A natural extension to the sail theory discussed above, is the question of the behaviour of a light inextensible membrane fixed at one end only, in effect a flag. It would appear that the only difference between a sail and a flag will be that the boundary condition that the trailing edge is fixed, $S^*(1, t^*) = 0$, will now be removed. However it should also be noted that the removal of this condition means that the sail is no longer required to deviate from the x-axis by only a small, order $\epsilon^{\frac{1}{2}}$, amount, as was the case with the sail.

The flag will be modelled, as the sail was, by a line of vortices. The scaling of the perturbation of S from the x-axis, will still be made with $c\epsilon^{\frac{1}{2}}$, where it is now assumed that $\alpha = O(\epsilon^{\frac{1}{2}})$. However since the trailing edge is free, the tension must be zero at this point. As the tension is constant, for the same reasons as in the sail problem, this implies zero tension throughout the flag. This would appear to contradict observations, however this condition only applies to a linear flag, and the ordinary flags one sees, flapping with tension in the flag, are clearly non-linear, since they deviate significantly from being a straight line. For a non-linear model of a flag, the reader is referred to Bäcker et al (1991) [2], who consider the industrial problem of artificial fibres in an airspinning process. Hence the equation for the flapping of a flag will be the unsteady sail equation, equation 2.31, with $\beta = 0$. Note that since

the flag has no preferred alignment, the initial angle of incidence of the cross-flow to the flag may be set to zero without loss of generality. Thus the flag equation is

$$\frac{1}{\pi}\int_0^1 \frac{S^*_{t^*t^*}}{\xi^* - x^*}d\xi^* = \mu(S^*_{x^*} + S^*_{t^*} - \alpha^*(t^*)), \tag{2.44}$$

with boundary conditions $S^*(0,t^*) = 0$ and $S_{x^*x^*}(1,t^*) = 0$, and initial conditions on S^* and $S^*_{t^*}$ as before, with α^* given. Since this now involves only first order derivatives in x^* these will be sufficient boundary conditions, and this gives a closed system, with the only parameter, μ, known *a priori*. Clearly the steady solution, corresponding to α and all t^*-derivatives being zero, will be $S^* = 0$, so in a steady flow the flag will merely align itself with the flow. This is not surprising as the flag has no tension, and in the unsteady case it is only the inertia of the flag that prevents it from being aligned with the flow.

The length condition, equation 2.11, which was of such importance with the sail equation, will also be replaced. This is partly because there is no 'excess' length as before, since the length of the flag is the only length in the problem. In the sail equation the non-dimensionalisation was made with respect to c, the distance between the ends of the sail. Since the distance between the ends of the flag is not known, in the flag problem the non-dimensionalisation must be made with respect to the length of the flag, which in this problem will be denoted by ℓ. This does not affect the equations derived, since to lowest order the length of the flag, or sail, and the distance between its ends, are the same. However it does appear that the length condition, equation 2.11, is violated, since in the steady case, with S being zero everywhere, the excess length is zero, but as soon as S is not zero the excess length will increase. This anomaly occurs because the distance between the ends of the flag will decrease when S deviates from zero, and so the correct dimensional expression for the length is

$$\ell = \int_0^c (1 + S_x)^2 dx,$$

where c is the x co-ordinate of the end-point of the flag. Using the same scalings as with the sail equation, this gives

$$c + \frac{1}{2}\epsilon\ell\int_0^{c/\ell} {S^*_{x^*}}^2 dx^* = \ell$$

and hence $\ell - c$ is order ϵ. The substitution $\kappa = \frac{\ell - c}{\ell}$ into the above equation gives, to lowest order,

$$\epsilon\int_0^1 {S^*_{x^*}}^2 dx^* = 2\kappa,$$

from which κ, and thus c, may be evaluated, if desired. Although in theory this shows that all the integrals in the flag equation are not from 0 to ℓ, but from 0 to c, or in the non-dimensionalised form of equation 2.44, not from 0 to 1 but from 0 to $1 - \kappa$, this does not affect the equation since to lowest order these expressions are the same. Thus there is no length condition analogous to that of the sail equation.

The absence of a length condition facilitates the stability analysis, as the problem is now linear. Furthermore, solutions may be sought of the form $S_0(x^*)e^{i\omega t^*}$. Substitution of this into the flag equation (equation 2.44) for $\alpha^* = 0$ gives the ordinary integro-differential equation

$$-\omega^2 \frac{1}{\pi} \int_0^1 \frac{S_0(\xi)}{\xi - x^*} d\xi = \mu(S_0(x^*) + i\omega S_0'(x^*)), \tag{2.45}$$

with the boundary condition $S_0(0) = 0$. This is then an eigenvalue problem for ω, with the solutions S_0 corresponding to the modes of a flapping flag in a uniform steady cross-flow.

However it is the unsteady sail equation for order 1 sail masses which is of most interest. Since no analytical solutions have been found for the steady equation, it seems likely that it will be difficult to find any for the unsteady equation, and none have as yet been found, except in the limiting cases described above. However, it is possible to solve the unsteady equation numerically, and results will be presented in chapter 3.

Chapter 3

Numerical Solution of the Unsteady Sail Equation

The unsteady sail equation is a singular partial integro-differential equation. There are few examples of such equations being solved, the most notable exception being the Benjamin-Ono equation (see section 8.3). It is hoped therefore, that solving the unsteady sail equation numerically will provide insight into the general problem of singular partial integro-differential equations, as well as being of interest in their own right.

The unsteady sail equation was derived in section 2.3, and for a sail of order 1 mass, where the scaled angle of incidence was order 1, was given by equation 2.31, namely

$$\frac{1}{\pi}\int_0^1 \frac{S_{tt} - \beta^2(t)S_{\xi\xi}}{\xi - x}d\xi = \mu(S_x + S_t - \alpha(t)), \tag{3.1}$$

with the boundary conditions $S(0,t) = S(1,t) = S_{xx}(1,t) = 0$ and the system closed, to permit evaluation of the unknown parameter $\beta(t)$, by the length condition

$$\frac{1}{2}\int_0^1 S_x^2 dx = 1. \tag{3.2}$$

Note that for the remainder of this chapter the asterisks used to denote non-dimensionalised variables have been omitted.

In principle this should be a tractable problem, since equation 3.1 may be inverted to give

$$S_{tt} - \beta^2 S_{xx} = -\frac{\mu}{\pi}\sqrt{\frac{1-x}{x}}\int_0^1 \sqrt{\frac{\xi}{1-\xi}}\frac{S_\xi + S_t}{\xi - x}d\xi + \mu\alpha\sqrt{\frac{1-x}{x}}, \tag{3.3}$$

an equation in which the singular integral transform affects only the first order derivatives, and so in the highest derivatives the equation is merely a second order hyperbolic partial differential equation. One of the purposes of this chapter is to determine what numerical problems are posed by having an integral transform. However there are two problems peculiar to this equation, or rather this system of equations in $S(x)$ and β, since β is not known *a priori*. The first of these is that, although equation 3.1 is linear in S, the presence of the $\beta^2 S_{xx}$ term means that it is not a linear system in the

two unknowns. The second problem is that it was shown in section 2.2.3 that that there is usually a square-root singularity in the second derivative of S at $x = 0$, which will affect the accuracy of the equations.

In the numerical solution to the steady problem obtained by Thwaites the non-linearity question was resolved by considering the problem when the tension parameter was known, and then obtaining from this an expression for the length of the sail. As a result of this a graph may be plotted for the length of the sail against the tension parameter, and so a complete picture of the sail may be found for any given sail length. Note that in Thwaites's formulation of the problem, the sail length plays a similar role to that of the angle of attack in the formulation given here, as a result of the non-dimensionalisation used by Thwaites (see section 2.2). However this method is inappropriate for the unsteady problem, since the tension parameter is now a function of time, and it is not realistic to solve the linear equation for all possible functions of time. Furthermore it is not possible to superimpose solutions for different tension parameters, as such solutions would not satisfy the non-linear length condition. For the steady problem, the singularity was dealt with by Thwaites by making the substitution $2x = 1 - \cos\theta$ and then solving for S as a function of θ. However this has does not resolve the problem of how to deal with the term outside the integral in equation 3.3, as any errors in the Hilbert transform will be multiplied by a factor of $x^{-\frac{1}{2}}$. This problem, and that of evaluating a principal value integral at all, may be overcome in the steady case by integrating equation 3.3 with respect to x, in which case (with all time derivatives equal to zero) all that remains is an ordinary integral equation with a kernel which has a logarithmic singularity, and which exhibits no singularity at $x = 0$, see section 2.2.2. However when considering the unsteady problem the S_{tt} term prevents this method from being used.

For these reasons the method used by Thwaites for numerical solution of the equation, in particular the substitution $2x = 1 - \cos\theta$, will not be used, and other methods are necessary to deal with the non-linearity and the singularity at zero.

Another method used for solving the steady sail equation is that of of Nielsen (1963) [63], who used a Fourier sine series. Similar methods include those of Chambers (1966) [15], who used a variational method based on Nielsen's method, and that of Tuck (1972) [97], who used a Fourier sine series method to solve the equation in the case where the sail has a rigid attachment. Another method particularly appropriate to the solution of singular integro-differential equations with a Cauchy kernel is the use of Chebychev polynomials, which have been used, for example by Frankel (1995) [39].

3.1 Finite Difference Schemes

It is easiest to think of the system of equations 3.1 and 3.2 (or, equivalently, 3.3 and 3.2) as being one singular partial integro-differential equation, equation 3.1, with a parameter, β, which is implicitly given by equation 3.2. Unfortunately, since β is a function of time, it will need to be determined

separately at each time step. Since there is no explicit formula for β it can only be found by a 'trial and error' method. In particular, Newton's method suggests itself for β. This may be applied by defining a variable ℓ, by

$$\ell = \frac{1}{2}\int_0^1 S_x^2 dx - 1. \tag{3.4}$$

Thus a solution is sought for β such that the S obtained from the solution of equation 3.1 satisfies $\ell = 0$. Hence at a given time, ℓ will depend on the choice of β and may be written as $\ell(\beta)$. Thus at each time step the problem is reduced to the solution of $\ell(\beta) = 0$, which may be solved by Newton's method, the iterative scheme being

$$\beta_{i+1} = \beta_i - \frac{\ell(\beta)}{\ell'(\beta)},$$

with β_i denoting the ith estimate of β at each time step. Unfortunately $\ell'(\beta)$ must be calculated numerically. Furthermore there is no reason for $\ell(\beta) = 0$ to have a unique solution at a given time, although this does prove to be the case in the examples discussed below. For the moment it may be assumed that β may be found by this method, in which case the question arises of finding a stable scheme for equation 3.1.

Since only highest derivatives are important in determining the stability of an equation, to find a stable difference scheme it is only necessary to examine the left-hand side of equation 3.1, or equivalently, equation 3.3, which just gives a variable speed wave equation. The fact that β varies does not contribute to any particular difficulty towards finding a stable difference scheme since, by a re-scaling defined by $\frac{d\tau}{dt} = \beta$, the highest derivatives of the equation give

$$\beta^2 S_{\tau\tau} + \beta\beta' S_\tau = \beta^2 S_{xx}$$

which, ignoring first order derivatives, is just the wave equation.

3.1.1 An Implicit Second Order Scheme

Two obvious finite difference schemes therefore present themselves to the solution of equation 3.3 with the appropriate boundary conditions, namely $S = 0$ at $x = 0$ and $x = 1$. The first of these is a direct second order scheme in terms of S, with S_i^j denoting the value of S at position ξ_i and time t_j. However the equation may also be written as a system of two first order equations in two variables, for example in terms of $u = S_x$ and $v = S_t$. (In this case one of the equations would be $u_t = v_x$). Firstly though, the second order equation will be discussed.

As with the slot injection problem, there are various methods of evaluating the singular integral on the right-hand side of equation 3.3. In the context of the slot injection problem, a further discussion of some of the methods available may be found in section 9.2. Here, the approximation will be made by taking the function to be transformed, h, to be constant over each mesh region, and evaluating the

transform at the centre of each mesh interval, $(\xi_i + \xi_{i+1})/2$. Hence

$$\int_0^1 \frac{h(\xi)}{\xi - x} d\xi \approx \sum_{k=0}^{n-1} h(\xi_k) \int_{\xi_k}^{\xi_{k+1}} \frac{d\xi}{\xi - x} = \sum_{k=0}^{n-1} h(\xi_k) \log \left| \frac{\xi_{k+1} - x}{\xi_k - x} \right|,$$

where $\{\xi_k\}$ is some mesh covering the region $[0, 1]$ with n points. The mesh used will be linear, with $\xi_i = i/n$, S_i^j denoting $S(x_i, t_j)$, and δx being the difference between mesh points. The expressions used to evaluate S_x and S_t at each mesh point will be given by central differences. Hence the following approximations will be made

$$\frac{1}{\pi}\sqrt{\frac{1-x}{x}} \int_0^1 \sqrt{\frac{\xi}{1-\xi}} \frac{S_\xi(\xi, t)}{\xi - x} d\xi \approx \sum_{k=0}^{n-1} R_{ik} S_k^j, \tag{3.5}$$

$$\frac{1}{\pi}\sqrt{\frac{1-x}{x}} \int_0^1 \sqrt{\frac{\xi}{1-\xi}} \frac{v(\xi, t)}{\xi - x} d\xi \approx \sum_{k=0}^{n-1} Q_{ik} v_k^j, \tag{3.6}$$

with v denoting S_t. The arrays Q_{ik} and R_{ik} are given by

$$Q_{ik} = \frac{1}{\pi}\sqrt{\frac{1-\xi_{i+\frac{1}{2}}}{\xi_{i+\frac{1}{2}}}} \sqrt{\frac{\xi_k}{1-\xi_k}} \log \left| \frac{2(k-i)+1}{2(k-i)-1} \right|, \tag{3.7}$$

$$R_{ik} = \frac{1}{2\pi}\sqrt{\frac{1-\xi_{i+\frac{1}{2}}}{\xi_{i+\frac{1}{2}}}} \left(\sqrt{\frac{\xi_{k-1}}{1-\xi_{k-1}}} \log \left| \frac{2(k-i)-1}{2(k-i)-3} \right| - \sqrt{\frac{\xi_{k+1}}{1-\xi_{k+1}}} \log \left| \frac{2(k-i)+3}{2(k-i)+1} \right| \right). \tag{3.8}$$

Using a central difference approximator for the second derivatives, S_{tt} and S_{xx}, and a central difference approximator for S_t, the following discretisation of equation 3.3 is obtained.

$$\begin{aligned} \frac{S_i^{j+1} - 2S_i^j + S_i^{j-1}}{\delta t^2} &= \beta^2 \frac{S_{i+1}^j + S_{i-1}^j - 2S_i^j}{\delta x^2} + \mu \alpha_j \sqrt{\frac{1-\xi_i}{\xi_i}} \\ &\quad - \mu Q_{ik} \left(\frac{S_k^{j+1} - S_k^{j-1}}{2\delta t} \right) - \mu R_{ik} S_k^j, \end{aligned} \tag{3.9}$$

where α_j denotes $\alpha(t_j)$. Note that this scheme is implicit, due to the S_k^{j+1} terms on the right-hand side. When applying von Neumann stability analysis to a scheme of this kind, all the terms except those corresponding to second order derivatives, i.e. the first term on each side, may be ignored. For justification of this, and further discussion of von Neumann analysis, see section 8.6 However it is also necessary to consider a perturbation in β. Hence, with the usual perturbation, $(S, \beta) \mapsto (S + Ae^{i(k\delta x - \omega\delta t)}, \beta + Be^{-i\omega\delta t})$, the expression obtained is

$$e^{i\omega\delta t} + e^{-i\omega\delta t} - 2 = \frac{\beta^2 \delta t^2}{\delta x^2}(2\cos k\delta x - 2) + 2\frac{Be^{-ik\delta x}}{A} \beta S_{xx} \delta t^2.$$

Since the last term will be order δt^2, it will be negligible compared to the other terms, so as expected the fact that β will vary with time will not *per se* affect the stability of any numerical scheme. Defining z to be $e^{-i\omega\delta t}$, the above equation is a quadratic in z of the form

$$z^2 - 2bz + 1 = 0,$$

where

$$b = 1 - 2\frac{\beta^2 \delta t^2}{\delta x^2} \sin^2 \frac{k\delta x}{2}.$$

Since the z^0 term in the quadratic equation is 1, the product of the roots will be one. If the roots are real and distinct then there will clearly be a root with $|z| > 1$, and the scheme will be numerically unstable. If there is a repeated root, or complex roots, then they will both satisfy $|z| = 1$ and so instabilities will neither grow nor decay, and the scheme will be numerically stable. Thus the scheme will be stable if and only if $b^2 < 1$, which will only be true for all values of k if and only if

$$c = \left| \frac{\beta \delta t}{\delta x} \right| < 1, \tag{3.10}$$

which defines the Courant number, c.

The boundary conditions using this method are simply that S_0^j and S_n^j are zero for all values of j.

3.1.2 An Explicit Scheme

Although the previous scheme is stable, it is also worth examining a scheme suggested by re-writing equation 3.3 as a system of two equations in two variables, to see if an explicit scheme may be obtained. There are various methods in which two variables may be defined to make this a system in two first order variables, one of which is given by defining $u = S_x$ and $v = S_t$. With these definitions the following system is obtained from equation 3.3.

$$v_t - \beta^2 u_x = -\frac{\mu}{\pi}\sqrt{\frac{1-x}{x}} \int_0^1 \sqrt{\frac{\xi}{1-\xi}} \frac{u+v}{(\xi - x)} d\xi + \mu\alpha\sqrt{\frac{1-x}{x}}, \tag{3.11}$$

$$u_t - v_x = 0. \tag{3.12}$$

The boundary conditions are now $v = 0$ at both ends of the sail, which will be sufficient. Moreover it is known that the integral of u over the whole region $(0, 1)$ is zero, and that u_x is zero at $x = 1$.

To ensure stability, a Lax-Friedrichs type of scheme will be applied (see section 9.3.1 for further details), with central differences, to give the following explicit scheme :

$$v_i^{j+1} = \frac{v_{i+1}^j + v_{i-1}^j}{2} + \frac{\beta^2 \delta t}{\delta x} \frac{u_{i+1}^j - u_{i-1}^j}{2} + \mu\alpha_j \delta t \left(\sqrt{\frac{1-\xi_i}{\xi_i}} - \mu Q_{ik} u_k^j - \mu Q_{ik} v_k^j \right), \tag{3.13}$$

$$u_i^{j+1} = \frac{u_{i+1}^j + u_{i-1}^j}{2} + \frac{\delta t}{\delta x} \frac{v_{i+1}^j - v_{i-1}^j}{2}. \tag{3.14}$$

For the purposes of stability analysis, the last term in the first equation may be ignored, as it does not contain any derivatives. On application to the scheme of a perturbation of a Fourier mode, with the perturbation to u being given by $Aze^{ik\delta x}$ and the perturbation to v being $Bze^{ik\delta x}$, where $z = e^{-i\omega\delta t}$, the following expressions are obtained :

$$Bz = B\cos k\delta x + A\frac{\beta^2 \delta t}{\delta x} i \sin k\delta x,$$

$$Az = A\cos k\delta x + B\frac{\delta t}{\delta x} i \sin k\delta x,$$

which will only have a non-trivial solution if

$$(z - \cos k\delta x)^2 = -\left(\frac{\beta\delta t}{\delta x}\right)^2 \sin^2 k\delta x,$$

hence

$$z = \cos k\delta x \pm \frac{\beta\delta t}{\delta x} i \sin k\delta x.$$

Therefore a necessary and sufficient condition for z to lie within or on the unit circle, and thus for the scheme to be stable, is the same condition as before, that the Courant number, c, defined by equation 3.10 is less than one.

Since this scheme is explicit it will naturally require fewer computations at each time step, so this method will be used for the calculations below. One slight disadvantage is that, since at each time step, the updated value of u, from equation 3.14, is independent of β, some care is needed to apply the length condition, equation 3.2. An expression using v is required, and this may be obtained by differentiating equation 3.2 with respect to time, to give the condition on β that v be chosen such that

$$\int_0^1 uv_x dx = 0$$

.

3.2 Initial and Boundary Conditions

With the second order central difference scheme given by equation 3.9, the boundary conditions $S(0) = 0$ and $S(1) = 0$ may simply be applied as $S_0^j = 0$ and $S_n^j = 0$ for all j. For the initial value problem S_i^0 and S_i^{-1} must also be given for all i. For the explicit scheme given by equations 3.13 and 3.14, the same boundary conditions must be applied by imposing v=0 at both ends (recalling that $v = S_t$). Hence v_0^j and v_n^j are zero for all values of j. The initial values of u may be found from the numerical solution of the steady problem detailed in section 2.2.2, with initial values of $v = 0$ used everywhere.

The values of u at the ends of the sail may simply be given by applying the second equation of the system, equation 3.12, namely $u_t = v_x$, at each end. However since central differences are used in the scheme for derivatives with respect to x (see equations 3.13 and 3.14), and there is no central difference approximator for $x-$derivatives at the ends, it is best to apply this equation at the centre of the interval between the end-point and the next mesh point. These points will be denoted by $x = \xi_{\frac{1}{2}}$ and $x = \xi_{n-\frac{1}{2}}$, with $\xi_{\frac{1}{2}}$ lying at the mid-point of ξ_0 and ξ_1, and $\xi_{n-\frac{1}{2}}$ lying at the mid-point of ξ_{n-1} and ξ_n. Central difference approximators may then be used for the values of the $x-$derivative at these points. Thus the following approximations are made

$$u_t|_{x=\xi_{\frac{1}{2}}, t=t_j} = \frac{1}{2}\left(\frac{u_0^{j+1} - u_0^j}{\delta t} + \frac{u_1^{j+1} - u_1^j}{\delta t}\right),$$

$$
\begin{aligned}
v_x|_{x=\xi_{\frac{1}{2}},t=t_j} &= \frac{v_1^j - v_0^j}{\delta x}, \\
u_t|_{x=\xi_{n-\frac{1}{2}},t=t_j} &= \frac{1}{2}\left(\frac{u_{n-1}^{j+1} - u_{n-1}^j}{\delta t} + \frac{u_n^{j+1} - u_n^j}{\delta t}\right), \\
v_x|_{x=\xi_{n-\frac{1}{2}},t=t_j} &= \frac{v_n^j - v_{n-1}^j}{\delta x},
\end{aligned}
$$

with, as elsewhere, forward differences used for derivatives with respect to time. Since all the v_0^j and v_n^j will be zero for all j, this gives the boundary conditions for the scheme given by equations 3.13 and 3.14 as

$$
\begin{aligned}
u_0^{j+1} &= u_0^j - (u_1^{j+1} - u_1^j) + 2\frac{\delta t}{\delta x}(v_1^j - v_0^j) \\
v_0^{j+1} &= 0 \\
u_n^{j+1} &= u_n^j - (u_{n-1}^{j+1} - u_{n-1}^j) + 2\frac{\delta t}{\delta x}(v_n^j - v_{n-1}^j) \\
v_n^{j+1} &= 0
\end{aligned}
$$

An alternative boundary condition for u would be to impose that $\int_0^1 u dx$ is zero, which is certainly true. However by not imposing this condition, since it is not implicit in the scheme, a useful check on the validity of the equations is obtained.

3.3 Convergence of the Schemes

For a function which is differentiable an infinite number of times, the approximations

$$
u_x(x_i, t_j) \approx \frac{u_{i+1}^j - u_{i-1}^j}{2\delta x} \qquad S_{xx}(x_i, t_j) \approx \frac{S_{i+1}^j + S_{i-1}^j - 2S_i^j}{\delta x^2}
$$

made in the previous section will be accurate to within order $u_{xx}\delta x$ and $S_{xxx}\delta x$ respectively. However in the case of the sail equation, it was shown in section 2.2.3, that S_{xx}, and thus u_x, will almost always exhibit a square-root singularity at $x = 0$. This reduces the accuracy of the above schemes from within an order of magnitude δx to within an order of magnitude of $\delta x^{\frac{1}{2}}$. This is a significant difference, and so it makes sense to subtract out the singularity. One way in which this may be achieved is to define $\overline{u} = u - \kappa x^{\frac{1}{2}}$, with κ chosen such that there is no singularity in $\overline{u}$ at $x = 0$. With such a choice of κ the error in the estimation of $\overline{u}_{xx}$ will now be of order δx.

However this will not in itself increase the accuracy of the overall scheme, since the accuracy of the evaluation of the Hilbert transform given by equation 3.6 (the same equation applies for evaluation of the integral involving u as for that involving v) has not yet been discussed in detail. In principle this should be accurate to within order δx, since the only approximation made was that the coefficient of the Cauchy kernel, $u\sqrt{\frac{x}{1-x}}$ should be constant over each interval. This is clearly going to be a poor approximation near $x = 1$, and so an improvement in the method for the Hilbert transform in this

model may be made by observing that since a substitution $z = \sqrt{\frac{x}{1-x}}$ gives

$$\frac{1}{\pi}\sqrt{\frac{1-x}{x}}\int\sqrt{\frac{\xi}{1-\xi}}\frac{d\xi}{(\xi-x)} = \frac{2}{\pi}\sqrt{\frac{1-x}{x}}\arcsin\sqrt{\xi} + \frac{1}{\pi}\log\left|\frac{\sqrt{\frac{\xi}{1-\xi}}-\sqrt{\frac{x}{1-x}}}{\sqrt{\frac{\xi}{1-\xi}}+\sqrt{\frac{x}{1-x}}}\right| = I(\xi,x),$$

thus defining $I(\xi,x)$, then it follows that

$$\frac{1}{\pi}\sqrt{\frac{1-x}{x}}\int_0^1\sqrt{\frac{\xi}{1-\xi}}\frac{u(\xi)}{(\xi-x)}d\xi \approx \sum_{k=0}^{n-1}\left(I(\xi_{k+1},x)-I(\xi_k,x)\right)u_k.$$

This suggests replacing the expression for Q_{ik} given by equation 3.7 with

$$Q_{ik} = I(\xi_{k+1},x_i) - I(\xi_k,x_i).$$

Although this solves the problem of the square-root singularity in the integrand at $\xi = 1$, the accuracy will only be to within order $(\delta x \log \delta x)$ as before, as the magnitude of the terms near $i = k$ (i.e. $\xi = x$) will be of order of magnitude $\delta x \log \delta x$. This does not affect accuracy much, as $\log \delta x$ tends to infinity so slowly. However the problem of the square-root singularity outside the integrand at $x = 0$ remains, as $I(\xi,x)$ will be asymptotically equal to $x^{-\frac{1}{2}}$ for small x. It is difficult to see how this problem may be resolved for small x, as it is not possible to integrate this singularity out in the unsteady equation. Hence it will be necessary to proceed with an error of order $\delta x^{\frac{1}{2}}$.

3.4 Results

The acceptance of an order $\delta x^{\frac{1}{2}}$ (i.e. $n^{-\frac{1}{2}}$) error in the numerical scheme is a serious problem. Although a significant amount of computational time is saved by using the explicit, rather than the implicit, scheme, the evaluation of the Hilbert transform, by whatever method, must take $O(n)$ calculations for each mesh point, and hence $O(n^2)$ calculations altogether. The condition that the Courant number (see equation 3.10) be less than one requires that $\delta t = O(\delta x)$, so that $\delta t = O(1/n)$, and so it will necessarily require $O(n)$ steps to reach a given time. Thus the number of computations to arrive at a solution for $t = t_1$, say, is $O(n^3 t_1)$. This will give an accuracy of $O(t_1 n^{-\frac{1}{2}})$. Hence to obtain a solution for t up to 5 to accuracy 0.01 would require $n \sim 2.5 \times 10^5$, and hence order 7.8×10^{16} calculations. Clearly some compromises will need to be made. In the computations described below, n was taken to be 1000, giving a reasonable accuracy of order $0.03t_1$. Unless otherwise stated, $\mu = 1$.

Several independent checks are available to test the validity of these results. Firstly the sail shape, S, may also be evaluated by integrating u with respect to x, and compared with the value obtained by integrating v. Secondly, from these values of S, it should be the case that $S = 0$ at $x = 1$. Thirdly, the length obtained for the sail shape may be compared over time : it should remain constant. Analysis of the errors in these checks indicate that the error at time t_1 is roughly $t_1 10^{-\frac{3}{2}}$, so the solutions for t_1 greater than about 3 must be treated with some caution. For clarity the sail shapes presented below

have been re-scaled, with $S(1)$ set to zero, by rescaling $S \mapsto \ell^{-1}(S - xS(1,t))$, where ℓ is chosen so that the length condition is satisfied. The values of $S(1,t)$ and $1-\ell$ were within the errors expected from the above discussion. The time taken for the computations up to time t_1 was typically around

$$50\mu^{\frac{1}{2}}\left(\frac{n}{1000}\right)^3 t_1$$

minutes.

Henceforth, the term 'concave' will be used to describe a sail in which the curvature is of the same sign throughout, which is equivalent to having S the same sign throughout. Concave sails will be described as 'positive' or 'negative' according to whether they lie above or below the positive $x-$axis.

3.4.1 Change of Sign of Camber

From equation 3.1, the obvious result that if (S,β) is a solution for a given α, then $(-S,\beta)$ is a solution for $-\alpha$ follows, as it does from the steady equation, equation 2.10. Considering only concave sails, one question of interest is the behaviour of the sail when the sail changes from a negative solution to a positive one. One example of a possible choice of $\alpha(t)$ for this would be to have an initial condition of $\alpha = 0$, with a negative sail (recalling that for $\alpha = 0$ both positive and negative concave sails are possible), and then to increase the value of α linearly to one. This choice of α will be denoted by $\alpha_1(t)$. Hence

$$\alpha_1(t) = \begin{cases} 0 & t < 0, \\ t & 0 < t < 1, \\ 1 & t > 1, \end{cases}$$

It would be expected in this case that the sail shape will change from a negative one to a positive one. Calculations were performed according to the scheme described above, with the sail shapes determined by integrating v, i.e. S_t with respect to time. For t taking integer values from zero to four the sail shapes obtained are shown in figure 3.1.

The sail shapes indicate the change, as expected, from a sail with negative camber to one with positive camber, although the similarity between the sail shapes for $t = 0$ and $t = 1$ suggest that the change is very slow at first. The final sail shape is similar to the steady state solution for $\alpha = 1$. In fact, virtually all concave steady sail shapes are very similar. This means that in order to analyse whether the sail has reached its 'final' position, it is important to examine the values of v, i.e. S_t, or more conveniently, the kinetic energy, given by $\frac{1}{2}\int_0^1 v^2 dx$. Figure 3.2 shows the values of the tension parameter, β, and the kinetic energy, plotted against time for t up to 5.

The sudden fall in the kinetic energy appears to indicate that the sail will approach the steady shape for $\alpha = 1$. However from the numerical solution of the steady sail in section 2.2.2, it is known that the steady shape for $\alpha = 1$ has a tension parameter of $\beta = 0.8089$, so at $t = 5$ there is clearly some way to go, and so the sail shape will remain in some kind of oscillatory behaviour until all the kinetic energy is dissipated.

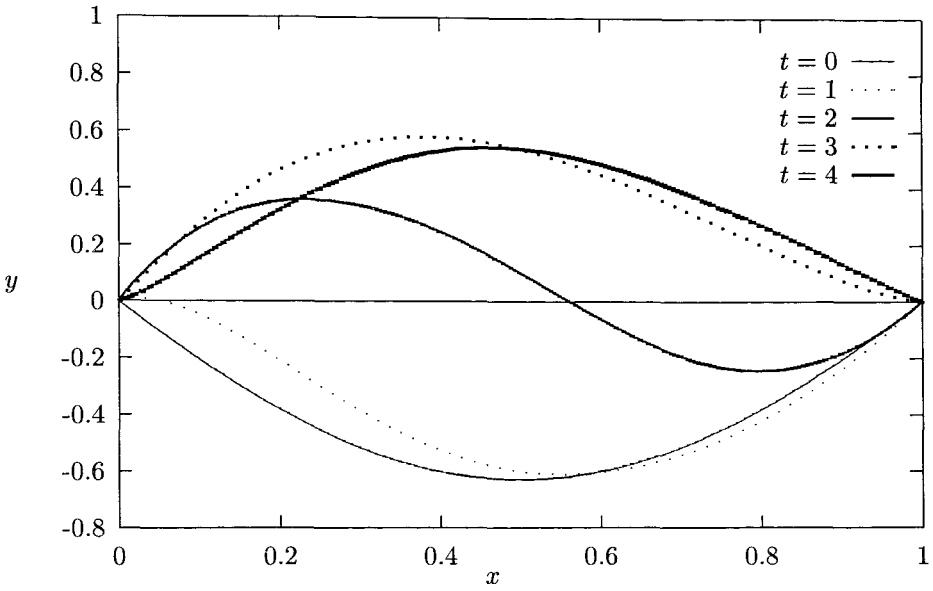

Figure 3.1: The Sail Shape for $\alpha = \alpha_1(t)$

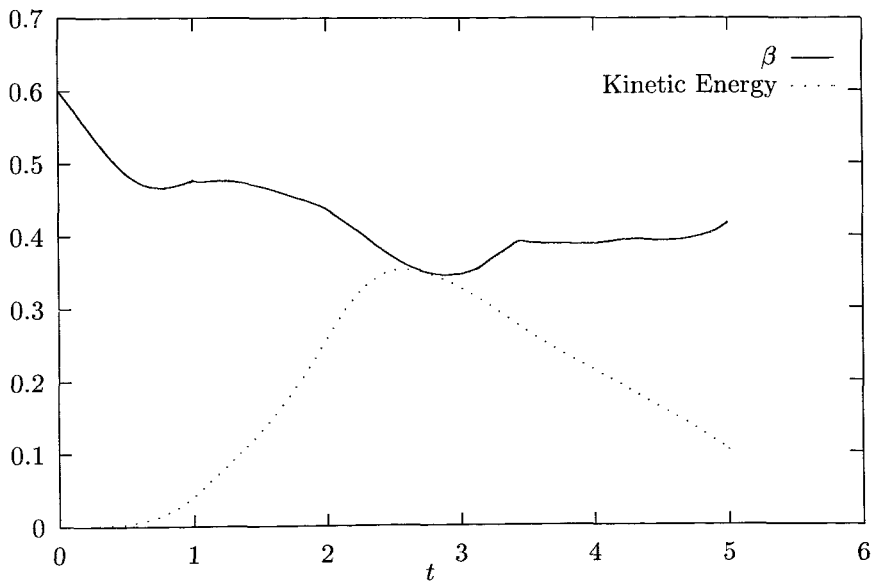

Figure 3.2: The Tension and Kinetic Energy of the Sail for $\alpha = \alpha_1(t)$

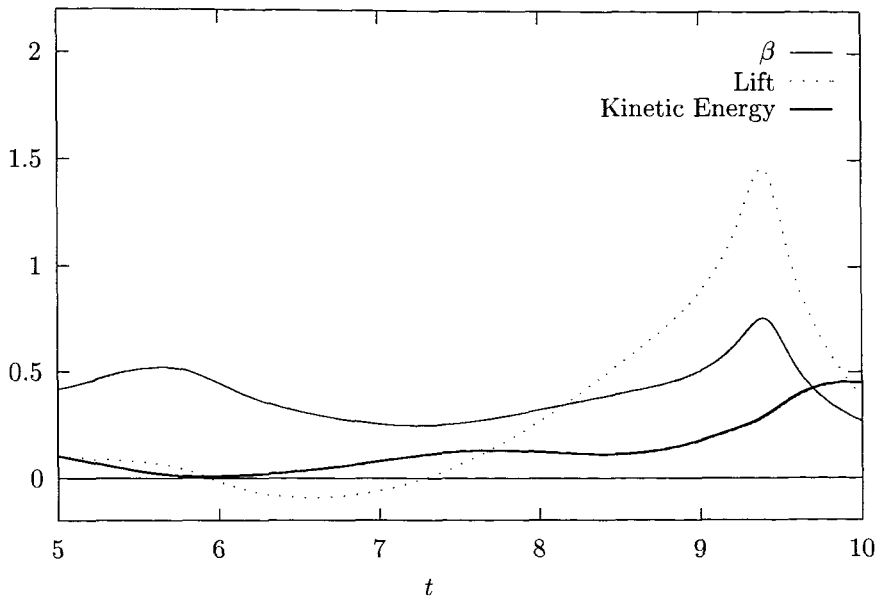

Figure 3.3: The tension parameter, β, lift, and kinetic energy of the sail for t between 5 and 10, $\alpha = \alpha_1(t)$.

Although the computational errors become significant for t much larger than 5, it is still instructive to examine the numerical solutions obtained, and these are shown in figure 3.3. These indicate that, from the fact that the lift becomes significantly positive, the shape found near $t = 9$ is close to that for the steady solution with positive camber. However the sail still possesses some kinetic energy at this stage, which may take some time to dissipate.

3.4.2 Changes to First Eigenvalue Solution

For the steady problem, when the angle of attack, α, is zero, there are two different solutions for each eigenvalue, differing only in sign. It would seem likely, therefore, that a perturbation to α could enable the sail to switch from one solution to the other, even if α then returns to zero. An example of a possible choice of α for which this could be attempted would be α increasing linearly from zero to one with $\alpha(t) = t$, and then decreasing linearly from one to zero, with $\alpha(t) = 2 - t$, then remaining thereafter at $\alpha = 0$. For this reason experiments will be attempted with $\alpha(t) = \alpha_2(t)$, where

$$\alpha_2(t) = \begin{cases} t & 0 < t < 1, \\ 2 - t & 1 < t < 2, \\ 0 & t < 0, t > 2. \end{cases}$$

Thus if the sail starts from the negative steady solution (i.e. that for which S is negative for all x), it would seem likely that it will change sign. With this choice of α the sail shapes obtained for t taking integer values from 0 to 10 are shown in figure 3.4

This suggests strong oscillatory behaviour, with the sail varying between positive and negative solutions. For t much larger than 10, the inaccuracies become too large for meaningful results to be obtained. The tension, lift and kinetic energy are plotted against time in figure 3.5.

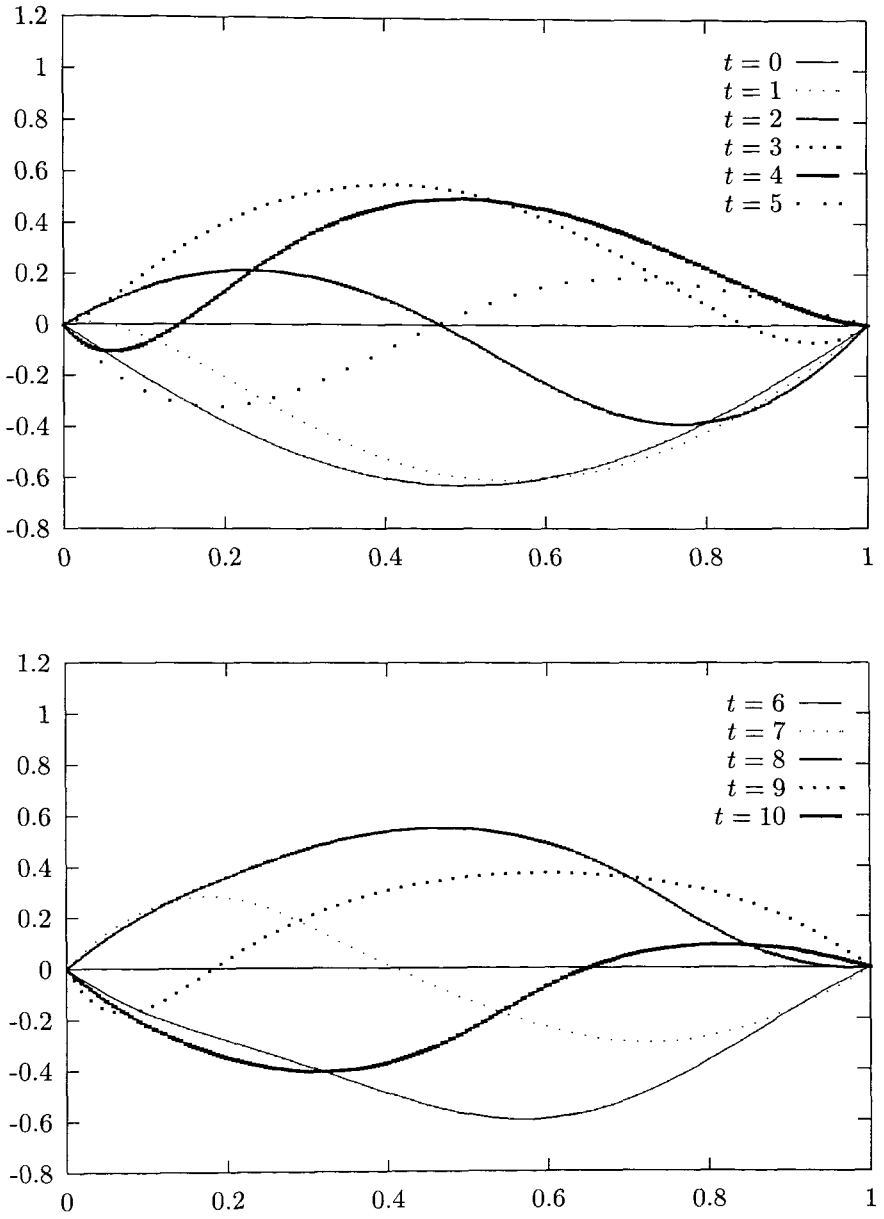

Figure 3.4: Sail Shapes for t From 0 to 10, for $\alpha = \alpha_2(t)$

These confirm the oscillatory behaviour. The fact that the peaks of the kinetic energy occur at roughly the same values appear to suggest that the motion is not damped. However this is not clear, and a more thorough stability analysis is needed to determine this. The question of stability will be addressed in a forthcoming paper.

Intuitively, it would seem that a smaller sail mass would result in faster changes to the sail shape. Thus, in the above example, the sail could change sign before the angle has been reduced to zero, and thus the desired change from a negative to a positive solution could occur. The above calculations

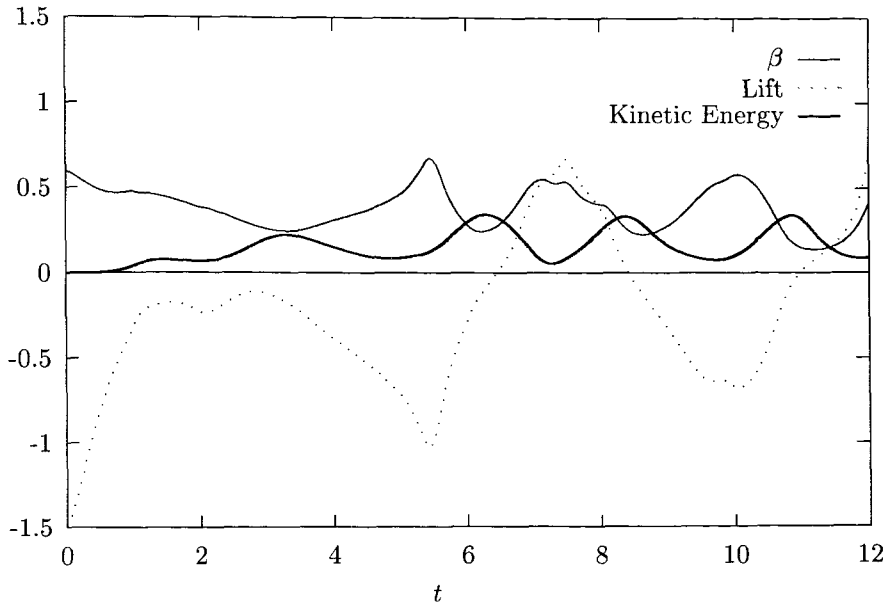

Figure 3.5: Tension, Lift and Kinetic Energy for $\alpha = \alpha_2(t)$

were therefore repeated, with $\mu = 5$, recalling that a low mass sail corresponds to a high value of μ. Unfortunately, increasing μ increases β (in the steady case β^2 is proportional to μ), and from equation 3.13 it follows that errors are proportional to β^2, so the accuracy of the scheme will decrease in this case. However the results produced indicate that the effect of changing the mass of the sail is not merely to increase the rate at which the shape changes, although this would appear to be the initial effect.

Figure 3.6 shows the sail shapes for t from 0 to 3, and although the sail initially moves towards a positive steady solution, it appears to move back. This is confirmed by figure 3.7, which shows the tension, lift and kinetic energy. This shows some sort of oscillatory behaviour, but it is not clear whether the sail will settle for the positive or negative steady solution, or oscillate indefinitely. One would expect oscillations to decay more quickly for high μ, from equation 2.42, but it is not clear here that this is the case. After t becomes approximately 0.35 numerical inaccuracies become significantly large, so it is not possible to find meaningful solutions for $n = 1000$.

Alternatively, with $\mu = 1$, α could be chosen so that it remains at $\alpha = 1$ for a non-zero length of time. The α chosen for this case is given by

$$\alpha_3(t) = \begin{cases} 0 & t \leq 0, \\ t & 0 \leq t \leq 1, \\ 1 & 1 \leq t \leq 2, \\ 3-t & 2 \leq t \leq 3, \\ 0 & t > 3. \end{cases}$$

For this example, the tension, lift, and kinetic energy are depicted in figure 3.8.

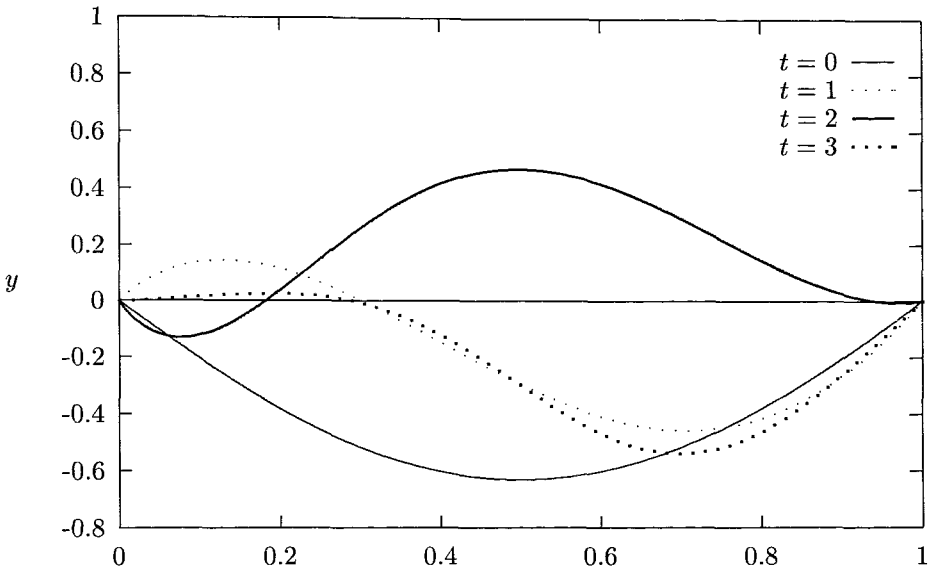

Figure 3.6: Sail Shapes for $\mu = 5$, $\alpha = \alpha_2(t)$

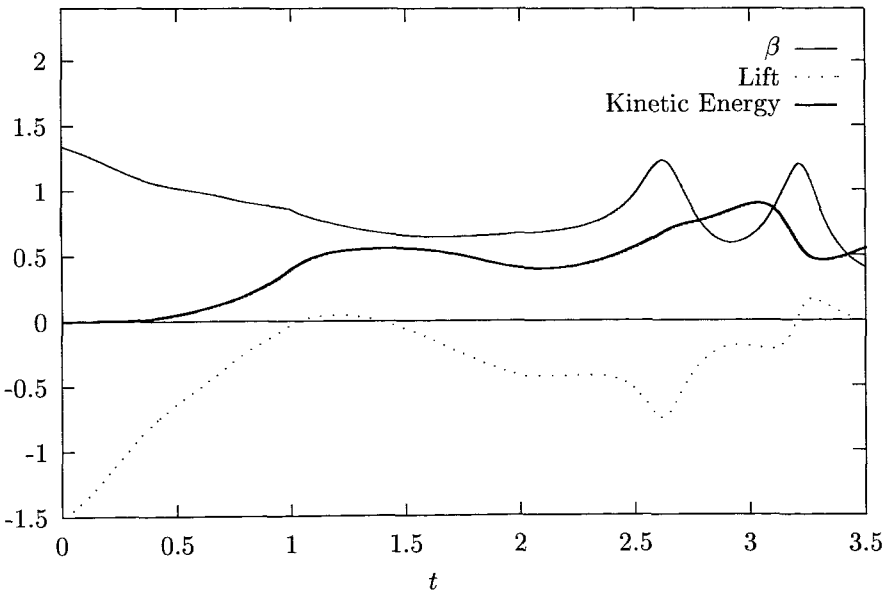

Figure 3.7: The tension, lift, and kinetic energy of the sail when $\mu = 5$, $\alpha = \alpha_2(t)$

Contrary to expectations, the solution does not appear to settle at the positive $\alpha = 0$ solution, but seems to oscillate somewhere between positive and negative solutions. This impression is confirmed by the sail shapes, depicted in figure 3.9.

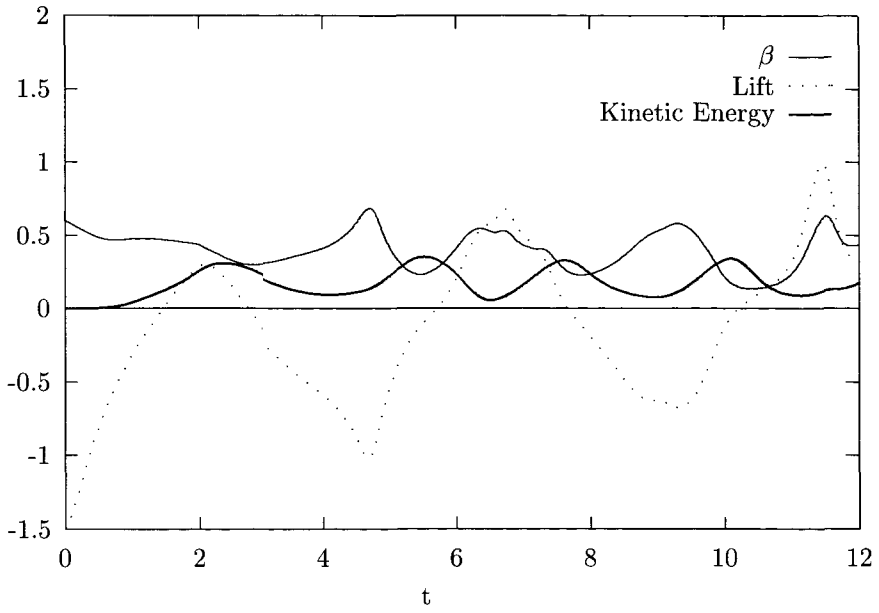

Figure 3.8: The Tension, Lift, and Kinetic Energy, for $\alpha = \alpha_3(t)$

Although, as mentioned earlier there is some doubt as to the accuracy of these values for large values of t, the behaviour of the lift, kinetic energy and tension do appear to obey some intuitive principles, suggesting that even for large values of t, the results are qualitatively correct. In particular, when the lift takes a maximum positive or negative value, the kinetic energy is at a minimum, and the tension is at a maximum. These points correspond to the extreme values of the sail. Conversely, the maximum values of the kinetic energy occurwhen the sail is at the middle of a transition from a negative solution to a positive solution. At these points, most of the aerodynamic force is expended on giving the sail motion, so the lift is zero, and the tension is at a minimum. The facts that the value about which the lift is oscillating increases, and that the maxima of the kinetic energy start to decrease slowly, suggest that the sail will eventualy settle to the positive $\alpha = 0$ solution. The oscillatory behaviour is a consequence of the hyperbolic nature of the sail equation, as in its highest derivatives it is just the wave equation. The energy dissipation must come from the sail doing work against the aerodynamic lift, when the motion of the sail is against the direction of the lift. However, when the motion of the sail is in the same direction as the lift, the sail will gain kinetic energy, so the energy of the sail will not decrease monotonically, and may not decay to zero at all.

3.4.3 Sails With Positive Camber

For concave sails whose camber does not change over time, the sail shapes in the steady case are all qualitatively similar, with the $\alpha = 0$ shapes and $\alpha \to \infty$ shapes represented in figure 3.10.

Since the sail shapes are so similar, it is to be expected that the unsteady case for change from one to another will be relatively simple, and take place over a much shorter time scale than the previous

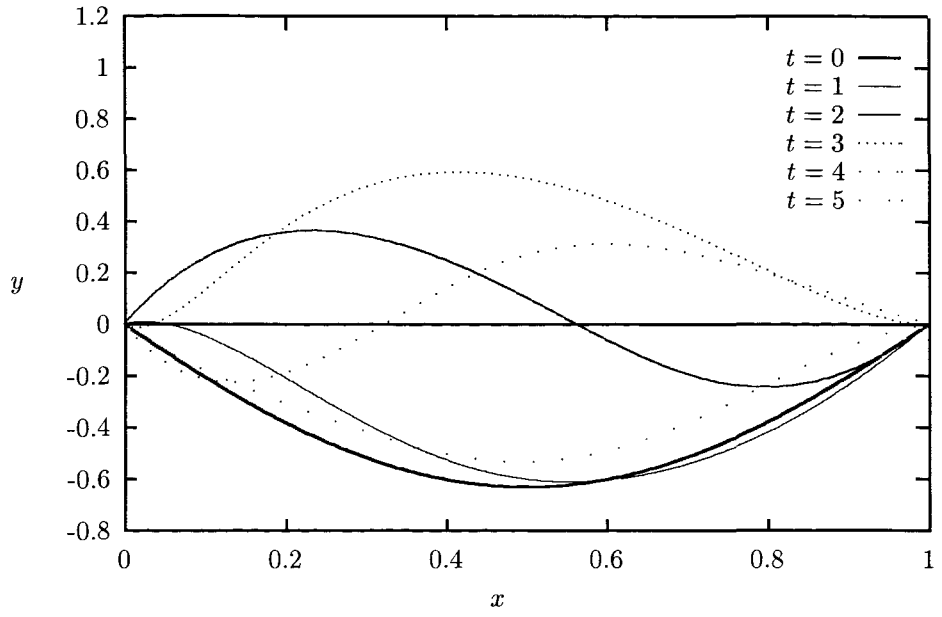

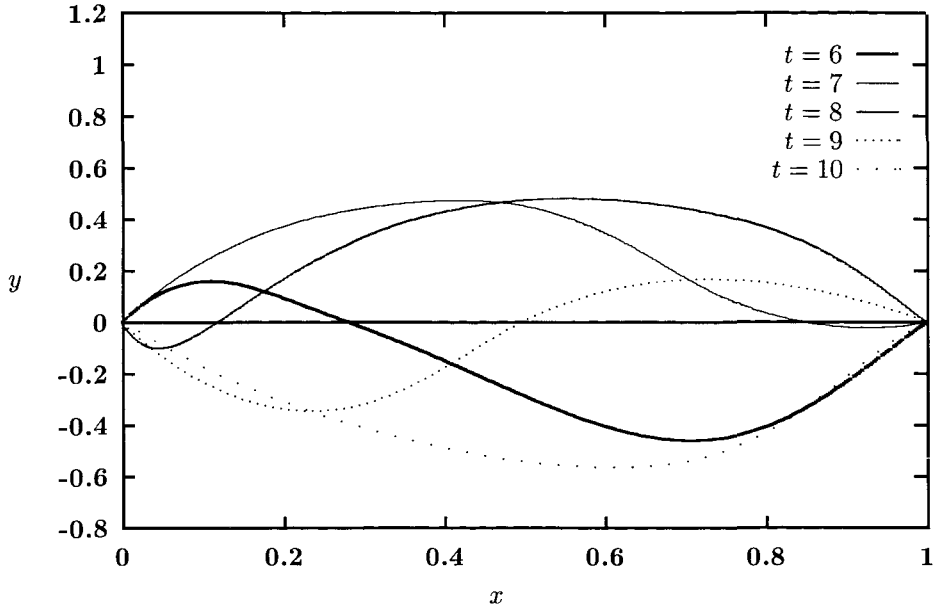

Figure 3.9: Sail Shapes for t from 0 to 10, with $\alpha = \alpha_3(t)$

examples. An example of this would be to examine the change as α increases from 0 to 1, and stays at $t = 1$, with the initial shape being the *positive* $\alpha = 0$ solution, so $\alpha = \alpha_1(t)$. Figure 3.11 shows the kinetic energy plotted against time for this case, and since the kinetic energy is small, it follows that the sail shape moves only very little. Figure 3.12 shows the sail shapes for $t = 0$ and $t = 1$. Computations were carried out for values of t up to seven, but for clarity these are not displayed as they are virtually identical to the shape for $t = 1$. Comparison with the shape for $t = 1$ in the steady state is made, and the difference is well within the expected computational error.

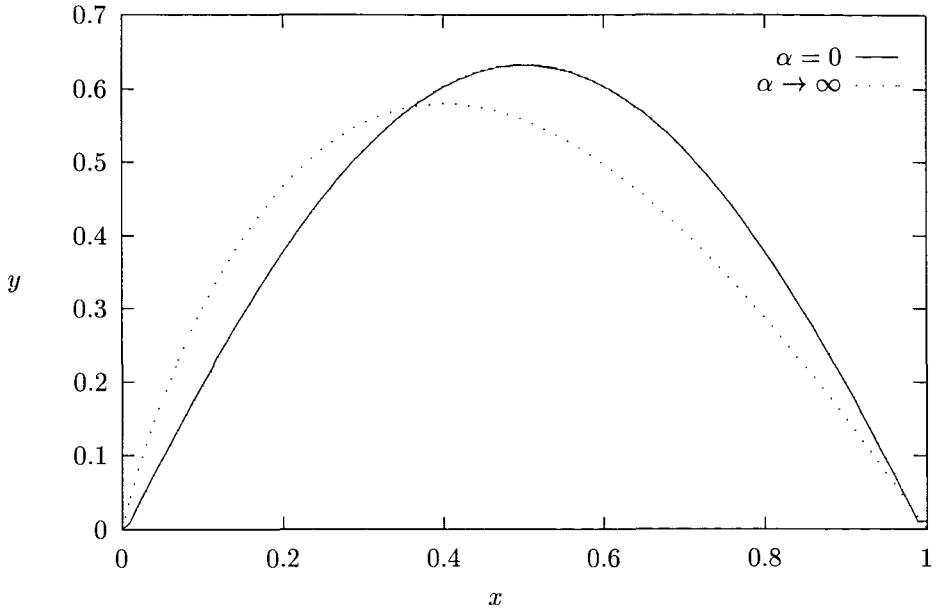

Figure 3.10: Sail Shapes for $\alpha = 0$ and $\alpha \to \infty$

It is therefore concluded that, although the sail is unlikely to be unstable in all cases, any oscillations may take a long time to decay, and in some cases may not decay at all. A more thorough analytical stability analysis is therefore required, and this will be conducted in a forthcoming paper.

However stability analysis is complicated by the fact that addition of a Fourier mode, $Ae^{i(k\delta x - \omega \delta t)}$ to any solution, must also satisfy the length condition, given by equation 3.2. Substitution of the added mode into the length condition yields

$$A \int_0^1 S_x e^{i(k\delta x - \omega t)} dx = 0.$$

This result cannot hold for all k unless A is 0, which suggests that stability analysis be conducted by another method. Haselgrove & Tuck (1976) [45] circumvented this problem by ignoring the length condition and assuming that the perturbation in the tension parameter was proportional to $e^{-i\omega\delta t}$, although the analysis is then that of a sail which is extensible to first order.

The above results give some indication in how to find numerical solutions for singular partial integro-differential equations. However, the low-mass sail equation (equation 2.34) is slightly harder to solve numerically as the highest x-derivative lies within the Hilbert transform, but the highest t-derivative lies outside, so the effect of the Hilbert transform will not be confined to highest order derivatives. A more detailed numerical analysis of such equations is presented in chapters 8 and 9, and a stable scheme for the low-mass equation is given in section 9.9. However, it is the order 1 mass case, for which results have already been presented, that is of most interest. Therefore attention will now be diverted from the sail equation to the problem of slot injection into a free stream.

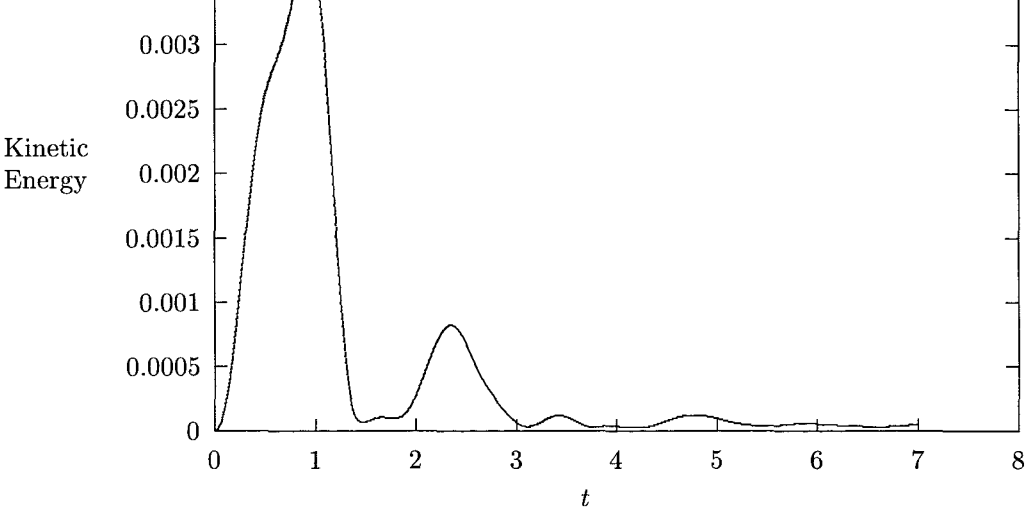

Figure 3.11: The kinetic energy plotted against time for a sail with $\alpha = \alpha_1(t)$, starting from a positive solution

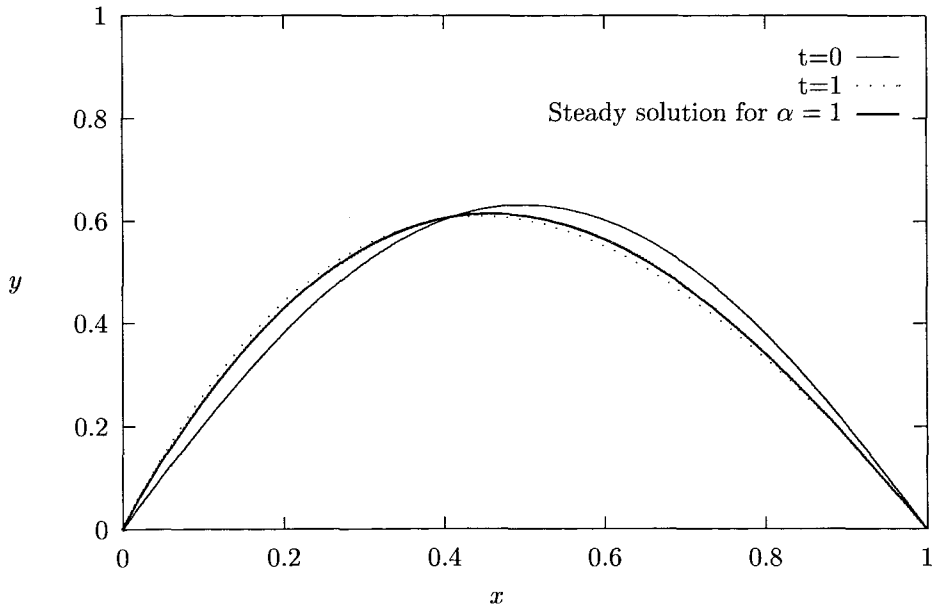

Figure 3.12: Sail Shapes for $\alpha = \alpha_1(t)$, Starting From a Positive Solution

Chapter 4

Injection Into a Free Stream

4.1 Introduction

Having examined the unsteady sail equation, similar techniques will be applied to the problem of unsteady slot injection into a free stream, which is particularly relevant to film cooling in turbine engines. Although the equations derived are similar, the equations for slot injection are significantly more complicated. However in order to justify the physical assumptions made in deriving the equations, it is necessary to examine the physical problem of slot injection into a free stream.

There exists a large amount of experimental and theoretical literature on the subject of slot injection into a free stream. Much of this is concerned with film cooling, i.e. the case where the injected fluid is cooler than the free stream, which has applications in, for example, turbine blades. This review will concentrate on theoretical studies made which employ careful order of magnitude estimates of all the terms in the equations of motion, and film cooling will be ignored, i.e. the temperature will be assumed to take the same value throughout. A review of the field of slot-injection was completed by Goldstein (1971) [42], and a more recent study has been completed by Fitt (1983) [30].

The importance of viscosity is dependent on the Reynolds number, defined by ratio of the product of the characteristic velocity, U, and length, L, to the dynamic viscosity, $Re = \frac{LU}{\nu}$. Of crucial importance is the ratio of the order of magnitude of the ratio of the blowing velocity out of the slot, v_w, to the free stream velocity U_∞, in comparison with the Reynolds number, Re, based on U_∞ and a characteristic length scale of the system, L. The length scale of the system chosen varies according to the system – in some, but not all models, it is the width of the slot, but in others it is the characteristic length scale of the external flow, which would be given, say, by the radius of curvature of the surface, or the height of the channel through which the crossflow travels. It is assumed throughout that $Re \gg 1$. When the region in which blowing takes place is finite, there will be a boundary layer on the plate upstream of the blowing, and the behaviour of this boundary layer will vary according to the blowing velocity. The following two-dimensional regimes have been considered for cases where v_w is a given function on a finite region of the surface of a flat plate, with the flow past the plate laminar, with typical velocity U_∞. In many cases the flow past the plate will be uniform. It is assumed that a boundary layer will

have formed before the onset of blowing, except in models where injection starts at the leading edge of the plate. Different regimes have been identified according to the order of magnitude of v_w/U_∞. There is no universally agreed terminology for the different regimes (weak, hard, etc.), the definitions used here are depicted in figure 4.1.

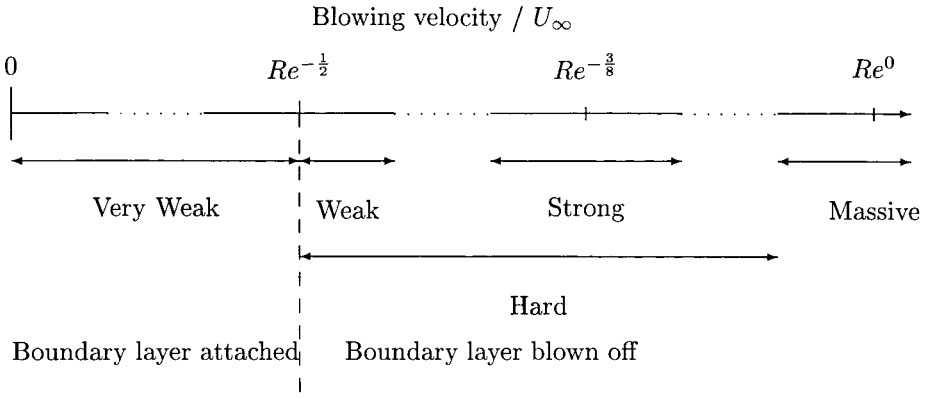

Figure 4.1: The Different Regimes for Injection into a Cross-Flow

4.2 Very Weak Blowing

Even in the absence of blowing, a boundary layer will form along the plate. According to boundary layer theory (see, for example, Stewartson (1964) [85]), the velocity in the boundary layer normal to the plate will be of order $U_\infty Re^{-\frac{1}{2}}$. Hence blowing velocities of an order of magnitude less than $U_\infty Re^{-\frac{1}{2}}$ will not affect the boundary conditions to the boundary layer equations to lowest order. However when $v_w = CU_\infty Re^{-\frac{1}{2}}$, where C is a constant of order 1, the blowing will affect the boundary conditions, the usual no-slip condition being replaced by the condition that $v = v_w$ on the plate. With this condition, Emmons & Leigh (1954) [28] showed that the system may be solved for constant blowing by the Blasius similarity transform provided $C < 0.6192$. The reason for this condition is that as $C \to 0.6192$ the boundary layer approaches a state of zero wall shear and is apparently blown off the plate. Thus the boundary layer will remain attached to the blowing surface only when $v_w < 0.6192U_\infty Re^{-\frac{1}{2}}$ and this regime will be referred to as *very weak* blowing.

4.3 Boundary Layer Separation

The form of the solution as $C \to 0.6192$ was obtained analytically by Kassoy (1970) [50] in the absence of a pressure gradient, and with a blowing velocity profile $v_w(x) \propto x^{-\frac{1}{2}}$. He separated the boundary layer into two regions : near the wall a linearised form of the Blasius equation applies subject to the boundary condition at the wall $v = v_w$, $u = 0$ (where u and v are the components of velocity in the x and y directions respectively). The other region is described by the full Blasius equation, with the boundary conditions being those of the free stream, the two regions being connected by an

asymptotic matching condition. The two regions are divided by a streamline that emanates from the onset of blowing, with the region below the dividing streamline consisting of injected fluid. The flow in the outer region is essentially that given by Lock's mixing layer system, see for example Lock (1951) [56]. As $C \to 0.6192$ the wall shear approaches zero smoothly as the effects of viscosity become less important in the region closer to the wall, and the streamline separating the two regions moves away from the wall, leading to a drastic thickening of the total boundary layer. Qualitatively the same behaviour will result for distributions of the injection velocity other than the distribution $v_w \propto x^{-\frac{1}{2}}$, which was assumed in order to facilitate analytic solutions.

The stability of separating boundary layers has been the focus of much study in various contexts, usually with the separation being caused by factors other than wall injection. A possible break-up mechanism for any boundary layer encountering any localised singularity was proposed by Smith (1989) [76]. Duck (1990a,1990b) [26, 25] considered three-dimensional separation, based on the triple-deck analysis of Stewartson (1969) [86]. He derived a non-linear, unsteady, system of partial differential equations, which was solved numerically, strongly suggesting that breakdown may occur at a finite time and finite spatial position. Peridier et al (1991) [67] computed the boundary layer solution for an unsteady boundary layer induced by the motion of a rectilinear vortex above an infinite plane wall using interacting boundary layer methods. Nonlinear breakup solutions were computed by Vickers & Smith (1994) [106] just beyond a breakaway-separation point, with a vortex sheet being produced near the smooth solid surface, with local inner-outer interaction. Further computations were performed by Cassel et al (1996) [13], who examined the viscous-inviscid interaction just upstream of the separation region and whose results suggest that any interaction can provoke a singularity of the type considered by Smith (1989). However in the work considered here, the behaviour of the boundary layer at separation is of less interest than the separated flow downstream.

4.4 Cole & Aroesty Theory

Cole & Aroesty (1968) [20] developed an inviscid model for blowing at a higher rate than that discussed above, with blowing velocity v_w/U_∞ small, but sufficiently large to blow the boundary layer off the plate. This large range of orders of magnitude will be referred to here as *hard* blowing. This model assumes a thin, inviscid injectant layer, with the effects of viscosity confined to the interface between the outer flow and the injected flow. This interface is a shear layer of negligible thickness. The shape of the shear layer is given by $y = \delta S(x)$ with $S(0) = 0$, thus assuming separation at the onset of blowing, since $x = 0$ is defined as the point at which blowing commences. Here δ is a small parameter defined by the condition that $S(1) = 1$. Their analysis showed that the order of magnitude of δ is $O\left(v_w/U_\infty\right)^{\frac{2}{3}}$. By expanding the terms in powers of δ they obtained an equation for $S(x)$ in terms of the pressure $P(x)$ and the blowing velocity $v_w(x)$ for compressible flow. For incompressible flow with

unit density this reduces to

$$S(x) = \frac{1}{\sqrt{2}} \int_0^x \frac{v_w(\xi)}{(P(\xi) - P(x))^{\frac{1}{2}}} d\xi. \tag{4.1}$$

A closed system for P and S for a given blowing velocity was obtained by applying results from thin aerofoil theory, i.e.

$$P(x) = \begin{cases} \frac{1}{\pi} \int_0^\infty \frac{S'(\xi)}{\xi - x} d\xi & \text{subsonic flow} \\ \frac{S'(x)}{(M_\infty^2 - 1)^{\frac{1}{2}}} & \text{supersonic flow.} \end{cases} \tag{4.2}$$

The constraints on the blowing velocity for this theory to apply are that $v_w/U_\infty \ll 1$, so that higher powers of δ may be ignored, that $v_w/U_\infty > 0.6192 Re^{-\frac{1}{2}}$ so that the boundary layer blows off, and that $v_w/U_\infty \gg Re^{-\frac{3}{5}}$, so that viscosity may be ignored in the injected region. Clearly for very large Reynolds numbers the last of these conditions is redundant.

4.5 Weak Blowing

Klemp & Acrivos (1972) [54] considered uniform flow of an incompressible fluid past a semi-infinite flat plate subject to a blowing velocity of $CU_\infty\ Re^{-\frac{1}{2}}$ where $C > 0.6192$ and is of order 1. The term *weak* blowing will be used to describe blowing of this order of magnitude, i.e. $v_w/U_\infty = O(Re^{-\frac{1}{2}})$, when it is sufficient to blow off the boundary layer. Their model followed from the Cole-Aroesty model, with separation assumed to take place at the onset of blowing, and a region underneath the boundary layer of injected fluid which is to first approximation inviscid, in which the horizontal velocity, u, is of order $U_\infty Re^{-\frac{1}{6}}$. The height of this region is $O(Re^{-\frac{1}{3}})$, while the blown off viscous boundary layer still has thickness $LRe^{-\frac{1}{2}}$, and is therefore thin in comparison with the blown layer for large values of Re. In this model viscous effects are confined to the boundary layer, since the external flow and the injected flow are inviscid. Expressions for the shape of the streamline dividing the boundary layer from the inviscid fluid were derived for velocity profiles $v_w = Re^{-\frac{1}{2}} x^{m-1}$, $0 < m \leq 1$, where $x = 0$ is the point at which blowing begins. However, as in the Cole-Aroesty model no solution was found for the case of uniform blowing over a region of infinite length.

Catherall et al (1965) [14] found that if v_w is constant and the blowing region is the entire plate (i.e. blowing commences at the leading edge of the semi-infinite plate, and continues to infinity) then separation will occur at a distance $0.7456 \frac{U_\infty^2 L}{v_w^2 Re}$ downstream from the leading edge of the plate. Smith & Stewartson (1973a) [78] argued that the adverse pressure gradient caused by the rapid thickening of the boundary layer in its neighbourhood may cause the separation point to move upstream. However the structure of the flow is not well understood near the separation point.

4.6 Strong Blowing

The term *strong* blowing is often used to refer to any blowing satisfying $Re^{-\frac{1}{2}} \ll v_w/U_\infty \ll 1$, e.g. by Smith (1973) [75]. However for the purposes of this review this rather broad range of blowing velocities

shall be referred to as *hard* blowing. In this review the term *strong* will be reserved for injection velocities satisfying the more precise condition that $v_w/U_\infty = O(Re^{-\frac{3}{8}})$. This follows the convention of Smith & Stewartson (1973a) [78], who conducted a study of slot injection with $v_w/U_\infty = O(Re^{-\frac{3}{8}})$ over an injection region $O(LRe^{-\frac{3}{8}})$. These scalings were chosen in order to balance the interaction between the boundary layer and the mainstream above it. Their study consisted of a triple-deck analysis of the kind considered by Stewartson & Williams (1969) [88], with the lower deck of thickness $O(L\epsilon^3)$, the boundary layer $O(L\epsilon^4)$, and the upper deck $O(L\epsilon^3)$ where $\epsilon = Re^{-\frac{1}{8}}$. This model was more complete than the Cole-Aroesty model in that it showed how the pressure builds up ahead of the slot and readjusts downstream of it. A crucial difference between this model and that of Cole-Aroesty is that in the Cole-Aroesty model separation of the boundary layer is presumed to occur at the onset of blowing, whereas in the model of Smith & Stewartson (1973a) [78] separation is allowed to occur at some point $x = x_s$ after the commencement of blowing at $x = x_0$, with $0 < x_s - x_0 \leq O(\epsilon^2)$. One advantage of this model is that it permits a constant blowing velocity profile without a pressure singularity : that this is not permissible in the Cole-Aroesty model was shown by Smith (1972) [74], (in the subsonic case it may be shown that $p(x) \sim \text{const}(-\log x)^{\frac{1}{3}}$ as $x \to 0$). In this model the pressure rises ahead of the slot, with the blowing being driven by a favourable pressure gradient.

This model was then extended to 'plate injection' by Smith & Stewartson (1973b) [79], in which the injection takes place over a distance of $O(L)$. In this model the separation takes place *before* the onset of blowing, i.e. $x_s < x_0$ with $L > x_0 - x_s \gg \epsilon^2 L$. The flow over the blowing region may be described completely, with the separated flow settled down to a fully developed state in which it is virtually at rest. There are thus four different regions : the region below the separated boundary layer before the onset of blowing, the blown region (below the boundary layer after the onset of blowing), the boundary layer, and the free stream. In a later study Stewartson (1974) [87] showed that a fully consistent solution of the Navier-Stokes equations could be constructed by dividing the flow field into seventeen regions. However there is no smooth transition between the models of slot blowing (blowing region of order $L\epsilon^3$) and plate blowing (blowing region of order L).

4.7 Massive Blowing

The term *massive* blowing refers to when the injection velocity satisfies $v_w/U_\infty = O(1)$. In this case there will be no shear layer produced, so the flow field will be analytic on the dividing streamline. Milne-Thomson (1949) [59] examined the case when the injection is so strong that a large, essentially inviscid disturbance is produced in the free stream from a point or a line source as in the theory of a Rankine solid. However Ting & Ruger (1965) [92] showed that should the ratio of the slot pressure to the external pressure, p_∞, drop below $\frac{1}{2}$ even an idealised model assuming laminar irrotational flow becomes a complicated free-boundary problem which must be solved numerically. Nevertheless theoretical analyses have been conducted by, for example, Inger & Gaitatzes (1971) [47], Thomas (1969)

[90], Wallace & Kemp (1969) [108], Roy & Nath (1992) [72], and Vasantha & Nath (1986) [103], with experimental work having been conducted by, for example, Hartunian & Spencer (1967) [44] and Bott (1968) [8].

4.8 Total Pressure Ratio

In all the above models, solutions have been found for a given injection velocity, v_w through the wall. However in practice this is difficult to set up experimentally, and it is more usual to have the fluid being injected from a slot, with the slot pressure being given. Fitt et al (1985) [34] (henceforth to be referred to as 'Fitt') considered slot injection into a free stream in which the pressure in the slot is given, see figure 4.2. The model is dependent on a small parameter, ϵ, which is defined by

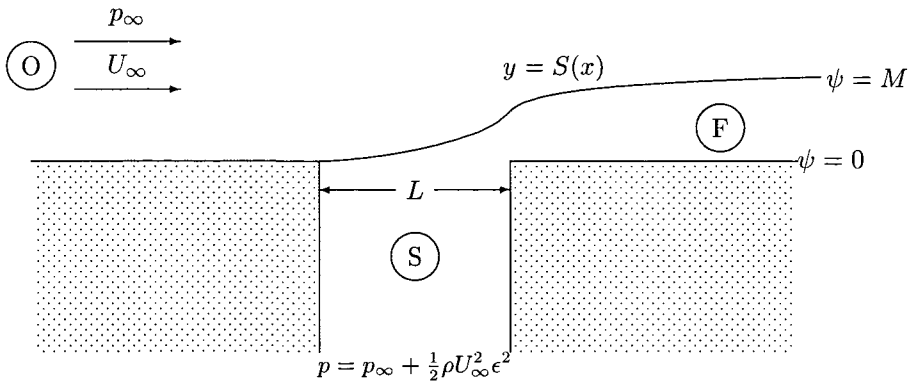

Figure 4.2: A Schematic Diagram of the Slot Injection Model

the slot pressure exceeding the free stream pressure by $\frac{1}{2}\rho U_\infty^2 \epsilon^2$ where U_∞ is the velocity of the free stream at infinity, and ρ is the density of the (incompressible) fluid. The model assumes subsonic flow throughout. His model combined the Cole-Aroesty theory discussed above with Rankine flow, i.e. flow past a series of sources. The parameter δ in the Cole-Aroesty model is roughly equivalent to ϵ^2. This is combined with a Rankine flow above the shear layer, with a series of sources of strength $O(\epsilon^2)$ which lead to a vertical velocity of $O(\epsilon^3)$ just above the shear layer after separation. The streamline exhibits a 'lid effect' with $S(0) = S'(0) = 0$, and the velocity normal to the flat surface being of order $U_\infty \epsilon^3$ over the slot region, except near the trailing edge where it may reach an order of magnitude of $U_\infty \epsilon$. By imposing continuity of pressure at the shear layer an integro-differential equation was derived for the shape of the dividing streamline $y = \epsilon^2 S(x)$ and solved numerically.

$$-\frac{1}{\pi} \int_0^\infty \frac{S'(\xi)}{\xi - x} = \begin{cases} -\frac{1}{2} & 0 < x < 1, \\ -\frac{1}{2} + \frac{1}{2}\frac{M^2}{S^2} & x > 1, \end{cases} \tag{4.3}$$

where M is the mass transfer out of the slot, and x is scaled with L, the slot width. The model assumes separation at the leading edge of the slot, with all the effects of viscosity being confined to a

shear layer of negligible thickness separating the blown region from the free stream. The mass transfer out of the slot was calculated and took a value of approximately $1.04LU_\infty\rho\epsilon^3$. This is another feature that makes this analysis an improvement on the methods described earlier : in this method the mass flow may be predicted from the pressure difference. The fact that the injection velocity increases by an order of magnitude near the trailing edge of the slot means that this model does not correspond exactly to any of the regimes described in figure 4.1.

The conditions for the validity of this model are that the blown region be inviscid, that the thickness of the shear layer is zero, and that the pressure difference, ϵ^2, be sufficiently small for linear asymptotics to be used. The assumption that the fluid in the blown region is inviscid may be tested by examination of the Navier-Stokes equation,

$$u_t + uu_x + vu_y = -\frac{1}{\rho}p_x + \nu\nabla^2 u.$$

From the scalings detailed above, all the non-viscous terms will be $O(\epsilon^2)$, with the viscous term being $O(\epsilon^{-3}Re^{-1})$. Thus it is required that $\epsilon^{-5} \ll Re$. For the thickness of the shear layer to be negligible, its thickness, which is $O(LRe^{-\frac{1}{2}})$ must be much less than that of the blown region, which is $O(L\epsilon^2)$. This gives the weaker condition that $\epsilon^{-4} \ll Re$. Hence the domain of validity of this model is that

$$Re^{-\frac{1}{5}} \ll \epsilon \ll 1. \tag{4.4}$$

This is a slightly weaker condition than that for the Cole-Aroesty model. This is because separation at the leading edge of the slot will occur whatever the pressure difference, due to the geometry of the system, whereas in the Cole-Aroesty model separation will only occur for sufficiently large values of v_w/U_∞. The assumption that the onset of separation occurs at a negligible distance from the leading edge of the slot may be justified by the work of Stewartson & Williams (1969) who for 'strong' blowing found that the separation point will lie at a distance of order $LRe^{-\frac{3}{8}}$ from the onset of blowing, which in this case corresponds to the leading edge of the slot.

That the system for pressure-driven injection of Fitt is similar to the velocity-driven Cole-Aroesty model may be seen from the fact, which has not previously been noted, that an equation similar to that of Fitt (equation 4.3) may also be obtained from the formula given by Cole & Aroesty when the injected velocity has a profile $v_w(x) = \delta(x-1)$, where δ is a Dirac delta function. Substitution of this velocity profile into equation 4.1 gives

$$S'(x) = \begin{cases} 0 & 0 < x < 1, \\ \frac{1}{\sqrt{2}}\frac{1}{\sqrt{P(1)-P(x)}} & x > 1. \end{cases}$$

Then substituting for P from equation 4.2 one obtains

$$\frac{1}{\pi}\int_1^\infty \frac{S'(\xi)}{\xi - x}d\xi = P(1) - \frac{1}{2S^2}.$$

The reason for the differences between this equation and equation 4.3 lies in part from the different way in which $S(x)$ is defined : Cole & Aroesty scaled $S(x)$ by the condition $S(1) = 1$, whereas Fitt scaled

S with $L\epsilon^2$. However this will lead only to the constants being different in the two equations. The more fundamental difference between this equation and that derived by Fitt is that Cole & Aroesty assume that separation takes place at the onset of blowing, i.e. at the *trailing* edge of the slot, where in this case the injected velocity is infinite. In Fitt's model the separation takes place at the leading edge of the slot, whereas almost all of the blowing takes place at the trailing edge of the slot. It seems plausible that the correct choice for v_w, with v_w being finite and positive for $0 < x < 1$, and tending to zero as x tends to zero, but behaving like a Dirac delta function at $x = 1$, would replicate the equation of Fitt, as now in both cases separation would occur at $x = 0$.

Fitt's model however, unlike the Cole-Aroesty model, gives a continuous model for the streamline without the pressure singularity required in the Cole-Aroesty model discussed earlier. There is a discontinuity in the pressure at $x = 1$, however this is caused by the fact that changes in the pressure take place over a typical length scale of $L\epsilon$ in this region, whereas in the rest of the system they take place over a region of length scale L. Thus by employing a complete analysis of the region near the trailing edge of the slot, a continuous expression for p may be found in terms of $(x/L\epsilon)$. However since this discontinuity only takes place over a region of length $O(L\epsilon)$ this will not have a significant effect on the solution for the streamline $S(x)$ or for the mass transfer M.

The effect of a slightly different slot geometry was considered by Fitt & Wilmott (1994) [35] who considered a slot in which the leading edge of the slot was higher than the trailing edge, and for which just upstream of the leading edge there was a separation ramp. This geometry encouraged clean separation at the leading edge. Expressions were derived for the mass flow for various shapes of separation ramps.

4.9 Trailing Edge Separation

The problem when separation takes place at the trailing edge as well, leading to the existence of two free boundaries has also been discussed, for example by Stojanovic (1988) [89] who proved that if the lower region (i.e. the region below the streamline which separates at the trailing edge) is assumed to have constant pressure then there exist continuous solutions for the two streamlines. This was also analysed by O'Malley (1988) [64] who assumed that the region below the dividing streamline at the trailing edge would be of constant pressure, and thence derived the equation

$$\frac{2}{\pi}\int_0^\infty \frac{S'(\xi)}{\xi - x}d\xi = \begin{cases} 1 & 0 < x < 1, \\ 1 - \frac{M^2}{S^2(x_r)} & 1 < x < x_r, \\ 1 - \frac{M^2}{S^2(x)} & x > x_r, \end{cases} \tag{4.5}$$

where x_r, to be found, is the end of the separation bubble, i.e. where the streamline that separates at the trailing edge of the slot re-attaches to the plane $y = 0$. O'Malley also derived the equation

$$\frac{2}{\pi}\int_0^\infty \frac{S'(\xi)}{\xi - x}d\xi = \begin{cases} 1 + 4\lambda x & 0 < x < 1, \\ 1 + 4\lambda x - \frac{M^2}{S^2(x)} & x > 1, \end{cases} \tag{4.6}$$

for flow where injection takes place into a free stream with a pressure gradient, with λ a measure of the strength of the pressure gradient. Asymptotic analysis and numerical solutions of these equations were performed by Fitt (1986) [31], who went on to consider a more realistic model for the separation bubble in the former of these equations. In this analysis the bubble is composed of two distinct regions, one in which the pressure is, as before, constant, and the other where the vorticity is constant. However this model differed from those considered previously in this context in that it allowed the slot pressure to be of an order of magnitude higher than in the problems previously considered in this context, so that the injected flow leaves the slot parallel to the slot walls. Re-attachment of the streamline separated at the trailing edge was taken to be tangential to the wall. This gave the equation

$$\frac{1}{\pi} \int_0^{x_r} S'(\xi) \left(\frac{1}{x-\xi} - \frac{1}{x_r-\xi} \right) d\xi = \begin{cases} S^2(1) & 0 < x < 1, \\ S^2(x) & 1 < x < x_r, \end{cases} \tag{4.7}$$

with boundary conditions $S(0) = S(x_r) = S'(x_r) = 0$ and $S'(0) = \infty$ (note that in this problem, unlike those discussed previously in this section, $x = 0$ corresponds to the trailing edge of the slot). Again an asymptotic expression was found for S both at $x = 0$ and as $x \to \infty$, and a numerical solution obtained for given values of x_r. Expressions were found for the jump in the Bernoulli constant in the separated region and for the singularity in $S'(0)$ as functions of x_r and it was conjectured that a limiting singularity strength may lead to a constant vorticity region of infinite length. However it was not possible for the numerical scheme used to confirm this.

4.10 Experimental Work

An experimental analysis of the blowing problem with a given pressure ratio was conducted by Fitt et al (1985) [34]. Pressure measurements were made at the wall for the cases when the slot had a sharp trailing edge, and where the slot had a 6mm trailing edge (the width of the slot was 40mm). It was found that at the lowest injection rates the mass flow was well above that predicted by linearised theory. As the injection rate increased, the results came closer to those predicted, and then deviated from the predicted result for larger injection rates. The reasons proposed for the discrepancies were that for lower injection rates the boundary layer thickness becomes as large as the injected layer and so viscous effects become important. For larger injection rates the separation at the trailing edge becomes significant, which accounts for the difference between the predicted result and that measured in the experiment in this case. The effect of rounding off the trailing edge of the slot was as predicted, but the effect on the mass flow was not marked. Shapes of the dividing streamlines were also given by experiment using a liquid crystal thermochromic indicator.

In the context of the rim seal problem discussed in chapter 1 comparisons of the predictions from Fitt et al (1985) [34] with experiment were made by Hamabe & Ishida (1992) [43] and Chew et al (1994) [18]. Again both sets of measurements showed good agreements with the predictions from the theory.

4.11 Suction From a Free Stream

The case when the pressure in the slot drops below the free-stream pressure, p_∞, is also of interest. If the pressure is maintained below p_∞ for long enough, slot suction from the free stream will ensue, which is clearly an undesirable situation in the context of film cooling of turbine blades, or to the rim seals described in chapter 1. A study of a physical problem similar to that discussed in the previous chapter for slot blowing, but with order one pressure differences permitted, was conducted by Dewynne et al (1989) [22]. This considered two-dimensional steady slot suction of a high-Reynolds-number, incompressible, fluid from a uniform flow. Unlike the slot blowing problem, however, a solution was found for the flow for order one pressure differences between the slot and the external flow, by use of hodograph techniques. It was found that the streamline that divides the fluid which enters the slot from that which remains outside does not re-attach at the trailing edge except at a critical value for the difference in slot pressures. For slot suction stronger than this critical value the stagnation point, where the re-attachment takes place, occurs downstream of the slot on the channel wall, and moves monotonically to infinity with increasing suction strength. For slot suction weaker than this the stagnation point is located on the wall of the slot, but the behaviour of the stagnation point is not monotonic with respect to suction strength in this case. In fact there is a finite suction strength for which the location of the stagnation point reaches a maximum distance from the corner, and for suction strength less than this the stagnation point moves towards the corner, and for small suction strengths is situated arbitrarily close to the corner. This is a result of the separation of the flow at the stagnation point.

Furthermore a linearised problem was discussed, where the pressure difference between the slot and the external flow was taken to be small as in the blowing problem. The exact solutions were shown to be asymptotically equal to the linearised solutions as the suction strength vanishes. The linearised three-dimensional problem, in which the slot is taken to be an infinitely long cylinder, was discussed by Dewynne et al (1990) [23]. Here, an eigenfunction expansion was obtained for the perturbation potential in terms of associated Legendre and trigonometric functions, giving an infinite system of linear equations for the eigenfunction coefficients which was then solved analytically. Thus an exact expression was found for the mass flow rate, and an analytic expression for the channel-wall pressure were found.

Prior to Dewynne et al (1989) [22] most 'suction' problems concentrated on flow fields with different geometries to the slot system. Milne-Thomson (1949) [59] considered the special case of a branch of a canal where the dividing streamline stagnates at the apex formed by the walls of the main channel and the branch. This may be thought of as a generalisation of the slot suction problem to slots which are not perpendicular to the uniform flow, however this work did not consider the separation of the flow at the leading edge of the slot which necessarily occurs with a perpendicular slot. Michell (1890) [57] considered the aperture problem in which instead of a slot there is an aperture in a wall dividing

the uniform flow from a stagnant region. The stagnant region is at a pressure lower than the static pressure far upstream in the region of uniform flow and hence fluid is drawn through the aperture. However in this problem the flow that is sucked through the aperture is bounded by free streamlines rather than the fixed slot walls. A relationship was deduced between the angle through which the flow through the aperture is turned and the static pressure drop across the wall far downstream. Watson (1946) [109] extended this to the case where the region of uniform flow is of infinite breadth, and Bliss (1982) [6] considered the three-dimensional problem with a slender aperture and a small static pressure drop.

For a slot which is not set perpendicular to the wall, Michell (1890) [57] showed that there is a critical value of the suction rate at which it is possible to have two constant pressure separated flow regions. Below this value of the suction rate, the streamline that separates at the trailing edge (due to the fact that the stagnation point lies downstream of the trailing edge) will re-attach, and that which separates at the leading edge will not. Above this critical value the streamline which separates at the leading edge will re-attach, and that which separates at the trailing edge will not. At the critical value neither streamline will re-attach. This critical suction rate is proportional to the square of the tangent of the angle of inclination, a fact which confirms that for a slot aligned perpendicularly to the wall the streamline separating at the leading edge will not re-attach.

Fitt & Lattimer (1996) [33] considered a linearised system in which a suction slot is placed downstream of an injection slot, following the work of Fitt et al (1985) and the linearised part of Deywnne et al (1989). A series of equations was derived according to whether the slot suction was sufficient to ingest all of the injected fluid or not. It was found that, for sufficiently weak slot suction, the 'suction' slot could be maintained at a pressure less than the free stream pressure, but still inject fluid into the free-stream, as a result of the interference caused by the upstream injection slot.

Experimental work on the steady suction problem was performed by Morland (1988) [60] both for weak suction and strong suction. The mass flow was controlled and static pressure measurements were made, from which the stagnation point and velocity minimum were inferred. This found reasonable quantitative agreement between the results predicted by the theory (which is the same as the theory used by Dewynne et al (1989) [22]) and the results found from experiment, and in particular the path taken by the stagnation point for various suction strengths concurred with that predicted by the theory. Some discrepancies were involved for strong sucking, probably due to the influence of the separated flow region present at the trailing edge. Experiments for weak suction agreed well with the linearised model except at the trailing edge of the slot. This was not surprising, however, as the linearised theory is not valid at the trailing edge.

Experiments were also conducted by Chew et al (1994) [18] in the context of the rim sealing problem discussed in chapter 1 . Measurements were made of the pressure for various values of annular axial flow. However the results did not agree well with the theory. Possible reasons for this include

circumferential pressure asymmetries in the annulus, and static pressure recovery in the seal. The former of these is not relevant to the two-dimensional theory described above, however, and so these results suggest that when considering rim sealing it may be necessary to examine three-dimensional effects.

4.12 Three-Dimensional Film Cooling

There are two possible approaches to extending the above work to three dimensions. The first is to consider the flow as extending over the half space $z > 0$ with a cylindrical, infinitely deep slot extending over the region $\{x^2 + y^2 < r, z < 0\}$, and then for blowing or sucking to impose a time dependent pressure difference at the bottom of the slot. For the steady case this has been examined for suction by Dewynne et al (1990) [23], although unlike the two-dimensional problem studied by Dewynne et al (1989) [22] only weak suction was studied, using linear asymptotics. Alternatively the rim sealing problem, discussed in chapter 1, gives an axisymmetric problem, relevant to modern gas turbines, which may be of interest, as Chew et al (1994) [18] have observed that it is necessary to study unsteady effects in the analysis of this problem. However with regard to the rim sealing problem Campbell (1978) [12] noted that circumferential pressure variations in the main gas flow path will affect ingestion of the hot gas. The pressure asymmetry may be caused by guide vanes, rotor blades or other disturbances, and so it would be of use to extend the work detailed above to the three-dimensional problems. However, since the unsteady problem has not previously been examined, it will be of use to study the two-dimensional slot injection and suction problems, and this will be the subject of the next two chapters.

Chapter 5

Unsteady Slot Injection

5.1 Steady Slot Injection

The work in this chapter will describe unsteady slot injection into a high-Reynolds-number cross-flow. As the most physically realistic way of imposing time-dependent injection is by controlling the pressure at the bottom of the slot, the model used will be that considered by Fitt et al (1985) [34] for steady slot injection, as discussed in section 4.8. The analysis assumed incompressible irrotational flow both in the injected flow and in the free stream, with a thin shear layer separating the two. The layer is assumed to separate at the leading edge of the slot, but not at the trailing edge. In practice there may be separation at both the leading and the trailing edge, depending sensitively on the local geometry near the edges of the slot : this is discussed in section 4.9. It may be assumed that the separation will take place at a small distance from the leading edge of the slot, although full triple-deck analysis similar to some of those described in section 4.3 is required for a detailed analysis of the boundary layer separation at the leading edge. Moreover, at the onset of separation, the flow will be in the $x-$direction, i.e. in the direction of the cross-flow. The effects of viscosity are confined to the shear layer, which is given by $y = S(x,t)$. The slot pressure is taken to be $p_\infty + \frac{1}{2}\rho U_\infty^2 \epsilon^2$, with p_∞ the free-stream pressure at infinity, ρ the density of the gas, and U_∞ the velocity of the flow at infinity. This defines ϵ which is a dimensionless parameter that is required to be much smaller than one for this analysis. The width of the slot is L. The domain of validity for this model is discussed in section 4.8, with the bounds on ϵ being given by equation 4.4. Figure 4.2 shows a schematic representation of the slot injection system.

By imposing the condition that pressure must be continuous across the shear layer, an integro-differential equation was found for $S(x)$ parametrised by a constant, M, which represents the mass flow out of the slot.

$$\frac{2}{\pi}\int_0^\infty \frac{S'(\xi)d\xi}{\xi - x} = \begin{cases} 1 & (0 < x < L), \\ 1 - \frac{M^2}{S^2} & (x > L). \end{cases} \tag{5.1}$$

By imposing that the shear layer is continuous the mass flow, and hence $S(x)$, and the pressure profile at the surface of the blade, were calculated, with the mass flow M being given by Fitt et al (1985)

[34] as approximately $1.04LU_\infty\rho\epsilon^3$.

5.2 The Interactive Case

For the purposes of this analysis the same assumptions as above will be made as in the steady case, except that the slot pressure will be taken to be $p_\infty + \frac{1}{2}\rho\epsilon^2 U_\infty^2 f(t)$, where $f(t)$ is a given function of time satisfying $f(t) > 0$ at all times. The region marked O in figure 4.2 is modelled by thin aerofoil theory, i.e. by considering the shear layer as a distribution of sources of strength $(2\pi)^{-1}\epsilon^2\gamma(x,t)$ along the positive x-axis. This gives a time-dependent potential $\Phi_O(x,y,t)$,

$$\Phi_O(x,y,t) = U_\infty x + \frac{\epsilon^2 U_\infty}{2\pi}\int_0^\infty \gamma(\xi,t)\log\left(\frac{(x-\xi)^2+y^2}{L^2}\right)d\xi. \tag{5.2}$$

In this analysis it is important to determine the order of magnitude of each term, so henceforth non-dimensionalised co-ordinates will be used. These are given by

$$\begin{aligned}
x &= Lx^*, \\
y &= \begin{cases} Ly^* & \text{in outer flow,} \\ L\epsilon^2 y^* & \text{in injected flow,} \end{cases} \\
S(x) &= L\epsilon^2 S^*(x^*), \\
t &= LU_\infty^{-1}\epsilon^{-1}t^*, \\
\Phi_O(x,y,t) &= U_\infty x + LU_\infty\epsilon^2\Phi_O^*(x^*,y^*,t^*), \\
\Phi_F(x,y,t) &= LU_\infty\epsilon\phi(x^*,y^*,t^*). \\
p &= p_\infty + \frac{1}{2}\rho U_\infty^2\epsilon^2 p^*,
\end{aligned}$$

where Φ_F denotes the velocity potential in the blown region F in figure 4.2.

Some care must be taken with the order of magnitude of these quantities. It is well known from thin aerofoil theory that a pressure difference of order ϵ^2 produces a disturbance of thickness order $L\epsilon^2$ (e.g. Woods (1961) [110]), and so the characteristic height of the blown region is of order $L\epsilon^2$. The order of magnitude of y will be the same in region F since here $0 < y < S(x,t)$. A pressure difference of order ϵ^2 over an order one length scale implies (for example from Bernoulli's equation) a velocity of order ϵ in region F, so the corresponding velocity potential is of order ϵ. Equation 5.2 implies that $\Phi_O - U_\infty x$ will be of order ϵ^2.

The characteristic time scale is also of some significance. The most obvious choice would be a time scale of LU_∞^{-1} since this is the characteristic time scale in the outer flow. However the flow in the F region has velocity of magnitude ϵU_∞ and so a time scale $LU_\infty^{-1}\epsilon^{-1}$ is also relevant. The time scale is determined by the pressure variations in the slot, and so it will be of interest to discuss more than one possible scaling of t. The case where t is scaled as above, i.e. with time scale $LU_\infty^{-1}\epsilon^{-1}$, will be referred to as the *interactive* case. In this case the flow above the shear layer will be quasi-steady and the flow below the shear layer will be unsteady. For any longer time scale the flow will be quasi-steady in both cases.

Bernoulli's equation states that the quantity $\rho\Phi_t + p + \frac{1}{2}\rho(u^2+v^2)$ (where p denotes pressure, ρ density, and (u,v) velocity) is independent of position for irrotational flow of an inviscid fluid. This may also be written

$$\rho\Phi_{Ot} + p + \frac{1}{2}\rho(\Phi_{Ox}^2 + \Phi_{Oy}^2) = F(t), \tag{5.3}$$

for some function of time, $F(t)$. In order to apply this equation it is necessary to evaluate the derivatives of Φ_O,

$$\Phi_{Ox} = U_\infty + \frac{\epsilon^2 U_\infty}{\pi}\int_0^\infty \frac{\gamma(\xi,t)(x-\xi)}{(x-\xi)^2+y^2}d\xi, \tag{5.4}$$

$$\Phi_{Oy} = \frac{\epsilon^2 U_\infty}{\pi}\int_0^\infty \frac{y\gamma(\xi,t)}{(x-\xi)^2+y^2}d\xi, \tag{5.5}$$

$$\Phi_{Ot} = \frac{\epsilon^2 U_\infty}{2\pi}\int_0^\infty \gamma_t(\xi,t)\log\left(\frac{(x-\xi)^2+y^2}{L^2}\right)d\xi. \tag{5.6}$$

The latter of the integrals may be expressed as a singular integral using integration by parts, since all time derivatives vanish at the limits of the integral.

When considering the outer flow only, the shear layer $y = S(x)$ is just the positive x-axis to lowest order, thus to compare the terms in Bernoulli's equation at the shear layer to the values taken at infinity, it is necessary to evaluate the left-hand side of equation 5.3 at $(x,0)$ and at $(-\infty,0)$. Immediately it can be seen that the Φ_{Oy} term will disappear, and the Φ_{Ox} term will equal U_∞ at infinity.

Substituting in the non-dimensionalised co-ordinates it may be seen that Φ_{Ot} is of order ϵ^3, Φ_{Oy} is of order ϵ^2, and $\Phi_{Ox} - U_\infty$ is order ϵ^2. Thus to lowest order, equation 5.3 may be re-written

$$p_\infty + \frac{1}{2}\rho U_\infty^2 = p_b + \frac{1}{2}\rho(\Phi_{Ox})^2,$$

where, p_∞ and U_∞ denote the pressure and velocity at infinity respectively, and p_b denotes the pressure at the shear layer (the condition that the pressure is continuous across the shear layer means that p_b denotes the pressure both just above and just below the shear layer). Substitution from equation 5.4 gives

$$\frac{p_b - p_\infty}{\frac{1}{2}\rho U_\infty^2} = -\frac{2\epsilon^2}{\pi}\int_0^\infty \frac{\gamma(\xi,t)(x-\xi)}{(x-\xi)^2+y^2}d\xi$$

According to the non-dimensionalisation used, the expression on the left-hand side of this equation is just $\epsilon^2 p_b^*$.

It may be seen that in the above integral the contribution from the region $(x-\epsilon, x+\epsilon)$ will be zero by symmetry, thus the singular integral may be evaluated as a Cauchy principal value. The above equation may be expressed in non-dimensionalised co-ordinates, observing that the y^2 terms can be ignored, to give

$$p_b^* = \frac{2}{\pi}\int_0^\infty \frac{\gamma(\xi^*,t^*)}{\xi^* - x^*}d\xi^*. \tag{5.7}$$

One difference between the unsteady case and the steady case is that the shear layer dividing the external flow from the blown region does not have to be a streamline in unsteady flow. This condition

is replaced by the kinematic condition, namely that

$$\frac{D}{Dt}(y - S(x,t)) = v - S_t(x,t) - uS_x(x,t) = 0 \tag{5.8}$$

must hold at $y = S(x,t)$. It is largely in this equation that the importance of the scale of the time changes becomes apparent, as the order of magnitude of the S_t term will depend on the time scale. This gives another condition from which the source strength, γ, may be found.

Observing that

$$\lim_{y\to 0^+} \frac{y}{(x-\xi)^2 + y^2} = \pi\delta(x-\xi),$$

u and v may be obtained in the limit as y tends to $S(x)$ from above by differentiating Φ_O to give

$$\begin{aligned} \lim_{y\to 0^+} u = \lim_{y\to 0^+} \Phi_{Ox} &= U_\infty - \frac{U_\infty \epsilon^2}{\pi} \int_0^\infty \frac{\gamma(\xi,t)}{\xi - x} d\xi, \\ \lim_{y\to 0^+} v = \lim_{y\to 0^+} \Phi_{Oy} &= \epsilon^2 U_\infty \gamma(x,t). \end{aligned}$$

Combining this with equation 5.8 gives that

$$\frac{v}{u} = \frac{\epsilon^2\gamma(x,t)}{1+O(\epsilon^2)} = S_x(x,t) + \frac{S_t(x,t)}{u}. \tag{5.9}$$

Writing this in terms of non-dimensionalised co-ordinates shows that

$$\epsilon^2\gamma(x^*,t^*) = \epsilon^2 S^*_{x^*}(x^*,t^*) + \epsilon^3 \frac{S^*_{t^*}(x^*,t^*)}{1+O(\epsilon)}. \tag{5.10}$$

This gives γ in terms of S, and hence it follows that, to lowest order,

$$\gamma(x^*,t^*) = S^*_{x^*}(x^*,t^*). \tag{5.11}$$

In order to analyse the F region of the fluid, the injected flow, we will assume that the flow is irrotational. Irrotational flow may seem unlikely at first, but since all velocities in the slot are small, the vorticity in the slot will be small (of order ϵ^3), and since vorticity is constant along streamlines in two-dimensional flow, a small vorticity in the slot will remain small in the cooling flow. Vorticity in the blown region can be significant, however, if the flow does not separate smoothly at the trailing edge. In this case a separation vortex may be set up in the vicinity of the trailing edge, and this may have significant effects which will lead to the different equations for this system described in section 4.9. However this phenomenon depends sensitively (i.e. on length scales of $L\epsilon$ or less) on the geometry of the slot near the trailing edge, and for the purpose of this analysis it will be assumed that the geometry of the slot is such that the separation is smooth, and so the flow will be irrotational.

The assumption of irrotational flow means that Laplace's equation holds for the velocity potential in the blown region. In non-dimensionalised co-ordinates, this gives

$$L^{-1}U_\infty\epsilon\phi_{x^*x^*} + L^{-1}\epsilon^{-3}U_\infty\phi_{y^*y^*} = 0.$$

Therefore to lowest order ϕ is linear in y^*, i.e.

$$\phi^* = A(x^*,t^*)y^* + B(x^*,t^*) + \epsilon^4\phi_1(x^*,y^*,t^*) + \ldots \tag{5.12}$$

Clearly the normal velocity must be zero at the fixed boundary $y^* = 0$. This implies that $A = 0$, and so to lowest order ϕ is a function of x^* and t^* only. This function B will henceforth be denoted by ϕ_0.

We may evaluate the pressure at the shear layer by use of Bernoulli's equation. The total pressure at the bottom of the slot is given as $p + \frac{1}{2}\rho U_\infty^2 \epsilon^2 f(t)$, and as this must be constant along streamlines it follows that this must be constant everywhere. Hence we have

$$p_b + \frac{1}{2}\rho({\Phi_F}_x^2 + {\Phi_F}_y^2) + \rho\Phi_{Ft} = p + \frac{1}{2}\rho U_\infty^2 \epsilon^2 f(t).$$

Using the non-dimensionalised variables, Φ_{Fx} will be $O(U_\infty \epsilon)$ and Φ_{Ft} will be $O(U_\infty \epsilon^2)$. However Φ_{Fy} will be $LU_\infty \epsilon^{-1}\phi_{y^*}$, which according to equation 5.12, is $U_\infty \epsilon^3 \phi_{1y^*}$, and so is much smaller than the other two terms. As in the steady case, all velocities are order $U_\infty \epsilon^2$ or less in the slot, and so the pressure will be constant above the slot. Hence in non-dimensional co-ordinates Bernoulli's equation reduces to

$$p_b^* = \begin{cases} f(t^*) & 0 < x^* < 1 \\ f(t^*) - \phi_{0x^*}^2 - 2\phi_{0t^*} & x^* > 1. \end{cases} \tag{5.13}$$

This may be combined with equations 5.7 and 5.11 to eliminate γ and p_b^*, leaving a relationship between S^* and ϕ_0. In order to close the system it is necessary to apply the kinematic condition in the region below the shear layer. In this region, the familiar equation

$$\phi_{y^*} = \phi_{x^*} S_{x^*}^* + S_{t^*}^*,$$

becomes, in non-dimensionalised variables,

$$LU_\infty \epsilon^3 \phi_{1y^*} = U_\infty \epsilon^3 \phi_{0x^*} S_{x^*}^* + U_\infty \epsilon^3 {S^*}_{t^*}. \tag{5.14}$$

Therefore it is necessary to evaluate ϕ_{1y^*}. This follows from Laplace's equation, which must be satisfied by ϕ. From equation 5.12 this reduces to

$$\phi_{0x^*x^*} + \phi_{1y^*y^*} = 0,$$

and so, as ϕ_0 is a function of x^* and t^* only,

$$\phi_{1y^*} = -\phi_{0x^*x^*} y^* + C(x^*, t^*).$$

The condition of zero normal velocity on $y^* = 0$ implies that $C = 0$, so at the shear layer ϕ_{1y^*} is just $-S^* \phi_{0x^*x^*}$. On substitution of this expression into equation 5.14 we are left with the desired equation relating ϕ_0 to S^*, namely

$$(\phi_{0x^*} S^*)_{x^*} + S_{t^*}^* = 0.$$

For convenience we will henceforth write ϕ for ϕ_0, and combine this result with the pressure balance equation suggested by equations 5.7, 5.11 and 5.13. Hence we have a system of two variables in ϕ and S^*, given by

$$\frac{2}{\pi}\int_0^\infty \frac{S_{\xi^*}^*}{\xi^* - x^*} d\xi^* = \begin{cases} f(t^*) & 0 < x^* < 1, \\ f(t^*) - {\phi_{x^*}^*}^2(x^*, t^*) - 2\phi_{t^*}^* & x^* > 1. \end{cases} \tag{5.15}$$

$$(\phi_{x^*}^* S^*)_{x^*} + S_{t^*}^* = 0. \tag{5.16}$$

The boundary conditions for this equation are S^* and $S^*_{x^*}$ are zero at $x^* = 0$, and it may be arbitrarily imposed that $\phi = 0$ at $x^* = 1$, as ϕ is the velocity potential. Initial conditions are also needed for ϕ and S^*. These equations will be referred to as the interactive equations for slot injection.

The mass transfer function will now depend on how far downstream of the slot it is evaluated. This function will be denoted by $M(x,t)$, and is given by

$$M = \int_0^{S(x)} \Phi_{Fx} dy = LU_\infty \epsilon^3 \int_0^{S^*} \phi_{0x^*} dy^* = LU_\infty \epsilon^3 \phi_{0x^*} S^* \tag{5.17}$$

in the blown region, $x^* > 1$. The physical interpretation of M in the region $0 < x^* < 1$ is less clear, but is irrelevant to the problem. This suggests that M be non-dimensionalised according to

$$M = LU_\infty \epsilon^3 M^*. \tag{5.18}$$

The interactive equations 5.15 and 5.16 may therefore be expressed in terms of M^* and S^* only, as they are in the steady state equations. In this form they are

$$\frac{2}{\pi} \int_0^\infty \frac{S^*_{\xi^*}}{\xi^* - x^*} d\xi^* = \begin{cases} f(t) & 0 < x^* < 1, \\ f(t) - \frac{M^{*2}(x^*,t^*)}{S^{*2}(x^*,t^*)} - 2\frac{\partial}{\partial t}\left(\int_0^{x^*} \frac{M^*(\xi^*,t^*)}{S^*(\xi^*,t^*)} d\xi^*\right) & x^* > 1, \end{cases} \tag{5.19}$$

$$M^*_{x^*} + S^*_{t^*} = 0. \tag{5.20}$$

Equation 5.20 suggests that the system may be expressed in terms of one variable, σ. This variable corresponds to the total mass of fluid that has been blown from the slot as far as distance x in time t, and is defined by the equations :-

$$\sigma_x = S, \tag{5.21}$$

$$\sigma_t = -M. \tag{5.22}$$

with $\sigma = 0$ at $x = 0$. The non-dimensionalised variable, σ^*, will just be $\sigma / L^2 \epsilon^2$.

Hence the time-dependent slot injection equation for the interactive case in terms of $\sigma^*(x^*, t^*)$ is

$$\frac{2}{\pi} \int_0^\infty \frac{\sigma^*_{\xi^*\xi^*}}{\xi^* - x^*} d\xi^* = \begin{cases} f(t) & 0 < x^* < 1, \\ f(t) - \left(\frac{\sigma^*_{t^*}}{\sigma^*_{x^*}}\right)^2 + 2\frac{\partial}{\partial t^*} \int_0^{x^*} \frac{\sigma^*_{t^*}}{\sigma_{x^*}} dx^* & x^* > 1, \end{cases} \tag{5.23}$$

with boundary conditions $\sigma^*(0,t^*) = \sigma^*_{x^*}(0,t^*) = \sigma_{x^*x^*}(0,t^*) = 0$ and appropriate initial conditions on σ^* and $\sigma^*_{t^*}$.

In whichever form they are presented, these equations pose a problem of significant complexity, being a non-linear system. Nonetheless it is felt that the equations derived with this non-dimensionalisation are the most important for the understanding of the slot injection problem, and so numerical approaches to this system are considered in chapters 8 and 9. Although it seems unlikely that analytic solutions will be found for this equation, an asymptotic analysis may be performed. This will give insight into the equations and results which are useful both to a physical understanding of the problem, and to the numerical analysis.

5.3 The Asymptotic Behaviour of the Shear Layer

5.3.1 Behaviour for Small x

The asymptotic behaviour of $S(x)$ at the leading edge of the slot may be determined fairly easily by inverting equations 5.19 and 5.20, according to the inversion formula given by equation A.3, giving

$$S^*_{x^*}(x^*,t^*) = -\frac{1}{2\pi}x^{*\frac{1}{2}}\int_1^\infty \frac{\phi^{*2}_\xi + 2\phi^*_t}{\xi^{\frac{1}{2}}(\xi - x^*)}d\xi + Cx^{*-\frac{1}{2}}, \tag{5.24}$$

where C is independent of x^*. It is immediately apparent that C is zero for all values of t^* from the boundary condition $S^*_{x^*}(0,t^*) = 0$. For $x^* < 1$ the above integral is not singular, so the asymptotic behaviour of S^* near zero will be given by

$$S^* = K(t^*)x^{*\frac{3}{2}} + O\left(x^{*\frac{5}{2}}\right). \tag{5.25}$$

In the quasi-steady case of section 5.4 the function $K(t)$ will be proportional to $f(t)$. However in the interactive case it not clear that this is the case, in other words the behaviour of the shear layer near the leading edge at a given time may not be dependent only on the slot pressure at that time, but may also be sensitive to the behaviour over a period of time. $K(t)$ may be found by letting x^* tend to zero in equation 5.24 to give

$$\frac{3}{2}K(t^*) = -\frac{1}{2\pi}\int_1^\infty \frac{\phi^{*2}_\xi + 2\phi^*_t}{\xi^{\frac{3}{2}}}d\xi. \tag{5.26}$$

5.3.2 Behaviour Near the Trailing Edge

Near $x^* = 1$ there is a jump discontinuity in the transform of $S^*_{x^*}$. Therefore there will be a logarithmic singularity in $S^*_{x^*}$ at $x^* = 1$, (see section A.4.3), so

$$S_{x^*} \sim K^\pm \log|1 - x^*| \text{ as } x^* \to 1^\pm,$$

where $K^\pm$ are constants. This implies that

$$S \sim C^\pm + K^\pm \log|1 - x^*| \text{ as } x^* \to 1^\pm,$$

however it is not obvious that C^+ and C^- are the same. It would seem possible for C^+ to be greater than C^- : this would correspond to there being a jump discontinuity in S^* at $x^* = 1$, with S^* taking a range of values at this point. This would certainly be the case were S_x to be an order of magnitude larger than $L\epsilon^2$ in some region $(1-\epsilon, 1+\epsilon)$. Suppose that the order of magnitude of S_x is ϵ^α at $x^* = 1$ for some $\alpha < 2$. Then from equation 5.11 this would lead to a source strength of order ϵ^α and hence a pressure difference of order ϵ^α. Since the pressure is continuous across the shear layer, this would lead to a similar pressure difference of order ϵ^α just below the shear layer, and so the horizontal component of the velocity, which is the largest component, in the blown region would be of order $\epsilon^{\frac{\alpha}{2}}$. Multiplying this velocity by the height of the shear layer at the trailing edge will give a mass flow of

order $\epsilon^{2+\frac{\alpha}{2}}$ which contradicts conservation of mass unless $\alpha = 2$ as the mass flow is of order ϵ^3 in the blown region. Hence S_x must be of order $L\epsilon^2$ at the trailing edge.

A jump discontinuity would still be possible for S_x order $L\epsilon^2$. However this would imply that S_x would behave like a Dirac delta function at the trailing edge, and it is known (see, for example, appendix 1 of Fitt (1983)), that this would imply a singularity of the form $1/(x^* - 1)$ at the trailing edge. This contradicts the fact that the pressure is constant for $x^* < 1$, as the pressure is the Hilbert transform of S_x in this region. Hence there can be no jump discontinuity at the trailing edge, and so C^+ will equal C^- (which equals C, say). Hence the asymptotic behaviour at $x^* = 1$ is given by

$$S \sim C + K^{\pm} \log|1 - x^*| \text{ as } x^* \to 1^{\pm}. \tag{5.27}$$

5.3.3 Behaviour for Large x

For large values of x^* it is necessary that $S^*_{x^*}$ tends to zero in order that the singular integral in equation 5.19, which is the expression for the value of the pressure at the shear layer, exists. In the steady case the behaviour at infinity is given by Fitt et al (1985) [34] as

$$S^* = M^* + O(1/x^*),$$

which implies that, as $\phi^*_{x^*} S^* = u^* S^* = M^*$,

$$\phi^* = x^* + O(\log x^*).$$

In the unsteady case it would appear reasonable for S^* to obey the same sort of behaviour. With this assumption it follows that the leading order terms in the expansions of both ϕ^* and S^* must be independent of time, otherwise the time-derivatives dominate equations 5.15 and 5.16. Note though that from equation A.13 that the Hilbert transform of a function with the asymptotic profile of x^{*-2} is asymptotically equal to $x^{*-2} \log x^*$. Hence the asymptotic expansion of S^* and ϕ^* must be given by

$$S^* = C_0 + C_1 x^{*-1} + C_2(t^*) x^{*-2} \log x^* + \ldots \tag{5.28}$$

$$\phi^* = \frac{1}{2} F(t^*) + x^* + K_1 \log x^* + K_2(t^*) x^{*-1} \log x^* + \ldots \tag{5.29}$$

where $F'(t) = f(t) - 1$. These give the results necessary from equations 5.15 and 5.16, that

$$f(t) - {\phi^*_{x^*}}^2 - 2\phi^*_t = O(x^{*-1}),$$

$$(\phi^*_{x^*} S)_{x^*} + S^*_{t^*} = 0.$$

Note in particular that C_0, C_1, and K_1 do not depend on time. This implies that both S^* and u^*, and thus M^*, are independent of time to within $O(x^{*-2} \log x^*)$. This is a surprising and counter-intuitive result, as one would normally expect the behaviour at infinity to vary with the slot-pressure in a subsonic flow. However it must be remembered that this regime is for changes on the interactive time

scale only, so implicitly it has been assumed that there is no variation on any other time scale. Thus it is more accurate to say that u^*, S^*, and M^* will only change by order $x^{*-2}\log x^*$ over a length of time of order $L/U_\infty\epsilon$. The asymptotic behaviour when variation takes place over both quasi-steady and interactive time scales is considered in section 5.6.

5.4 The Quasi-Steady Case

The system becomes quasi-steady if the changes in the slot pressure take place over a time scale of $LU_\infty^{-1}\epsilon^{-2}$ or longer. In this case all the time derivatives will be an order of magnitude smaller than in the interactive case, and the equation (in terms of M and S) will be as follows, with the same boundary conditions as before :-

$$\frac{2}{\pi}\int_0^\infty \frac{S^*_{\xi^*}}{\xi^*-x^*}d\xi^* = \begin{cases} f(t^*) & 0<x^*<1, \\ f(t^*)-\frac{M^*(t^*)^2}{S^*(x^*,t^*)^2} & x^*>1. \end{cases} \tag{5.30}$$

Since there are no time derivatives, t^* will behave as a parameter. The equation derived from conservation of mass beneath the shear layer will now reduce to $M^*_{x^*}=0$, which is the justification for writing $M^*=M^*(t^*)$ in the above equation. The boundary conditions $S^*_{x^*}=S^*=0$ at $x=0$ are sufficient information to find a solution and determine M^*, as in the steady case. At a given time, the equation will be the same as that for a steady system with slot pressure $p_\infty+\frac{1}{2}\rho U_\infty^2\epsilon^2 f(t)$. Thus the solution for this will be a family of steady state solutions parametrised by t^* given by

$$\begin{aligned} S(x,t) &= f(t)S_0(x), \\ M(t) &= f(t)^{\frac{3}{2}}M_0, \\ \phi_x(x,t) &= f(t)^{\frac{1}{2}}\frac{M_0}{S_0(x)}, \end{aligned} \tag{5.31}$$

where $S_0(x)$ is the solution of equation 5.1, the steady state injection equation, and M_0 is the corresponding mass transfer. The prediction that the mass flow is proportional to $f(t)^{\frac{3}{2}}$ has not previously been recognised, and is physically very significant, as it is the mass flow that is of most interest, particularly downstream of the slot. The importance of this relation is underlined by the fact that the mass flow far downstream of the slot does not vary with time over the interactive time scale, as was shown in section 5.3.3. It will also be shown in section 5.5 that it does not vary over shorter time scales, so far downstream this relationship between slot pressure and mass transfer is valid over all time scales.

5.5 The Fast Unsteady Case

Changes occurring over a time scale of order LU_∞^{-1} present a different problem to those discussed above, since the time scale of variations in the slot pressure is now an order of magnitude smaller than the natural time scale of the flow in the blown region. Furthermore the flow in the outer region

will now be fully unsteady, which is a contrast to the interactive case where it is quasi-steady, so time derivatives will become significant in this part of the flow. However, over the new time scale, there will be no motion in the blown layer in a finite time, since the velocity in this region is $O(U_\infty \epsilon)$. By conservation of mass therefore, the height of the shear layer must remain constant in this region. This means that, even if the slot pressure only varies over a time scale of L/U_∞, the height of the shear layer, and the velocity of the fluid in the blown region underneath it, can only vary to lowest order over a time scale of $L/U_\infty \epsilon$, although lower order terms will vary over the shorter time scale. Note that although the height of the shear layer is not varying with time in the blown region, it will vary over the slot.

Since all time derivatives are zero in the blown region to lowest order, the only effect of the change in the slot pressure is in the region above the slot. Here, the pressure changes will affect the height of the shear layer. The equation describing this may be derived in essentially the same way as for the interactive case, except that time derivatives are now significant. In particular, from equation 5.9 it follows that the source strength, $\epsilon^2\gamma$, will be given by

$$\epsilon^2\gamma = S_x + \frac{S_t}{U_\infty} + O(\epsilon^3),$$

just above the shear layer. Furthermore, the Φ_{Ot} term, given by equation 5.6, becomes significant. This may be integrated by parts, as before, but particular care must be taken with this integration, since a jump discontinuity in S, i.e. σ_x, is likely at $x = L$, as S is unsteady for $x < 1$ but steady for $x > L$. Hence it is prudent to split this integral into two parts. For convenience, as before, σ will be defined such that $\sigma_x = S$, and $\sigma = 0$ at $x = 0$. Hence, from equation 5.6, using the above expression for γ,

$$\Phi_{Ot} = \frac{\epsilon^2 U_\infty}{2\pi}\left(\int_0^L d\xi + \int_L^\infty d\xi\right)\left\{\left(\sigma_{\xi\xi t} + U_\infty^{-1}\sigma_{\xi tt}\right)\log\left(\frac{(x-\xi)^2+y^2}{L^2}\right)\right\},$$

from which,

$$\begin{aligned}\lim_{y\to 0^+}\Phi_{Ot} &= -\frac{\epsilon^2 U_\infty^2}{\pi}\int_0^\infty \frac{U_\infty^{-1}\sigma_{\xi t} + U_\infty^{-2}\sigma_{tt}}{\xi - x}d\xi \\ &+ \frac{\epsilon^2 U_\infty}{2\pi}\left(\left[\left(\sigma_{\xi t} + U_\infty^{-1}\sigma_{tt}\right)\log\frac{(x-\xi)^2}{L^2}\right]_{\xi=0}^{\xi=L^-} + \left[\left(\sigma_{\xi t} + U_\infty^{-1}\sigma_{tt}\right)\log\frac{(x-\xi)^2}{L^2}\right]_{\xi=L^+}^{\xi=\infty}\right).\end{aligned}$$

Of the two terms in square brackets, the contributions from 0 and ∞ will be zero, as in the interactive case, but the two terms from $x = L$ need not cancel, since the value for L^+ will be zero, as the flow is steady for $x > L$, but the value for L^- may be non-zero. Therefore let the contribution from L^- be denoted by $2N(t)U_\infty \log\left|\frac{L-x}{L}\right|$. Then

$$N(t) = \epsilon^2 U_\infty^{-1}\left(\sigma_{xt} + U_\infty^{-1}\sigma_{tt}\right)\Big|_{x=L}. \tag{5.32}$$

The expression obtained for Φ_{Ot} is therefore

$$\lim_{y\to 0^+}\Phi_{Ot} = -\frac{\epsilon^2 U_\infty^2}{\pi}\int_0^\infty \frac{U_\infty^{-1}\sigma_{\xi t} + U_\infty^{-2}\sigma_{tt}}{\xi - x}d\xi + \frac{\epsilon^2 U_\infty^2}{\pi}N(t)\log\left|\frac{L-x}{L}\right|.$$

Hence from equation 5.3, i.e. Bernoulli's equation for the external flow, by substituting the expression from equation Φ_{Ox} as before, it follows that

$$\frac{p_b}{\rho} + \frac{1}{2}U_\infty^2 - \frac{\epsilon^2 U_\infty^2}{\pi}\int_0^\infty \frac{\sigma_{\xi\xi} + 2U_\infty^{-1}\sigma_{\xi t} + U_\infty^{-2}\sigma_{tt}}{\xi - x}d\xi + \frac{U_\infty^2\epsilon^2}{\pi}N(t)\log\left|\frac{L-x}{L}\right| = F(t),$$

where $F(t)$ is some function of time only. In fact, by letting $x \to \infty$, it follows that $F(t) = \rho^{-1}p_\infty + \frac{1}{2}U_\infty^2$, and so

$$\frac{p_b - p_\infty}{\frac{1}{2}\rho U_\infty^2\epsilon^2} = \frac{2}{\pi}\int_0^\infty \frac{\sigma_{\xi\xi} + 2U_\infty^{-1}\sigma_{\xi t} + U_\infty^{-2}\sigma_{tt}}{\xi - x}d\xi - \frac{2N(t)}{\pi}\log\left|\frac{L-x}{L}\right|. \tag{5.33}$$

This describes the behaviour above the shear layer, and it is imposed that $p_b - p_\infty = \frac{1}{2}\rho U_\infty^2\epsilon^2 f(t)$ in the slot region, so the behaviour of the shear layer above the slot is given by

$$f(t) = \frac{2U_\infty}{\pi}\int_0^\infty \frac{\sigma_{\xi\xi} + 2U_\infty^{-1}\sigma_{\xi t} + U_\infty^{-2}\sigma_{tt}}{\xi - x}d\xi - \frac{2N(t)}{\pi}\log\left|\frac{L-x}{L}\right|. \tag{5.34}$$

Since all time-derivatives are zero in the blown region, over the time scale chosen, L/U_∞, the value of σ in the blown region will just equal its initial value, which must be given from the initial conditions. Hence the above equation is sufficient to describe the shear layer everywhere, with the only unknowns being the value of σ in the region $(0,1)$ and $N(t)$. In non-dimensionalised co-ordinates, with the non-dimensionalised variables defined in the same way as previously, except

$$\begin{aligned} \sigma &= L^2\epsilon^2\sigma^*, \\ t &= LU_\infty^{-1}t^*, \end{aligned}$$

this may be written as

$$\frac{2}{\pi}\int_0^1 \frac{\sigma^*_{\xi\xi} + 2\sigma^*_{\xi t^*} + \sigma^*_{t^*t^*}}{\xi - x^*}d\xi = f(t^*) + \frac{2N(t^*)}{\pi}\log|1 - x^*| - \frac{2}{\pi}\int_1^\infty \frac{S^*_\xi(\xi,0)}{\xi - x^*}d\xi, \tag{5.35}$$

which is valid for $x^* < 1$. The boundary conditions for this equation at $x^* = 0$ are $\sigma^* = 0$, from the definition of σ^*, $\sigma^*_{x^*} = 0$, from the definition of S^*, since $\sigma^*_{x^*} = S^*$, and $\sigma^*_{x^*x^*} = S^*{}_{x^*} = 0$, since smooth separation must occur at the leading edge. Thus a solution for σ^* may be obtained, which will be dependent on time for $x^* < 1$ (i.e. the region above the slot), and independent of time for $x^* > 1$, i.e. the blown region. This will lead to a jump discontinuity at $x = L$ in the solution found for S^*. However this merely indicates that the above analysis is invalid in a region of width $L\epsilon$ near the trailing edge, $x^* = 1$. Near $x^* = 1$ it is therefore to be expected that $S^*_{x^*}$ will tend to infinity.

Equation 5.35 may be solved, by use of the inversion formula detailed in section A.2.2, and the inversion for $\log 1 - x^*$ given in appendix B. The boundary conditions are that $\sigma^* = \sigma^*_{x^*} = \sigma^*_{x^*x^*} = 0$ at $x^* = 0$, so the inversion used will be that of equation A.6. The inverse of $f(t)$, which will just be $f(t)$ multiplied by the inverse of 1, is given by equation A.8. Hence

$$\sigma^*_{x^*x^*} + 2\sigma^*_{x^*t^*} + \sigma^*_{t^*t^*} = \frac{1}{2}f(t)\sqrt{\frac{x^*}{1-x^*}} - g_1(x^*) + \frac{N(t)}{\pi}b(x^*). \tag{5.36}$$

where $b(x^*)$ is the inverse of $\log|1-x^*|$, and is given in appendix B, and $g_1(x^*)$ is the inverse of

$$\frac{1}{\pi}\int_1^\infty \frac{S^*_\xi(\xi,0)}{\xi - x^*}d\xi.$$

This may be solved by use of the change of co-ordinates $\zeta = x^* - t^*$, $\eta = x^* + t^*$, to give

$$\begin{aligned}\sigma &= a_1(x^*-t^*) + (x^*+t^*)a_2(x^*-t^*) - g_2(x^*) \\ &+ \int_0^{x^*}\int_0^{\xi}\left(\frac{1}{2}f(z-x^*+t^*)\sqrt{\frac{z}{1-z}} + \frac{1}{\pi}N(z-x^*+t^*)b(z)\right)dz\,d\xi,\end{aligned}$$

where $g_2'' = g_1$ and $g_2(0) = g_2'(0) = 0$. From the boundary conditions that $\sigma = \sigma_x = 0$, it follows that a_1 and a_2 are zero. Therefore, changing the order of integration gives

$$\sigma = -g_2(x^*) + \frac{1}{2\pi}\int_0^{x^*}(1-z)\left(\sqrt{\frac{z}{1-z}}f(z-x^*+t^*) + N(z-x^*+t^*)b(z)\right)dz.$$

Although N is as yet unknown, it may be determined from an ordinary integro-differential equation by substituting the above expression into equation 5.32. Hence σ, and therefore S^* may be found, since $S^* = \sigma^*_{x^*}$. For more details of how this is done, the suction problem of chapter 6 discusses an almost identical system of equations, derived in section 6.2, and solved in sections 6.3, 6.4, and 6.5. The function $g_2(x^*)$ may be easily found from the initial conditions, observing that if $f(t^*) = 1$ for all t^*, the steady state solution will be recovered, with $N(t^*) = 0$, and hence

$$g_2'(x^*) = -S^*(x^*,0) + \sqrt{x^*}\sqrt{1-x^*}.$$

Solutions are not presented here, as it is not the behaviour of the shear layer above the slot that is of interest, but the mass transfer, and the velocity, downstream of the slot, and these are constant on the time scale described here. Hence it is the interactive case that is of most interest, as only changes on this time scale, i.e. $L/U_\infty\epsilon$, or longer, can affect the mass flow.

5.6 Variation Over Two Time Scales

So far it has been assumed that the variation in the slot pressure may be said to take place over any time scale. However for a function such as $f(t) = t$, for $t > 0$, the slot pressure will vary over all time scales. Moreover, since the equations derived are non-linear, it is not possible to super-impose solutions of the different time scales. Here, a system in which changes take place over both the quasi-steady and the interactive time scale will be considered. A suitable example of such a time scale would be $f(t) = \sin t/t_1 + \sin t/t_2$, where $t_1 = L/U_\infty\epsilon^2$ and $t_2 = L/U_\infty\epsilon$. In such a case particular care must be taken with the non-dimensionalisation, and a 'two-tier' non-dimensionalisation must be applied for time,

$$\begin{aligned}x &= Lx^*, \\ t &= LU_\infty^{-1}\epsilon^{-2}t^{(q)} + LU_\infty^{-1}\epsilon^{-1}t^{(i)},\end{aligned}$$

$$
\begin{aligned}
S &= L\epsilon^2\left(S^{(q)}(x^*,t^{(q)}) + S^{(i)}(x^*,t^{(q)},t^{(i)})\right),\\
\phi &= LU_\infty\epsilon\left(\phi^{(q)}(x^*,t^{(q)}) + \phi^{(i)}(x^*,t^{(q)},t^{(i)})\right),\\
f(t) &= f^{(q)}(t^{(q)}) + f^{(i)}(t^{(i)}).
\end{aligned}
$$

The functions $S^{(q)}$ and $\phi^{(q)}$ are the quasi-steady solutions, given by equation 5.31. The functions $S^{(i)}$ and $\phi^{(i)}$ are the deviations from the quasi-steady solutions, which will take place on the interactive time scale, and which are of the same order of magnitude as $S^{(q)}$ and $\phi^{(q)}$ respectively. On application of this non-dimensionalisation into the usual equations, i.e. the pressure balance (equations 5.7,5.11 and 5.13), and the kinematic condition (equation 5.8) the following equations, which are similar to the interactive equations in the form given by equations 5.15 and 5.16 are obtained.

$$
\frac{2}{\pi}\int_0^\infty \frac{S_\xi^{(q)} + S_\xi^{(i)}}{\xi - x^*}d\xi = \begin{cases} f^{(q)} + f^{(i)} & 0 < x^* < 1, \\ f^{(q)} + f^{(i)} - \left(\phi^{(q)} + \phi^{(i)}\right)^2_{x^*} - 2\phi^i_{t^{(i)}} & x^* > 1, \end{cases}
$$

$$
\left\{\left(\phi^{(q)}_{x^*} + \phi^{(i)}_{x^*}\right)\left(S^{(q)} + S^{(i)}\right)\right\}_{x^*} + S^{(i)}_{t^{(i)}} = 0,
$$

observing that all derivatives with respect to $t^{(q)}$ will be an order of magnitude smaller than any other terms. Since $S^{(q)}$ and $\phi^{(q)}$ are the solutions for the quasi-steady equations, i.e. equation 5.30 with $\phi^{(q)}_{x^*}S^{(q)} = M^{(q)}$ a function of $t^{(q)}$ only, the terms in the above equations containing only quasi-steady terms may be subtracted out. Hence the system of equations for variations over the interactive time scale, with variations also taking place over the quasi-steady time scale is

$$
\frac{2}{\pi}\int_0^\infty \frac{S_\xi^{(i)}}{\xi - x^*}d\xi = \begin{cases} f^{(i)} & 0 < x^* < 1, \\ f^{(i)} - 2\phi^{(q)}_{x^*}\phi^{(i)}_{x^*} - {\phi^{(i)}_{x^*}}^2 - 2\phi^{(i)}_{t^{(i)}} & x^* > 1, \end{cases} \tag{5.37}
$$

$$
0 = \left(\phi^{(i)}_{x^*}S^{(q)} + \phi^{(q)}_{x^*}S^{(i)} + \phi^{(i)}_{x^*}S^{(i)}\right)_{x^*} + S^{(i)}_{t^{(i)}}. \tag{5.38}
$$

Here, $f^{(i)}$ is given, and $S^{(q)}$ and $\phi^{(q)}$ are given by equation 5.31.

The asymptotic expressions as x tends to infinity will be similar to those given for the interactive case by equations 5.28 and 5.29. The only difference is that some of the terms which were constant will now be given by functions of $t^{(q)}$. Hence

$$
S^{(i)} = C_0(t^{(q)}) + C_1(t^{(q)})x^{*-1} + C_2(t^{(q)},t^{(i)})x^{*-2}\log x^* + \ldots, \tag{5.39}
$$

$$
\phi^{(i)} = \frac{1}{2}F^{(i)}(t^{(i)}) + x^* + K_1(t^{(q)}) + K_2(t^{(q)},t^{(i)})x^{*-1} + \ldots. \tag{5.40}
$$

Here, as before, $F^{(i)}$ is defined according to $F^{(i)'} = f^{(i)} - 1$. From the definition of $S^{(i)}$ it follows that C_0 and K_1 must be zero, as these contribute to $S^{(q)}$.

Variation over fast and unsteady time scales simultaneously is complicated by the fact that to calculate the pressure in the blown region for the fast case to the same order of magnitude as in the interactive case, i.e. $\rho U_\infty^2\epsilon^2$, it is necessary to examine second order terms in the velocity potential. Nevertheless, the same principles will apply.

5.7 Stability

The stability of the shear layer need only be considered on the interactive time scale, since on the fast time scale the shear layer does not change, and on the quasi-steady time scale the shear layer will scale with $f(t)$. To consider the stability of the shear layer, $S_0^*(x^*)$ may be taken to be a steady-state solution of the system. A test for stability may be conducted by perturbing the steady state solution with a Fourier mode, defined by

$$\begin{aligned} S^*(x^*,t^*) &= S_0^*(x^*) + L\epsilon^2 A e^{i(\omega t^* - kx^*)} \\ \phi^*(x^*,t^*) &= \phi_0^*(x^*) + LU_\infty \epsilon B e^{i(\omega t^* - kx^*)} \end{aligned}$$

where A and B are much less than one (but larger than ϵ) and $\phi_0^*(x^*)$ is the steady state solution. Substitution of this into the interactive equations, i.e. equations 5.15 and 5.16, gives, to first order, for $x^* > 1$,

$$Aike^{-ikx^*}\frac{1}{\pi}\int_0^\infty \frac{e^{ik\xi}}{\xi - x^*}d\xi - iku_0^*B + i\omega B = 0, \tag{5.41}$$

$$Au_{0x^*}^* + Au_0^*ik + BS_0^*(ik)^2 + BS_{0x^*}^*ik - i\omega A = 0, \tag{5.42}$$

where $u_0^* = \phi_{0x^*}^*$. Note that for $x^* < 1$ the only term in the first equation is the Hilbert transform term, which is proportional to zero, and hence A is zero, implying that B is zero so there can be no instabilities. It is therefore sufficient to consider the region $x^* > 1$. In this region, for large k, equation 5.42 may be simplified to

$$(iku_0^* - i\omega)A - k^2 S_0^* B = 0. \tag{5.43}$$

The integral in equation 5.41 may also be simplified, by observing that, if k is positive,

$$\begin{aligned} e^{-ikx^*}\frac{1}{\pi}\int_0^\infty \frac{e^{ik\xi}}{\xi - x^*}d\xi &= \frac{1}{\pi}\int_{-k^{-1}x^*}^\infty \frac{e^{iu}}{u}du, \\ &= \frac{1}{\pi}\int_{-\infty}^\infty \frac{e^{iu}}{u}du - \frac{1}{\pi}\int_{-k^{-1}x^*}^\infty \frac{e^{iu}}{u}du, \\ &= i - O(k^{-1}). \end{aligned} \tag{5.44}$$

For negative k, the result $-i + O(k^{-1})$ is obtained, and so equation 5.41 may be simplified to

$$-A|k| = -(iku_0^* - i\omega)B = 0. \tag{5.45}$$

With these simplifications, it follows from equations 5.43 and 5.45 that non-trivial solutions will exist for A and B only if

$$S_0^* k^2 |k| = -(iku_0^* - i\omega)^2.$$

Hence for sufficiently large k values of ω with negative imaginary part may exist, and so $e^{-i\omega t}$ may grow exponentially. This means that the flow is linearly unstable for $x^* > 1$.

Linear instabilities of separated flow have been studied by many authors, with it known experimentally that a separating laminar flow may break down abruptly as the flow becomes turbulent, see for example Van Dyke (1982) [100]. Non-linear instability was studied by Brown et al (1988) [10], who considered separation from an aerofoil, with a region of constant vorticity beneath the aerofoil, and found instabilities by essentially the same method as described above. Similarity solutions for the breakdown region were then found and solved for both subsonic and supersonic flow. For subsonic flow above a region of zero vorticity, as in the slot injection problem, a symmetric cusped region was found, with the height of the shear layer, the velocity and the pressure being given analytically (equation 5.4 of Brown et al (1988)).

It seems likely that the instabilities for slot injection will be similar, although it is not clear how far downstream of the slot they will occur. The fact that instabilities arise is not entirely surprising, as both the external and the injected region are modelled as being inviscid, with an unstable vortex sheet separating them. However in practice the lower order effects of viscosity often act in order to stabilise the flow, so instabilities may not occur until a considerable distance downstream of the slot. There is some experimental evidence of this in the fact that the shear layers observed by Fitt et al (1985) [34] were observed to be stable. Nevertheless the onset of instabilities and turbulent mixing is an important aspect of film cooling, and would be a useful area for further research.

Chapter 6

Unsteady Slot Suction

6.1 Steady Suction Into a Slot

The unsteady analysis of slot suction detailed in this chapter will follow the two-dimensional analysis of Dewynne et al (1989) [22], in the asymptotic case for low strength slot suction, and so will be similar in kind to the analysis of the blowing problem. Section 4.11 contains further details of the models that have been used for slot suction.

In the steady case the slot pressure will be $p_\infty - \frac{1}{2}\rho U_\infty^2 \epsilon^2$, and the model for the external flow is now that of a series of sinks in the region $0 < x < L$ along the x-axis. A schematic representation is shown in figure 6.1 The streamline that separates at the point $(0,0)$ will be denoted by $\Psi = 0$,

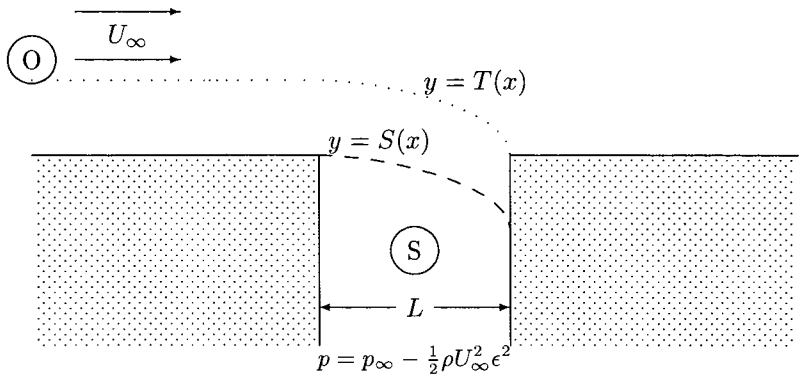

Figure 6.1: Slot suction in a steady system

where Ψ is the stream function for the outer flow. For $x < 0$ it will simply lie on the x-axis, but for $0 < x < L$ it will separate, and the equation of this streamline will be given by $y = L\epsilon^2 S(x)$ in this region.

The crucial difference between linear slot suction and slot injection is that there is no 'blown' region with suction analogous to region F in the injection case. The only two regions are the perturbed

free-stream, and the region beneath the shear layer, in which all velocities are zero. Furthermore since the mass flow is inwards, it comes from the fast moving free-stream, and thus is an order of magnitude larger than in the injection case : as before, the height of the perturbation will be of order $L\epsilon^2$, so as the suction velocity is necessarily U_∞, the mass flow will now be of order $LU_\infty\rho\epsilon^2$, as opposed to the order $LU_\infty\rho\epsilon^3$ appropriate for the injection problem. The conditions on ϵ are that it be small, so that linear asymptotics may be applied, and that the shear layer be of negligible width. As this shear layer is of thickness $O(LRe^{-\frac{1}{2}})$, and the height of the streamline is $O(L\epsilon^2)$, this gives the bounds on ϵ for this model to apply as being

$$Re^{-\frac{1}{4}} \ll \epsilon \ll 1.$$

Non-dimensionalising is done in the same way as in the 'injection' case, except that the mass flow will now be of magnitude $LU_\infty\epsilon^2$. Imposing the condition that the slope of the flow just above this streamline will be $L\epsilon^2 S^{*\prime}(x)$ as before, this leads to a stream function in the outer region given by

$$\Psi = LU_\infty y - \frac{LU_\infty\epsilon^2}{\pi}\int_0^L S^{*\prime}(\xi)\arctan\left(\frac{y}{\xi - x}\right)d\xi. \tag{6.1}$$

(This is just the imaginary part of the complex potential corresponding to the slot injection problem, given by equation 5.2, but with a sign change).

Applying Bernoulli's equation above and below the flow, imposing continuity of pressure across the shear layer, and neglecting velocities in the slot as before, leads to the result that, to lowest order,

$$-\frac{p_b - p_\infty}{\frac{1}{2}\rho U_\infty^2\epsilon^2} = 1 = -\frac{2}{\pi}\int_0^1 \frac{S^{*\prime}(\xi^*)}{\xi^* - x^*}\,d\xi^*. \tag{6.2}$$

This equation, obtained by matching pressures, is the governing equation of the flow, since the stream function may be obtained in terms of S (see equation 6.1). The boundary conditions, as for the analogous slot equation, are derived from the assumption of smooth separation at the leading edge, and are that $S^* = S^*_{x^*} = 0$ at $x^* = 0$.

The solution of this is for $S^{*\prime}$ given in section A.2.3, as being proportional to $\sqrt{\{x/(1-x)\}}$, with the choice of solution determined by the fact that S^* and $S^{*\prime}$ are zero at $x^* = 0$. Integration of this with respect to x^* gives

$$S^*(x^*) = \frac{\sqrt{x^*}\sqrt{1-x^*}}{2} - \frac{\arcsin(\sqrt{x^*})}{2}. \tag{6.3}$$

The streamline which touches the point $(1,0)$ is also of some interest. This is the streamline which divides the part of the flow which will enter the slot from the part which will pass over the slot. This streamline will be denoted by $y = L\epsilon^2 T^*(x^*)$, with the value of Ψ on this streamline given by $\Psi = M$. As with slot injection, ρM will measure the mass transfer into the slot, although now M^* is defined by $M = LU_\infty\epsilon^2 M^*$. With these definitions, $T^*(x^*)$ will be given by

$$LU_\infty\epsilon^2 T^*(x^*) + \frac{LU_\infty\epsilon^2}{2\pi}\int_0^1 \sqrt{\frac{\xi}{1-\xi}}\arctan\left(\frac{\epsilon^2 T^*(x^*)}{\xi - x^*}\right)d\xi = LU_\infty\epsilon^2 M^*. \tag{6.4}$$

The mass flow, M, may be found by evaluating it the top of the slot. This may be done since the vertical velocity, $-\Psi_x$ is known in this region, and may be evaluated along this line using equation 6.3

$$M = \int_0^L \Psi_x(x,0)\,dx = -U_\infty \epsilon^2 \int_0^L S'(x)\,dx = \frac{\pi}{4} L U_\infty \epsilon^2. \tag{6.5}$$

Thus equation 6.4 becomes

$$\epsilon^2 T^*(x^*) + \frac{\epsilon^2}{2\pi} \int_0^1 \sqrt{\frac{\xi}{1-\xi}} \arctan\left(\frac{\epsilon^2 T^*(x^*)}{\xi - x^*}\right) d\xi = \frac{\pi}{4}\epsilon^2 \tag{6.6}$$

Differentiating this equation with respect to x^* produces the result that, to lowest order, T is given by

$$T^{*\prime}(x^*) = \begin{cases} -\frac{1}{2}\sqrt{\frac{x^*}{1-x^*}} & 0 \le x^* < 1, \\ 0 & x^* \le 0, x^* > 1. \end{cases} \tag{6.7}$$

and so the line $y = T^*(x^*)$ is given by

$$T^*(x^*) = \begin{cases} \frac{\pi}{4} & x^* \le 0, \\ \frac{\pi}{4} + \frac{1}{2}\sqrt{x^*}\sqrt{1-x^*} - \frac{1}{2}\arcsin\sqrt{x^*} & 0 \le x^* \le 1 \\ 0 & x^* \ge 1. \end{cases} \tag{6.8}$$

This is consistent with thin aerofoil theory since the velocity in the $y-$direction is given by $-\lim_{y\to 0+} \Psi_x$. Since $T(x)$ and $S(x)$ are both streamlines, they must both be given by $\frac{v}{u} = T'(x) = S'(x)$ both above the slot and in the region to the left of the slot. Since they are both of height $O(L\epsilon^2)$, they are both at $y = 0$ to lowest order, and so the expressions for u and v at $y = T$ and $y = S$ will be the same, so T' and S' will be the same.

6.2 Unsteady Suction

As with the injection problem, the time-dependency of the system in which gas is sucked in the slot will be introduced by making the slot pressure equal to $p - \frac{1}{2}\rho U_\infty^2 \epsilon^2 f(t)$, where $f(t) > 0$. The non-dimensional variable t^* will be defined by $t = L/U_\infty t^*$ so that pressure variations take place over a time scale of unit order of magnitude. This is the natural time scale of the flow, as the velocity is $O(U_\infty)$ throughout the flow. Hence any changes over a time scale larger than this will be quasi-steady.

By modelling the flow outside the slot by potential flow with a series of sources as before, and choosing a source strength such that

$$\frac{D}{Dt}(y - L\epsilon^2 S(x,t)) = 0,$$

one may express the velocity potential in terms of $S(x,t)$

$$\Phi = U_\infty x + \frac{U_\infty \epsilon^2}{2\pi} \int_0^L (S_\xi(\xi,t) + U_\infty^{-1} S_t(\xi,t)) \log\left(\frac{(x-\xi)^2 + y^2}{L^2}\right) d\xi. \tag{6.9}$$

Note that, as in the injection case, $S(x,t)$ is no longer a streamline is the shear layer dividing the external flow from the static flow in the slot.

The mass transfer at the top the slot, $LU_\infty\epsilon^2 M_0(t)$ may be evaluated to give

$$LU_\infty\epsilon^2 M_0(t) = -\int_0^1 \Phi_y(x,0,t)\,dx = -U_\infty\epsilon^2(\sigma_x(1,t) + U_\infty^{-1}\sigma_t(1,t)). \tag{6.10}$$

where $\sigma(x,t)$ is defined by $\sigma_x = S$ and $\sigma(0,t) = 0$. Bernoulli's equation will now contain a Φ_t term and, taking the limit as y tends to $S(x,t)$ from above, the pressure at the boundary will be given by

$$\begin{aligned}\frac{p_b - p_\infty}{\frac{1}{2}\rho U_\infty^2\epsilon^2} &= -\frac{\Phi_x^2|_{y=S(x,t)} + 2\Phi_t|_{y=S(x,t)} - \Phi_x^2|_\infty - 2\Phi_t|_\infty}{U_\infty^2\epsilon^2} \\ &= \frac{2}{\pi}\int_0^L \frac{U_\infty^{-2}\sigma_{tt} + 2U_\infty^{-1}\sigma_{\xi t} + \sigma_{\xi\xi}}{\xi - x}\,d\xi + \frac{2}{\pi}M_0'(t)\log\left(\frac{L-x}{L}\right).\end{aligned}$$

Since velocities are zero in the slot, the left-hand side of the equation will be equal to the non-dimensionalised static pressure at the bottom of the slot, which is maintained at $-f(t)$. In non-dimensionalised co-ordinates this reduces to

$$-f(t) = \frac{2}{\pi}\int_0^1 \frac{\sigma^*_{t^*t^*} + 2\sigma_{\xi^*t^*} + \sigma^*_{\xi^*\xi^*}}{\xi^* - x^*}\,d\xi^* + \frac{2}{\pi}M_0{}'(t^*)\log(1-x^*). \tag{6.11}$$

This is the unsteady version of equation 6.2, and may be expressed entirely in terms of σ by applying the non-dimensionalised version of equation 6.10. The boundary conditions on σ^* are that $\sigma^* = \sigma_{x^*} = \sigma_{x^*x^*} = 0$, since the flow is assumed to separate smoothly. Initial conditions are needed for σ and σ_{t^*}. This equation may be inverted according to the formulae described in section A.2.2, with the condition that all the derivatives of σ^* up to second order in x^* are zero implying that the formula used in equation A.6 is the required version to use, with no singularity in the inverse transform at $x^* = 0$. This gives

$$\sigma_{x^*x^*} + 2\sigma_{x^*t^*} + \sigma_{t^*t^*} = -\frac{f(t^*)}{2}\sqrt{\frac{x^*}{1-x^*}} - \frac{1}{\pi}M_0{}'(t^*)b(x^*), \tag{6.12}$$

where $b(x^*)$ is given by

$$b(x^*) = -\frac{1}{\pi}\sqrt{\frac{x^*}{1-x^*}}\int_0^1 \sqrt{\frac{1-\xi}{\xi}}\frac{\log(1-\xi)}{\xi - x^*}\,d\xi,$$

to give

$$b(x^*) = 2\left(\arcsin\sqrt{x^*} - \log 2\sqrt{\frac{x^*}{1-x^*}}\right), \tag{6.13}$$

(see appendix B). Note that the system of equations given by equation 6.12 and 6.10 is very similar to those for fast injection, given by equations 5.36 and 5.32, with N replaced by $-M_0'$. This result has implications for the problem where injection and suction both take place over a period of time and is discussed in section 7.4.

For a given M_0, equation 6.12 is a parabolic second order partial differential equation. This may be solved by changing co-ordinates from (x^*, t^*) to $(\xi, \eta) = (x^* + t^*, x^* - t^*)$ and integrating twice with respect to ξ. Hence σ is given in terms of M_0 as

$$\sigma = a_1(x^* - t^*) + (x^* + t^*)a_2(x^* - t^*)$$

$$- \int_0^{x^*} \int_0^{x_1} \frac{1}{2} f(x_2 - x^* + t^*) \sqrt{\frac{x_2}{1-x_2}}\, dx_2\, dx_1$$
$$- \frac{1}{\pi} \int_0^{x^*} \int_0^{x_1} M_0'(x_2 - x^* + t^*) b(x_2)\, dx_2\, dx_1, \qquad (6.14)$$

where a_1 and a_2 are functions which may be determined from the boundary conditions. As the boundary conditions are $\sigma = \sigma_{x^*} = 0$ at $x^* = 0$ it turns out that a_1 and a_2 are identically equal to zero.

The solution for σ above assumes that $f(t)$ and $M_0(t)$ are defined for all t, including $t < 0$. This requires some care when solving the equations. In particular if suction commences at $t = 0$ (with $f(t) = 1$ for all $t > 0$, say), with the system being described by free stream flow with no suction for all $t < 0$ then the correct form for $f(t)$ is $f(t) = H(t)$ which will *not* give the same solution as $f(t) = 1$. This means that the form of the solution at a given time depends not only on the strength of the suction, but on the history of the strength of the suction.

On substitution of equation 6.10 into the expression for σ defined by equation 6.14, an integral equation may be obtained for $M_0(t^*)$,

$$M_0(t^*) = \int_0^1 \frac{1}{2} f(x_1 - 1 + t^*) \sqrt{\frac{x_1}{1-x_1}}\, dx_1 + \frac{1}{\pi} \int_0^1 M_0'(x_1 - 1 + t^*) b(x_1)\, dx_1. \qquad (6.15)$$

From the linearised part of the theory of Dewynne et al (1989) [22] it is known that the particle path that attaches at the trailing edge is within order $L\epsilon^3$ of the particle path that divides the part of the flow that is sucked into the slot from the part that is not. Therefore these may be considered as the same particle path, and will be denoted by $y = L\epsilon^2 T^*(x^*, t)$. This particle path may be evaluated, as in the steady case, from the equation

$$\epsilon^2 M(x^*, t^*) = \epsilon^2 T(x^*, t^*) - \frac{1}{\pi} \int_0^1 (S^*_{\xi^*} + S^*_{t^*}) \arctan\left(\frac{\epsilon^2 T(\xi^*, t^*)}{\xi^* - x^*}\right) d\xi^*,$$

by differentiating with respect to time. However in the steady case the equation derived from this condition was found to be equivalent to that obtained from the condition that the line $y = L\epsilon^2 T(x,t)$ is a streamline, i.e. $\frac{D}{Dt}(y - L\epsilon^2 T(x,t)) = 0$ on $y = L\epsilon^2 T(x,t)$. Re-writing this as

$$v = uT_x + T_t,$$

expressions for $T(x,t)$ may be found in the three regions of the flow, since $v = \Phi_y$ is given in terms of $\sigma(x,t)$ from equation 6.9, and $u = U_\infty$ to lowest order.

- For $x < 0$, $v = 0$ to lowest order and $u = U_\infty$ so this condition leads to $T^*_{x^*} + T^*_{t^*} = 0$, or $T^*(x^*, t^*) = c_1(x^* - t^*)$ in this region.
- For $0 < x < L$, $v = L\epsilon^2(S^*_{x^*} + S^*_{t^*})$ and hence $T^*(x^*, t^*) = S^*(x^*, t^*) + c_2(x^* - t^*)$ in this region.
- For $x > L$, $v = 0$ to lowest order, so again $T^*_{x^*} + T_{t^*} = 0$, or $T^*(x^*, t^*) = c_3(x^* - t^*)$ in this region. Since T^* is defined by the condition that $T^*(1, t^*) = 0$ for all t^*, c_3 must be identically equal to zero in this region. Hence T^* is everywhere zero in this region.

The functions $c_1(x^* - t^*)$ and $c_2(x^* - t^*)$ may be found by imposing continuity of $T(x,t)$ at $x^* = 0$ and $x^* = 1$. This gives $c_1(\xi) = c_2(\xi) = -S^*(1-\xi)$. Thus $T^*(x^*,t^*)$ may be found given $S^*(x^*,t^*)$. Since the integral equation for $S^*(x^*,t^*)$ involves $M_0(x^*,t^*)$ the next step is to solve the integral equation for $M_0(x^*,t^*)$ for a given $f(t^*)$, i.e. equation 6.15, which will henceforth be referred to as the *mass transfer equation.*

6.3 General Solution of the Mass Transfer Equation

Henceforth the asterisk notation used to denote non-dimensional quantities will be omitted. The mass transfer equation, equation 6.15 may therefore be written in the form.

$$M_0(t) = \int_0^1 \frac{1}{2} f(x_1 - 1 + t)\sqrt{\frac{x_1}{1-x_1}}\, dx_1 + \frac{1}{\pi}\int_0^1 M_0'(x_1 - 1 + t)b(x_1)\, dx_1.$$

An immediate feature of the mass transfer equation is that it exhibits a linear dependence on $f(t)$, i.e. if $M_0^{(1)}(t)$ is a solution for $f^{(1)}(t)$ and $M_0^{(2)}(t)$ is a solution for $f^{(2)}(t)$ then $M_0^{(1)}(t) + kM_0^{(2)}(t)$ is a solution for $f^{(1)}(t) + kf^{(2)}(t)$ for any constant k. It may also be differentiated through with respect to time, so that if M_0 is a solution for f, then M_0' will be a solution for f'. Furthermore the steady state solution, $M_0(t) = \frac{\pi}{4}$, is clearly a solution when $f(t) = 1$, agreeing with the previous steady analysis. Two different solution techniques have been used to solve this equation analytically, suitable for different choices of $f(t)$: the method of degenerate kernel, and the use of integral transformations.

6.3.1 The Method of Degenerate Kernel

The method of degenerate kernel is suitable when the function $f(t)$ satisfies the condition that $f(x - t + 1)$ may be written as a linear combination of a finite number of separable functions, i.e.

$$f(x - t + 1) = \sum_{i=1}^{n} a_i(x)b_i(t),$$

where all of the functions $b_i(t)$ satisfy the same condition, i.e.

$$b_i(x - t + 1) = \sum_{j=1}^{n} c_i(x)b_i(t),$$

the solution is $M_0 = \sum A_i b_i(t)$ where the A_i may be found by direct substitution. Examples of possible functions $f(t)$ for which this method is applicable include $f(t) = t$ and $f(t) = \sin \nu t$. Although neither of these is a valid choice for $f(t)$ in this system since a condition for the validity of this model is that $f(t) > 0$, the solutions are of interest owing to the property of linearity which means that given the solution for $f(t) = \sin t$ a more physically useful solution such as that for $f(t) = 1 + \sin t$ may easily be obtained. They also apply to the case where injection and suction both take place over a period of time, discussed in section 7.4. Furthermore the solution for $f(t) = t$ should provide a guide as to the behaviour of $f(t) = tH(t)$ (where $H(t)$ is the Heaviside step function) for large t. Other possible

choices for $f(t)$ for which this method could be applied include any linear combination of $f(t) = t^n$, where n is a non-negative integer, and trigonometric and exponential functions. The solutions for $f(t) = t$ and $f(t) = \sin \nu t$ are given in sections 6.4.1 and 6.4.2 respectively.

6.3.2 Solution Using Integral Transformations

The integral transformations used to solve the mass transfer equation are Laplace and Fourier transforms : this method is suitable when $f(t)$ is a linear combination of functions which possess a Fourier or Laplace transform. Realistic examples of functions $f(t)$ for which Laplace transforms may be used include $H(t)$, $tH(t)$, $H(t)\sin \nu t$, $H(t)e^t$; examples for which Fourier transforms are applicable include $\sin \nu t$ and $\delta(t)$.

Before taking Laplace transforms it is convenient to re-write the integrals in the mass transfer equation (equation 6.15), as being over the range $(0, \infty)$, i.e.

$$\begin{aligned} M_0(t) = & \frac{1}{2}\int_0^\infty f(x_1 - 1 + t)\sqrt{\frac{x_1}{1-x_1}}H(1-x_1)\,dx_1 \\ + & \frac{1}{\pi}\int_0^\infty M_0(x_1 - 1 + t)b(x_1)H(1-x_1)\,dx_1. \end{aligned} \tag{6.16}$$

The two integrals on the right-hand side are convolutions. This follows as they may both be written in the form

$$\int_{-\infty}^{\infty} h_1(x_1 - 1 + t)h_2(1 - x_1)dx_1,$$

where $h_1(x_1)$ is zero for negative x_1 and $h_2(x_1)$ is zero outside the region $[-1, 1]$. The first function will be zero for $x_1 < 1 - t$ and the second will be zero for $x_1 > 1$, so the value of the above integral will not be changed if the limits of the integral are replaced by $1 - t$ and 1. On substitution of $u = 1 - x_1$, the above integral is

$$\int_0^t h_1(t-u)h_2(u)du,$$

which is the usual form for a convolution.

It is now necessary to evaluate the transforms of the part of the integrands that are functions of x_1 only. The first of these is

$$\begin{aligned} \int_0^\infty \sqrt{\frac{x}{1-x}}e^{-px}H(1-x)\,dx &= \int_0^1 \sqrt{\frac{x}{1-x}}e^{-px}\,dx \\ &= -\frac{d}{dp}\int_0^1 \frac{e^{-px}}{x^{\frac{1}{2}}(1-x)^{\frac{1}{2}}}\,dx \\ &= -\frac{d}{dp}\int_0^\pi e^{-\frac{p}{2}}e^{\frac{p}{2}\cos\theta}d\theta. \end{aligned}$$

The modified Bessel function $I_0(p)$ is given by the integral representation (see, for example, Abramowitz & Stegun (1964) [1])

$$I_0(z) = \frac{1}{\pi}\int_0^\pi e^{\pm z\cos\theta}d\theta.$$

Hence the above integral is

$$\begin{aligned}\int_0^\infty \sqrt{\frac{x}{1-x}}e^{-px}H(1-x)\,dx &= -\pi\frac{d}{dp}\left(e^{-\frac{p}{2}}I_0\left(-\frac{p}{2}\right)\right)\\ &= \frac{\pi}{2}e^{-\frac{p}{2}}I_0\left(\frac{p}{2}\right)+\frac{\pi}{2}e^{-\frac{p}{2}}I_0'\left(-\frac{p}{2}\right)\\ &= \frac{\pi}{2}e^{-\frac{p}{2}}\left(I_0\left(\frac{p}{2}\right)-I_1\left(\frac{p}{2}\right)\right),\end{aligned} \tag{6.17}$$

using elementary properties of the modified Bessel functions. The other transform required is the Laplace transform of $b(x_1)H(1-x_1)$. In order to evaluate this integral it is necessary to evaluate the Laplace transform of $H(1-x_1)\arcsin\sqrt{x_1}$.

$$\int_0^\infty e^{-px}\arcsin\sqrt{x}H(1-x)\,dx = \int_0^1 e^{-px}\arcsin\sqrt{x}\,dx$$

$$\begin{aligned}&= \left[\frac{e^{-px}}{-p}\arcsin\sqrt{x}\right]_0^1+\frac{1}{p}\int_0^1\frac{e^{-px}}{2}x^{-\frac{1}{2}}(1-x)^{-\frac{1}{2}}\,dx\\ &= \frac{\pi e^{-p}}{-2p}+\frac{\pi}{2p}e^{-\frac{p}{2}}I_0\left(\frac{p}{2}\right)\\ &= \frac{\pi}{2}e^{-\frac{p}{2}}\left(\frac{I_0\left(\frac{p}{2}\right)}{p}-\frac{e^{-\frac{p}{2}}}{p}\right).\end{aligned}$$

The Laplace transform of b is then a linear combination of this expression and that obtained from equation 6.17 according to the expression for $b(x)$ given by equation 6.13.

Now, by taking Laplace transforms of equation 6.16 and writing the Laplace transforms of $M_0(t)$ and $f(t)$ as $\overline{M}_0(p)$ and $\overline{f}(p)$ respectively, the following expression may be obtained for $\overline{M}_0$.

$$\overline{M}_0(p) = \frac{\pi}{4}\overline{f}(p)\frac{I_0\left(\frac{p}{2}\right)+I_1\left(\frac{p}{2}\right)}{I_0\left(\frac{p}{2}\right)+p\log 2\left(I_0\left(\frac{p}{2}\right)+I_1\left(\frac{p}{2}\right)\right)}. \tag{6.18}$$

This is valid when $f(t)=0$ for all $t\le 0$ and $M_0(t)=0$ for all $t\le 0$.

If $f(t)$ is non-zero for $t<0$ then it is necessary, where possible, to take Fourier transforms, which leads to the similar formula

$$\tilde{M}_0(\omega) = \frac{\pi}{4}\tilde{f}(\omega)\frac{J_0\left(\frac{\omega}{2}\right)+iJ_1\left(\frac{\omega}{2}\right)}{J_0\left(\frac{\omega}{2}\right)+i\omega\log 2\left(J_0\left(\frac{\omega}{2}\right)+J_1\left(\frac{\omega}{2}\right)\right)}. \tag{6.19}$$

where J_0, J_1 denote Bessel functions and $\tilde{f}$ and $\tilde{M}_0$ denote the Fourier transforms of f and M_0 respectively. This expression is valid for Fourier transformable functions f such as $f(t)=\sin\nu t$, for which a solution is given in section 6.4.2.

6.3.3 The singularities of $\overline{M}_0$

In order to invert this integral it is necessary to determine the poles of $\overline{M}_0$ and evaluate the residues. It is clear from equation 6.18 that poles of $\overline{f}(p)$ will be poles of $\overline{M}_0$, and since I_0 and I_1 are analytic everywhere the only other singularities will be poles of the denominator in the right-hand side, which will henceforth be denoted by $g(p)$, i.e.

$$g(p) = I_0\left(\frac{p}{2}\right)+p\log 2\left(I_0\left(\frac{p}{2}\right)+I_1\left(\frac{p}{2}\right)\right).$$

Since the function $g(p)$ satisfies

$$g(\overline{p}) = \overline{g}(p),$$

the poles occur in conjugate pairs. All the poles may therefore be written as $-\lambda_i \pm i\mu_i$ where the λ_i are all real and the μ_i are positive real numbers. Using the Newton-Raphson method 320 pairs of simple roots have been found, of which the corresponding values of λ_i and μ_i for the first 6 roots are shown in the table below.

	$i=1$	$i=2$	$i=3$	$i=4$	$i=5$	$i=6$
λ_i	2.530	3.774	4.277	4.609	4.857	5.056
μ_i	1.983	8.976	15.409	21.763	28.088	34.400

It may be shown from the asymptotic analysis in section 6.3.4 that there are an infinite number of poles. The residue of $e^{pt}\overline{M}_0(p)$ at the poles, $-\lambda_i \pm i\mu_i$ is given by

$$\frac{\pi}{4}\sum_{i=1}^{\infty} e^{-\lambda_i t}(\alpha_i \cos\mu_i t + \beta_i \sin\mu_i t),$$

where the α_i and β_i are real numbers given by

$$\alpha_i - i\beta_i = 4\overline{f}(p_i)\frac{I_0\left(\frac{p_i}{2}\right) + I_1\left(\frac{p_i}{2}\right)}{I_0\left(\frac{p_i}{2}\right)\log 2\,(2+p_i) + I_1\left(\frac{p_i}{2}\right)(1+p_i\log 2)}, \tag{6.20}$$

with $p_i = -\lambda_i + i\mu_i$.

Clearly the assumption that all the poles p_i lie to the left of the imaginary axis in the $p-$plane, i.e. all the λ_i are positive, is necessary in order to prevent an exponentially increasing mass transfer function in those of the above examples where Laplace transforms are used. It is also relevant to the case when Fourier transforms are used, for example when $f(t) = 1$. In this case it is to be expected that the only solution is $M_0(t) = \frac{\pi}{4}$, i.e. the steady state solution. However substitution of $f(t) = 1$ into equation 6.19 gives

$$M_0(t) = \frac{1}{2\pi}\frac{\pi}{4}\int_{-\infty}^{\infty} \frac{-2e^{i\omega t}}{i\omega}\frac{J_0\left(\frac{\omega}{2}\right) + iJ_1\left(\frac{\omega}{2}\right)}{J_0\left(\frac{\omega}{2}\right) + i\omega\log 2\left(J_0\left(\frac{\omega}{2}\right) + iJ_1\left(\frac{\omega}{2}\right)\right)}, \tag{6.21}$$

since $\tilde{f}(\omega) = -\frac{2}{i\omega}$. The integral on the right-hand side of the above equation may be evaluated using a contour which closes in the upper half-plane, and in the neighbourhood of the pole at $\omega = 0$ takes the shape of a semi-circle, the radius of which will tend to zero. The other poles of the integrand will be at ip_i, i.e. $\mp\mu_i - i\lambda_i$. Hence the assumption that all the p_i (or, more precisely, all the p_i with non-zero residue) lie to the left-hand side of the imaginary axis is equivalent to all of the poles in the integrand above being outside the contour. If this is the case then evaluation of the above integral gives $M_0(t) = \frac{\pi}{4}$otherwise there will be additional terms of the form $e^{-\lambda_i t}(\alpha_i \cos\omega t + \beta_i \sin\mu_i t)$. Hence the assumption that the p_i lie to the left of the imaginary axis is equivalent to $M_0(t) = \frac{\pi}{4}$ being the unique solution when $f(t) = 1$. Due to the linearity of the mass transfer equation this is also equivalent to the statement that

$$M_0(t) = \frac{1}{\pi}\int_0^1 M_0'(x-1+t)b(x)\,dx$$

has no non-zero solution.

The question of whether $g(p)$ has any multiple roots is also of interest, since this will affect the form of the solution for $M_0(t)$. If there were a multiple root then $g'(p)$ would have to equal zero at a root of $g(p)$. In other words the equations

$$\begin{aligned} g(p) &= (1+p\log 2)\, I_0(p/2) + (p\log 2)\, I_1(p/2) = 0, \\ g'(p) &= \left(\log 2 + \frac{1}{2}p\log 2\right) I_0(p/2) + \left(\frac{1}{2} + \frac{1}{2}p\log 2\right) I_1(p/2) = 0. \end{aligned}$$

must have a simultaneous solution. By comparing the ratios of the coefficients of I_0 and I_1 this requires that

$$\frac{1+p\log 2}{p\log 2} = \frac{2\log 2 + p\log 2}{1+p\log 2}.$$

The solution to the above equation is

$$p = \frac{1}{2\log 2(\log 2 - 1)}.$$

which is clearly a real number, and so will not be a root of $g(p) = 0$, since $g(p)$ has no real roots. Hence the functions $g(p)$ and $g'(p)$ have no common roots and so $g(p)$ will have no multiple roots.

6.3.4 Asymptotic Behaviour of the Poles of $\overline{M}_0$

Another feature of the poles p_n that is of interest is the nature of them as $n \to \infty$. In order to simplify this problem the transformation $\omega = ip$ will be used, so that the function $g(p)$ becomes

$$g(\omega) = J_0\left(\frac{\omega}{2}\right) - i\omega\log 2\left(J_0\left(\frac{\omega}{2}\right) - iJ_1\left(\frac{\omega}{2}\right)\right).$$

The asymptotic behaviour of the Bessel functions J_0 and J_1 for large z is given by, from e.g. Abramowitz & Stegun (1964) [1],

$$\begin{aligned} J_0(z) &\sim \sqrt{\frac{2}{\pi z}}\left(\sin\left(z+\frac{\pi}{4}\right) - \frac{1}{8z}\cos\left(z+\frac{\pi}{4}\right) + o(z^{-2}\sin z)\right), \\ J_1(z) &\sim -\sqrt{\frac{2}{\pi z}}\left(\cos\left(z+\frac{\pi}{4}\right) - \frac{3}{8z}\sin\left(z+\frac{\pi}{4}\right) + o(z^{-2}\sin z)\right), \end{aligned}$$

for $|\arg z| < \pi$. Substituting this into the expression for $g(\omega)$ gives

$$g(\omega) \sim \sqrt{\frac{4}{\pi\omega}}\begin{pmatrix} \omega\log 2\cos(\frac{\omega}{2}+\frac{\pi}{4}) - i\omega\log 2\sin(\frac{\omega}{2}+\frac{\pi}{4}) \\ +\frac{i\log 2}{4}\cos(\frac{\omega}{2}+\frac{\pi}{4}) + (1-\frac{3}{4}\log 2)\sin(\frac{\omega}{2}+\frac{\pi}{4}) + o(w^{-1}\sin\frac{w}{2}) \end{pmatrix}. \tag{6.22}$$

This expression will be valid for all positive x, where $\omega = x + iy$. The fact that the roots of $g(p)$ are of the form $-\lambda_i \pm i\mu_i$, where λ_i and μ_i are positive real numbers, means that the roots of $g(\omega)$ will be of the form $\pm x + iy$ where x is positive and y is negative. Hence it is sufficient to look for the roots in the right-hand half of the complex plane. In the above expression the dominant terms for large values of ω, once the common factor has been divided out, will be

$$\omega\log 2\left(\cos\left(\frac{\omega}{2}+\frac{\pi}{4}\right) - i\sin\left(\frac{\omega}{2}+\frac{\pi}{4}\right)\right) = \omega\log 2\exp\left(-i\left(\frac{\omega}{2}+\frac{\pi}{4}\right)\right) = O(\omega e^{\frac{y}{2}}).$$

At a root of $g(\omega)$, this term will have to cancel with the next largest term, which will be of order $\cos\left(\frac{\omega}{2}\right)$, i.e. $e^{|\frac{y}{2}|}$. This is clearly not possible for positive y, since the above term will be $\omega e^{\frac{y}{2}}$, which will not cancel with $e^{\frac{y}{2}}$ for large values of ω. Hence it is necessary to look for values of ω in the lower half of the complex plane, i.e. $y < 0$. When this is the case, cancellation will occur provided $e^{\frac{y}{2}}$ is of the same order of magnitude as $\omega e^{-\frac{y}{2}}$. This requires $e^y \sim x$.

Substituting $\omega = x + iy$ into equation 6.22, and ignoring terms which are of an order of magnitude less than $e^{-\frac{y}{2}}$ gives

$$2x\log 2e^{-\frac{ix}{2}}e^{\frac{y}{2}}e^{-\frac{i\pi}{4}} - (1-\frac{3}{4}\log 2)ie^{\frac{ix}{2}}e^{\frac{-y}{2}}e^{\frac{i\pi}{4}} + \frac{i}{4}\log 2e^{\frac{ix}{2}}e^{-\frac{y}{2}}e^{\frac{i\pi}{4}} = 0,$$

and hence

$$2x\log 2 = (\log 2 - 1)e^{ix}e^{-y}.$$

From the last equation it follows that e^{ix} must be a negative real number (since $\log 2 - 1$ is negative), and hence

$$x = (2n+1)\pi, \qquad n \text{ an integer.}$$

From this, y may be calculated to give

$$y = \log\left(\frac{1-\log 2}{2x\log 2}\right).$$

This analysis shows that there are no roots of $g(\omega)$ in the upper half plane, and so there are no roots of $g(p)$ in the right half plane, for large values of $|p|$. Since there are no roots of $g(p)$ for small p (since the $I_0(p)$ term, which is non-zero dominates), this means that if any roots of $I(p)$ in the right-hand plane were to exist, they would necessarily be of order 1. As no such roots have been found, and any such roots would imply non-uniqueness of the steady solution (see section 6.3.3), it will henceforth be assumed that no such roots exist.

The asymptotic behaviour for the λ_n and μ_n as $n \to \infty$ is given by the above expressions for x and y as being

$$\begin{aligned}\mu_n &= (2n+1)\pi + o(1/n),\\ \lambda_n &= \log\left(\frac{2\log 2(2n+1)\pi}{1-\log 2}\right) + o(1/n).\end{aligned}$$

Values of this asymptotic profile are plotted against the calculated values of $-\lambda_i + i\mu_i$ in figure 6.2, and these show that the calculated values tend quickly to the asymptotic behaviour.

This asymptotic behaviour is crucial in determining the convergence of the series which makes up the 'correction term' in the expressions given above for the mass transfer M_0, i.e.

$$\sum_{i=1}^{\infty} e^{-\lambda_i t}(\alpha_i \cos\mu_i t + \beta_i \sin\mu_i t).$$

Clearly it is necessary that this series converges for the above results to be meaningful. A question that also arises in the calculation of the height of the shear layer, $S(x,t)$, is whether the first and

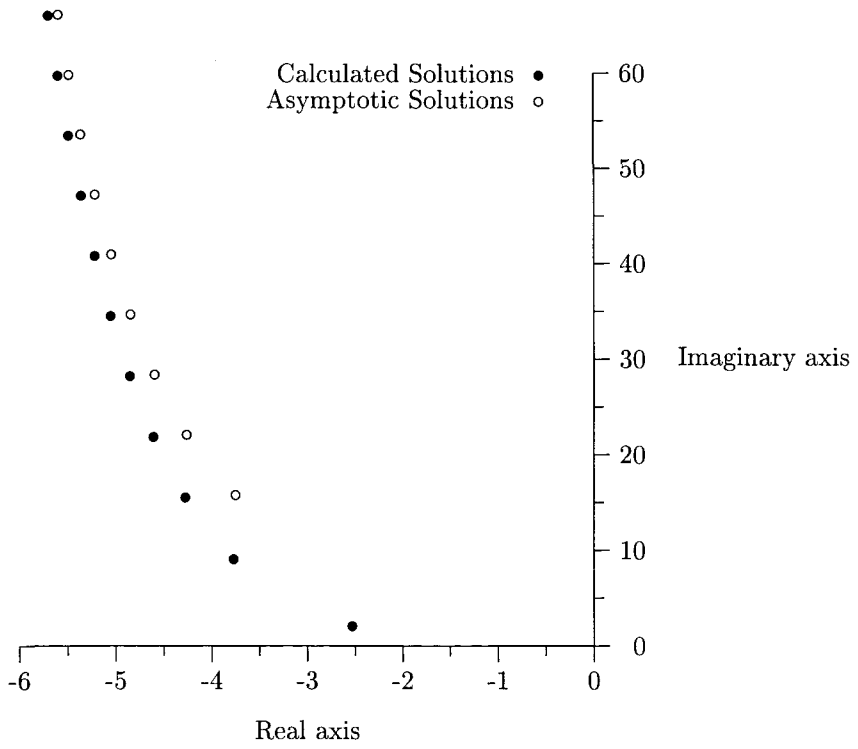

Figure 6.2: The First Eleven Poles of $g(p)$ in the Upper Half-Plane

second derivatives of the following series will converge. Since the α_i depend on the function $f(t)$, this will depend crucially on the function $f(t)$. On substitution of the appropriate asymptotic expansion for the modified Bessel functions into equation 6.20, the following asymptotic expression is obtained for α_i and β_i :

$$\alpha_i - i\beta_i = 4\overline{f}(p)\frac{i}{ip_i \log 2 + \log 2e^{-p} - \frac{1}{2}e^{-p}}. \tag{6.23}$$

Substitution of $p_i = -\lambda_i + \mu_i$ into the above equation gives an expression for α_i and β_i which will be of order $\frac{\overline{f}(p_i)}{p_i}$. Since for large values of i the p_i resemble odd multiples of π, the sum of the α_i and β_i will be convergent for any function $f(t)$ provided $\overline{f}(p)$ tends to zero for large p. (The sum of the α_i will be equal to the correction term in the mass transfer function at $t = 0$). Thus the functions chosen above, $f(t) = H(t)$, $f(t) = tH(t)$ etc will all satisfy these conditions and so the mass transfer will be finite. However it will not always be possible to differentiate term by term, since with each differentiation a factor of μ_n comes out. For example with $f(t) = H(t)$ the α_n will be of order n^{-2} and so the terms $\mu_n\alpha_n$ will be of order n^{-1} and so the series will not converge at $t = 0$. However the term $e^{-\lambda_n t}$ will be of order n^{-t} (since $\lambda = o(\log \mu) = o(\log n)$ and so for positive t the series will converge. Hence the expression obtained for the correction to the mass transfer will be differentiable for all positive t, but the mass transfer will not be differentiable for $t = 0$.

6.4 Particular Solutions of the Mass Transfer Equation

6.4.1 $f(t) = t$

When $f(t) = t$, the solution expected from the method of degenerate kernel will be $M_0 = At+B$, where A and B are constants. This may easily be verified, and A and B evaluated, by direct substitution into the mass transfer equation (equation 6.15) to give

$$At + B = \frac{1}{2}\int_0^1 (x-1)\sqrt{\frac{x}{1-x}}\,dx + \frac{1}{2}t\int_0^1 \sqrt{\frac{x}{1-x}}\,dx + \frac{1}{\pi}\int_0^1 Ab(x)\,dx.$$

Since this must be true for all t, the coefficients of t must be equal to give

$$A = \frac{1}{2}\int_0^1 \sqrt{\frac{x}{1-x}}\,dx = \frac{\pi}{4},$$

and hence

$$B = -\frac{1}{2}\int_0^1 \sqrt{\frac{x}{1-x}} + \frac{1}{4}\int_0^1 b(x)\,dx = \frac{\pi}{16} - \frac{\pi}{4}\log 2.$$

This gives the solution for $M_0(t)$ for the case when $f(t) = t$ as

$$M_0(t) = \frac{\pi}{4}t + \frac{\pi}{16} - \frac{\pi}{4}\log 2. \tag{6.24}$$

Since the fact that $f(t) < 0$ for $t < 0$ means that such a choice for $f(t)$ is not strictly valid, nevertheless it does provide a clear and simple example of how this method of solution works. Furthermore since this method may be applied for any polynomial function, a solution may be found using this method for any function $f(t)$ satisfying $f(t) = \sum a_n t^n$. Furthermore this method may be expected to be a good approximation for large t in the case when $f(t) = tH(t)$, and it is shown in example 6.4.3 that this is indeed the case.

6.4.2 $f(t) = \sin \nu t$

A more useful example for which the method of degenerate kernel may be used is that for which $f(t) = \sin \nu t$ for all t, where ν is a positive real number. Although $f(t) = \sin t$ is not itself a valid choice of $f(t)$ for the suction problem, the mass transfer function for choices of $f(t)$ such as $f(t) = 1 + \sin \nu t$ and $f(t) = \sin^2 \nu t$ are easily deduced from the solution for $f(t) = \sin \nu t$. As in the previous example, the integrands may be separated by elementary trigonometric formulae with the solution for $M_0(t)$ being $M_0(t) = A\cos \nu t + B \sin \nu t$. By substituting this into the mass transfer equation, A and B may be found directly via some involved algebra. However it is simpler to solve the equation using Fourier transforms. The Fourier transform of $f(t) = \sin \nu t$ is given by $\tilde{f}(\omega) = \pi i(\delta(\nu + \omega) - \delta(\nu - \omega))$. Substituting this into equation 6.19 gives

$$\tilde{M_0}(\omega) = \frac{\pi}{4}\frac{(J_0\left(\frac{\omega}{2}\right) + iJ_1\left(\frac{\omega}{2}\right))\pi i(\delta(\nu+\omega) - \delta(\nu-\omega))}{J_0\left(\frac{\omega}{2}\right) + i\omega\log 2\left(J_0\left(\frac{\omega}{2}\right) + J_1\left(\frac{\omega}{2}\right)\right)}.$$

Inverting this transform gives (for $\nu \geq 0$).

$$M_0(t) = \frac{\pi}{4} \cdot \frac{\pi i}{2\pi} \begin{bmatrix} e^{-i\nu t}\left(\frac{(J_0(\frac{-\nu}{2})+iJ_1(\frac{-\nu}{2}))}{J_0(\frac{-\nu}{2})-i\nu\log 2(J_0(\frac{-\nu}{2})+J_1(\frac{-\nu}{2}))}\right) \\ - \quad e^{i\nu t}\left(\frac{(J_0(\frac{\nu}{2})+iJ_1(\frac{\nu}{2}))}{J_0(\frac{\nu}{2})+i\nu\log 2(J_0(\frac{\nu}{2})+J_1(\frac{\nu}{2}))}\right) \end{bmatrix},$$

which yields

$$M_0(t) = A_\nu \cos \nu t + B_\nu \sin \nu t, \tag{6.25}$$

where

$$A_\nu = \frac{\pi}{4} \frac{J_0\left(\frac{\nu}{2}\right) J_1\left(\frac{\nu}{2}\right) - \nu \log 2 \left(J_0^2\left(\frac{\nu}{2}\right) + J_1^2\left(\frac{\nu}{2}\right)\right)}{J_0^2\left(\frac{\nu}{2}\right) - 2\nu \log 2 J_0\left(\frac{\nu}{2}\right) J_1\left(\frac{\nu}{2}\right) + \nu^2 (\log 2)^2 \left(J_0^2\left(\frac{\nu}{2}\right) + J_1^2\left(\frac{\nu}{2}\right)\right)}, \tag{6.26}$$

$$B_\nu = \frac{\pi}{4} \frac{J_0^2\left(\frac{\nu}{2}\right)}{J_0^2\left(\frac{\nu}{2}\right) - 2\nu \log 2 J_0\left(\frac{\nu}{2}\right) J_1\left(\frac{\nu}{2}\right) + \nu^2 (\log 2)^2 \left(J_0^2\left(\frac{\nu}{2}\right) + J_1^2\left(\frac{\nu}{2}\right)\right)}. \tag{6.27}$$

This result may be confirmed by direct substitution. Thus for all real positive ν it follows that $A_\nu < 0$ and $B_\nu \geq 0$. Hence the mass transfer and the pressure difference will never be in phase, with the phase lag taking a value between 0 and $\frac{\pi}{2}$ for all ν. A phase lag of $\frac{\pi}{2}$ will only occur when 2ν is a root of the Bessel function J_0 and a phase lag of zero will only occur for $\nu = 0$. In the limit as $\nu \to \infty$ both A and B will tend towards zero, with $\nu A_\nu = O(1) = \nu^2 B_\nu$ in the limit.

6.4.3 $f(t) = tH(t)$

Laplace transforms provide the simplest method for solving the mass transfer equation when $f(t) = tH(t)$. Substituting into equation 6.18 gives

$$\overline{M}_0(p) = \frac{\pi}{4} \frac{1}{p^2} \frac{I_0\left(\frac{p}{2}\right) + I_1\left(\frac{p}{2}\right)}{I_0\left(\frac{p}{2}\right) + p \log 2 \left(I_0\left(\frac{p}{2}\right) + I_1\left(\frac{p}{2}\right)\right)}. \tag{6.28}$$

The residue of $e^{pt}\overline{M}_0(p)$ at the double pole $p = 0$ is given by

$$\frac{d}{dp}\left(\frac{\pi}{4} e^{pt} \frac{I_0\left(\frac{p}{2}\right) + I_1\left(\frac{p}{2}\right)}{I_0\left(\frac{p}{2}\right) + p \log 2 \left(I_0\left(\frac{p}{2}\right) + I_1\left(\frac{p}{2}\right)\right)}\right)\Bigg|_{p=0} = \frac{\pi}{4} t + \frac{\pi}{16} - \frac{\pi}{4} \log 2.$$

Thus the solution for the mass transfer equation when $f(t) = tH(t)$ is given by

$$M_0(t) = \frac{\pi}{4} H(t) \left(t + \frac{1}{4} - \log 2 + \sum_{i=1}^{\infty} e^{-\lambda_i t} (\alpha_i \cos \mu_i t + \beta_i \sin \mu_i t)\right) \tag{6.29}$$

where the α_i and β_i are given by equation 6.23. Hence a slot pressure which increases linearly with time will give a mass transfer function which is linear with an oscillating exponentially decaying correction function. In the limit as $t \to \infty$ it will be the same as the solution given in equation 6.24 for $f(t) = t$. The mass transfer in this case is plotted against time in figure 6.3.

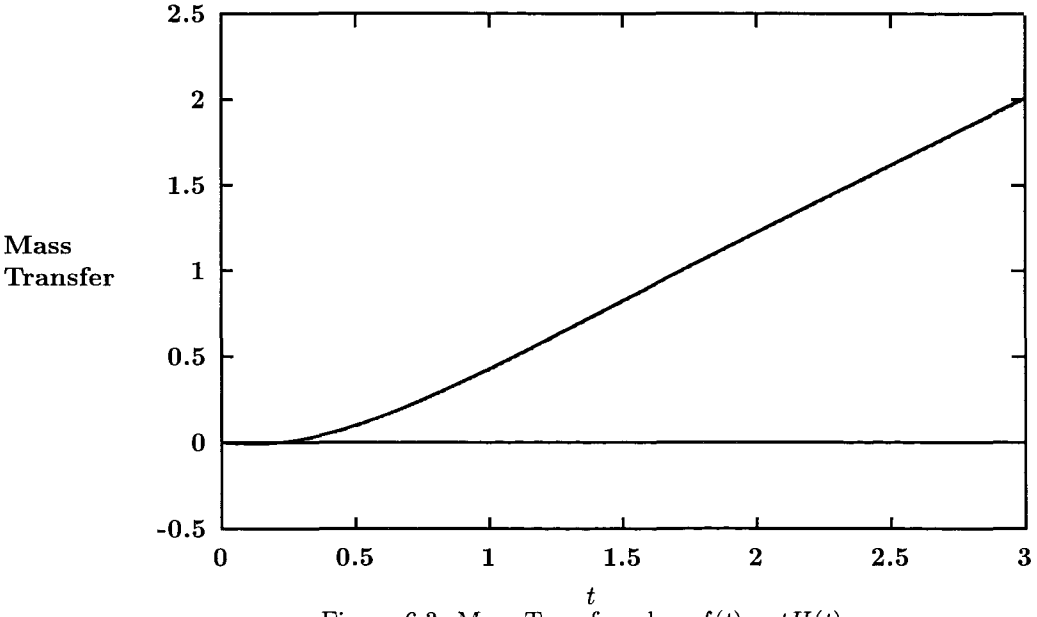

Figure 6.3: Mass Transfer when $f(t) = tH(t)$

6.4.4 $f(t) = H(t)$

The Laplace transform of $H(t)$, the Heaviside function is equal to $1/p$. Hence the Laplace transform of $M_0(t)$ will have a simple pole at the origin as well as at the simple poles $p_i = -\lambda_i \pm i\mu_i$. From equation 6.18 the residue of $e^{pt}\overline{M}_0(p)$ at $p = 0$ will be equal to

$$\frac{\pi}{4}\frac{I_0(0) + I_1(0)}{I_0(0) + 0\log 2(I_0(0) + I_1(0))} = \frac{\pi}{4}.$$

This will lead to a solution

$$M_0(t) = \frac{\pi}{4}H(t)\left(1 + \sum_{i=1}^{\infty} e^{-\lambda_i t}(\alpha_i \cos\mu_i t + \beta_i \sin\mu_i t)\right), \tag{6.30}$$

where the λ_i and μ_i are as before, but the α_i and β_i are given by

$$\alpha_i - i\beta_i = 4\frac{1}{p_i}\frac{I_0\left(\frac{p_i}{2}\right) + I_1\left(\frac{p_i}{2}\right)}{I_0\left(\frac{p_i}{2}\right)\log 2\,(2 + p_i) + I_1\left(\frac{p_i}{2}\right)(1 + p_i \log 2)}. \tag{6.31}$$

Figure 6.4 shows the behaviour of the mass transfer function in this case.

6.4.5 $f(t) = \sin\nu t H(t)$

The Laplace transform of $\sin\nu t H(t)$ is given by

$$\overline{f}(p) = \frac{\nu}{p^2 + \nu^2}.$$

Substitution of this into equation 6.18 gives

$$e^{pt}\overline{M}_0(p) = \frac{\pi}{4}e^{pt}\frac{\nu}{p^2 + \nu^2}\frac{I_0\left(\frac{p}{2}\right) + I_1\left(\frac{p}{2}\right)}{I_0\left(\frac{p}{2}\right) + p\log 2\left(I_0\left(\frac{p}{2}\right) + I_1\left(\frac{p}{2}\right)\right)},$$

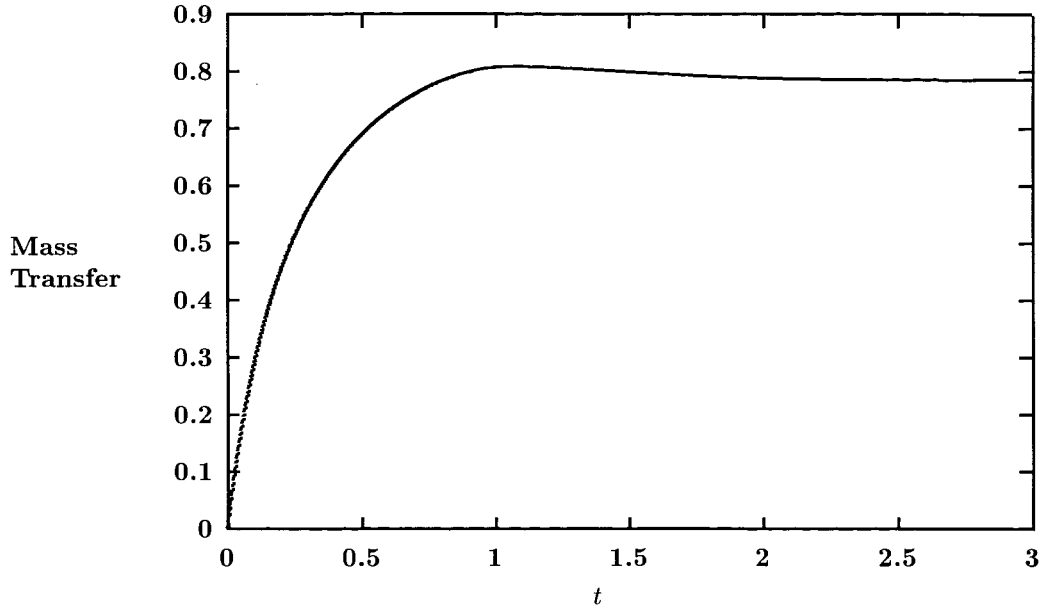

Figure 6.4: Mass Transfer when $f(t) = H(t)$

which has poles at $p = \pm i\nu$ and at $p = p_i = -\lambda_i \pm i\mu_i$. The residues at $p = \pm i\nu$ sum to $A_\nu \cos \nu t + B_\nu \sin \nu t$, where A and B are given by equation 6.26. The poles at $p = p_i$ give residues of the form $e^{-\lambda_i t}(\alpha_i \cos \mu_i t + \beta_i \sin \mu_i t)$. Hence the solution for the mass transfer function in this case is

$$M_0(t) = A_\nu \cos \nu t + B_\nu \sin \nu t + \frac{\pi}{4} \sum_{i=1}^{\infty} e^{-\lambda_i t}(\alpha_i \cos \mu_i t + \beta_i \sin \mu_i t), \tag{6.32}$$

where the α_i and β_i are given by

$$\alpha_i - i\beta_i = 4\frac{\nu}{p_i^2 + \nu^2} \frac{I_0\left(\frac{p_i}{2}\right) + I_1\left(\frac{p_i}{2}\right)}{I_0\left(\frac{p_i}{2}\right) \log 2\,(2 + p_i) + I_1\left(\frac{p_i}{2}\right)(1 + p_i \log 2)}. \tag{6.33}$$

As expected, in the limit as $t \to \infty$ this will tend to the solution found for $f(t) = \sin \nu t$ in section 6.4.2. In fact, as figure 6.5 shows, it will tend to the asymptotic solution very quickly.

6.5 Evaluation of the Height of the Shear Layer

Given the mass transfer, the shear layer $S(x,t)$ may be evaluated from equation 6.14, recalling that $S(x,t) = \sigma_x(x,t)$. In the case when $f(t) = H(t)$, the expression for the mass transfer $M_0(t)$ is given in section 6.4.4, and $S(x,t)$ is

$$\begin{aligned} S(x,t) &= -\frac{1}{2}H(t)\,(a'(x) - H(x-t)(a'(x-t) + ta''(x-t)) - \frac{1}{4}tH(t)H(x-t)b'(x-t) \\ &- \frac{1}{4}\sum_{i=1}^{\infty} \int_0^x \int_0^{x_1} (-\lambda_i^2 - \mu_i^2) e^{-\lambda_i(x_2 - x + t)} \cos \mu_i(x_2 - x + t) b(x_2)\, dx_2\, dx_1 \\ &- \frac{1}{4}\sum_{i=1}^{\infty} \int_0^x \left(-\lambda_i \cos \mu_i(x_1 - x + t) - \mu_i \sin \mu_i(x_1 - x + t) e^{-\lambda_i(x_1 - x + t)}\right) b(x_1)\, dx_1, \end{aligned}$$

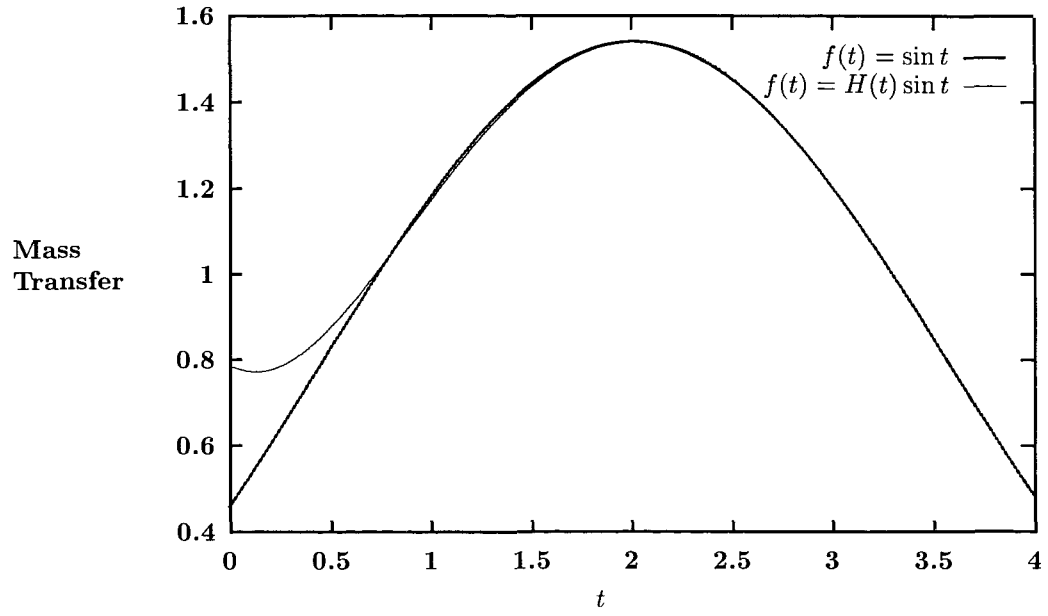

Figure 6.5: Mass Transfer when $f(t) = \sin tH(t)$

where

$$a(x) = \frac{1}{2}\sqrt{x}\sqrt{1-x}\left(x - \frac{3}{2}\right) + \arcsin\sqrt{x}\left(\frac{3}{4} - x\right). \tag{6.34}$$

This may be simplified slightly, since the double integral in the expression for S may be written as a single integral, by reversing the order of integration and observing that the integrand does not depend on x_1. Hence

$$\begin{aligned} S(x,t) &= -\frac{1}{2}H(t)\left(a'(x) - H(x-t)(a'(x-t) + ta''(x-t)\right) - \frac{1}{4}tH(t)H(x-t)b'(x-t) \\ &- \frac{1}{4}\sum_{i=1}^{\infty}\int_0^x (1-x_2)(-\lambda_i^2 - \mu_i^2)e^{-\lambda_i(x_2-x+t)}\cos\mu_i(x_2 - x + t)b(x_2)\,dx_2 \\ &- \frac{1}{4}\sum_{i=1}^{\infty}\int_0^x \left(-\lambda_i\cos\mu_i(x_1 - x + t) - \mu_i\sin\mu_i(x_1 - x + t)e^{-\lambda_i(x_1-x+t)}\right)b(x_1)\,dx_1, \end{aligned}$$

The values of $S(x,t)$ for the case $f(t) = H(t)$ are plotted in figure 6.6, for t taking the values 0.2,0.4,0.6,0.8,1. The shape for $t = 1$ is almost indistinguishable from the steady state solution given by equation 6.3

Similarly, in the case when $f(t) = tH(t)$ the shear layer is given by

$$\begin{aligned} S(x,t) &= -\frac{1}{2}H(t)(a_1(x) - (x-t)a(x)) \\ &- \frac{1}{2}H(t)H(x-t)((x-t)(a(x-t) + ta'(x-t)) - (a_1(x-t) + ta'_1(x-t))) \\ &- \frac{1}{4}H(t)B(x) - H(t)H(x-t)((B(x-t) + tb(x-t))) \\ &- \frac{1}{4}\sum_{i=1}^{\infty}\int_0^x (1-x_2)(-\lambda_i^2 - \mu_i^2)e^{-\lambda_i(x_2-x+t)}\cos\mu_i(x_2 - x + t)b(x_2)\,dx_2 \end{aligned}$$

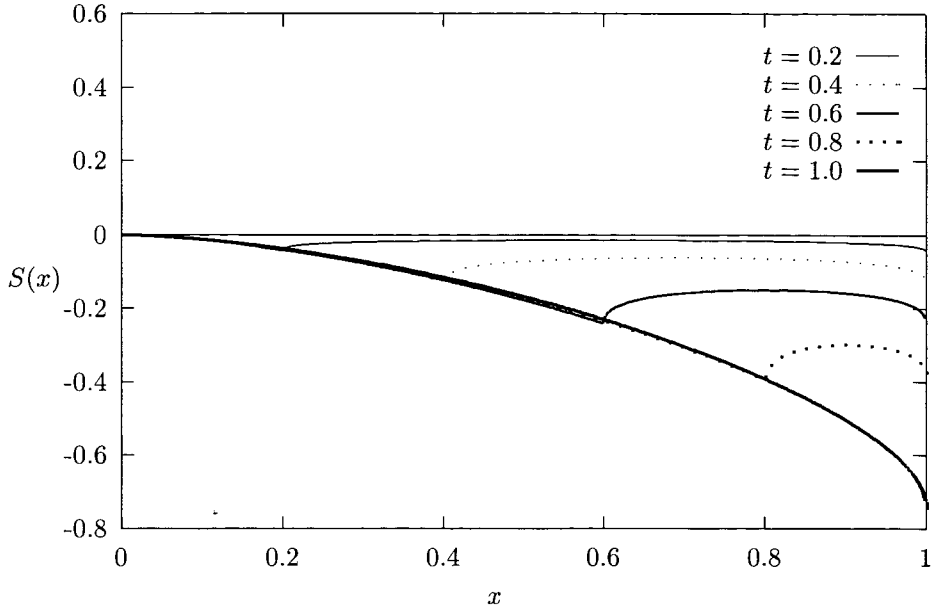

Figure 6.6: The Shear Layer, $S(x)$, with $f(t) = H(t)$

$$- \frac{1}{4}\sum_{i=1}^{\infty}\int_0^x (-\lambda_i)\cos\mu_i(x_1 - x + t) - \mu_i \sin\mu_i(x_1 - x + t)e^{-\lambda_i(x_1 - x + t)}b(x_1)\,dx_1 \quad (6.35)$$

where $B(x)$ is given by $B'(x) = b(x)$, i.e.

$$B(x) = (2x - 1 - 2\log 2)\arcsin\sqrt{x} + (1 + 2\log 2)\sqrt{x}\sqrt{1-x}. \quad (6.36)$$

In the above expressions, the integrals may be expressed as products of exponential and Bessel functions. However the resulting expressions are long-winded, and not particularly helpful, and so are not presented here.

6.6 Asymptotic Behaviour as $t \to 0$

For a system which is steady for $t < 0$ the behaviour for small t is of interest. This may be derived from equations 6.10 and 6.12. For example if $f(t) \sim t^n$ as $t \to 0$ for some constant positive n, then if $\sigma \sim t^m$, say, then equation 6.10 implies that $M_0 \sim t^{m-1}$, and so from equation 6.12 it follows that $m - 2 = n$, so that in a system in which the difference between the slot pressure and the external pressure behaves asymptotically for small t as t^n, $S(x,t)$ will behave as t^{n+2} and the mass transfer as t^{n+1}.

A dimensional argument leads to the same result : the dimensions of M_0 are $LU_\infty = L^2/T$ (with T denoting time), the dimension of the height of the shear layer is L, and the dimension of the pressure difference is $\rho U_\infty^2 = M^2/T^2$ (with M denoting mass). Hence it is to be expected that changes in the mass transfer will be slower than changes in the pressure difference and faster than the changes in $S(x,t)$ by a factor of t. Note that all changes will still occur over a time scale of L/U_∞, as this is the

natural time scale of the flow. Nevertheless there is a significant time delay evident from the fact that for small t, the mass transfer will be a factor of t smaller than the slot pressure.

The question of the behaviour of small values of $f(t)$ opens up the larger problem in which the slot pressure function $f(t)$ changes sign, so that injection and suction both occur over a period of time. The next chapter will therefore consider the transition between injection and suction.

Chapter 7

Combining Suction and Injection

So far the cases of injection and suction have been treated completely separately : the slot pressure has always been taken to be always greater than the external pressure or always less than the external pressure. However a case of some interest is that concerning a slot pressure which over a period of time takes values both greater than and less than the external pressure. In discussion of the suction case in section 6.2 onwards it was observed that there is a time lag between changes in the slot pressure and the mass transfer. Since the difference between blowing and sucking is determined by whether the mass transfer is into or out of the slot it is to be expected that the change from sucking to blowing will not take place at the time when $f(t) = 0$ but at a finite time after $f(t)$ has changed sign, at the time when the mass transfer is zero.

Note that in this chapter the asterisks used to denote non-dimensionalised variables have been omitted.

7.1 Transition from Suction to Injection

For a system in which sucking changes to blowing it is expected that the equations derived in section 5.2 will remain valid until some time $t = t_i$. In the suction case, as depicted in figure 6.1 there were two paths of interest : the shear layer dividing the flow into the slot from the static fluid already in the slot, $y = S(x)$, and the particle path that re-attaches at the trailing edge of the slot and divides the fluid that will enter the slot from that which will not, $y = T(x)$. It is to be expected that as the difference between the slot pressure and the external pressure decreases these two paths will begin to converge, and in the limiting case as $t \to t_i$ they will be the same line. Thus t_i may be defined equivalently as satisfying $M_0(t_i) = 0$, $S(1, t_i) = 0$ or even $M(x, t_i) = 0$ for all x. For $t > t_i$ the system may be considered as an injection case and the equations derived in section 6.2 will be applicable to the problem, with initial conditions for $S(x)$ on $0 < x < 1$ given by the value of $S(x)$ as $t \to t_i$.

7.2 Transition from Injection to Suction

When the system changes from blowing to sucking, t_i may be defined as before as satisfying $S(1, t_i) = 0$. However the 'blown' layer of fluid which has already been blown out of the slot will affect the flow (see figure 7.1) so the system will not be simply a case of slot suction with the appropriate boundary conditions. Instead the external flow will have to be modelled as uniform flow, with a series of

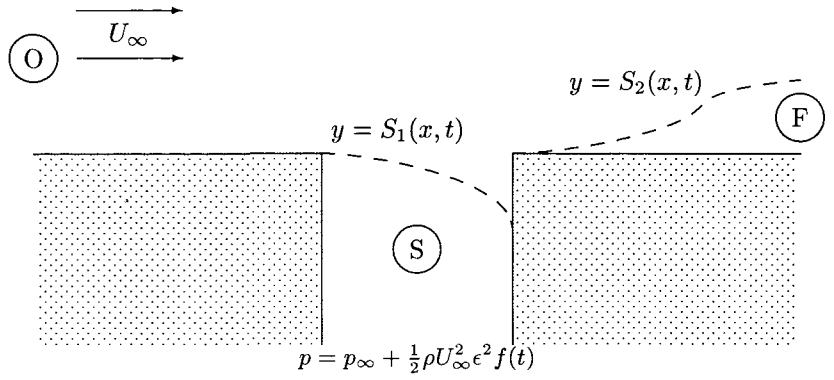

Figure 7.1: The Transition from Injection to Suction

sinks at the top of the slot as before, but with the blown layer also remaining as a series of sources along some region of the positive $x-$axis. Initially this region will simply be $x > 1$, but as the blown region of fluid is blown further downstream the region will be $x > x_0(t)$ where x_0 will be the point at which the blown region of fluid commences. Note that the blown region cannot become completely disconnected from the trailing edge, as the vortex sheet cannot emanate from a wall, but instead must emanate from the separation at the trailing edge. However the height of the vortex sheet may be less than $O(\epsilon^2)$ up to a point x_0, and thus it may be said that the blown region commences downstream of the slot.

The fact that this problem contains features of both injection and suction at the same time, in that although suction is occurring there is still a blown layer, suggests that it would be helpful to seek a unifying equation for both slot injection and suction.

7.3 A Unified Interactive Equation

The purpose of this section is to find an equation which describes both suction and injection for a slot when changes to the slot pressure take place over a time scale of $L/U_\infty\epsilon$. Note that this time scale is the quasi-steady time scale for slot suction. The slot pressure will be defined by $p_\infty + \frac{1}{2}\rho U_\infty^2 \epsilon^2 f(t)$ so that a positive $f(t)$ corresponds to slot injection while a negative $f(t)$ corresponds to slot suction. With this definition the equations in terms of S and ϕ (where ϕ denotes the velocity potential of the

blown region) are

$$\frac{2}{\pi}\int_0^\infty \frac{S_\xi}{\xi - x}d\xi = \begin{cases} f(t) & 0 < x < 1, \\ f(t) - \phi_x^2 - 2\phi_t & x > 1, \end{cases} \tag{7.1}$$

$$(\phi_x S)_x + S_t = 0, \text{ for } x > 1, \tag{7.2}$$

for slot injection, and

$$\frac{2}{\pi}\int_0^1 \frac{S_\xi}{\xi - x}d\xi = f(t) \tag{7.3}$$

for slot suction. The slot injection equations are equations 5.15 and 5.16 which were derived in section 5.2. The suction equation for this time scale is equation 6.11, derived in section 6.2, with the time derivatives omitted, since this is the quasi-steady time scale for suction. The omission of the time derivatives means that it is now convenient to work in terms of S, rather than σ, recalling that $\sigma_x = S$. The boundary conditions for the equations are the same, i.e. $S = S_x = 0$ at $x = 0$, with $\phi(1) = 0$.

There are two crucial differences between the injection and suction equations : the first is the variable ϕ which does not appear in the suction equations. This is not an insurmountable problem as it means that any definition of ϕ for the suction problem will not affect the equation. The second problem is that the suction equation is only valid over the region $(0, 1)$, and indeed physically $S(x, t)$ is only defined over this region. In fact when there is a transition from injection to suction, as in figure 7.1, there are two shear layers : the shear layer in the slot, separating the ingested flow from the static flow in the slot, and the shear layer separating the blown fluid from the external flow. Although these could both be termed $S(x, t)$, according to whether x is greater than or less than 1, this could be confusing, so they will be termed $S_1(x, t)$ and $S_2(x, t)$, with S_1 representing the height of the shear layer in or above the slot, and valid for $0 < x < 1$, and S_2 representing the height of the blown region, and valid for $x > 1$. It follows from this that S_1 may take either sign according to whether the system is sucking or blowing, but S_2 must be non-negative, although in the suction only case it will be zero, as there is no blown region. With this notation the injection equations 7.1 and 7.2 may be written

$$\frac{2}{\pi}\int_0^1 \frac{S_{1\xi}}{\xi - x}d\xi + \frac{2}{\pi}\int_1^\infty \frac{S_{2\xi}}{\xi - x}d\xi = \begin{cases} f(t) & 0 < x < 1, \\ f(t) - \phi_x^2 - 2\phi_t & x > 1, \end{cases} \tag{7.4}$$

$$(\phi_x S_2)_x + S_{2t} = 0, \text{ for } x > 1. \tag{7.5}$$

The boundary conditions for this are that S_1 and S_{1x} are 0 at $x = 0$. Furthermore, since in the original injection problem S had to be continuous, $S_1(1) = S_2(1)$.

For this to be a unifying equation for suction and injection, the above equations must also be satisfied when there is no injection. The second equation, equation 7.5 will clearly be satisfied if $S_2 = 0$ for $x > 1$, i.e. everywhere. This makes physical sense, as in the suction only case there is no blown region, which intuitively is the same as there being a blown region of zero height. This also means that equation 7.4 will be satisfied in the region $x < 1$. However some care must be used for the region $x > 1$. Physically both the suction equation and equation 7.4 are derived from a pressure

balance. However if there is no blown region, then there is no need for a pressure balance on $x > 1$, which is then a fixed boundary. This illustrates the danger in equating a blown region of thickness zero with no blown region. This problem may be overcome, however, by a correct definition of ϕ. Since if there is no blown region $S_2 = 0$, any value of ϕ chosen will automatically satisfy equation 7.5. This makes sense because if there is no blown region, the velocity potential in the blown region is an open question. However if the lack of a blown region is to be modelled as a blown region of zero thickness, then ϕ must be chosen so as to be the velocity potential that would achieve a pressure balance for $x > 1$ at the shear layer. If this is done then the pressure balance equation, equation 7.4 will be valid for $x > 1$. Thus equations 7.4 and 7.5 are the unifying equations in the interactive case. The boundary conditions on S_1 and ϕ_1 are that $S_1 = S_{1x} = \phi(1) = 0$. The boundary condition on S_2 is that if $S_1(1)$ is positive then, by continuity of the shear layer, $S_2(1) = S_1(1)$, and if $S_1(1)$ is negative, then, since the slot is now a suction slot, $S_2(1) = 0$.

If $f(t)$ is positive, equations 7.4 and 7.5 reduce to the interactive injection equations 7.1 and 7.2, and if $f(t)$ is negative the solution of the equations will be, using the analysis of steady suction, (see equation 6.3,

$$\begin{aligned} S_1(x,t) &= \frac{1}{2} f(t) \left(\sqrt{x}\sqrt{1-x} - \arcsin\sqrt{x} \right), \\ S_2(x,t) &= 0. \end{aligned}$$

The solution for ϕ must be chosen so that the right-hand side of equation 7.4 balances, so for $x > 1$,

$$f(t) \int_0^1 \sqrt{\frac{1-\xi}{\xi}} \frac{d\xi}{\xi - x} = f(t) - \phi_x^2 - 2\phi_t.$$

The integral above, which for $x > 1$ is a non-singular integral, may be evaluated, reducing the above equation to

$$\phi_x^2 + \phi_t = f(t)\sqrt{\frac{x}{x-1}},$$

with $\phi(1) = 0$. This may be solved using Charpit's equations, see, for example, Sneddon (1957) [83], although the solution is not given here, as it has no physical relevance. However this does indicate that the system of equations 7.4 and 7.5 can describe problems in which both injection and suction occur. The boundary conditions are that $S_1 = S_{1x} = 0$ at $x = 0$, that $\phi = 0$ at $x = 1$ for all t, and that $S_2(1) = \max(S_1(1), 0)$. Appropriate initial conditions are also required for ϕ, S_1 and S_2. It may also be necessary to impose that S_2 is non-negative.

7.4 A Unified Equation in the Fast Regime

The fast regime, where the slot pressure changes over a time scale of order L/U_∞, is important to the study of problems like the rim seal problem, discussed in chapter 1, where slot injection is desired, but changes in the external pressure over a short time scale mean that some suction may occur. For the

suction only case, the equations for changes on this time scale were derived in section 6.2 and solved in sections 6.3, 6.4 and 6.5. The equations in terms of σ and M_0, where M_0 represents the mass flow evaluated at the top of the slot, were given by equations 6.12 and 6.10 and, in non-dimensionalised variables, were

$$\begin{aligned} \sigma_{xx} + 2\sigma_{xt} + \sigma_{tt} &= -\frac{f(t)}{2}\sqrt{\frac{x}{1-x}} - \frac{1}{\pi}M_0' b(x), \\ M_0 &= -(\sigma_x + \sigma_t)|_{x=1}. \end{aligned}$$

For the same time scale, the corresponding equations for slot injection were derived in section 5.5 and were given by equations 5.36 and 5.32 to give

$$\sigma_{xx} + 2\sigma_{xt} + \sigma_{tt} = \frac{f(t)}{2}\sqrt{\frac{x}{1-x}} - g_1(x) + \frac{N(t)}{\pi}b(x), \tag{7.6}$$

$$N = (\sigma_{xt} + \sigma_{tt})|_{x=1}. \tag{7.7}$$

Here, g_1 may be determined from the initial conditions. Both sets of equations are valid in the region $0 < x < 1$. These equations are very similar. Clearly $N(t)$ corresponds to $-M_0'(t)$. The change in the sign of $f(t)$ is to be expected, as the suction equations were derived assuming a slot pressure of $p_\infty - \frac{1}{2}\rho U_\infty^2 \epsilon^2 f(t)$, whereas the injection equations assumed a slot pressure of $p_\infty + \frac{1}{2}\rho U_\infty^2 \epsilon^2 f(t)$. Here, $f(t)$ will be defined in the positive direction, as for injection, so the slot pressure will be $p_\infty + \frac{1}{2}\rho U_\infty^2 \epsilon^2 f(t)$. Now the only difference between the sets of equations for slot injection and slot suction is the function $g_1(x)$ which exists for slot injection. It is not surprising that the two physical problems give similar equations, as in this regime the injected region is effectively steady, so will not interact with the region above the slot. The only difference is that in fast slot injection, there is a region (which does not move) of blown fluid, which will affect the pressure distribution. This is manifested in the slot injection equations in the function $g_1(x)$ which represents the contribution to the pressure from the blown region. Since for slot suction there is no blown region, $g_1(x)$ is zero in this case.

Thus the fast slot injection equations, given by equations 7.6 and 7.7, and repeated here, are the unified equations for slot injection and slot suction over the fast time scale. The function $g_1(x)$ may be determined from the initial conditions, as in section 5.5. These equations may be solved in the same way as the slot suction equations may be solved, for which solutions are presented in sections 6.3, 6.4 and 6.5. The only difference between the solutions of the transition equations and the suction equations (apart from the change in the way $f(t)$ is defined) will be the effects of the function g_1. As the equations are linear, this will just result in addition of a term g_2 to σ, where $g_2'' = g_1$, and $g_2'(0) = g_2(0) = 0$. Thus the solutions for S and M_0 will only be changed by addition of $g_2'(x)$ and $-g_2'(1)$ respectively. If the initial conditions are taken to be those of slot injection, then the mass transfer into the slot will be of order $LU_\infty\rho\epsilon^2$, as for slot suction, and may be measured by M_0. The mass transfer out of the slot will be of order $LU_\infty\rho\epsilon^3$. If the initial conditions are those of slot suction,

then M_0 will still correspond to the mass transfer while suction is taking place, but has no physical meaning while injection is taking place. In this case the mass transfer out of the slot will be zero to lowest order, as the injected region of flow starts of as being zero, and so must remain as zero (i.e. $S(x) = 0$ for all $x > 0$). Since the flow in the injected region has a velocity of order $U_\infty \epsilon$, there will be an injected region of height $O(\epsilon^2)$ within a distance of order $L\epsilon$ from the trailing edge set up within this time scale. The injection mass transfer in such a case will still be of order $LU_\infty \rho \epsilon^3$, and to evaluate this term it is necessary to examine lower order terms. In this case another singular partial linear integro-differential equation will be derived, with time-derivatives of both σ and ϕ both being significant.

However it is the case where over the longer time scale, injection is taking place that is of most relevance to the rim seal problem. The fact that closed form solutions may be found for this equation is a particularly useful result that may measure the mass transfer when there is a sudden dip in the slot pressure (or a sudden increase in the external pressure) over a time scale of L/U_∞.

7.5 Equal Mass Suction and Injection

For ordinary slot suction the mass transfer is order $LU_\infty \rho \epsilon^2$, whereas for slot injection it is order $LU_\infty \rho \epsilon^3$. This shows that for the interactive unified equations (equations 7.4 and 7.5), in which both suction and injection occur over the interactive time scale, the mass of fluid ingested into the slot will be an order of magnitude greater than the fluid injected into the free stream. Hence to consider a system in which both mass flows are equal, either the injection must take place for a much longer time than the suction, or the strength of the injection, defined by $\epsilon^2 f(t)$, must be much stronger than the strength of the suction. If the injection takes place for a longer time than the suction, then for the mass flows to be of the same order of magnitude the difference in the time scales must be by a factor of ϵ^{-1}. If the injection time scale is order $\epsilon^{-2} L/U_\infty$ and the suction time scale is order $\epsilon^{-1} L/U_\infty$, then the problem is quasi-steady both for suction and injection. If the injection time is order $\epsilon^{-1} L/U_\infty$, and the suction time is order L/U_∞ then both problems are fully unsteady. In this case the transition will take place over the shorter time scale, and the flow will be described by the unified equations for fast transition, i.e. equations 7.6 and 7.7.

If the injection and suction pressures both vary over the same time scale then same order mass flow may still result if the injection and suction pressures are of different orders of magnitude. For this to occur, ϵ_i^3 must be of the same order as ϵ_s^2, where ϵ_i and ϵ_s define the injection and suction slot pressures according to the usual relationship $p = p_\infty + \frac{1}{2}\rho U_\infty^2 \epsilon^2 f(t)$, with $f(t)$ of order 1. Hence $\epsilon_s = \epsilon_i^{\frac{2}{3}}$, so, to lowest order, the shear layer once suction has commenced will be at a height of zero, and the suction will not affect the blown region downstream.

However, for most realistic cases it is felt that the pressure difference is unlikely to change by an order of magnitude. Since the most interesting case for transition is given by time changes for

injection over an order $\epsilon^{-1}t/\mathrm{L}U_\infty$ time scale, i.e. the interactive time scale, the numerical solution of the interactive equations will be the subject of the next two chapters.

Chapter 8

Numerical Analysis of the Interactive Equations

8.1 Brief Description of the System of Equations

This chapter is concerned only with the initial value problem for the system of equations for unsteady slot injection derived in section 5.2. As previously mentioned, the system of equations may be expressed in many different ways : in terms of any two of u, S and M or in terms of a single variable σ, (note that in this chapter the asterisks used to denote non-dimensionalised variables will be omitted). Naturally the choice of variables does not fundamentally affect the nature of the system of equations, although it will affect any numerical scheme. To obtain an equation in terms of one variable, without the necessity for any integrals other than the integral transform, it is necessary to differentiate equation 5.23 with respect to x. Note that as $\sigma_{xx} = S_x = 0$ at both ends of the singular integral, it is permissible to differentiate through the integral transform (see section A.5). This gives the injection equation in the form

$$\frac{1}{\pi}\sigma_x^3 \int_0^\infty \frac{\sigma_{\xi\xi\xi}(\xi,t)}{\xi - x} d\xi = \begin{cases} 0 & x < 1, \\ \sigma_t^2\sigma_{xx} + \sigma_x^2\sigma_{tt} - 2\sigma_x\sigma_t\sigma_{xt} & x > 1. \end{cases} \tag{8.1}$$

Hence the equation is a non-linear partial differential equation, containing an integral transform. The situation is further complicated by the fact that the integral transform is strongly singular, and by the fact that the equation must be separated into two distinct regions. A more serious problem though is that, unlike the unsteady sail equation of chapters 2 and 3, the highest derivatives (σ_{xxx} and σ_{tt}) occur neither both inside nor both outside the integral transform. Although linear and quasi-linear partial differential equations are relatively well understood, and there is some understanding of both non-linear partial differential equations and linear singular integro-differential equations, no literature has been found on the numerical solution of singular partial integro-differential equations. Under the usual definitions the presence of the integral transform in the highest derivative means that it is not even possible to apply the usual techniques of partial differential equations to this equation, for example to find the characteristics or eigenvalues of the problem.

The attempts to solve the equations numerically may be classified into two types : the first consists of variations on the normal finite difference type scheme, whereas the other consists of an iterative method of solving the equation, based on inverting the Hilbert transform, which is related to the method of solving the steady equation used by Fitt et al (1985) [34]. This type of method for unsteady equations will be referred to as 'sequential iteration'. However first it is worth examining analytic solutions of the equations, in particular to see if any similarity solutions exist.

8.2 Similarity Solutions

Although the presence of the inhomogenous term $f(t)$ in the original formulation of the equations, i.e. equations 5.19 and 5.20, will preclude similarity solutions as a solution of practical use (in equation 8.1, where the $f(t)$ term has been eliminated by differentiation, the inhomogeneity is effectively introduced by the boundary conditions) it is still of interest to find them as solutions for the equation. However even without the inhomogeneity the difference between the two expressions for the Hilbert transform over $(0,1)$ and $(1,\infty)$ mean that it is not possible to find non-trivial similarity solutions over the whole region. To see this consider equation 8.1 and consider any value of $x > 1$ at a given time. Then assuming a similarity solution exists, there exist an α and a β such that $\sigma(x,t) = t^\beta f(\eta)$ where $\eta = xt^{-\alpha}$. Then observing that the Hilbert transform of such a function will be in the same form,

$$\int_0^\infty \frac{t^\beta f(\xi t^{-\alpha})}{\xi - x} d\xi = \int_0^\infty \frac{t^\beta f(\zeta)}{\zeta - \eta} d\zeta = t^\beta H(\eta), \tag{8.2}$$

for any function f for which the Hilbert transform is H, and that this Hilbert transform is zero for $x < 1$, it must be that the Hilbert transform is zero for all values of η and thus all values of x. Since the only functions for which this is true are proportional to $x^{-\frac{1}{2}}$ (see section A.1.1), and the right-hand side of equation 8.1 must be zero for $x < 1$, this gives only the solution $t^0 x^{-\frac{1}{2}}$. Hence it is more helpful to consider only the region $x > 1$.

Considering only the region $x > 1$, and setting $\sigma = 0$ outside this region, equation 8.1 is invariant under the transformation $(x-1, t, S) \mapsto (\lambda(x-1), \lambda^\gamma, \lambda^{4-2\gamma} S)$. Hence solutions exist of the form $\sigma(x,t) = t^{4\alpha-2} f(xt^{-\alpha})$ where f must satisfy the non-linear ordinary singular integro-differential equation

$$\frac{1}{\pi} f'^3 \int_1^\infty \frac{f'''(\xi)}{\xi - \eta} d\xi = (4\alpha - 2)^2 f'' f^2 + \alpha\eta(1-\alpha) f'^3 - 2(2\alpha - 1)^2 f'^2 f. \tag{8.3}$$

Solutions of the form $f(x - ct)$, where c is a constant, may often be found for partial differential equations, as both derivatives will be of the same form. However, they will not be applicable to this equation as the semi-infinite integral transform of such a function is given by

$$\begin{aligned} \int_0^\infty \frac{f(\xi - ct)}{\xi - x} d\xi &= \int_{-ct}^\infty \frac{f(u)}{u - (x - ct)} d\xi \\ &= \int_0^\infty \frac{f(u)}{u - (x - ct)} du + \int_{-ct}^0 \frac{f(u)}{u - (x - ct)} du. \end{aligned}$$

The first integral in the above expression is a function of $x - ct$, but the second will not be, unless $f(u)$ is zero for all $u < 0$. However if this were to hold, $f(x - ct)$ would be zero everywhere for large values of t, so this will not be a particularly helpful solution. Similarly non-zero functions of the form $f(x + ct)$ cannot be solutions.

8.3 The Benjamin-Ono Equation

The most well-known singular partial integro-differential equation is the Benjamin-Ono equation (Brooke Benjamin (1967) [9], Ono (1975) [66]), given by

$$u_t + 2uu_x + \frac{1}{\pi} \int\!\!\!\!\!\!- _{-\infty}^{\infty} \frac{u_{\xi\xi}(\xi, t)}{\xi - x} d\xi = 0.$$

The crucial difference between this equation and the singular partial integro-differential equations examined here, is that the range of integration is the whole real axis. This permits solutions of the form $u(x - ct)$ and $u(x + ct)$, which cannot be found for the equations studied for the sail and slot problems of chapters 2,5, and 6, as the range of integration has a finite boundary (see section 8.2). Brooke Benjamin (1967) found a solitary wave solution, which was shown to be a soliton solution by Chen et al (1979) [17], who found N-soliton solutions. The equation possesses many other special features, making it the focus of much study, partly in relation to the Korteg-de Vries equation (Korteg & de Vries (1895) [55]),

$$u_t + 6uu_x + u_{xxx} = 0,$$

which was first introduced in the theory of long surface water waves. Bock & Kruskal (1979) [7] showed that the Benjamin-Ono equation has an infinite number of conserved densities, and hence derived linearised equations, by use of a Miura transformation,

$$u = k(e^w - 1) + \frac{1}{2} i \left(w_x - i \int\!\!\!\!\!\!- _{-\infty}^{\infty} \frac{w_\xi}{\xi - x} d\xi \right).$$

Other properties of the Benjamin-Ono equation include the relationship between the linear eigenvalue problem and an inverse scattering transform (Fokas & Ablowitz (1983) [38]), and the fact that the equation possesses two non-local linear operators, which generate infinitely many commuting symmetries and constants of the motion (Fokas & Fuchssteiner (1981) [37]). However, no detailed work has been found on numerical solutions of this equation, nor for the non-linear equations of Santini et al (1987) [73] which also examined singular partial differential equations in the context of inverse scattering theory. In any case, it is not clear that such work would be applicable to the interactive slot injection problem, in which the range of integration is semi-infinite, rather than infinite.

There is more literature on integro-differential equations in only one variable, with a method of reducing integro-differential equations with Cauchy kernel to integral equations given by Gakhov (1965) [41]. Closed form solutions for a class of integro-differential equations with Cauchy kernels over the semi-infinite range have also been found by Varley & Walker (1989) [102]. Stability conditions have

been found for integro-differential equations by Drozdov (1996) [24], and existence and uniqueness theorems have been found for weakly singular convolution kernels by Engler (1996) [29]. However, all of the above apply to linear equations only, with there being very few analytical results available on non-linear integro-differential equations with Cauchy kernel. However such equations occur frequently in a range of physical problems, in particular thin aerofoil theory (e.g. Fitt et al (1985) [34], and King & Tuck (1993) [53]), and the behaviour of cracks (e.g. Kaya & Erdogan (1987b) [51], Fitt et al (1995) [32]), and have been solved numerically, usually by iterative methods.

8.4 Description of the Method of Sequential Iteration

For this method the formulation used for the interactive slot injection equations will be that used in section 5.2, given by equations 5.19 and 5.20. In order to solve the equations it is convenient to re-write the two equations in a different form, inverting the Hilbert transform in equation 5.19 according to the methods detailed in section A.1.2 (note that the particular inversion taken will be that compatible with the boundary conditions). This gives the following equation

$$S_x(x,t) = \frac{1}{2\pi}\int_1^\infty \left\{ \frac{M^2(\xi)}{S^2(\xi)} + 2\frac{\partial}{\partial t}\left(\int_1^\xi \frac{M}{S}dz\right)\right\} \frac{\sqrt{x}}{\sqrt{\xi}(\xi - x)}d\xi.$$

This equation may be integrated with respect to x to give an expression for $S(x,t)$. Similarly equation 5.20 may be integrated with respect to x. Note that the value of M at infinity, which will henceforth be denoted by M_∞, is known from the initial conditions, as it will remain constant, according to the asymptotic analysis of section 5.3.3. Hence the system of two equations may be written

$$S(x,t) = \frac{1}{2\pi}\int_1^\infty \left(\frac{M^2}{S^2} + 2\int_1^\xi \left(\frac{M}{S}\right)_t dz\right)\left(-2\sqrt{\frac{x}{\xi}} + \log\frac{\sqrt{\xi}+\sqrt{x}}{|\sqrt{\xi}-\sqrt{x}|}\right)d\xi, \tag{8.4}$$

$$M(x,t) = -\int_\infty^x S_t d\xi + M_\infty. \tag{8.5}$$

For the moment only cases where $f(t)$ is one for negative t will be considered. When $f(t)$ is identically equal to one all time derivatives may be ignored and the second equation reduces to $M = M_\infty$, so M will now be a constant. The problem then becomes that for the steady state system solved by Fitt et al (1985) [34]. However the method used there will not be applicable to this more general problem, since it uses a rescaling $S = M_\infty^{\frac{2}{3}}T$ to give

$$T(x) = \frac{1}{2\pi}\int_1^\infty T^{-2}(\xi)\left\{-2\sqrt{\frac{x}{\xi}} + \log\frac{\sqrt{\xi}+\sqrt{x}}{|\sqrt{\xi}-\sqrt{x}|}\right\}d\xi, \tag{8.6}$$

thus eliminating M_∞. M_∞ is then found from the condition that $M_\infty = S_\infty = T^3(\infty)$. The above equation is sufficient to determine T, and hence S, with an iterative numerical relaxation scheme. However when $f(t)$ is not a constant, the unsteady term in equation 8.4 means that a similar rescaling will no longer be possible, and so it will no longer be possible to eliminate M_∞ and reduce the problem to a single equation in one variable only.

One apparently unwelcome result of the inversion of the Hilbert transform is the fact that the function $f(t)$ has now disappeared from the problem since it does not appear in either equation, nor in the boundary conditions. This may seem a little peculiar since it is to be expected that the height of the shear layer and the mass flow are dependent on the slot pressure. This is analogous to the steady state problem in which, after the re-scaling, the equation is reduced to

$$\frac{2}{\pi}\int_0^\infty \frac{T_\xi}{\xi - x}d\xi = \begin{cases} M_\infty^{-\frac{2}{3}} & 0 < x < 1, \\ M_\infty^{-\frac{2}{3}} - T^{-2} & x > 1, \end{cases} \tag{8.7}$$

from which the unknown constant M_∞ disappears upon inversion. In fact it would appear that the constant M_∞ cannot be determined from the above equation with the usual boundary conditions ($T(0) = T_x(0) = 0$), and that a one-parameter family of solutions will result. However from physical considerations it is possible to impose another constraint upon the system that is sufficient to determine M_∞ and $T(x)$ uniquely, namely continuity at $x = 1$. It may be seen from numerical solutions to this problem that if a value of M_∞ other than the correct value is chosen, the solution derived will satisfy the above equation, but the value of $T(1)$ determined by integrating T_x from 0 to 1 will differ from that determined by integrating from 1 to infinity by a value depending on M_∞. The reason for this is that the expression for T_x derived in equation 8.6 was obtained by integrating the expression obtained by inverting the original Hilbert transform, and so assumes that there are no jump discontinuities. However the expression obtained for T_x has a logarithmic singularity at $x = 1$ (see section 5.3.2) and so such a solution may exist. The values of $T(x)$ are given at two points however : at $x = 0$, T is given by the boundary conditions, and as $x \to \infty$ T is given as being equal to $M_\infty^{\frac{1}{3}}$ by an asymptotic analysis similar to that described in section 5.3.3. Hence the correct value of M_∞ to satisfy continuity is given by the equation

$$\int_0^1 T_\xi d\xi + \int_1^\infty T_\xi d\xi = M_\infty^{\frac{1}{3}}.$$

In the interactive problem, as mentioned earlier, it will not be as simple to solve the problem since it is not possible to eliminate M_∞ with a re-scaling. Although it would seem from equations 8.4 and 8.5 that it will be possible to solve the equations by a predictor-corrector method, as the equations have been integrated and all the boundary conditions been applied, the function $f(t)$ has disappeared from the equations. Again this is because it is possible to choose a value of M such that equations 8.4 and 8.5 are satisfied, but the function S has a jump discontinuity at $x = 1$. In order to prevent this discontinuity, it is necessary to impose another condition on the equations. As in the steady state, this equation arises from the fact that the Hilbert transform must be zero at infinity. Since the Hilbert transform at infinity is given by the right-hand side of equation 5.19 it follows that

$$f(t) = \frac{M_\infty^2}{S_\infty^2} + 2\int_1^\infty \left(\frac{M}{S}\right)_t d\xi. \tag{8.8}$$

Thus M and S must satisfy equations 8.4, 8.5 and 8.8 at each time step.

The method used to solve this system of equations, given S and M at time $t = 0$, say, will then be as follows.

1. Make an estimate for M at the new time. A possible estimate would be $M(x,t+\delta t) = 2M(x,t) - M(x,t-\delta t)$ as this assumes linear variations in M.

2. Using this estimate for M, find the solution for S from equation 8.4 using a method similar to that employed in the steady state case (possible now since M is now 'known'), by repeated iteration until convergence is obtained to within a specified limit.

3. From equation 8.5 a new estimate for M may now be obtained.

4. Repeat steps 2 and 3 until convergence is obtained to within a specified limit.

5. If the values of M and S obtained do not satisfy equation 8.8, then re-scale M according to equation 8.8 and repeat step 2.

6. Advance another time step.

An alternative would be to apply step 3 before convergence is reached in step 2, in other words to obtain the second estimate for M after only one iteration of equation 8.4. However although this is quicker, it would seem that the system may be less likely to converge.

8.5 A Test Problem for Sequential Iteration

In order to test the accuracy and validity of the above method of solution a test problem has been constructed, to which the analytic solution is known. The problem chosen is the system of equations in M and S,

$$\frac{2}{\pi} \int_0^\infty \frac{S_\xi}{\xi - x} d\xi = S + M - G(t), \tag{8.9}$$

$$M_x + S_t = 0, \tag{8.10}$$

where $G(t)$ is any given function of t.

Appropriate initial conditions will also be given so that the solution will be

$$S(x,t) = H(x-t)(F(x-t) - 1), \tag{8.11}$$

$$M(x,t) = H(x-t)(F(x-t) + 1) + G(t), \tag{8.12}$$

where $F(x)$ is given as the function of one variable which satisfies $F(0) = 1$, $F(\infty) = 0$ and

$$\frac{1}{\pi} \int_0^\infty \frac{F'(\xi)}{\xi - x} d\xi = F(x). \tag{8.13}$$

That the solution for S and M is given by equations 8.11 and 8.12 to the system defined by equations 8.9 and 8.10 may be seen from the fact that substitution of these solutions into equation 8.9 just gives equation 8.13, by which F is defined, and substitution into equation 8.12 gives $M_x = F'(x-t)$ and $S_t = -F'(x-t)$.

Expressions for the function F in terms of Laplace transforms are given by Stewartson (1960) [84] and Varley & Walker (1989) [102]. The expression given by Stewartson for $F(x)$ is

$$F(x) = \frac{1}{\pi}\int_0^\infty \frac{e^{-sx}}{(1+s^2)^{\frac{3}{4}}} \exp\left[-\frac{1}{\pi}\int_0^s \frac{\log u}{1+u^2}du\right].$$

The method used to solve this will be essentially the same as the first method of solving the equations for the interactive case discussed above. However some modifications have had to be made due to the linearity of this system, since in equation 8.9 an arbitrary multiple of $F(\frac{1}{2}x)$ may be added to S to give another solution for a given M. Hence it is necessary for each iteration of this equation to ensure that $S(0) = 0$. It is not thought that a similar situation will arise in the interactive problem, as there are sufficient boundary conditions for the problem to be well posed.

8.6 Stability Analysis of the Test Problem

Due to the complexity of the problem, the method for analysis of the numerical stability of these equations will be the von Neumann method rather than the matrix method (for details, see, for example, Smith (1965) [80]). Although application of this method will not conclusively prove the stability or otherwise of a numerical scheme, as some of the equations are non-linear and the expected solution is not periodic, this type of analysis often gives useful results even when the theoretical basis for it is not rigorously justified, see for example Richtmyer (1967) [71]. Considering for now the test problem given by equations 8.9 and 8.10, with the numerical scheme described above, and ignoring for now the effect of boundary conditions, a Fourier perturbation will be added to an exact solution (S, M) to give $(S + Ae^{i(kx-\omega t)}, M + Be^{i(kx-\omega t)})$ where k is real and A and B are small. Recalling that the numerical scheme is obtained, as in the 'real' problem by inverting the Hilbert transform and integrating with respect to x, so that the equations may be written

$$S(x,t) = \frac{1}{2\pi}\int_0^\infty \left(-2\sqrt{\frac{x}{\xi}} + \log\frac{\sqrt{\xi}+\sqrt{x}}{|\sqrt{\xi}-\sqrt{x}|}\right)(S(\xi,t)+M(\xi,t))d\xi,$$

$$M(x,t) = -\int_\infty^x S_t d\xi + G(t) + M_\infty.$$

The domain, namely $[0,\infty)$, will be discretised into n equally spaced regions (x_j, x_{j+1}) with $x_{n+1} = x_{max}$, say, and defining $S_\ell^j = S(x_\ell, t_j)$, leaving open for now the question of the time difference. This yields the following discretisation of the above equations :

$$\begin{aligned} S_\ell^j &= \sum_{p=0}^{n} A_{\ell p}(S_p^j + M_p^j) + Q_\ell, \\ M_{\ell+1}^j &= M_{\ell-1}^j + 2\delta x\left(\frac{S_\ell^j - S_\ell^{j-1}}{\delta t}\right), \end{aligned}$$

where $\delta x = x_j - x_{j-1}$, $\delta t = t_j - t_{j-1}$, and $A_{\ell p}$ and Q_ℓ are given by

$$2n\pi A_{\ell p} = 2\ell^{\frac{1}{2}}(p^{\frac{1}{2}} - (p+1)^{\frac{1}{2}}) + (p+1-\ell)\log\left|\frac{(p+1)^{\frac{1}{2}}+\ell^{\frac{1}{2}}}{(p+1)^{\frac{1}{2}}-\ell^{\frac{1}{2}}}\right| - (p-\ell)\log\left|\frac{p^{\frac{1}{2}}+\ell^{\frac{1}{2}}}{p^{\frac{1}{2}}-\ell^{\frac{1}{2}}}\right|,$$

$$Q_\ell = -4\pi^{-\frac{3}{2}}\sqrt{\frac{x_\ell}{x_{max}}}.$$

Note that the asymptotic expression for the solution $F'(x) \sim -(\pi x)^{-\frac{3}{2}}$, which was first noted by Stewartson (1960) [84], but is relatively simple to calculate, was used to calculate the Q_ℓ.

With this discretisation, application of the Fourier perturbation, cancellation of the first order terms, and ignoring all terms of second or higher order in A and B, or first order in δx or δt, gives the following equations

$$\begin{aligned} A(1-e^{i\omega\delta t})\frac{\delta x}{\delta t} - Bi\sin k\delta x &= 0, \\ (A+B)e^{-ikx}\sum_{p=0}^{\infty} A_{\ell p}e^{ipk\delta x} &= A. \end{aligned}$$

Thus for there to be non-zero solutions of A and B, and writing the coefficient of $(A+B)$ in the second equation as $C \doteq C_R + iC_I$,

$$\frac{\delta x}{\delta t}(1-e^{i\omega\delta t})C = -i\sin k\delta x(C-1),$$

and hence

$$\begin{aligned} e^{i\omega\delta t} &= 1 + \frac{C-1}{C}\frac{\delta t}{\delta x} i\sin k\delta x, \\ |e^{i\omega\delta t}| &= \left|1 + \frac{\delta t}{\delta x}\sin k\delta x \frac{-C_I + i(|C|^2 - C_R)}{|C|^2}\right|. \end{aligned} \tag{8.14}$$

The numerical scheme will be unstable if there are values of k such that the perturbations will grow in amplitude over time. Since k is real, the amplitude of the perturbations is proportional to $|e^{-i\omega\delta t}|$ and so for the perturbations to be stable, the term on the right of equation 8.14 must have a modulus of *greater* than unity. Although no analytic expression for C has been found, some calculations have been done to calculate the size of this term for various values. These consistently give values for $|e^{-i\omega\delta t}|$ which are less than unity, thus suggesting the scheme is stable. Moreover this is independent of whether the expression for S_t in equation 8.10 is given by forward difference, $\delta t^{-1}(S_\ell^j - S_\ell^{j-1})$, or using the Lax-Friedrichs formulation, $\frac{1}{2}\delta t^{-1}(2S_\ell^j - S_{\ell+1}^{j-1} - S_{\ell-1}^{j-1})$ (see section 9.3.1). Computations carried out using the scheme described above prove to be stable, with the numerical solution produced within $O(\delta x)$ of the analytical solution. Figure 8.1 shows the numerical solution for S compared with its correct value. Calculations were performed with 100 mesh points, with $x_{max} = 10$, and $\delta t = \delta x$. The error is, as expected, of order 0.1, which is the maximum of δx and x_{max}.

However since it is assumed that S and M tend to zero as x tends to infinity in evaluating the integral, it is important that x_{max} is sufficiently large, so that $F(x-t)$ is small, so the numerical solution is only valid while $t \ll x_{max}$.

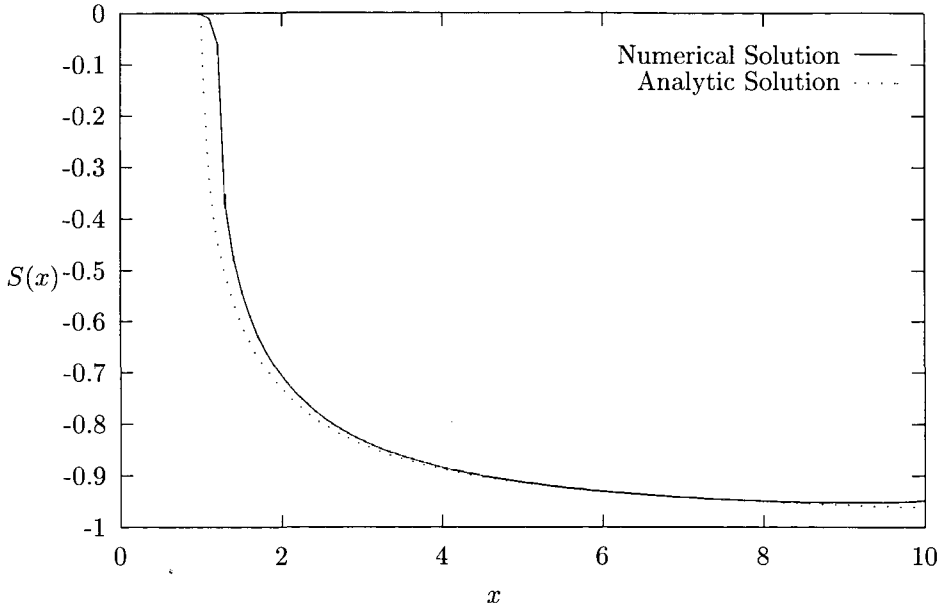

Figure 8.1: Comparison of numerical and analytic solutions for the test problem using sequential iteration

8.7 Stability Analysis of the Interactive Problem

For the interactive problem, i.e. equations 5.19 and 5.20 the same approach was used. In this problem there is the added complication of the fact that the equations are different in the two regions. For the purposes of stability analysis, though, only the second region will be considered. The effect of the first region on the system of equations is twofold : it affects the boundary conditions at $x = 1$, since continuity is imposed there, and it gives another term in equation 5.19, which will be the part of the integral over the region $(0, 1)$. However, considering the solution over the region $(0, 1)$ as 'known', addition of this term will not affect stability. Hence analysis will be applied to the following system :

$$\frac{1}{\pi}\int_0^\infty \frac{S_\xi}{\xi - x}d\xi = \frac{1}{2}f(t) - \frac{1}{2}\phi_x^2 - \phi_t, \tag{8.15}$$

$$M_x + S_t = 0, \tag{8.16}$$

$$\phi_x = \frac{M}{S}. \tag{8.17}$$

with the discretisation given by

$$S_i^{j+1} = -\sum_{p=0}^{n} A_{ip}\left(\frac{M_p^{j+1\,2}}{2S_p^{j+1\,2}} + \frac{\phi_p^{j+1} - \phi_p^j}{\delta t}\right),$$

$$0 = M_{i+1}^{j+1} - M_{i-1}^{j+1} + \frac{\delta x}{\delta t}(S_i^{j+1} - \frac{1}{2}(S_{i+1}^j + S_{i-1}^j)),$$

$$\phi_{i+1}^j - \phi_i^j = \frac{M_i^j}{S_i^j}\delta x.$$

Clearly there are many possible discretisations, for example the Lax-Friedrichs type formulation of the mass conservation equation (the second equation in the above system) could be dropped in favour

of the forward difference formulation. In that and the other equations forward difference approximations to first derivatives could be replaced by central difference approximations. However both experimentally, i.e. by applying different discretisations, and theoretically, by use of von Neumann stability analysis, it can be seen that these adjustments do not have a significant effect on the stability of this system. Applying the von Neumann analysis to this system with (S, M, ϕ) being perturbed to $(S + Ae^{i(kx-\omega t)}, M + Be^{i(kx-\omega t)}, \phi + Ce^{i(kx-\omega t)})$ gives the following system of equations.

$$\begin{aligned}
\sum_{p=l}^{n-1} A_{ip} e^{ipk\delta x} \left(\frac{BM}{S^2} e^{-i\omega\delta t} - A\frac{M^2}{S^3} e^{-i\omega\delta t} + C\frac{1 - e^{i\omega\delta t}}{\delta t} \right) &= A, \\
2Bi \sin k\delta x e^{-i\omega\delta t} + \frac{\delta x}{\delta t} A(e^{-i\omega\delta t} - \cos k\delta x) &= 0, \\
\frac{B}{S} - \frac{M}{S^2} A &= C\frac{e^{ik\delta x} - 1}{\delta x}.
\end{aligned}$$

From the requirement that there be a non-trivial solution for A, B and C an expression may be obtained for $e^{-i\omega\delta t}$. However in practice evaluating it will not be a trivial exercise, particularly since it will be strongly dependent on the values of M and S, which are unknown except in the steady state case where $f(t)$ is constant. Although it seems likely that values of $e^{-i\omega\delta t}$ greater than unity will be possible, it is best that numerical experiments are performed in order to see if this scheme works. Unfortunately in all cases the iteration failed to converge after a few time steps, irrespective of the choice of relaxation parameter, or accuracy of iteration. For the few time steps, if any, for which values are obtained, the growth of instabilities is evident. For example, with $\xi_{max} = 1.9$, $n = 10$, $f(t) = 1$, and a relaxation parameter in the iteration of $\theta = 0.1$, the iteration fails to converge after three time steps. Furthermore only the first two steps approximate well to the expected steady solution. The solutions for $S(x)$ are displayed in figure 8.2.

Minor variations to this scheme such as increasing the number of mesh points or the value of ξ_n, working in terms of S and ϕ, rather than S and M, altering the values of $\delta t/\delta x$ and the relaxation parameter θ, and using the Lax-Friedrichs formulation for $x-$derivatives, all failed to improve the stability of this scheme. Part of the difficulty in finding a stable scheme lies in the fact that stability analysis of the sequential iteration method is more complicated than for standard finite difference schemes. For this reason a stable finite difference scheme for the equations was sought, and this is discussed in chapter 8.

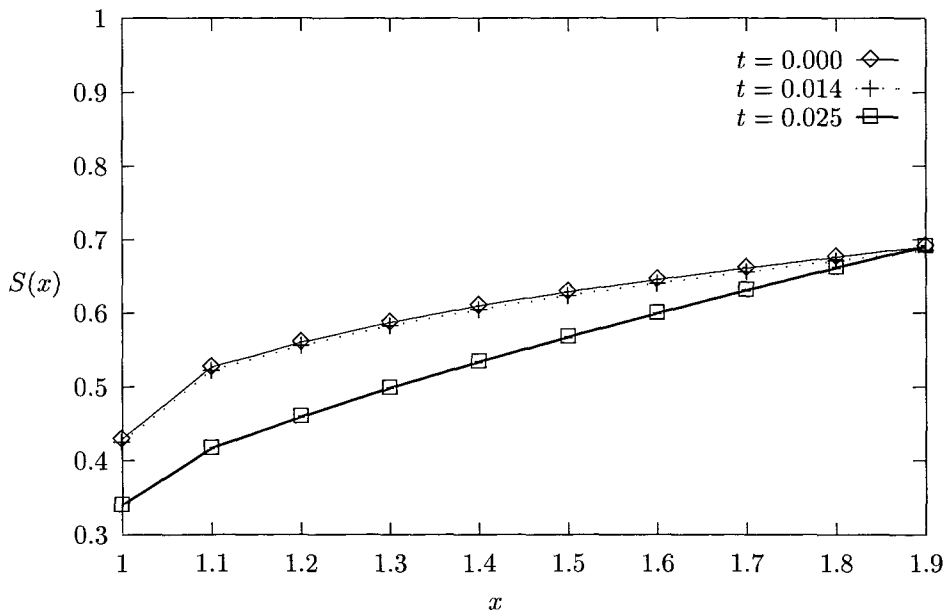

Figure 8.2: Output from the sequential iteration scheme for the interactive problem for the first 3 time steps

Chapter 9

Explicit Finite Difference Methods

9.1 Finite Difference Methods

Although the sequential iteration method has its advantages, it is less obvious than traditional finite difference methods of solving the equation, as would be applied to a standard partial differential equation (i.e. one without a singular integral). The main disadvantage of using finite difference methods, and one of the reasons that the sequential iteration method was originally conceived, is that the inversion of the Hilbert transform followed by integration that was used in the sequential iteration method, and which leads to a logarithmically singular integral, rather than the strongly singular Cauchy integral, is no longer possible. Hence it is now necessary to find some method of numerically evaluating a Cauchy principal value integral. However there are notable advantages to finite difference methods : since no iteration is used, there is no requirement that the iterative scheme converges at each time step, and the absence of iteration will mean that fewer computations will be needed. Furthermore von Neumann stability analysis will be simpler using this method. As with the sequential iteration method it is important to examine a number of test equations to examine how the stability or otherwise of the interactive equation is affected by features such as non-linearity and, more importantly, the Hilbert transform. In particular the question arises of which partial differential equation will provide the best analogy to the full interactive problem. In Tuck (1991) [96] an integro-differential equation is compared to the equivalent differential equation with the Hilbert transform ($\int dx$) operator replaced by the differential operator $\frac{d}{dx}$. This is justified on two counts : their inverses are unique to within addition of a one parameter family of functions, and asymptotically they have the same effect on the $\sin x$ and $\cos x$, an important consideration in that particular study but less so in this one. For this type of problem it seems more appropriate to replace the Hilbert transform operator with the identity operator, and one of the aims of this chapter is to explain why it is felt that for numerical purposes this is the best way to approach the question of finding numerical solutions to this equation. Naturally no replacement of the Hilbert transform operator can give even a qualitative approximation for the solution, but for the purposes of understanding the equation it is felt that the 'equivalent' partial differential equation is worth discussing, as the properties of partial differential

equations are so much better understood.

9.2 Finding Numerical Approximations to Hilbert Transforms

As mentioned in the previous section, the disadvantage of using the finite difference method is that it now becomes necessary to evaluate the Hilbert transform of the function S_x. This is particularly difficult as the Cauchy kernel $(\xi - x)^{-1}$ does not lend itself well to numerical solutions, as to evaluate the Cauchy principal value integral directly it is necessary to ignore a region arbitrarily close to the singularity, which will lead to at least two terms in the integral expression which will be unbounded as the size of the mesh tends to zero. Although in theory these terms should cancel there is a danger that errors will become larger. Furthermore as the mesh size becomes smaller, the size of this singularity will increase. This suggests using indirect methods of evaluating the integral.

Here, the notation H_i will be used for the approximation of the singular integral $\int g(\xi)(\xi - \xi_i)^{-1}$. The most obvious way to evaluate the integral is to approximate the integrand, $g(\xi)(\xi - \xi_i)^{-1}$ by a piecewise constant function, taking the values $g_k(\xi_k - \xi_i)^{-1}$ over each region (ξ_k, ξ_{k+1}). The intervals bounded by ξ_i are omitted, as these correspond to the region $(x - \epsilon, x + \epsilon)$, which is omitted in the integral when a Cauchy principal value integral is performed. Considering for the moment only functions integrated over the integral $(0, 1)$ with an even mesh this leads to the expression

$$H_i \approx \sum_{\substack{j=0 \\ j \neq i, i-1}}^{n-1} \frac{S_j}{j - i}, \tag{9.1}$$

However this is undesirable, largely because the function $g(\xi)(\xi - x)^{-1}$ will have a very large derivative near $\xi = x$, and hence the approximation of the integrand to a piecewise constant function becomes inaccurate, although not as much as one would suppose as if g is well behaved there is some cancellation of terms to the left and right of $\xi = x$. Nevertheless a better approximation is to take the function g to be piecewise constant. Furthermore to avoid evaluating the transform at a mesh point, which means that it will not be possible to integrate over either of the regions which have ξ_i as an end-point, the approximation $H_i = \frac{1}{2}(H_{i-\frac{1}{2}} + H_{i+\frac{1}{2}})$ can be made, where $H_{i\pm\frac{1}{2}}$ denotes the evaluation of the transform at $\xi_{i\pm\frac{1}{2}} = \frac{1}{2}(\xi_i + \xi_{i\pm1})$. This gives

$$H_i = \frac{1}{2} \sum_{i=0}^{n-1} g_k \log \left| \frac{2(k-i)+3}{2(k-i)-1} \right|. \tag{9.2}$$

This method may be further refined by use of a spline to approximate $g(\xi)$. This is particularly appropriate when the function g, whose transform is to be evaluated, is of the form $g = h'$, where h is the unknown variable. Further details on methods for increasing the accuracy are discussed by Piessens et al (1976) [68].

For the purposes of this study the function g to be transformed is of the form $g = h'$, where h is given only at the discrete set of points ξ_i. Hence any advantage gained by using a more sophisticated

method of numerical integration to improve accuracy may be lost if insufficient care is taken over the approximation used for h'. Veldman (1979) [104] and Veldman & Dijkstra (1980) [105] used integration by parts to obtain the following expression

$$\int_a^b \frac{h'(\xi)}{\xi - x} d\xi = -\int_a^b h''(\xi) \log|\xi - x| d\xi \approx -\sum_{k=0}^{n-1} \frac{h_{k+1} + h_{k-1} - 2h_k}{\delta x^2} \int_{\xi_k}^{\xi_{k+1}} \log|\xi - x| d\xi, \qquad (9.3)$$

assuming h' is zero at both ends of the integral. This has the advantage that the integral is no longer a Cauchy principal value, but instead contains only an integrable singularity. However this requires a numerical approximation to h'' which is particularly inappropriate in our case as it was shown in section 5.3 that the function S, which will be analogous to h in the solution of the interactive equations, has a logarithmic singularity in the first derivative at $x = 1$. Hence it makes more sense to apply the method used by Davis & Werle (1982) [21] and apply the integration by parts the other way round to give

$$\int_a^b \frac{h'(\xi)}{\xi - x} d\xi = \frac{h(b)}{b - x} + \int_a^b \frac{h(\xi)}{(\xi - x)^2} d\xi \approx \frac{h(b)}{b - x} + \sum_{k=0}^{n-1} h_k \int_{\xi_k}^{\xi_{k+1}} \frac{d\xi}{(\xi - x)^2}, \qquad (9.4)$$

where the integrals on the right-hand side must be interpreted in the Hadamard sense, and it has been assumed that $h(a)$ is zero. Again it is necessary that the function is evaluated at points other than the mesh points, and so the approximation $H_i = \frac{1}{2}(H_{i+\frac{1}{2}} + H_{i-\frac{1}{2}})$ will be used again. The behaviour of the sum obtained by using this expression is qualitatively different from the previous methods, as there is no Cauchy principal value. However the sum produced,

$$H_{i+\frac{1}{2}} = \frac{1}{\delta x} \sum_{k=0}^{n-1} \frac{4h_k}{1 - 4(k - i)^2}, \qquad (9.5)$$

still leads to singularities as the coefficient of g_k will tend to infinity as $\delta x \to 0$. This will now be cancelled by the sum of the rest of the terms, which will all have a negative coefficient of g_k. This differs from the Cauchy principal value type integrals where the coefficients of terms at equal distances from $\xi = x$ cancel out pairwise to within order 1.

When dealing with an integro-differential equation over the region $(-\infty, \infty)$ resulting from boundary layer separation, Peridier et al (1991) [67] made a transformation of the type $\xi = \tan(\frac{\pi}{2}\theta)$. This has the advantage that it is no longer necessary to find an estimate for the tail of the integral (i.e. the integral between the last mesh point and infinity). Furthermore the equation was made second order accurate by taking the function to be transformed, h', to be piecewise linear rather than piecewise constant. In other words, in each interval $h(x)$ will be approximated by the linear function that satisfies $h(\xi_i) = \xi_i$ and $h(\xi_{i+1}) = \xi_{i+1}$, namely

$$h(x) = h_k + \frac{h_{k+1} - h_k}{\xi_{k+1} - \xi_k}(x - \xi_k) \qquad x \in [\xi_k, \xi_{k+1}]. \qquad (9.6)$$

Other methods of evaluating integrals with Cauchy coefficients include using product integration methods, which are detailed, for example, by Baker (1977) [3]. Some other useful formulae are detailed by Kaya & Erdogan (1987a) [52].

As a test of the accuracy of some of the methods described above, numerical approximations to the transform of the derivative of $h(x) = (1+x)^{-1}$ will be obtained. The correct value of the transform is given by

$$\int_0^\infty -\frac{1}{(1+\xi)^2}\frac{1}{\xi - x}d\xi = \frac{\log x}{(1+x)^2} + \frac{1}{1+x}.$$

This choice of function was used as it has a similar asymptotic expansion to that of the shear layer, $S(x)$, in the interactive problem, i.e. h_x is $O(x^{-2})$ (see section 5.3.3). In the calculations a uniform mesh was used, with the $\xi_n = 10$, unless stated otherwise. The non-singular part of the integral, i.e. $\xi > 10$, was obtained by using the asymptotic formula

$$h(x) = \frac{h(\xi_n)\xi_n}{x} + O(x^{-2}).$$

From this the values of h at a further n mesh points, $\{\xi_i\}_{i=n+1}^{2n}$, may be calculated. This means that the assumption implicit in the above approximations, that x is not being evaluated near the end of the range of integration, will be valid for large values of x.

Applying the same asymptotic expansion for $\xi > \xi_n$, $h'(\xi)$ will be given, to within order x^{-3}, by $-h(\xi_n)\xi_n/x^2$. Therefore the 'tail' of the integral may be approximated by

$$\int_{\xi_{2n}}^\infty \frac{h'(\xi)}{\xi - x}d\xi \approx -h(\xi_n)\xi_n \int_{\xi_{2n}}^\infty \frac{1}{\xi^2}\frac{1}{\xi - x}d\xi = \frac{h(\xi_{2n})\xi_{2n}}{x^2}\left(\frac{x}{\xi_{2n}} + \log\frac{\xi_{2n} - x}{\xi_{2n}}\right).$$

Calculated errors for this function are displayed in figure 9.1. The methods used to evaluate it are based on the methods described above. The first two are based on the integration by parts described by equations 9.4 and 9.3 respectively, and the third is the more straightforward method defined by equation 9.2.

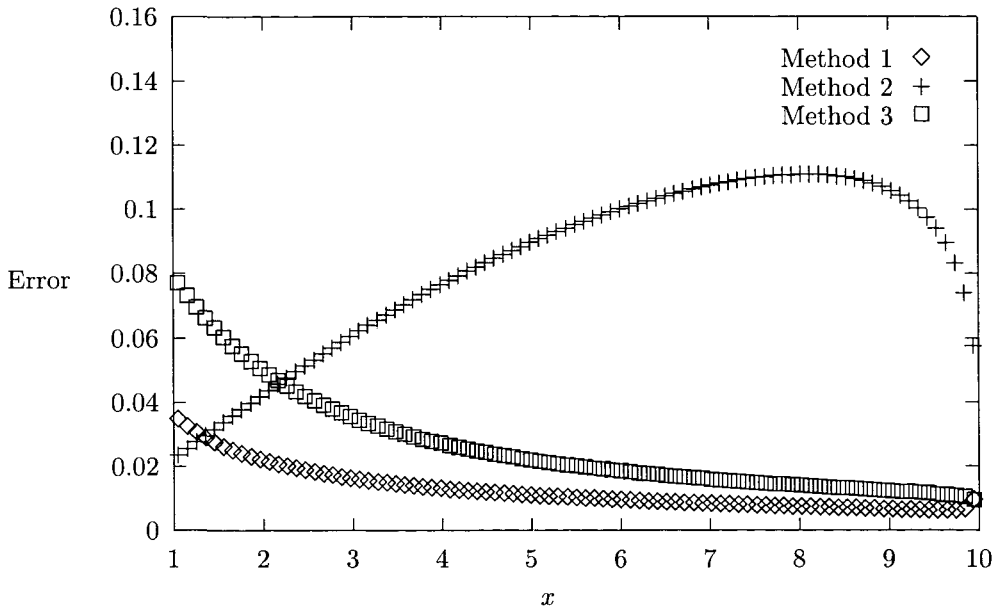

Figure 9.1: Errors in the different ways of numerically evaluating Hilbert transforms

Since the error in the singular integral is $O(\delta x)$, it is to be expected that in this case, with $n = 100$ and $\delta x = 0.1$, that an order 0.1 error will result. This is confirmed by figure 9.1, but the first method, that used by Davis & Werle (1982) [21], proves the most effective. Results for the first few mesh points, near $x = 0$, are not displayed, and do not prove to be small for the first few mesh points. This is because the assumption that x is not near the boundary of the domain of integration is not valid here. To estimate these values it is best to use an asymptotic series. However this problem is not relevant to the interactive slot injection problem of equations 5.15 and 5.16, as the Hilbert transform here only needs to be evaluated for $x > 1$.

9.3 The Test Problem for the Interactive Equation

As discussed earlier, when discussing properties such as stability of the interactive equations it is permissible to ignore the region $(0, 1)$ and concentrate instead on the problem posed in the other region. Hence the test problem will be chosen to be similar to the interactive equations, equations 5.15 and 5.16, except without the integral transforms. Throughout this chapter the equations will be expressed in terms of ϕ and S, rather than M and S, as was the case in the previous chapter. Replacing the Hilbert operator by the identity the following 'test' system of equations is derived.

$$S_x + \frac{1}{2}\phi_x^2 + \phi_t = \frac{1}{2}f(t), \tag{9.7}$$

$$(\phi_x S)_x + S_t = 0. \tag{9.8}$$

Note that the choice of coefficient of S_x chosen in the first equation is entirely arbitrary — that term could equally well be replaced by, for example, $-S_x$ since the kernel of the transform $(\xi - x)^{-1}$ will take both positive and negative values.

As with the interactive problem, these test equations can be combined to give a single equation by differentiating equation 9.7 with respect to x. Hence

$$\sigma_x^3 \sigma_{xxx} = \sigma_t^2 \sigma_{xx} + \sigma_x^2 \sigma_{tt} - 2\sigma_x \sigma_t \sigma_{xt}, \tag{9.9}$$

where $\sigma_x = S$, $\sigma_t = -\phi_x S$. This will have similarity solutions of the same form as those of the interactive equations, namely $\sigma(x,t) = t^{4\alpha-2} f(xt^{-\alpha})$, where f must satisfy the non-linear ordinary differential equation

$$f'^3 f''' = (4\alpha - 2)^2 f'' f^2 + \alpha\eta(1-\alpha) f'^3 - 2(2\alpha - 1)^2 f'^2 f. \tag{9.10}$$

The single equation form of the problem, equation 9.9, shows that the system of equations 9.7 and 9.8 is a quasi-linear third order system of partial differential equations. Writing this as a system of equations in S, ϕ and u, where $u = \phi_x$, gives

$$\begin{pmatrix} 1 & \frac{u}{2} & 0 \\ 0 & 1 & 0 \\ u & 0 & S \end{pmatrix} \begin{pmatrix} S \\ \phi \\ u \end{pmatrix}_x + \begin{pmatrix} 0 & 1 & 0 \\ 0 & 0 & 0 \\ 1 & 0 & 0 \end{pmatrix} \begin{pmatrix} S \\ \phi \\ u \end{pmatrix}_t = \begin{pmatrix} \frac{f(t)}{2} \\ u \\ 0 \end{pmatrix}.$$

The characteristics of this system are given by $\frac{dt}{dx} = \lambda$ where the λ are the roots of the equation $|B - \lambda A| = 0$ when the above equation is written as $A\boldsymbol{\omega}_x + B\boldsymbol{\omega}_t = \boldsymbol{a}$ where $\boldsymbol{\omega}$ is the column vector with components (S, ϕ, u). The cubic equation this gives for λ is $\lambda^3 S = 0$, so the only characteristics are given by $dt = 0$. Thus the necessary conditions to solve the problem on the region $(1, \infty)$ will be the initial values of S and ϕ, and the values of S, ϕ and u on $x = 1$. In the interactive problem S and S_x are given by analysis of the region $(0, 1)$, using the fact that $S(0) = S_x(0) = 0$, and it may be arbitrarily imposed that $\phi(1) = 0$.

The most straightforward difference scheme for this system of equations, using the usual notation, is the following :-

$$\begin{aligned} \phi_i^{j+1} &= \phi_i^j + \delta t \left(\frac{f(t)}{2} - \frac{1}{2} \left(\frac{\phi_{i+1}^j - \phi_{i-1}^j}{2\delta x} \right)^2 - \frac{S_{i+1}^j - S_{i-1}^j}{2\delta x} \right), \\ S_i^{j+1} &= S_i^j - \frac{\delta t}{\delta x^2} \left(\frac{(\phi_{i+1}^j - \phi_{i-1}^j)(S_{i+1}^j - S_{i-1}^j)}{4} + S_i^j(\phi_{i+1}^j + \phi_{i-1}^j - 2\phi_i^j) \right). \end{aligned} \tag{9.11}$$

Applying the von Neumann stability analysis, with $(S, \phi) \to (S + Ae^{i(k\delta x - \omega t)}, \phi + Be^{i(k\delta x - \omega t)})$ to this scheme gives the following system of equations for A and B.

$$A \left(\frac{\delta t}{\delta x} i \sin k\delta x \right) + B \left(e^{-i\omega\delta t} - 1 + u \frac{\delta t}{\delta x} i \sin k\delta x \right) = 0, \tag{9.12}$$

$$A \left(e^{-i\omega\delta t} - 1 + ui \frac{\delta t}{\delta x} \sin k\delta x + u_x \delta t \right) + B \left(\frac{\delta t}{\delta x} S_x i \sin k\delta x + \frac{\delta t}{\delta x^2} S(2\cos k\delta x - 2) \right) = 0, \tag{9.13}$$

where $u = \phi_x$. Note that at this stage the following terms may be ignored as they will be an order of magnitude smaller than the other terms : the $u_x \delta t$ term in the coefficient of A in the second equation will certainly be smaller than the other terms in that bracket, as will the $\frac{\delta t}{\delta x} S_x i \sin k\delta x$ term in the coefficient of B in the second equation. Thus for there to be a non-trivial solution for A and B the following equation must hold

$$\left(e^{-i\omega\delta t} - 1 + u \frac{\delta t}{\delta x} i \sin k\delta x \right)^2 = i \sin k\delta x \frac{\delta t^2}{\delta x^3} S(2\cos k\delta x - 2).$$

If $\frac{\delta t}{\delta x}$ is order 1, then the term on the right-hand side will dominate and values of $|e^{-i\omega\delta t}|$ greater than one will certainly be possible. Hence the ratio of interest, which must be order 1, is $\delta t^2/\delta x^3$, which will henceforth be denoted by r^2. If this is order 1 then $\frac{\delta t}{\delta x}$ will be small and hence

$$e^{-i\omega\delta t} = 1 \pm 2r\sqrt{S} \sin \frac{k\delta x}{2} e^{\frac{3i\pi}{4}} \sqrt{\sin k\delta x} + O(\delta x^{\frac{1}{2}}). \tag{9.14}$$

Clearly the above expression permits values for $e^{-i\omega\delta t}$ greater than unity, since the last term is a complex number with a non-zero real part, and so one of the possible solutions will have a real part greater than one. Hence the above scheme is unstable and it will be necessary to examine other numerical schemes.

9.3.1 Lax-Friedrichs Scheme

The Lax-Friedrichs scheme, as discussed earlier, is particularly useful for hyperbolic equations, and first order partial differential equations, for example $u_t + u_x = 0$ for which the scheme

$$u_i^{j+1} = u_i^j - \frac{\delta t}{\delta x}\frac{(u_{i+1}^j - u_{i-1}^j)}{2},$$

is unstable, since the usual perturbation gives

$$e^{-i\omega\delta t} = 1 - \frac{\delta t}{\delta x} i \sin k\delta x, \tag{9.15}$$

which will always have a modulus greater than one for some values of k. However by replacing the term u_i^j in the approximation for u_t by its average over the neighbouring mesh points to obtain the scheme

$$u_i^{j+1} = \frac{u_{i+1}^j + u_{i-1}^j}{2} - \frac{\delta t}{\delta x}\left(\frac{u_{i+1}^j - u_{i-1}^j}{2}\right),$$

the "1" in the expression for $e^{-i\omega\delta t}$ (equation 9.15) is replaced by a "$\cos k\delta x$", giving

$$e^{-i\omega\delta t} = \cos k\delta x - \frac{\delta t}{\delta x} i \sin k\delta x.$$

which will have a modulus of less than one provided $|\frac{\delta t}{\delta x}|$ is less than one.

In this test problem, therefore, the equivalent change in the approximations for S_t and ϕ_t will have the same effect, namely in the stability analysis the "1" in each of equations 9.12 and 9.13 will be replaced by a $\cos k\delta x$, so equation 9.14 will become

$$\begin{aligned} e^{-i\omega\delta t} &= \cos k\delta x \pm 2r\sqrt{S}\sin\frac{k\delta x}{2} e^{\frac{3i\pi}{4}}\sqrt{\sin k\delta x} + O(\delta x^{\frac{1}{2}}), \\ &= 1 - 2s^2 \pm \sqrt{8r^2 S} e^{\frac{3i\pi}{4}} s^{\frac{3}{2}}\sqrt{1-s^2}. \end{aligned} \tag{9.16}$$

where $s = \sin\frac{k\delta x}{2}$. Noting that $\sqrt{8r^2S}$ is real, this means that there will always be a value of $e^{-i\omega\delta t}$ with a real part greater than one, since for small values of s the real part of the right-hand side will be $1 \pm \sqrt{8r^2S}s^{\frac{3}{2}}$ to within order s^2. Hence use of the Lax-Friedrichs formulation alone will not provide a stable solution for this problem.

9.3.2 The Crank-Nicolson Method

The Crank-Nicolson method is often used in the context of parabolic equations. Used with the heat equation it has the effect of making any difference scheme stable regardless of the size of $\frac{\delta t}{\delta x^2}$. To see this it is necessary to apply the normal perturbation to the ordinary explicit difference scheme

$$u_i^{j+1} = u_i^j + \frac{\delta t}{\delta x^2}(u_{i+1}^j + u_{i-1}^j - 2u_i^j),$$

to give

$$e^{-i\omega\delta t} = 1 - 4\frac{\delta t}{\delta x^2}\sin^2\frac{k\delta x}{2}.$$

Therefore values of $e^{-i\omega\delta t}$ with modulus greater than one are permissible if $\frac{\delta t}{\delta x^2}$ is greater than $\frac{1}{2}$. However the Crank-Nicolson method changes the scheme in that instead of using the forward time difference $\delta t^{-1}(u_i^{j+1} - u_i^j)$ at the time-step corresponding to j and equating it to the central second derivative approximation at time j, it uses central difference approximators at the time step $j + \frac{1}{2}$, using linear interpolation where necessary. This gives the scheme

$$u_i^{j+1} = u_i^j + \frac{\delta t}{\delta x^2}\frac{1}{2}\left(u_{i+1}^j + u_{i-1}^j - 2u_i^j + u_{i+1}^{j+1} + u_{i-1}^{j+1} - 2u_i^{j+1}\right),$$

and hence

$$e^{-i\omega\delta t} = 1 + \frac{1}{2}\frac{\delta t}{\delta x^2}(1 + e^{-i\omega\delta t})(-4\sin^2 k\delta x)$$

$$\Rightarrow e^{-i\omega\delta t} = \frac{1 - 2\frac{\delta t}{\delta x^2}\sin^2\frac{k\delta x}{2}}{1 + 2\frac{\delta t}{\delta x^2}\sin^2\frac{k\delta x}{2}}.$$

Thus the effect of this scheme in general is to replace a scheme of the form

$$u_i^{j+1} = u_i^j + A_{ik}u_k^j,$$

for some matrix $\{A_{ik}\}$, with one of the form

$$u_i^{j+1} = u_i^j + A_{ik}\frac{1}{2}(u_k^{j+1} + u_k^j),$$

which changes the stability criterion from something of the form

$$e^{-i\omega\delta t} = 1 - a \tag{9.17}$$

to

$$\begin{aligned} e^{-i\omega\delta t} &= 1 - \frac{1}{2}a(1 + e^{-i\omega\delta t}), \\ \Rightarrow e^{-i\omega\delta t} &= \frac{2-a}{2+a} = 1 - \frac{2a}{2+a} = -1 + \frac{4}{2+a} \end{aligned}$$

Thus the Crank-Nicolson scheme will be stable as long as a is positive. In particular it stabilises a scheme where the instability is caused by the term a in a stability criterion such as that of equation 9.17 becoming too positive, so that $e^{-i\omega\delta t}$ becomes less than -1. However this does not apply in the test problem, as from equation 9.14 the problem is that "a" is allowed to be negative. In this case the Crank-Nicolson is unhelpful, as from the above equation if a is negative unbounded values of $e^{-i\omega\delta t}$ may occur.

9.3.3 Averaging

Another possible way to improve the stability is to apply the above formulae for all S_i^{j+1} and ϕ_i^{j+1} and then to take the average value of the next and previous mesh points, i.e. apply

$$S_i^{j+1} = \frac{1}{2}\left(\overline{S}_{i+1}^{j+1} + \overline{S}_{i-1}^{j+1}\right),$$

where $\overline{S}$ denotes the expression for S_i^{j+1} obtained by applying a previous scheme. To consider the effect this will have on stability, suppose that the previous scheme yields the stability relation

$$e^{-i\omega\delta t} = a,$$

where a in general will depend on $k\delta x$, and, for a non-linear equation, on S, ϕ, etc. Then, when the above formula for the averaging process is applied, the new relation will be

$$e^{-i\omega\delta t} = \frac{1}{2}a(e^{ik\delta x} + e^{-ik\delta x}) = a\cos k\delta x.$$

This is a partial improvement, and will certainly not lead to new instabilities, but it will only be able to make an unstable scheme stable if the original expression for $e^{-i\omega\delta t}$ became greater than unity only for values of $k\delta x$ where $\cos k\delta x$ is small. This is not the case in any of the schemes for the interactive test problem, so averaging will not in itself give a stable scheme.

Although this suggests the above schemes will be unstable, use of von Neumann analysis does not provide a rigorous proof. Hence the above schemes were tried for the test problem. All were found to become unstable quickly, as predicted from the von Neumann analysis. The computations were performed with $f(t) = 1$, and boundary conditions $\phi(1,t) = S(1,t) = S_x(1,t) = 0$. The region over which the equations were solved was $(0, 10)$. The initial conditions were $S = 1$ and $\phi = x$. With these conditions, the solution should be $S = 1$ and $\phi = x$ for all t. Figure 9.2 shows the behaviour of S at $t = 2$ for three sets of computations, all using 100 mesh points. The graph denoted 'A' was used for the scheme defined by equation 9.11. The graph labelled 'B' used the Lax-Friedrichs scheme, and graph 'C' used Lax-Friedrichs and averaging. Clearly instabilities have arisen. The time steps in these computations were given by $\delta t/\delta x^{\frac{3}{2}} = 0.9$, but in practice the instabilities arose irrespective of the size of the time steps used.

9.4 A Simpler Test Problem

The difficulty in finding a solution for the above equations has so far been in the fact that the system is third order, a fact which is most easily seen from equation 9.9. However replacing the σ_{xxx} with σ_{xx} will change this equation to a more familiar looking second order equation. One way of achieving this without making drastic changes to the test problem given by equations 9.7 and 9.8 is to replace the S_x term in equation 9.7 with S to give the following system of equations

$$S + \frac{1}{2}\phi_x^2 + \phi_t = \frac{1}{2}f(t), \tag{9.18}$$

$$(\phi_x S)_x + S_t = 0. \tag{9.19}$$

These are effectively the interactive equations over the region $x > 1$ with the Hilbert transform of S_x replaced by S. However this is a more fundamental change than replacing the Hilbert transform of S_x with S_x as the system is now second order.

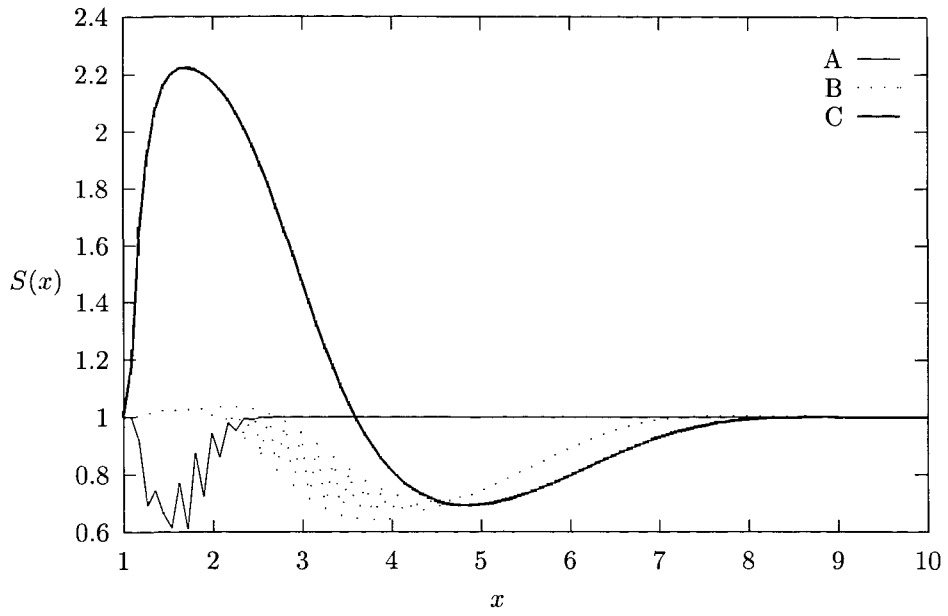

Figure 9.2: Numerical Instabilities for the Test Problem Without Hilbert Transform

This is now a hyperbolic second order system of equations. Differentiation of the first equation with respect to x means they may be written as a system of two first order equations in two variables, S and $u = \phi_x$.

$$\begin{pmatrix} 1 & u \\ u & S \end{pmatrix} \begin{pmatrix} S \\ u \end{pmatrix}_x + \begin{pmatrix} 0 & 1 \\ 1 & 0 \end{pmatrix} \begin{pmatrix} S \\ u \end{pmatrix}_t = \begin{pmatrix} 0 \\ 0 \end{pmatrix}.$$

Writing this as $A\boldsymbol{\omega}_x + B\boldsymbol{\omega}_t = \mathbf{0}$ as before, except with $\boldsymbol{\omega} = (S, u)$, the characteristics are given by $\frac{dx}{dt} = \lambda$ where the λ are given by the solutions of the equation $|A - \lambda B| = 0$. Thus $\lambda = u \pm \sqrt{S}$, and so for S non-zero the characteristics are real and distinct.

As before this system will have similarity solutions, this time of the form $S = t^{2\alpha-2} f(\eta)$, $u = t^{\alpha-1} g(\eta)$, where $\eta = xt^{-\alpha}$ and f and g satisfy

$$-\alpha\eta g' + gg' + f' + (\alpha - 1)g = 0, \tag{9.20}$$

$$(fg)' - \alpha\eta f' + (2\alpha - 2)f = 0. \tag{9.21}$$

Although it is often preferable to solve hyperbolic equations by changing to characteristic co-ordinates, this will not be done here as there is no such analogy with the more complicated third order problem. Instead a numerical scheme similar to those used in the preceding chapter will be used. Using the Lax-Friedrichs formulation for differentiation with respect to time, and replacing the S_x term with S, equations 9.11 will be replaced by

$$\phi_i^{j+1} = \frac{1}{2}(\phi_{i+1}^j + \phi_{i-1}^j) + \delta t \left(\frac{1}{2} f(t) - \frac{1}{2} \left(\frac{\phi_{i+1}^j - \phi_{i-1}^j}{2\delta x} \right)^2 - S_i^j \right), \tag{9.22}$$

$$S_i^{j+1} = \frac{1}{2}(S_{i+1}^j + S_{i-1}^j) - \frac{\delta t}{\delta x^2} \left(\frac{(\phi_{i+1}^j - \phi_{i-1}^j)(S_{i+1}^j - S_{i-1}^j)}{4} + S_i^j(\phi_{i+1}^j + \phi_{i-1}^j - 2\phi_i^j) \right). \tag{9.23}$$

Application of the usual perturbation, as in the previous section, will lead to an equation similar to equations 9.12 and 9.13. However use of the Lax-Friedrichs formulation will mean that the two terms of the form $e^{-i\omega\delta t} - 1$ will be replaced by $e^{-i\omega\delta t} - \cos k\delta x$. Furthermore the change of S_x to S in the first equation means that in equation 9.12, the coefficient of A will change from $\frac{\delta t}{\delta x} i \sin k\delta x$ to δt. The condition that A and B are non-zero now becomes

$$\left(e^{-i\omega\delta t} - \cos k\delta x + u\frac{\delta t}{\delta x} i \sin k\delta x\right)^2 = \frac{\delta t^2}{\delta x^2} S(2\cos k\delta x - 2). \tag{9.24}$$

Note that the ratio of importance is now $\frac{\delta t}{\delta x}$ as expected, since this is a second order hyperbolic equation. This ratio will henceforth be denoted by r. The above result shows that, with this scheme, if $k\delta x = \pi$ then $e^{-i\omega\delta t}$ will equal $-1 \pm 2ir\sqrt{S}$, which will clearly have a modulus of greater than one. However this problem would not arise if the $\cos k\delta x$ term were replaced by a $\cos 2k\delta x$ term. As this term arises in the approximation for ϕ_{xx} it is necessary to reconsider the approximation used for ϕ_{xx} in the scheme. In the scheme of equations 9.22 and 9.23 this approximation appears in the very last term, and was

$$\phi_{xx}(\xi_i, t_j) = \frac{\phi^j_{i+1} + \phi^j_{i-1} - 2\phi^j_i}{\delta x^2} + O(\delta x).$$

Here, this will be replaced with

$$\phi_{xx}(\xi_i, t_j) = \frac{\phi^j_{i+2} + \phi^j_{i-2} - 2\phi^j_i}{4\delta x^2} + O(\delta x).$$

The reasons why this is necessary are rather subtle and need not be discussed here. The change in the perturbation analysis will be in the right-hand side of equation 9.24, where the term in brackets, $(2\cos k\delta x - 2)$, will be replaced by $(\cos 2k\delta x - 1)/2$. Hence

$$\left(e^{-i\omega\delta t} - \cos k\delta x + uir \sin k\delta x\right)^2 = r^2 S(\cos 2k\delta x - 1)/2. \tag{9.25}$$

On taking the square-root of this, it follows that

$$e^{-i\omega\delta t} = \cos k\delta x - ir(u \pm \sqrt{S}) \sin k\delta x$$

Therefore the scheme will always be stable provided $r(u + \sqrt{S}) < 1$. This is the expected result since $u + \sqrt{S}$ is the largest eigenvalue of the problem, so $r(u + \sqrt{S})$ is the Courant number. In practice a Courant number of 0.95 is often chosen in order to exclude non-linear instabilities. Note that choice of a Courant number less than one will mean that the scheme will satisfy the CFL condition and be convergent, as well as stable (see, for example, Smith (1965) [80]).

Applying this scheme with initial conditions for ϕ and S, and boundary conditions at $x = 0$ for S and ϕ_x the following results may be produced for Courant numbers of less than 1. The mesh used was even, with $\xi_n = 10$, with a Courant number of 0.9, and boundary conditions $S = 1$ and $\phi = 0$ at $x = 1$. The initial conditions were $S = 1$ and $\phi = x$, with $f(t) = 1$ for $t < 0$, and $f(t) = 1 + t/(1 + t)$ for positive t. The choice of a function $f(t)$ which is discontinuous in the second derivative appears

to give a singularity in S along $x = t$, but this does not cause any numerical problems. The solutions found for S are shown in figure 9.3, for various values of n, where n is the number of mesh points, and show convergence with an error of order $O(\delta x)$. For a Courant number greater than one the numerical solution quickly diverges, as expected.

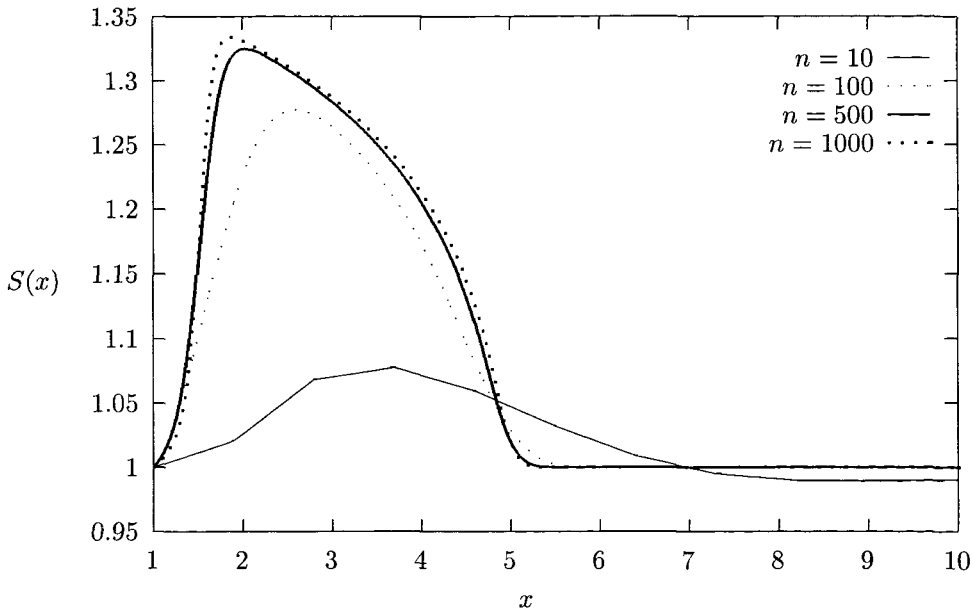

Figure 9.3: Numerical solutions to the second order test problem without a Hilbert transform for various numbers of mesh points

9.5 The Effect of the Hilbert Transform

Although the simpler second order test problem has now been solved numerically, the question of how to attack the interactive problem remains open. There are two crucial differences between the problem solved in the preceding section and the interactive problem : the fact that the interactive problem is third order, and the presence of the Hilbert transform in the interactive problem. It has already been shown that the presence of the extra x-derivative in the interactive equation, even when the Hilbert transform is excluded, poses formidable problems from a numerical point of view, however the effect of the Hilbert transform has not yet been discussed in any detail. One point of interest is the question of to what extent the 'order' of any partial differential equation containing a Hilbert transform may be defined, as a transform of S_x may also be interpreted as a transform of S or S_{xx} etc, by a change of kernel obtained by integration by parts (as in equations 9.3 and 9.4). Indeed, as has already been mentioned, a case could be made for arguing that the presence of a Hilbert transform has the effect of increasing the order of the equation by 1, on the grounds that the inverse of the Hilbert transform has the same dimension of non-uniqueness as the inverse of differentiation, and furthermore that in the form in which the kernel is integrable without recourse to a Cauchy principal value, i.e. that of

equation 9.3, the transform is of the function S_{xx}. Nevertheless, in this analysis, for the purposes of finding numerical solutions the singular partial integro-differential equation which will be compared to that of the last section will be the second order equation with the S replaced by the Hilbert transform of S.

This may partly be justified by considering Fourier transforms with respect to x and t. Suppose a function $f(x,t)$ has a Fourier transform $\tilde{f}(k,\omega)$, where k and ω are the x and t transform variables respectively. The transforms of f_x and f_t will then be $-ik\tilde{f}$ and $-i\omega\tilde{f}$. However the Fourier transform of the infinite-range Hilbert transform will just be $i\pi\mathrm{sgn}(k)$. This suggests that in stability analyses the growth of unstable modes will only be affected by infinite range Hilbert transforms to within multiplication by a constant.

For the purposes of this analysis the method used to estimate the Hilbert transform of a function S, with $S(\xi_p) = S_p$, will be given by $\sum A_{ip}S_p$, where

$$A_{ip} = \begin{cases} \frac{1}{\pi}\log\left(\frac{2(p-i)+1}{2(p-i)-1}\right) & i \neq p, \\ 0 & i = p. \end{cases} \tag{9.26}$$

Note that this is not quite enough to give a good approximation to the Hilbert transform, especially at large values of i, as the range of integration is $(0,\infty)$ whereas the sum defined above is only an approximation over the range $(0,\xi_n)$. However it will be assumed that ξ_n is sufficiently large that S is small for values of S larger than ξ_n and that, for the moment, only instabilities far from the boundary of the mesh region are being considered.

The contribution to the stability condition from the Hilbert transform term of a function S, at $x = \xi_\ell$, $t = t_j$, is obtained by evaluating the sum when the S_ℓ^j are replaced by $S_\ell^j + Ae^{i(k\delta x - \omega\delta t)}$ and the order A term divided by $e^{i(kx-\omega t)}$, as the other terms were. Applying this to the sum evaluated at the mesh point $\xi_\ell = \ell\delta x$ gives

$$\sum_{p=0}^{n-1} A_{\ell p}S_p \to \sum_{p=0}^{n-1} A_{\ell p}e^{i(p-\ell)k\delta x}.$$

The first feature to observe in this expression is that each term is order one, unlike a term corresponding to an $x-$derivative, say, in which there would be a factor δx^{-1}. This justifies the hypothesis that in some sense the Hilbert transform operator 'corresponds' with the identity operator.

To simplify this sum, note that from equation 9.26, $A_{\ell,\ell-p} = -A_{\ell,\ell+p}$, and assume that $\ell < \frac{1}{2}n$ (the corresponding expression for $\ell > \frac{1}{2}n$ is only slightly different), to give an expression for the sum. Let this sum be denoted by $2iC^2$, then

$$2iC^2 = \sum_{q=1}^{\ell} 2iA_{\ell,\ell+q}\sin qk\delta x + \sum_{p=2\ell+1}^{n-1} A_{\ell p}e^{i(p-\ell)k\delta x}. \tag{9.27}$$

From equation 9.26 it follows that $A_{\ell p}$ is of order $(\ell-p)^{-1}$ for large values of $\ell - p$. Since $\ell\delta x = x$, it follows that everywhere except near $x = 0$, ℓ is large, and so in the second sum of equation 9.27

the values of $\ell - p$ will be large. Thus this sum will tend to a sum of terms of the form $e^{ip\theta}/p$, where $\theta = k\delta x$, and it is well known, e.g. from Gradshteyn & Ryzhik (1965) (page 38), that this sum is convergent for non-zero values of θ, with the sum of the series being given by

$$\sum_{p=1}^{\infty} \frac{e^{ip\theta}}{p} = -\frac{1}{2}\log 4\sin^2\frac{\theta}{2} + i\frac{\pi - \theta}{2},$$

for $0 < \theta < 2\pi$. For order 1 values of $k\delta x = \theta$, therefore, the second sum of equation 9.27 will be convergent, and since the largest terms are of order $(\ell - p)^{-1}$, this series will be of order $(\ell - p)^{-1}$, although for small values of $\theta = k\delta x$, it will be of order $\log k\delta x(\ell - p)^{-1}$.

By the same reasoning the first sum of equation 9.27 is convergent, although since there are no cosine terms, there is no logarithmic singularity for small values of $k\delta x$. Hence C is a real number, which may be obtained by numerically evaluating the sum. The possible largest value of C, which is the value of most interest, will be obtained in the limit as $k\delta x \to 0$. Hence C is given by, from equation 9.27,

$$C^2 = \sup_{0<\theta<2\pi} \sum_{q=1}^{\infty} \log\frac{2q+1}{2q-1}\sin q\delta x, \tag{9.28}$$

which may be evaluated numerically to about 1.55. (This is the value obtained for 5000 terms with $\theta = 0.01$). A maximum value of $\pi/2$ is obtained for the related series $q^{-1}\sin q\delta x$, and this seems likely to be close to C. This ties in well with the fact that the expected perturbation from the Fourier mode, is $\pm 2iC$, whereas the effect of a Hilbert transform on the Fourier transform of a function is known to be to multiply it by $\pm i\pi$. Thus it may be said, that for the purposes of Fourier analysis of numerical schemes for partial differential equations with Hilbert transforms, that in the same way that differentiation with respect to x and t have the effect of multiplication by ik and $-i\omega$ respectively, so the Hilbert transform has the effect of multiplying by $\pm i\pi$. This result will hold for all singular partial integro-differential equations with Hilbert transforms, and regardless of whether the Hilbert transform is over a finite, infinite, or semi-infinite region, although for the finite and semi-infinite cases the instability criteria will be different near the boundaries.

9.6 A Test Problem With a Hilbert Transform

Replacement of the function S in equation 9.18 with the semi-infinite range Hilbert transform gives the following test problem

$$\frac{1}{\pi}\int_0^{\infty} \frac{S(\xi,t)}{\xi - x}d\xi + \frac{1}{2}\phi_x^2 + \phi_t = \frac{1}{2}f(t), \tag{9.29}$$

$$(\phi_x S)_x + S_t = 0. \tag{9.30}$$

The presence of similarity solutions will not be affected by the Hilbert transform, as shown by equation 8.2, and they will take the same form as the similarity solutions of equations 9.18 and 9.19, namely $S = t^{2\alpha-2}f(\eta)$, $u = t^{\alpha-1}g(\eta)$, where $\eta = xt^{-\alpha}$ and f and g will satisfy a very similar pair of

equations to equations 9.20, i.e.

$$-\alpha\eta g' + gg' + \frac{1}{\pi}\int_0^\infty \frac{f'(\xi)}{\xi-\eta}d\xi + (\alpha-1)g = 0, \tag{9.31}$$

$$(fg)' - \alpha\eta f' + (2\alpha-2)f = 0. \tag{9.32}$$

For the purposes of finding a numerical solution to this system, the calculation of the Hilbert transform at each mesh point ξ_i will be given by the integral over the region $(0,\infty)$, taking S to be equal to S_k over each interval (ξ_k, ξ_{k+1}). This gives a numerical scheme, using the Lax-Friedrichs formulation as before, similar to that for the previous problem, for which the scheme was given by equations 9.22 and 9.23. The only change is the introduction of the Hilbert transform, which gives

$$\phi_i^{j+1} = \frac{1}{2}(\phi_{i+1}^j + \phi_{i-1}^j) + \delta t\left(\frac{1}{2}f(t) - \frac{1}{2}\left(\frac{\phi_{i+1}^j - \phi_{i-1}^j}{2\delta x}\right)^2 - \sum_{p=0}^{n-1} A_{ip}S_p^j\right), \tag{9.33}$$

$$S_i^{j+1} = \frac{1}{2}(S_{i+1}^j + S_{i-1}^j) - \frac{\delta t}{\delta x^2}\left(\frac{(\phi_{i+1}^j - \phi_{i-1}^j)(S_{i+1}^j - S_{i-1}^j)}{4} + S_i^j(\phi_{i+1}^j + \phi_{i-1}^j - 2\phi_i^j)\right), \tag{9.34}$$

where the A_{ip} define the singular integral and are given by equation 9.26.

From section 9.5 it follows that the effect of a Hilbert transform in the stability analysis is to introduce a factor $\pm 2iC^2$, where C^2 is defined by equation 9.28 and is roughly $\pi/2$. Given C^2, the expression for the stability of the numerical scheme described above by equations 9.33 and 9.34 becomes that of equation 9.24 (which gave the value of $e^{-i\omega\delta t}$ for the test problem of section 9.4, in which there was no Hilbert transform), with the right-hand side being multiplied by $2iC^2$, giving

$$\left(e^{-i\omega\delta t} - \cos k\delta x + u\frac{\delta t}{\delta x} i \sin k\delta x\right)^2 = \frac{\delta t^2}{\delta x^2} 2iC^2 S(2\cos k\delta x - 2),$$

and hence

$$e^{-i\omega\delta t} = \cos k\delta x - ir\left(u\sin k\delta x \pm (1+i)C\sqrt{S}\sin\frac{k\delta x}{2}\right). \tag{9.35}$$

This may be expanded in powers of $k\delta x$, in which case the real part of $e^{-i\omega\delta t}$ will be

$$1 \pm Cr\sqrt{S}\frac{k\delta x}{2} - 2(k\delta x^2)^2 + O(k\delta x)^3.$$

Therefore instabilities may grow for $k\delta x$ small. However, this analysis is only relevant for $k\delta x \gg \delta x$, and for finite values of δx it is likely that there will be no $k\delta x$ for which both $k \gg 1$ and $k\delta x$ is sufficiently small for $e^{-i\omega\delta t}$ to be greater than one. For order 1 values of $k\delta x$, the highest value for $|e^{-i\omega\delta t}|$ obtained from equation 9.35 will be when the $\pm$ sign is taken to be positive, and $\sin k\delta x = -sin\frac{k\delta x}{2}$, so that imaginary terms are of the same sign. In this case the expression may be given in terms of $y = \sin\frac{k\delta x}{2}$.

$$e^{-i\omega\delta t} = 1 - 2y^2 + rC\sqrt{S}y + iy\left(ru + rC\sqrt{S}\right).$$

$|e^{-i\omega\delta t}|^2$ will therefore be a quartic in y, with a maximum near $y = 0$, and tending towards infinity for positive and negative y. Note though that since $y = \sin\frac{k\delta x}{2}$, only values of y between -1 and 1

need be considered. The minima will be reached near the value of given by $2y^2 = 1 + rC\sqrt{S}$, as the real part of $e^{-i\omega\delta t}$ is zero here. For sufficiently small r this will be in the region $(-1, 1)$. Hence the condition for $e^{-i\omega\delta t}$ to be less than one everywhere except in the region near $y = 0$ may be obtained by imposing that it is less than one at $y = \pm 1$. This will hold provided

$$r^2\{(C\sqrt{S} - 1)^2 + (u + C\sqrt{S})^2\} < 1,$$

where C is given by equation 9.28.

Thus a Courant number, c, may usefully be defined by

$$c = \{(C\sqrt{S} - 1)^2 + (u + C\sqrt{S})^2\}^{\frac{1}{2}} \frac{\delta t}{\delta x}.$$

It is expected (although not conclusively proven) that numerical experiments performed with a Courant number of less than one will be stable and converge to the correct solution. However, as a result of the instability near $k\delta x = 0$, for larger values of n a smaller value of r may be needed. Naturally convergence cannot be tested until the correct solution is known, so in order to test the validity of this analysis, the equation was modified slightly so that there will be a known analytical solution with which the numerical solution may be compared. Since both stability and convergence are dependent only on the highest derivatives in a problem, the stability analysis considered above will also be valid for the following system of equations on the region $(1, \infty)$

$$\begin{aligned} \frac{1}{\pi} \int_0^\infty \frac{S(\xi, t)}{\xi - x} d\xi &= \begin{cases} 0 & x < 1, \\ \phi_t + \frac{1}{2}\phi_x^2 - \frac{3x^2h'^2 + (1-x^2)hh'' + \frac{1}{2}axh^2 - 2ahx^{\frac{3}{2}}h'}{h^2} & x > 1, \end{cases} \\ (\phi_x S)_x + S_t &= 0. \end{aligned}$$

where h is an arbitrary function of time, a is an arbitrary constant, and S is given over the region $(0, 1)$. The solution of this system is

$$S = \frac{h(t)}{x^{\frac{1}{2}}}, \qquad \phi = \frac{2}{3}cx^{\frac{3}{2}} - \frac{h'(t)}{h(t)}(x^2 - 1).$$

The method used to evaluate the Hilbert transform was that used in the above stability analysis, i.e. H_i was given by $A_{ip}S_p$ where A_{ip} was given by equation 9.26. However in order to prevent large errors occurring for values of x near the last mesh point x_{max} it is necessary to numerically estimate the values of S over the region $(x_{max}, 2x_{max})$ and apply the singular integral transform over the region $(0, 2x_{max})$, then adding a tail. This may be done by asymptotic methods, observing that S behaves like $x^{-\frac{1}{2}}$ over this region. Although this observation is based upon the known solution, it is usually possible to obtain some sort of asymptotic expression at infinity when the solution is not known, as was done with the interactive equations in section 5.3. It is necessary to do this as the largest terms in the sum are those immediately either side of x, which must cancel each other out to lowest order, and so it is necessary that sufficient terms are always taken either side of x for this cancellation to occur.

Because of the non-linearity of the problem it is important that the assumptions made previously about S and u, namely that they are both positive and order 1, are true, and so h and a must be chosen accordingly. The examples used below are those of the steady problem with $h = 1$, $a = 1$, and the unsteady problem with $h = 4 - t$, $a = 0$ with $t < 4$. The boundary values necessary are $S(1,t) = h(t)$ and $\phi(1,t) = 0$, with initial values given for S and ϕ by $h(0) = 4$, $h'(0) = 0$.

Applying the above scheme, numerical experiments were run, for both the steady and the unsteady problem. The graphs below on the whole show good agreement with the known analytic solution, for sufficiently low Courant number, thus confirming the hypothesis that the Hilbert transform is not *per se* an obstacle to finding a numerical scheme for a singular partial integro-differential equation which is stable and convergent. The maximum value of the Courant number before the solutions stabilise was found to be about 1.3 for $n = 100$. Figure 9.4 indicates the solutions found for Courant numbers of 1.3 and 1.4 for the steady state problem.

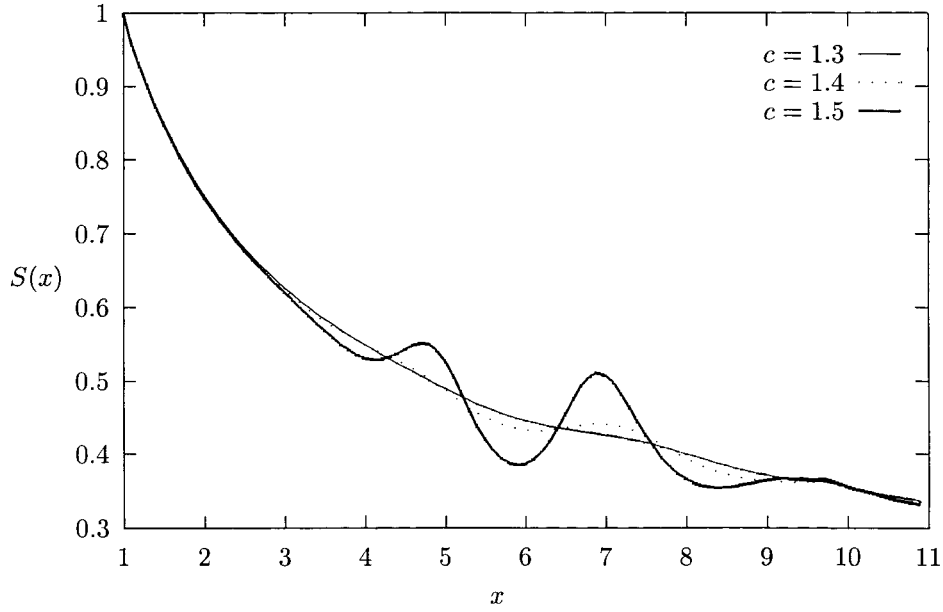

Figure 9.4: Solutions to the second order test problem with different Courant numbers at $t = 10$.

For the unsteady problem, the solution found for S at $t = 2$ is shown for $n = 10$, $n = 100$, and $n = 500$, in figure 9.5, and compared with the analytic solution $S = h(t)x^{-1/2}$. This shows that the solution is converging to the correct solution. As expected, a lower Courant number is needed for higher values of n so the Courant number was taken to be 0.8 in these computations, with x_{max} set to 10 for $n = 10$ and $n = 100$, and $n = 23$ for $n = 1000$. The motivation behind this choice of x_{max} is that the accuracy is limited by two factors : the thickness of the mesh, which gives an error of $O(\delta x)$, i.e. $O(x_{max}/n)$, and the estimation of the tail of the integral, in which there is an error of $O(x_{max}^{-1})$. Thus for a given n, the optimal choice will be when these errors are of an equal order of magnitude,

so

$$\frac{x_{max}}{n} \sim x_{max}^{-1},$$

implying that $x_{max} \sim n^{\frac{1}{2}}$. With this choice of x_{max}, the error will be $O(n^{-\frac{1}{2}})$. Figure 9.5 shows the numerical solution converging to the analytic solution as n increases.

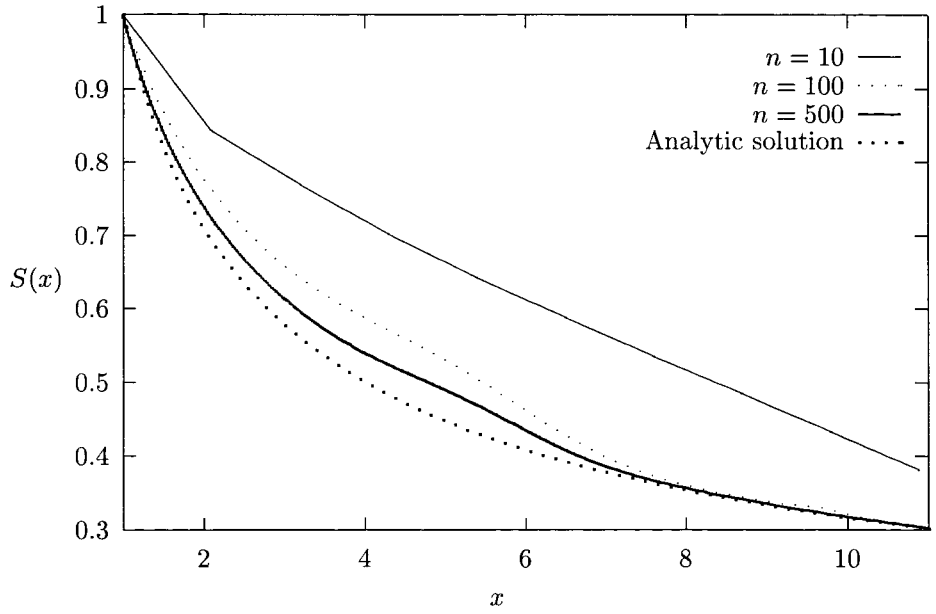

Figure 9.5: Numerical solution of the unsteady second order test equation for various mesh sizes

9.7 The Linearised Third Order Equation

Before looking at other schemes often used to improve stability it is worth noting that the stability of any scheme is determined by its highest derivatives only. This is manifested in the above stability analysis by the observation that some of the terms in the expression for $e^{-i\omega\delta t}$ were less than order 1 when r is order 1. These terms correspond to the $\phi_x S_x$ term in equation 9.8 and the $\frac{1}{2}\phi_x^2$ term in equation 9.7. Furthermore the effect of the non-linearity on the stability of the equations is now confined to the coefficient of r in the final expression for $e^{-i\omega\delta t}$ (e.g. equation 9.14 or equation 9.16) being multiplied by a factor of $\sqrt{S}$. However S is positive and order 1, and furthermore, since in the steady problem it varies only by a factor of 2 in the region in which this stability analysis is being conducted, setting this term equal to 1 is unlikely to vary the fundamental properties of this equation with regard to stability. Hence before examining other, more complicated, stability it is better to examine the 'simplified' form of the equations, in which all derivatives save those of the highest order are set to zero, and the remaining terms linearised where necessary. In other words the $\frac{1}{2}\phi_x^2$ term in equation 9.7 is set to zero, and the $(\phi_x S)_x$ term in equation 9.8 is replaced by ϕ_{xx}. This leads to the

following system

$$\begin{aligned} S_x + \phi_t &= 0, \\ \phi_{xx} + S_t &= 0, \end{aligned}$$

or, expressing it as a single equation in σ as before, by differentiating the first equation with respect to x and imposing $\sigma_x = S$,

$$\sigma_{xxx} = \sigma_{tt}. \tag{9.36}$$

Note that this is the equation that one would expect to arrive at after making the same simplifications to equation 8.1, and that it has the same properties with regard to characteristics, etc, as the original equation. Hence any search for a stable numerical scheme for the interactive problem must focus on this equation, with the assumption that any stable scheme for this equation will also be stable for the test problem defined by equations 9.7 and 9.8. The fact that once a numerical scheme had been found for the second order test problem, the introduction of the Hilbert transform did not present an insurmountable obstacle suggests that such a scheme may give, with certain modifications, a numerically stable solution to the interactive problem.

The fact that it has not been possible to find a numerical solution to the third order test problem of section 9.3 suggests that the sticking point in finding a stable numerical scheme for the interactive problem is not related to the Hilbert transform, or to the non-linearity of the problem, but to the usual difficulties in finding stable schemes for third order problems, and in particular the third order problem $\sigma_{xxx} = \sigma_{tt}$, the linearised simplified version of the full interactive problem. The methods described above (Lax-Friedrichs, Crank-Nicolson, etc) fail to provide a stable numerical scheme for this equation for the same reasons as they fail for the interactive problem, so further discussion of this equation, which is considerably easier to analyse than the full interactive problem, is necessary to obtain a better understanding. One possible starting point is to examine the stability of separable solutions to the linearised equation, since the general solution may be written in the form

$$\sigma = \int_{-\infty}^{\infty} f(\mu) X(x;\mu) T(t;\mu) d\mu,$$

where the $X(x;\mu)T(t;\mu)$ are the separable solutions parametrised by μ.

Setting $\sigma(x,t) = X(x)T(t)$ and substituting into the linearised equation $\sigma_{xxx} = \sigma_{tt}$ gives $X'''/X = T''/T$ =constant. The linearly independent solutions for X are thus $X = e^{\mu x}$, $e^{-\frac{1}{2}\mu x}\cos\frac{\sqrt{3}}{2}\mu x$, and $e^{-\frac{1}{2}\mu x}\sin\frac{\sqrt{3}}{2}\mu x$, where μ is a real constant. The solutions for T are either sinusoidal or exponential depending on the sign of μ. Whether a boundary value problem permits growing exponential modes or not depends on the boundary conditions. Given the boundary conditions $X(0) = 0$ with X and X' tending to zero as x tends to infinity, there is no non-zero solution if μ is negative. If μ is positive $a = \mu^{\frac{2}{3}}$ is real and positive. In this case the solution for X is $e^{-\frac{1}{2}\mu x}\sin\frac{\sqrt{3}}{2}\mu x$, with a general solution for σ of $Xe^{at} + Xe^{-at}$, and so exponentially growing modes are possible. Alternatively the boundary

conditions $X(0) = X'(0) = 0$, with X tending to zero as x tends to infinity permit no non-zero solution. This demonstrates the importance of boundary conditions with regard to stable solutions.

One of the disadvantages of the linearisation that led to this equation is that the corresponding boundary conditions are not clear. The absence of the Hilbert transform will mean that one fewer conditions will be needed. Furthermore in order to convert the system of equations into an equation in one variable, the equation involving $f(t)$ had to be differentiated, thus $f(t)$ enters the equation only through the boundary conditions. In the interactive problem S and S_x are given as being zero at $x = 0$, and thus are given implicitly at $x = 1$ by the inversion. Note that only the condition that $S(0,t) = 0$ is related to the corresponding partial differential equation, as the condition that $S_x(0,t) = 0$ provides information regarding the inversion of the Hilbert transform (this is why the original steady equation required two boundary conditions, even though it was only first order with regard to differentiation). The missing boundary condition must therefore involve $f(t)$, and so must arise from the fact that the Hilbert transform must tend to zero for large x. From equation 5.20 it then follows that $\phi_t + \frac{1}{2}\phi_x^2$ tends to $f(t)$ as x tends to infinity, and, since for the purposes of this linearised equation the term ϕ_x^2 has been ignored as it does not feature a highest derivative, this gives the condition $\phi_t \to f(t)$ as $x \to \infty$. Differentiating this, and expressing it in terms of σ gives $\sigma_{tt} \to 0$, and so, bearing in mind that for the separable solutions σ_{tt} is proportional to σ, the appropriate boundary conditions are $\sigma \to 0$ as $x \to \infty$, along with $\sigma(0,t) = 0$ (from the definition of σ) and $\sigma_x(0,t) = 0$. The fact that these conditions permit no non-zero solutions suggest that this equation has been over-simplified.

If the procedures as followed above are used, save the ignoring of the non-linear terms, the equation in terms of one variable, with no Hilbert transform, and no terms in any but the highest derivatives, may be written

$$\sigma_x \sigma_{xxx} = \sigma_{tt}. \tag{9.37}$$

In some ways this is more desirable than the linearised version above, as the boundary condition $\sigma(0,t) = \sigma_x(0,t) = \sigma(\infty,t) = 0$ will not necessarily lead to a non-zero solution. Furthermore it is invariant under the transformation $x \mapsto -x$, and so more appropriate to a physical situation. However since it is non-linear, separable solutions are not as easy to find, and the previous problems with numerical stability remain. Clearly, further study of this equation would be helpful to finding a stable scheme for the interactive equations, and this would be a useful area into which further research could be conducted.

9.8 The Full Interactive Problem

The success of the numerical scheme for equations 9.29 and 9.30 relies upon the fact that from a numerical point of view, the Hilbert transform does not behave like a derivative, but like the identity operator. However this is not a desirable feature for the interactive equations, since no scheme has

yet been found for the third order problem without the Hilbert transform. For this reason it is to be expected that any approximation to the Hilbert transform of S_x which is of the form

$$\int \frac{S_\xi}{\xi - x} d\xi \approx \sum_{i=0}^{n-1} A_{ik}(S_x)_k,$$

(where $(S_x)_k$ denotes the numerical derivative S at the mesh point k by, for example, a central difference operator) will be unstable. This proves to be the case in numerical experiments. However an approximation that applied integration by parts, as in equation 9.4, would be preferable, as S is no longer explicitly differentiated. The approximation corresponding to this form is that of equation 9.5, and applying the usual perturbation to this gives a first order error of

$$H_{p+\frac{1}{2}} \to e^{-ikx} \frac{1}{\delta x} \sum_{q=0}^{n-1} \frac{4e^{iqk\delta x}}{1 - 4(q-p)^2}.$$

The term in the above sum corresponding to $q = p$ is $4\delta x^{-1}$, and the sum of the terms corresponding to $q = p \pm 1$ is $-\frac{8}{3}\delta x^{-1} \cos k\delta x$, etc. Thus the first order error, for order 1 values of $k\delta x$, will be of order δx^{-1}, as is the first order for differentiation. Thus although the differentiation in this method is implicit, as far as von Neumann analysis is concerned, the operation that takes S to the Hilbert transform of S_x is still a derivative. The averaging process $H_p = \frac{1}{2}(H_{p-\frac{1}{2}} + H_{p+\frac{1}{2}})$ has no effect on this phenomenon. Numerical experiments have been carried out which confirm this, and the interactive equations become unstable very quickly, even when the function S is given over the region $(0, 1)$. Examples of the growth of instabilities for the interactive problem, with $x_{max} = 11$, a Courant number of 0.9 and a slot pressure $f(t) = 1$, which should yield the steady solutions, are shown in figure 9.6.

Although a stable numerical scheme has not been found for the interactive injection equations, it has been shown that the presence of a Hilbert transform need not *per se* pose an insurmountable obstacle to finding such schemes. In particular it seems that the main obstacle to the interactive problem is caused by the fact that it is third order, and thus of a similar type to the linearised equation, equation 9.36. It is therefore suggested that a stable scheme must be found for this equation, with a stable scheme for the non-linear integro-differential equation likely to be found by a similar method. One possible way to find such a solution would be to add a term to equation 9.36 of the form $\delta x \sigma_{xxxx}$, which will tend to zero in the limit as $\delta x \to 0$, but may have a stabilising effect. This would be a similar kind of scheme to the Lax-Friedrichs scheme described earlier (section 9.3.1), which may be thought of as addition of a term of the kind $\delta x S_{xx}$.

One final conclusion from the numerical analysis of these equations is that if a partial integro-differential equation can be expressed in such a way that the integral transform contains no terms in the highest derivatives of the equation, then the integral transform will not affect numerical stability of the equation. A corollary of this is that in the case that the integral transform is invertible, an integro-differential equation in which the integral transform contains *only* highest derivatives will also

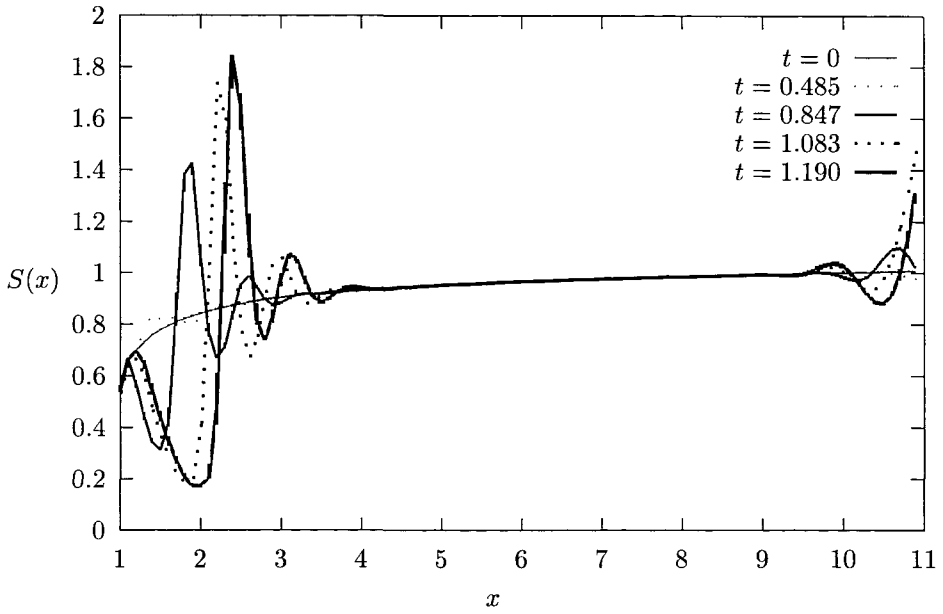

Figure 9.6: Growth of numerical instabilities for solution of interactive problem using finite difference methods

be solvable numerically, provided the partial differential equation consisting of the highest derivatives is solvable, as is the case with the unsteady sail equation solved in chapter 3. Since the unsteady sail equation (equation 2.31), in terms of its highest derivatives was just the wave equation, any stable scheme for the wave equation will be stable for the unsteady sail equation.

9.9 The Low Mass Sail and Flag Equations

The equation given for an unsteady sail in the limit as its mass tends to zero was given by equation 2.32. In this case μ is large, but $\mu^{-1}\beta^2$ is order 1. Ignoring all terms save those in the highest derivatives, this equation may be written

$$-\frac{1}{\pi}\frac{\beta^2}{\mu}\int_0^1 \frac{S_{\xi\xi}}{\xi - x}d\xi = S_t, \tag{9.38}$$

with the boundary conditions given by $S = 0$ at $x = 0$ and $x = 1$, and $S_{xx} = 0$ at $x = 1$, and initial conditions on S, as before.

This appears to be similar to the heat equation, with the Cauchy kernel, and its consequent change of sign at $\xi = x$, indicating that the ratio of S_t to S_{xx} will have to be considered as taking both positive and negative values. However there is a fundamental difference between the ordinary heat equation,

$$u_t = u_{xx},$$

and the backwards heat equation

$$u_t = -u_{xx},$$

in that if $f(t)$ is a solution for one of the above equations, then $f(-t)$ will be the solution for another. This has serious implications for stability, as if a scheme is found for the first equation, for which $|e^{-i\omega\delta t}| \leq 1$, then naturally $|e^{i\omega\delta t}| \geq 1$, which suggests that the same scheme when applied to the second equation will be unstable, unless $e^{-i\omega\delta t}$ is identically equal to one. Some research has been conducted on such 'forward-backward' heat equations, for example by Turfus (1986) [98], and Freidlin & Weinberger (1993) [40]. However it must be recalled, from section 9.5, that the effect of the Hilbert transform is not multiplication by ± 1, but $\pm i$. This changes the stability criterion completely and a stable difference scheme may be found for the low-mass sail equation (equation 9.38), using a three-level time difference scheme, that is

$$S_p^{j+1} = S_p^{j-1} - 2\frac{\delta t}{\delta x^2}\frac{\mu}{\pi\beta^2}\left(H_{p+1}^j + H_{p-1}^j - 2H_p^j\right)$$

where as usual S_p^j denotes $S(\xi_p, t_j)$, and H_p^j denotes some evaluation of the Hilbert transform at the point ξ_p, typically given by an expression of the form

$$H_p^j = \sum_{q=0}^{n-1} A_{pq} S_q^j,$$

where the A_{pq} are given by equation 9.26. Since it is known from section 9.5 that applying the usual von Neumann perturbation to H_i gives $\pm i$, it follows that

$$e^{-i\omega\delta t} = e^{i\omega\delta t} \pm 2\frac{\mu}{\beta^2}\frac{\delta t}{\delta x^2} i\left(2\cos k\delta x - 2\right).$$

For convenience, the notation $z = e^{-i\omega\delta t}$, $r = \delta t/\delta x^2$ will be introduced. With this notation, the above equation is a quadratic in z of the form

$$z^2 - 2ibz - 1 = 0,$$

where b is a real number given by

$$b = \pm 4r\frac{\mu}{\beta^2}\sin^2\frac{k\delta x}{2}.$$

The product of the roots will therefore be 1. Hence for there to be no roots of modulus greater than one, they must both be of modulus one. This will happen if the roots are complex, or there is a double root. For convenience, y will be defined by $y = iz$. With this definition, $|y| = |z|$. The quadratic for y is then

$$y^2 - 2by + 1 = 0.$$

The equation for y has real coefficients, with the product of the roots equalling 1. Therefore, if the roots are a complex conjugate pair then, since their moduli must be equal, they must both be equal to 1. This condition will be satisfied provided the above equation has no real roots, i.e. provided

$$b^2 < 1.$$

Hence stability for this three-level difference scheme may be achieved provided

$$\left| 4r\frac{\mu}{\beta^2} \right| < 1.$$

This shows that stable schemes are possible for singular partial integro-differential equations, even where the transform contains a highest derivative. This case is particularly interesting, as the associated partial differential equation is not unconditionally stable under the equivalent scheme if the Hilbert transform is replaced by a constant, but only stable if the constant is of the right sign. Furthermore, in its highest derivatives the low-mass sail equation is the same as the Benjamin-Ono equation, discussed in section 8.3, with the domain of integration and the non-linearity in the first-order x-derivative being the only significant differences. Therefore it is anticipated that the above scheme, with the obvious modifications, would be applicable to the Benjamin-Ono equation.

The stable scheme for the low-mass equation, along with the results successfully obtained for the test equation of section 9.6, shows that it is sometimes possible to find numerical solutions to singular partial integro-differential equations, and how the stability analysis must proceed in order to determine whether a scheme will be successful.

Chapter 10

Conclusions

10.1 Summary of Results

The results presented show that although singular partial integro-differential equations pose particular problems, these problems are not necessarily insurmountable. In particular, the numerical work on the unsteady sail equation in chapter 3, the test problem of section 9.6, and the stability analysis of the low-mass sail equation of section 9.9, show that numerical solutions may sometimes be found for them. However the von Neumann analysis of chapter 9 shows that in order to be able to find a stable numerical scheme for a singular partial integro-differential equation, it is necessary to consider the corresponding partial differential equation, with the integral transform replaced by a positive or negative constant. If there are no stable schemes for the corresponding partial differential equation, then there are unlikely to be any for the singular partial integro-differential equation. This poses particular problems for finding numerical solutions of the interactive equations of section 5.2. However for equations for which the corresponding partial differential equation has stable numerical schemes, a numerical scheme may sometimes be obtained. In general the effect of a Hilbert transform on a stability condition will be for a factor of $\pm i\pi$ to appear.

For the physical problem of the unsteady sail, the results presented in section 3.4 show how the shape of the sail, the lift and the tension vary with the angle of attack. In particular it is shown that for a variation between concave sail shapes with the same sign camber, the sail shape approaches that of the steady state with virtually no oscillatory behaviour. However, when the sail shape changes camber, the sail shape does not change monotonically with time to the new sail shape, but oscillates between sail shapes of opposite camber. The problem is less complicated for the high-mass sail of section 2.6, which is unaffected by the aerodynamic flow, and so will be stationary. The low-mass sail of section 2.5 is likely to behave similarly to the order 1 mass sail, although the numerical results presented in section 3.4.2 suggest that instabilities are likely to become more significant. The analytic solutions found for the low-mass sail (equation 2.33) for particular angles of attack, also indicate that a non-zero angle of attack can still generate zero lift, as in the steady case. The problem where the relative angle of incidence is large may also be solved entirely analytically (section 2.7). In this case

the sail shape remains constant and the tension is proportional to the angle of incidence. The analysis of the flag equation also provides an eigenvalue problem for possible modes of a flapping flag in a steady cross-flow, given by equation 2.45.

For the injection and suction problems a variety of useful results have been obtained. The analysis of the quasi-steady injection (section 5.4) gives a result, not previously observed, that the mass flow will depend on the slot pressure to the power of 1.5. Furthermore, analysis of the fast case (section 5.5) indicates that for the purposes of computing the mass flow, only changes over the interactive time scale, $L/U_\infty\epsilon$, need be considered. The analysis of the interactive case indicates that changes far downstream may only occur on the quasi-steady time scale, $L/U_\infty\epsilon^2$, and gives the asymptotic expression for the changes at infinity. The stability analysis of section 5.7 indicates that the shear layer separating the injected region from the free stream is unstable, which has led to problems in the numerical analysis of the interactive equations.

For the suction problem, the mass transfer and the height of the shear layer were solved analytically in chapter 6. The solution for a slot pressure function $H(t)$ in section 6.4.4 indicates that over a short period of time the mass transfer for a given slot pressure may be higher if the slot pressure has been increased from a lower value than for the steady state, as the mass transfer does not depend monotonically on the slot pressure function. The results for a sinusoidal slot pressure function in section 6.4.2 also indicate that the mass transfer will never be in phase with the slot pressure function, with the phase lag given by equations 6.25 and 6.26. Furthermore the fact that the equations may be solved analytically for any slot pressure which is a linear combination of polynomial, exponential or sinusoidal or other Laplace transformable or Fourier transformable functions indicates that an expression may be obtained for the length of time for which the slot pressure will need to exceed zero for the system to change from suction to injection.

The discussion of the transition between injection and suction of chapter 7 indicates how research into this problem could proceed, with the behaviour of the system being described by the unified equations 7.4 and 7.5. However to solve this equation numerically it is necessary to solve the interactive slot injection equations, which will prove difficult because of their inherent instability. Nevertheless the slot suction equations are sufficient for it to be possible to analytically compute the length of time for a suction slot to become an injection slot, for a given slot pressure profile. The order of magnitude of this time will be L/U_∞, as this is the time scale of changes to slot suction. However, the changes will only be noticeable at an order L distance downstream of the slot after a time of order $L/U_\infty\epsilon$, and far downstream of the slot after a time of order $L/U_\infty\epsilon^2$. The conclusion of section 7.4, show how closed form expressions may be found for the mass transfer and height of the shear layer when the transition is over the fast time scale, L/U_∞. This is a particularly useful result for problems such as the rim seal problem, where slot injection is desired, but suction may occur over small time scales as a result of external pressure variations.

10.2 Avenues for Future Research

From the results presented for the sail equation, it is clear that a more thorough stability analysis is required to determine the stability of the sail. Accuracy of the numerical solutions found may also be improved, possibly by use of a Galerkin method. Galerkin methods, in particular by using some useful well-known properties of Chebychev polynomials, are frequently used in the context of integro-differential equations over a finite range, for example by Frankel (1995) [39]. Future work might examine the stability of such methods, as well as how they might be used to improve accuracy. A stability analysis may also be performed for the flag equation. This will be a slightly simpler problem, as there is no length condition as there was for the sail. For the interactive slot injection equations, examination of the instabilities found for the shear layer in the injected region would also be of interest, particularly as the mixing of the free-stream is particularly relevant to the film cooling problem. It seems likely that instabilities will be similar to those found for high-Reynolds-number flow over a separated recirculating eddy by Brown et al (1988) [10].

Other possible extensions to the theory applied here include extending the study to three dimensions. For the slot injection and suction problems there is the axisymmetric rim seal problem, and the problems of suction into and injection from a cylindrical slot. These have been studied for steady flow (by Chew et al (1994) [18], Dewynne et al (1990) [23] and Fitt (1983) [30], respectively), but the unsteady case has not yet been considered.

In order to find a numerical solution to the interactive slot injection equations, it would be useful to find a solution to the linearised equation, equation 9.36, i.e.

$$\sigma_{xxx} = \sigma_{tt}.$$

Although there are severe difficulties in finding stable numerical schemes for such an equation, one possible method would be to add a term of the form $\delta x \sigma_{xxxx}$. In the limit as δx tends to zero, the equation would still be the same, but the fourth order derivative may have a stabilising effect. Although such a scheme may not necessarily be stable when applied to the full non-linear equation with the Hilbert transform, it seems likely that it would help such a scheme to be found.

Appendix A

Useful Results Regarding Singular Integrals

All of the results in this appendix may be found in Muskhelishvili (1953) [61] and Gakhov (1965) [41], (henceforth referred to as 'Muskhelishvili' and 'Gakhov') to which the reader is referred for a comprehensive analysis on one-dimensional singular integrals. For a discussion of the properties of multidimensional singular integrals the reader is referred to Mikhlin (1965) [58]. A comprehensive survey on the infinite range Hilbert transformation was completed by Titchmarsh (1948) [93], and Pipkin (1991) [69], completed a less comprehensive, but still valuable, study of Cauchy principal value integrals. Note that here the term Hilbert transform will be used for any integral transform with a Cauchy kernel $(\xi - x)^{-1}$, although in some parts of the literature the term is restricted to the case where the domain of integration is the entire real axis. Under this definition it is necessary to classify Hilbert transforms over real domains into three types, according to whether the domain of integration is infinite at both ends, infinite at one end, or finite. Thus a real function $f(x)$, assuming it satisfies the appropriate integrability conditions will have a finite Hilbert transform, a semi-infinite Hilbert transform and an infinite Hilbert transform, given respectively by

$$\frac{1}{\pi}\int_0^1 \frac{f(\xi)}{\xi - x}d\xi, \qquad \frac{1}{\pi}\int_0^\infty \frac{f(\xi)}{\xi - x}d\xi, \qquad \frac{1}{\pi}\int_{-\infty}^\infty \frac{f(\xi)}{\xi - x}d\xi.$$

Note that the multiplication of the reciprocal of π is usually, but not always, given as part of the definition of the Hilbert transform. Sometimes the π is replaced by $i\pi$, which, in the case of the infinite transform makes it self-inverting for some classes of function. Clearly for a semi-infinite region other than $(0, \infty)$ or a finite region other than $(0, 1)$ the results described below will still apply, subject to some trivial modifications.

A.1 Properties of Semi-Infinite Hilbert Transforms

A.1.1 Non-Uniqueness of Inverse

Since over any interval the Hilbert transform is a linear operator the question of non-uniqueness of the inverse of a function (assuming that the inverse exists) will be related to the number of functions whose Hilbert transform is zero. It may easily be shown that

$$\frac{1}{\pi}\int_0^\infty \frac{\xi^{-\frac{1}{2}}}{\xi - x}d\xi = 0, \tag{A.1}$$

and it is shown in Muskhelishvili that constant multiples of $x^{-\frac{1}{2}}$ are the only functions whose Hilbert transform is zero. Hence all inverses will be unique only to within addition of a one parameter family of solutions.

A.1.2 Inversion Formulae

Inversion of a Hilbert transform is equivalent to solution of the equation

$$\frac{1}{\pi}\int_0^\infty \frac{f(\xi)}{\xi - x}d\xi = g(x),$$

which has a solution given by the explicit formula

$$f(x) = -\frac{1}{\pi}\int_0^\infty \sqrt{\frac{\xi}{x}}\frac{g(\xi)}{\xi - x}d\xi + Cx^{-\frac{1}{2}} \tag{A.2}$$

$$= -\frac{1}{\pi}\int_0^\infty \sqrt{\frac{x}{\xi}}\frac{g(\xi)}{\xi - x}d\xi + Cx^{-\frac{1}{2}}, \tag{A.3}$$

where C is an arbitrary constant. Either of the above expressions may be used, since they are both equivalent, provided $g(x)$ tends to zero sufficiently quickly for the integral in the first expression to exist. To see that this is so, observe that the difference between the two expressions is given by

$$\frac{1}{\pi}\int_0^\infty \frac{g(\xi)}{\sqrt{\xi x}}d\xi,$$

which is a constant multiple of $x^{-\frac{1}{2}}$ provided the integral exists. The inversion formula may be verified by use of the Bertrand-Poincaré formula, and is valid for Hölder continuous functions, g, i.e. functions for which there exist A and μ such that

$$|g(x_1) - g(x_2)| < A|x_1 - x_2|^\mu$$

for all x_1 and x_2 within the domain of integration.

A.2 Properties of Finite Hilbert Transforms

A.2.1 Non-Uniqueness of Inverse

As with the semi-infinite Hilbert transform, there is only one linearly independent function with Hilbert transform equal to zero, given by $x^{-\frac{1}{2}}(1-x)^{-\frac{1}{2}}$. As before it is fairly easy to show that

$$\frac{1}{\pi}\int_0^1 \sqrt{\frac{1}{\xi(1-\xi)}}\frac{1}{\xi - x}d\xi = 0, \tag{A.4}$$

by use of the substitution $t^2 = \xi/(1-\xi)$.

A.2.2 Inversion Formulae

As with the semi-infinite Hilbert transform, the solution to the equation

$$\frac{1}{\pi} \fint_0^1 \frac{f(\xi)}{\xi - x} d\xi = g(x)$$

may be written in more than one way, any of which are equivalent, and all of which contain an arbitrary constant, C. The explicit formula for the inversion, again valid for Hölder continuous functions, then becomes

$$f(x) = -\frac{1}{\pi} \frac{1}{\sqrt{x(1-x)}} \fint_0^1 \sqrt{\xi(1-\xi)} \frac{g(\xi)}{\xi - x} d\xi + \frac{C}{\sqrt{x}\sqrt{1-x}} \tag{A.5}$$

$$= -\frac{1}{\pi} \sqrt{\frac{x}{1-x}} \fint_0^1 \sqrt{\frac{1-\xi}{\xi}} \frac{g(\xi)}{\xi - x} d\xi + \frac{C}{\sqrt{x}\sqrt{1-x}} \tag{A.6}$$

$$= -\frac{1}{\pi} \sqrt{\frac{1-x}{x}} \fint_0^1 \sqrt{\frac{\xi}{1-\xi}} \frac{g(\xi)}{\xi - x} d\xi + \frac{C}{\sqrt{x}\sqrt{1-x}}. \tag{A.7}$$

A.2.3 Inverse of 1

It may easily be found that

$$\frac{1}{\pi} \fint_0^1 \sqrt{\frac{\xi}{1-\xi}} \frac{1}{\xi - x} d\xi = -\frac{1}{\pi} \fint_0^1 \sqrt{\frac{1-\xi}{\xi}} \frac{1}{\xi - x} d\xi = 1, \tag{A.8}$$

and so the inverse of 1 is given by $\pm \left(\frac{x}{1-x}\right)^{\pm\frac{1}{2}}$ plus an arbitrary multiple of $x^{-\frac{1}{2}}(1-x)^{-\frac{1}{2}}$.

A.3 A Property of All Hilbert Transforms

Another result which is useful for a variety of reasons, particularly for giving an independent numerical check, is valid for all Hilbert transforms of a function which is square integrable over the domain of integration. In Fitt (1986) [31] this property is attributed to a suggestion by P. Wilmott, although in fact it is a simple, but important, consequence of Parseval's theorem as given by Tricomi (1951) [94],

$$\int_L \phi_1(x)\overline{\phi}_2(x) + \phi_2(x)\overline{\phi}_1(x) dx = 0, \tag{A.9}$$

(where $\overline{\phi}_1$ represents the Hilbert transform of ϕ_1 over the range L) in the particular case where $\phi_1 = \phi_2$. This theorem relies on the fact that the above integral is

$$\int_L \fint_L \frac{\phi_1(x)\phi_2(\xi) + \phi_2(x)\phi_1(\xi)}{\xi - x} d\xi dx,$$

which is antisymmetric in ξ and x and so must be zero *assuming the order of integration may be reversed.* Hence $\phi_1\phi_2$ must be L^1, i.e. its modulus must be Lebesgue integrable, in order that Fubini's theorem may apply, and so the order of integration may be reversed. Note that if $\phi_1 = \phi_2$ the criterion

for the theorem to apply is that ϕ_1 must be square integrable, see for example, Tricomi (1951) [95]. In this case the more specific rule

$$\int_L \phi_1(x) \fint_L \frac{\phi_1(\xi)}{\xi - x} d\xi \, dx = 0 \tag{A.10}$$

applies.

A.4 Asymptotic Behaviour of Hilbert Transforms

A.4.1 Asymptotic Behaviour at a Boundary

Consider the behaviour of the finite or semi-infinite transform of a function $f(x)$ near $x = 0$. A constant L will be defined as the upper limit of the domain of integration, so that $L = 1$ corresponds to a finite Hilbert transform and a semi-infinite transform corresponds to L tending to infinity. With this notation, in the case where L is finite, the Hilbert transform may be written

$$\frac{1}{\pi} \fint_0^L \frac{f(\xi)}{\xi - x} d\xi = \frac{1}{\pi} \int_0^L \frac{f(\xi) - f(x)}{\xi - x} d\xi + \frac{1}{\pi} f(x) \log \frac{L - x}{x}.$$

If f is differentiable at $x = 0$, therefore, there will be a logarithmic singularity at $x = 0$ of strength $\pi^{-1} f(x) \log L$.

If f is not differentiable at $x = 0$ then it is convenient to define a variable y such that

$$x \ll y \ll 1.$$

With this notation the Hilbert transform of $f(x)$ will be

$$\begin{aligned} \frac{1}{\pi} \fint_0^L \frac{f(\xi)}{\xi - x} d\xi &= \frac{1}{\pi} \fint_0^y \frac{f(\xi)}{\xi - x} d\xi + \frac{1}{\pi} \int_y^L \frac{f(\xi)}{\xi - x} d\xi, \\ &= \frac{1}{\pi} \fint_0^y \frac{f(\xi)}{\xi - x} d\xi + \frac{1}{\pi} \int_y^L \frac{f(\xi)}{\xi} d\xi + O\left(\frac{x}{y}\right). \end{aligned} \tag{A.11}$$

This confirms the previous result, that there will be a logarithmic singularity if f is differentiable, since the singular integral from 0 to y will just be $f(0) \log \frac{y}{x}$, to lowest order, and as a choice of y as a power of x, e.g. $x^{\frac{1}{2}}$, is consistent with the definition of y, this term is just proportional to $\log x$. The second term will also exhibit a dependence on $\log y$, and thus $\log x$. Note that in the case $f(0) = 0$, both terms will be zero and so there is no singularity, with the Hilbert transform approaching a constant as x tends to zero. This constant will be given by

$$\frac{1}{\pi} \lim_{x \to 0} \fint_0^L \frac{f(\xi)}{\xi - x} d\xi = \frac{1}{\pi} \int_0^L \frac{f(\xi)}{\xi} d\xi.$$

If f has a power-law singularity, $f(x) \sim x^{-p}$, then the second term in equation A.11 for the Hilbert transform will be of order y^{-p}, which by a suitable choice of y may be defined to be smaller than any negative power of x, and so may be ignored. The first term will be the singular integral from 0 to y,

and thus will only depend on the behaviour of $f(x)$ near $x = 0$. Using the result, from Pipkin (1991) [69], that for p between 0 and 1, and x between 0 and 1

$$\frac{1}{\pi}\int_0^1 \frac{dt}{t^p(1-t)^{1-p}(t-x)} = \frac{\cot p\pi}{t^p(1-t)^{1-p}},$$

it follows that the asymptotic behaviour of the transform of any function with a power-law singularity will be a power-law singularity of the same index, with the exception of the case where $f(x) \sim x^{-\frac{1}{2}}$, in which case the singularity will be zero and so the transform will tend towards a constant.

To summarise, therefore, as $x \to 0$,

$$\int_0^L \frac{f(\xi)}{\xi - x}d\xi \sim \begin{cases} \text{const.} & \text{if } f(x) \to 0, \\ \text{const.} & \text{if } f(x) - kx^{-\frac{1}{2}} \to 0 \text{ for some } k, \\ kf(0)\log x & \text{if } f(x) \to f(0), \\ x^{-p} & \text{if } f(x) \sim x^{-p},\ 0 < p < 1. \end{cases} \tag{A.12}$$

Clearly the same results will be obtained near $x = 1$ for the finite integral.

A.4.2 Asymptotic Behaviour at Infinity

For the behaviour as x tends to infinity, (this applies to semi-infinite and infinite transforms only) it is useful to define y slightly differently, by

$$1 \ll y \ll x,$$

although again, y may be chosen to be a power of x. The singular integral for large x, is now given by

$$\frac{1}{\pi}\int_0^\infty \frac{f(\xi)}{\xi - x}d\xi = \frac{1}{-x\pi}\int_0^y \frac{f(\xi)}{\xi}\left(1 + \frac{\xi}{x} + \ldots\right)d\xi + \frac{1}{\pi}\int_y^\infty \frac{f(\xi)}{\xi - x}d\xi.$$

This shows that the asymptotic behaviour of the transform for large x will depend entirely on the behaviour of the function f for large x, save for a contribution of order at most x^{-1}. Since from Pipkin (1991) [69] it is known that for x and p both between 0 and 1,

$$\frac{1}{\pi}\int_0^\infty \frac{d\xi}{\xi^p(\xi - x)} = \frac{\cot p\pi}{x^p},$$

it follows that a function which asymptotically behaves as a power law will have a transform with the same behaviour (with the exception, as before, of $x^{-\frac{1}{2}}$, which will give zero contribution). Furthermore the result that

$$\int_0^\infty \frac{dt}{(1+t)(t-x)} = -\frac{\log x}{x+1}$$

shows that for any function for which $f(x) \sim x^{-1}$ as $x \to \infty$, the transform will behave as $\frac{\log x}{x}$, and the result that

$$\int_0^\infty \frac{dt}{(1+t)^2(t-x)} = -\frac{1}{x+1} - \frac{\log x}{(x+1)^2}$$

shows that for any function for which $f(x) \sim x^{-2}$, the transform will behave as x^{-1}.

These results may be summarised as before to give, for $x \to \infty$,

$$\int_0^\infty \frac{f(\xi)}{\xi - x} d\xi \sim \begin{cases} x^{-1} + O\left(\frac{\log x}{x^2}\right) & \text{if } f(x) \sim x^{-2}, \\ x^{-1} & \text{if } f(x) - kx^{-\frac{1}{2}} \sim x^{-2} \text{ for some } k, \\ \frac{\log x}{x} & \text{if } f(x) \sim x^{-1}, \\ x^{-p} & \text{if } f(x) \sim x^{-p},\ 0 < p < 1. \end{cases} \tag{A.13}$$

The asymptotic behaviour of transforms of functions with logarithmic or power-logarithmic asymptotic behaviour is discussed by Gakhov (1965) [41].

A.4.3 Effect of Jump Discontinuities

If $f(x)$ has a jump discontinuity at a point $x = a$, say, then its Hilbert transform will not exist at that point. However, provided the discontinuities are integrable and occur at only discrete values of x, the transform will exist at other values of x. Since the transform is linear, and any jump discontinuity may be cancelled out by subtraction of a Heaviside step function, it is only necessary to examine the transform of a step function, $H(x)$. Since, for example,

$$\int_0^\infty \frac{H(\xi - 1) - H(\xi - 2)}{\xi - x} d\xi = \log\left|\frac{2 - x}{1 - x}\right|,$$

it follows that a jump discontinuity will always result in a logarithmic singularity in the Hilbert transform at the same point, although not necessarily of the same strength. From the inversion formulae it also follows that a logarithmic singularity will result in a jump discontinuity.

A.5 The Derivative of a Hilbert Transform

The effect of differentiating a Hilbert transform is essentially the same for finite, semi-infinite and infinite range transforms. The expression for the derivative, assuming the function f, to be transformed, is differentiable, and that f' is integrable, is given by, from the definition of a Cauchy principal value,

$$\frac{d}{dx} \int_a^b \frac{f(\xi)}{\xi - x} d\xi = \int_a^b \frac{f'(\xi)}{\xi - x} d\xi + \frac{f(b)}{x - b} + \frac{f(a)}{a - x}. \tag{A.14}$$

In order to prove this, it is necessary to consider $Hi(x + h) - Hi(x)$, where $Hi(x)$ is the value of the transform evaluated at x. This difference is given by

$$\left(\int_a^{x+h-\epsilon} d\xi + \int_{x+h+\epsilon}^b d\xi\right)\left(\frac{f(\xi)}{\xi - x - h}\right) - \left(\int_a^{x-\epsilon} d\xi + \int_{x+\epsilon}^b d\xi\right)\left(\frac{f(\xi)}{\xi - x}\right),$$

in the limit as ϵ tends to zero. Consider the region $(x - \epsilon, x + \epsilon)$ in the first integral. In this region the integrand will be $O(h^{-1})$, so the integral over this region will be at most $O(\epsilon h^{-1})$. In the limit as ϵ tends to zero therefore, this term will be zero. Similarly the region $(x + h - \epsilon, x + h + \epsilon)$ in the second term will be zero in the limit. Hence both integrals are over the same region, giving the expression

$$\left(\int_a^{x-\epsilon} d\xi + \int_{x+\epsilon}^{x+h-\epsilon} d\xi + \int_{x+h+\epsilon}^b d\xi\right)\left(\frac{f(\xi)}{\xi - x - h} - \frac{f(\xi)}{\xi - x}\right).$$

This may be integrated by parts to give

$$-\left(\int_a^{x-\epsilon} d\xi + \int_{x+\epsilon}^{x+h-\epsilon} d\xi + \int_{x+h+\epsilon}^{b} d\xi\right)\left(f'(\xi)\log\left|\frac{\xi-x-h}{\xi-x}\right|\right) + f(b)\log\frac{b-x-h}{b-x}$$
$$-f(x+h+\epsilon)\log\frac{\epsilon}{h+\epsilon} + f(x+h-\epsilon)\log\frac{\epsilon}{h-\epsilon} - f(x+\epsilon)\log\frac{h-\epsilon}{\epsilon}$$
$$+f(x-\epsilon)\log\frac{h+\epsilon}{\epsilon} - f(a)\log\frac{a-x-h}{a-x}.$$

In the limit as $\epsilon \to 0$, the second and third non-integral terms will cancel, as will the fourth and fifth. The integral term will contain only a logarithmic singularity, so addition of the region $(x+h-\epsilon, x+h+\epsilon$ to the domain of integration will not affect the value of the integral. Hence the above expression is given by

$$-\left(\int_a^{x-\epsilon} d\xi + \int_{x+\epsilon}^{b} d\xi\right)\left(f'(\xi)\log\left|\frac{\xi-x-h}{\xi-x}\right|\right) + f(b)\log\frac{b-x-h}{b-x} - f(a)\log\frac{a-x-h}{a-x}.$$

The integral in the above expression clearly exists. Expanding the whole of the above expression in powers of h gives

$$h\left(\int_a^b \frac{f'(\xi)}{\xi-x}d\xi + \frac{f(b)}{x-b} + \frac{f(a)}{a-x}\right) + O(h^2).$$

This gives the required result.

Note that the requirement that f' is integrable is an important one and does not immediately follow from the fact that f is differentiable, as there are functions such as $x^{-\frac{1}{2}}$ which have a Hilbert transform (when integrated from 0 to 1), but whose derivatives do not, as they are not integrable.

Appendix B

The Derivation of $b(x)$

The function $b(x)$, discussed in sections 5.5, 6.2 and 7.4, is defined by

$$\frac{1}{\pi}\int_0^1 \frac{b(\xi)}{\xi - x}d\xi = \log(1-x). \tag{B.1}$$

Inverting this integral by the methods detailed in section A.1.2 gives

$$b(x) = -\frac{1}{\pi}\sqrt{\frac{x}{1-x}}\int_0^1 \sqrt{\frac{1-\xi}{\xi}}\frac{\log(1-\xi)}{\xi - x}d\xi, \tag{B.2}$$

where the inversion was taken so as to ensure that $b(0) = 0$. The above integral may be calculated by use of the substitution $z^2 = \frac{\xi}{1-\xi}$ to give the expression

$$b(x) = \frac{2}{\pi(1-x)}\int_0^\infty \frac{\log(1+z^2)}{(z^2+1)(z^2 - \frac{x}{1-x})}dz.$$

Since the integrand in the above equation is even, the above integral may be expressed as an integral over the whole real axis. By taking branch cuts from i to infinity and $-i$ to infinity along the imaginary axis the above integral may be found by contour integration by using a key-hole contour around the part of the branch cut in the upper half plane.

A less time consuming method to solve for the function $b(x)$ is to differentiate equation B.1 to find an expression for the Hilbert transform of $b'(x)$. Unfortunately care must be taken with this since $b(x)$ has a square root singularity at $x = 1$. Thus it will be necessary to subtract off the singularity at this point. In order to do this it is necessary to examine the behaviour of $b(x)$ as $x \to 1$. It may be shown from equation B.2 that as $x \to 1$

$$\begin{aligned}
b(x) &= \frac{1}{\pi}\sqrt{\frac{x}{1-x}}\int_0^1 \frac{\log 1-\xi}{\sqrt{\xi}\sqrt{1-\xi}}d\xi + O(\sqrt{1-x}) \\
&= \frac{1}{\pi}(1-x)^{-\frac{1}{2}}\frac{d}{dp}\int_0^1 (1-\xi)^{p-1}\xi^{-\frac{1}{2}}d\xi\Big|_{p=\frac{1}{2}} + O(\sqrt{1-x}) \\
&= \frac{1}{\pi}(1-x)^{-\frac{1}{2}}\frac{d}{dp}\beta\left(p,\frac{1}{2}\right)\Big|_{p=\frac{1}{2}} + O(\sqrt{1-x}) \\
&= \frac{1}{\pi}(1-x)^{-\frac{1}{2}}\beta\left(\frac{1}{2},\frac{1}{2}\right)\left(\Psi\left(\frac{1}{2}\right) - \Psi(1)\right) + O(\sqrt{1-x}) \\
&= -2\log 2(1-x)^{-\frac{1}{2}} + O(\sqrt{1-x}),
\end{aligned}$$

where β represents the Beta function and Ψ represents the digamma function. Similarly it may be shown that near $x = 0$

$$b(x) = (2 - 2\log 2)x^{\frac{1}{2}} + O(x^{\frac{3}{2}}).$$

Hence it may be deduced that the function $c(x)$ given by

$$c(x) = b(x) + 2\log 2\sqrt{\frac{x}{1-x}}$$

will be continuous and finite at both $x = 0$ and $x = 1$. It may then be easily shown from equation B.1, using equation A.8, that

$$\frac{1}{\pi}\int_0^1 \frac{c(\xi)}{\xi - x}d\xi = \log(1-x) + 2\log 2.$$

Differentiation of the above equation and integration by parts, which is now permissible since $c'(x)$ will have only a square root singularity at each end of the integral, and $c(x)$ is well behaved, (see section A.5) gives

$$\frac{1}{\pi}\int_0^1 \frac{c'(\xi)}{\xi - x}d\xi - \frac{1}{\pi}\frac{c(1)}{1-x} = -\frac{1}{1-x},$$

recalling that $b(0) = 0$, so $c(0)$ must equal zero. By applying the inversion formula for finite range Hilbert transforms (see section A.2.2) it may be seen that

$$c'(x) = (c(1) - \pi)\delta(1-x) + \frac{K}{\sqrt{x}\sqrt{1-x}}.$$

In order to satisfy the asymptotic expressions for $c(x)$ which follow from those derived for $b(x)$ it follows that $K = 1$ and $c(1) = \pi$. Hence

$$c(x) = 2\arcsin\sqrt{x}$$

and so b is given as being

$$b(x) = 2\arcsin\sqrt{x} - 2\log 2\sqrt{\frac{x}{1-x}} \tag{B.3}$$

References

[1] M. Abramowitz and I. A. Stegun. *Handbook of Mathematical Functions.* Dover Publications, 1964.

[2] M. Bäcker, H. Neunzert, and S. Younis. The fluttering of fibres in airspinning processes. In H. Wacker and W. Zulehner, editors, *Proceedings of the Fourth European Conference on Mathematics in Industry*, pages 197–205. B. G. Teubner Stuttgart and Kluwer Academic Publishers, 1991.

[3] C. T. H. Baker. *The numerical treatment of integral equations.* Clarendon Press, 1977.

[4] R. Barakat. Incompressible flow around porous two-dimensional sails and wings. *J. Math. Phys.*, 47:327–349, 1968.

[5] J. Barry. The aerodynamic penalties associated with blade cooling. Technical report, VKI LS 83, 1976.

[6] D. B. Bliss. Aerodynamic behaviour of a slender slot in a wind tunnel wall. *AIAA Journal*, 20(9):1244–1252, 1982.

[7] T. L. Bock and M. D. Kruskal. A two-parameter Miura transform of the Benjamin-Ono equation. *Physics Letters A*, 74:173–176, 1979.

[8] J. F. Bott. Massive blowing experiments. *AIAA Journal*, 6:613–619, 1968.

[9] T. Brooke Benjamin. Internal waves of permanent form of fluids of great depth. *J. Fluid Mech.*, 29:559–592, 1967.

[10] S. N. Brown, H. K. Cheng, and F. T. Smith. Nonlinear instability and break-up of separated flow. *J. Fluid Mech.*, 193:191–216, 1988.

[11] J. W. Bugler. *On the Application of Potential Flow Theory to the Aerodynamics of Sails.* PhD thesis, College of Aeronautics, Cranfield Institute of Technology, 1957.

[12] D. A. Campbell. Gas turbine disc sealing system design. In *Proc. AGARD Conf. on Seal Technology in Gas Turbine Engines*, 1978. AGARD-CP-237.

[13] K. W. Cassel, F. T. Smith, and J. D. A. Walker. The onset of instability in unsteady boundary-layer separation. *J. Fluid Mech.*, 315:223–256, 1996.

[14] D. Catherall, K. Stewartson, and P. G. Williams. Viscous flow past a flat plate with uniform injection. *Proc. Roy. Soc. London.*, 284:370–396, 1965.

[15] LL. G. Chambers. A variational formulation of the Thwaites sail equation. *Q. J. Mech. Appl. Math.*, 19:221–231, 1966.

[16] A. Q. Chapleo. A review of two-dimensional sails. Technical report, University of Southampton, April 1968. S. U. Y. R. report no. 23.

[17] H. H. Chen, Y. C. Lee, and N. R. Pereira. Algebraic internal wave solitons and the integrable calogero-moser-sutherland n-body problem. *Phys. Fluids*, 22:187–188, 1979.

[18] J. W. Chew, T. Green, and A. B. Turner. Rim sealing of rotor-stator wheelspaces in the presence of external flow. *ASME paper*, 1994.

[19] V. Cisotti. Moto con scia di un profilo flessible. *Accad. Nat. dei Lincei*, 15:116–173, 1932.

[20] J. D. Cole and J. Aroesty. The blowhard problem — inviscid flows with surface injection. *Int. J. Heat Mass Transfer*, 11:1167–1183, 1968.

[21] R. T. Davis and M. J. Werle. Progress on interacting boundary-layer computations at high Reynolds number. In T. Cebeci, editor, *Numerical and Physical Aspects of Aerodynamic Flows.* Springer, 1982.

[22] J. N. Dewynne, S. D. Howison, J. R. Ockendon, L. C. Morland, and E. J. Watson. Slot suction from inviscid channel flow. *J. Fluid Mech.*, 200:265–282, 1989.

[23] J. N. Dewynne, L. C. Morland, and E. J. Watson. Weak suction from a channel flow into a circular orifice. *Q. J. Mech. Appl. Math.*, 32:517–534, 1990.

[24] A. Drozdov. Stability of integro-differential equations with periodic operator co-efficients. *Q. J. Mech. Appl. Math.*, 49, 1996.

[25] P. W. Duck. Triple-deck flow over unsteady surface distributions : the three-dimensional development of Tollmien Schlichting waves. *Computers Fluids*, 18:1, 1990.

[26] P. W. Duck. Unsteady three-dimensional marginal separation, including breakdown. *J. Fluid Mech.*, 220:85–98, 1990.

[27] J. P. Dugan. A free-streamline model of the two-dimensional sail. *J. Fluid Mech.*, 42(3):433–446, 1970.

[28] H. W. Emmons and D. Leigh. Tabulation of the Blasius function with blowing and suction. *Aero. Res. Counc. Current Paper*, (157), 1954.

[29] H. Engler. Global smooth solutions for a class of parabolic integrodifferential equations. *Trans. Amer. Math. Soc.*, 348(1):267–290, 1996.

[30] A. D. Fitt. *Theoretical Aspects of Film Cooling.* PhD thesis, Oxford University, 1983.

[31] A. D. Fitt. Numerical solution of a certain class of non-linear singular integrodifferential equations. Technical report, Cranfield Institute of technology mathematics and ballistics group, 1986. Report no. MB 7/86.

[32] A. D. Fitt, A. D. Kelly, and C. P. Please. Crack propagation models for rock fracture in a geothermal energy reservoir. *SIAM J. Appl. Math.*, 55(6):1592–1608, 1995.

[33] A. D. Fitt and T.R.B. Lattimer. A high-Reynolds-number cross-flow with injection and suction. *Q. J. Mech. Appl. Math.*, 49(4), 1996. Preprint.

[34] A. D. Fitt, J. R. Ockendon, and T. V. Jones. Aerodynamics of slot-film cooling : Theory and experiment. *J. Fluid Mech.*, 160:15–27, 1985.

[35] A. D. Fitt and P. Wilmott. Slot film cooling — the effect of separation angle. *Acta Mechanica*, 103:79–88, 1994.

[36] P. D. Fleming and S. D. Probert. Flexible sail wind-turbines : Review of pertinent theoretical analyses. *Applied Energy*, 18:89–99, 1984.

[37] A. Fokas and B. Fuchssteiner. The hierarchy of the Benjamin-Ono equation. *Physics Letters A*, 86:341–345, 1981.

[38] A. S. Fokas and M. J. Ablowitz. The inverse scattering transform for the Benjamin-Ono equation — a pivot to multidimensional problems. *Stud. Appl. Math.*, 68:1–10, 1983.

[39] J. I. Frankel. A Galerkin solution to a regularized Cauchy singular integrodifferential equation. *Q. Appl. Math.*, 53(2):245–258, June 1995.

[40] M. Freidlin and H. Weinberger. On a backward-forward parabolic equation and its regularization. *J. Diff. Equ.*, 105(2):264–295, 1993.

[41] F. D. Gakhov. *Boundary Value Problems.* Pergamon Press, 1965.

[42] R. J. Goldstein. Film cooling. *Adv. in Heat Trans.*, 7:321–379, 1971.

[43] K. Hamabe and K. Ishida. Rim seal experiments and analysis of a rotor-stator system with non-axisymmetric main flow. *ASME paper*, 92-GT-160, 1992.

[44] R. A. Hartunian and D. J. Spencer. Experimental results for massive blowing studies. *AIAA Journal*, 5:1397–1401, 1967.

[45] M. K. Haselgrove and E. O. Tuck. Stability properties of the two-dimensional sail model. In *New England Yacht Symposium*, 1976.

[46] S. Hubbard and N. Riley. Boundary-layer control by heat and mass transfer. *Int. J. Heat Mass Transfer*, 38(17):3209–3217, 1995.

[47] G. R. Inger and G. A. Gaitatzes. Strong blowing into supersonic laminar flows around two-dimensional and axisymmetric bodies. *AIAA Journal*, 9:436–443, 1971.

[48] P. S. Jackson. A simple model for elastic two-dimensional sails. *AIAA Journal*, 21(1):153–155, 1983.

[49] A. Kapila and D. Drew, editors. *Third Workshop on Mathematical Problems in Industry.* RPI, 1987.

[50] D. R. Kassoy. On laminar boundary blowoff. *SIAM J. Appl. Math.*, 18:29–40, 1970.

[51] A. C. Kaya and F. Erdogan. On the solution of integral equations with a generalized Cauchy kernel. *Q. Appl. Math.*, 45(3):455–469, October 1987.

[52] A. C. Kaya and F. Erdogan. On the solutions of integral equations with strongly singular kernels. *Q. Appl. Math.*, 45(1):105–122, April 1987.

[53] A. C. King and E. O. Tuck. Thin liquid layers supported by steady air-flow surface traction. *J. Fluid Mech.*, 251:709–718, 1993.

[54] J. B. Klemp and A. Acrivos. High Reynolds number flow past a flat plate with strong blowing. *J. Fluid Mech.*, 51:337–356, 1972.

[55] D. J. Korteg and G. De Vries. On the change of form of long waves advancing in a rectangular canal and a new type of long stationary waves. *Phil. Mag.*, 39(5):422, 1895.

[56] R. C. Lock. The velocity distribution in the laminar boundary layer between parallel streams. *Q. J. Mech. Appl. Math.*, 4:42–63, 1951.

[57] J. H. Michell. On the theory of free stream lines. *Phil. Trans. Roy. Soc. A*, 181:389–431, 1890.

[58] S. G. Mikhlin. *Multidimensional Singular Integrals and Integral Equations.* Pergamon Press, 1965.

[59] L. M. Milne-Thomson. *Theoretical Hydrodynamics.* Macmillan, 1949.

[60] L. C. Morland. *Mathematical Models for a Fluid Flow Arising in Turbine Blade Cooling Passages.* PhD thesis, Oxford University, 1988.

[61] N. I. Muskhelishvili. *Singular Integral Equations.* Noordhoff Groningen Holland, 1953.

[62] K. L. E. Nickel. A theory of sail-wings. *Zeit. Flugwiss. Welt.*, 11:321–328, 1987.

[63] J. Nielsen. Theory of flexible aerodynamic surfaces. *J. Appl. Mech. : Trans. ASME*, 30:435–442, 1963.

[64] K. O'Malley. *An Experimental and Theoretical Study of Slot Injection and Flow Separation.* PhD thesis, Oxford University, 1988.

[65] K. O'Malley, A. D. Fitt, T. V. Jones, J. R. Ockendon, and P. Wilmott. Models for high Reynolds number flow down a step. *J. Fluid Mech.*, 222:139–155, 1991.

[66] H. Ono. Algebraic solitary waves in stratified fluids. *J. Phys. Soc. Japan*, 39(4):1082–1091, 1975.

[67] V. J. Peridier, F. T. Smith, and J. D. A. Walker. Vortex-induced boundary-layer separation. part 2. unsteady interacting boundary-layer theory. *J. Fluid Mech.*, 232:133–165, 1991.

[68] R. Piessens, M. van Roy-Branders, and I. Mertens. The automatic evaluation of Cauchy principal value integrals. *Angewandte Informatik*, 18:31–35, 1976.

[69] A. C. Pipkin. *A Course on Integral Equations.* Springer-Verlag, 1991.

[70] L. Prandtl. Tragflügeltheorie I. *Nachr. Ges. Wiss. Goettingen Math. Phys. Kl.*, 24:451–477, 1918.

[71] R. D. Richtmyer and K. W. Morton. *Difference methods for initial-value problems.* Interscience Publishers, 1967.

[72] S. Roy and G. Nath. Unsteady laminar compressible swirling flow with massive blowing. *AIAA Journal*, 30(11):2604–2605, 1992.

[73] P. M. Santini, M. J. Ablowitz, and A. S. Fokas. On the inital value problem for a class of nonlinear integral evolution equations including the sine-Hilbert equation. *J. Math. Phys.*, 28(10):2310–2316, 1987.

[74] F. T. Smith. *Theoretical and Experimental Study of Airflow past a Porous Surface with Strong Blowing.* PhD thesis, Oxford University, 1972.

[75] F. T. Smith. On strong blowing into an incompressible airstream. *J. Fluid Mech.*, 60:241–255, 1973.

[76] F. T. Smith. Finite-time break up can occur in any unsteady interacting boundary layer. *Mathematika*, 35:256–273, 1989.

[77] F. T. Smith and D. S. Riley. A model of convector heating from a flat plate. *Int. J. Heat Mass Transfer*, 22:309–319, 1979.

[78] F. T. Smith and K. Stewartson. On slot injection into a supersonic boundary layer. *Proc. Roy. Soc. London.*, 332:1–22, 1973.

[79] F. T. Smith and K. Stewartson. Plate injection into a separated supersonic boundary layer — part I. *J. Fluid Mech.*, 58:143–159, 1973.

[80] G. D. Smith. *Numerical solution of partial differential equations : finite difference methods.* Oxford University Press, 1965.

[81] R. Smith and W. Shyy. Computation of unsteady laminar flow over a flexible two-dimensional membrane wing. *Phys. Fluids*, 7(9):2175–2184, 1995.

[82] R. Smith and W. Shyy. Computational model of flexible membrane wings in steady laminar flow. *AIAA Journal*, 37(10):1769–1777, 1995.

[83] I. N. Sneddon. *Elements of partial differential equations.* McGraw-Hill, 1957.

[84] K. Stewartson. A note on lifting line theory. *Q. J. Mech. Appl. Math.*, 13:49–56, 1960.

[85] K. Stewartson. *The Theory of Laminar Boundary Layers in Compressible Fluids.* Oxford University Press, 1964.

[86] K. Stewartson. On the flow near the trailing edge of a flat plate II. *Mathematika*, 16:106–121, 1969.

[87] K. Stewartson. Plate injection into a separated supersonic boundary layer — part II. *J. Fluid Mech.*, 62:289–304, 1974.

[88] K. Stewartson and P. G. Williams. Self-induced separation. *Proc. Roy. Soc. A.*, 312:181–206, 1969.

[89] S. Stojanovic. Injection of ideal fluid from a slot into a stream — 2 free boundaries. *IMA J. Appl. Math.*, 41:237–253, 1988.

[90] P. D. Thomas. Flow over a finite flat plate with massive injection. *AIAA Journal*, 7:681–687, 1969.

[91] B. Thwaites. The aerodynamic theory of sails. *Proc. Roy. Soc. London.*, 261:402–422, 1961.

[92] L. Ting and C. J. Ruger. Oblique injection of a jet into a stream. *AIAA Journal*, 3:534–576, 1965.

[93] E. C. Titchmarsh. *Introduction to the theory of Fourier integrals.* Oxford, 1948.

[94] F. G. Tricomi. On the finite Hilbert transformation. *Quart. J. Math.*, 2:199–211, 1951.

[95] F. G. Tricomi. *Integral Equations.* Pergamon, 1964.

[96] E. O. Tuck. Ship-hydrodynamic free-surface problems without waves. *J. Ship Res.*, 35(4):277–287, Dec 1991.

[97] E. O. Tuck and M. Haselgrove. An extension of two-dimensional sail theory. *J. Ship Res.*, 16:148–152, 1972.

[98] C. Turfus. Diffusion from a continuous source near a surface in steady reversing shear flow. *J. Fluid Mech.*, 172:183–209, 1986.

[99] M. van Dyke. *Perturbation methods in fluid mechanics.* Academic Press, 1964.

[100] M. van Dyke. *An album of fluid motion.* Parabolic Press, 1982.

[101] J. M. Vanden-Broeck. Nonlinear two-dimensional sail theory. *Phys. Fluids*, 25(3):420–423, 1982.

[102] E. Varley and J. D. A. Walker. A method for solving singular integrodifferential equations. *IMA J. Appl. Math.*, 43:11–45, 1989.

[103] R. Vasantha and G. Nath. Boundary-layer flow past a cylinder with massive blowing. *AIAA Journal*, 24(11):1874–1875, 1986.

[104] A. E. P. Veldman. NLR TR 79023 U. Technical report, Nat. Aerospace Lab, 1979.

[105] A. E. P. Veldman and D. Dijkstra. In *7th Int. Conf. on Numerical Methods in Fluid Dynamics.* Stanford, 1980.

[106] I. P. Vickers and F. T. Smith. Theory and computations for breakup of unsteady subsonic or supersonic separating flows. *J. Fluid Mech.*, 268:147–173, 1994.

[107] K. Voelz. Profil und Auftrieb eines Segels. *Zeit. Angew. Math. Mech.*, 30:301–317, 1950.

[108] J. Wallace and N. H. Kemp. Similarity solutions to the massive blowing problem. *AIAA Journal*, 7(7):1517–1523, 1969.

[109] E. J. Watson. Free streamline suction slots. Technical Report 2177, Aeronautical Research Council, 1946.

[110] L. C. Woods. *The theory of subsonic plane flow.* Cambridge University Press, 1961.